# A SPIN-LABEL ESR STUDY OF DRUG BINDING TO DNA

by

Richard William Strange

Submitted for the degree of PhD

at the University of Keele,

Staffordshire.

1985

## ABSTRACT

A spin-labelled derivative of the drug Proflavine was prepared and its interactions with natural DNA in fibres were investigated using the technique of electron spin resonance (ESR). Computer simulations of the ESR spectra showed that spin-labelled proflavine adopts a preferred orientation in each of the different DNA conformations. In A- and C-form DNA the binding geometry is explained by an external interaction between the drug molecules and the phosphate groups of the double helix. In B-form DNA the drug molecules exhibited some form of rotational motion. Simulations indicated that this motion was directed about the helix axis, a conclusion which is consistent with an intercalative mode of binding. An examination of the B-form X-ray diffraction patterns confirmed that intercalation had occurred.

A difference was observed in the binding of the drug to different species of DNA, suggesting that some form of site specific interaction is involved. The importance of drug concentration on the conformational properties of DNA was recognised.

The binding of several Phenothiazine tranquilisers to DNA was also investigated. The solution ESR spectra of these (oxidised) drug molecules showed that the distribution of unpaired spin density over the heterocyclic ring depends upon the substituted groups present. However, in DNA fibres the different drug species adopted the same binding geometry. Although the ESR results were consistent with both intercalation and external binding, the large spread of drug orientations estimated from computer simulations suggests that external binding is more likely.

DNA from the bacteriophage dW-14 was spin-labelled in order to determine the conformation of the putrescine groups attached to the thymine bases. The information obtained from these experiments suggests that the putrescine groups project into the major groove in B- and C-form DNA,

whereas in the A-conformation they lie close to each other in the hollow interior of the helix.

## ACKNOWLEDGEMENTS

I should like to thank Professor Watson Fuller, Head of the Physics Department, Keele University, for the provision of facilities for carrying out this research.

I wish to thank my supervisor Dr. E. F. Slade for the encouragement and advice he has given me throughout the project.

I am especially grateful to Dr. D. V. Griffiths for the time he invested in the many spin-labelling experiments we carried out.

I am particularly grateful to Dr. A. Mahendrasingham for the many discussions we had as well as for his invaluable aid in taking the X-ray diffraction pictures shown in this thesis. I should also like to thank Mr. David Keeble for allowing me more than my fair share of time on the ESR spectrometer.

I should like to express my gratitude to several members of the technical staff of the Physics Department. In particular, my thanks go to Mr. Jim Minshull, without whom the experimental work would have been far from easy, to Mr. Mike Daniels for the photographic work, and to Mr. Fred Rowerth, the Laboratory Superintendant, who gave me assistance whenever it was needed.

Finally, I should like to express my thanks to my parents, for their help and encouragement, and to Susan for keeping me sane.

## CONTENTS

# CHAPTER 1

# INTRODUCTION

## 1.1 DNA Structure and Function

The nucleic acids, **deoxyribose nucleic acid** (DNA) and **ribose nucleic acid** (RNA), are present in the cells of all living organisms. DNA is found mainly in the nucleus while RNA is found both in the nucleus, where it is synthesised, and in the cytoplasm, where protein synthesis takes place.

The fundamental role of DNA is the transmission of genetic information from one generation of cells to the next. This information is decoded by the messenger RNA-ribosome transfer-RNA system and used to synthesise enzymes and structural proteins for the new cell.

Nucleic acids consist of pentose sugars, nitrogeneous bases and phosphoric acid. In DNA the pentose is deoxyribose and the bases are the pyrimidines thymine (T) and cytosine (C), and the purines, adenine (A) and guanine (G). In RNA ribose replaces deoxyribose and uracil (U) replaces thymine (Fig. 1.1). The combination of a sugar, a phosphate and a base is called a "nucleotide" (Fig. 1.2).

In DNA the pentose molecules are linked by C3' - C5' phosphate - diester bonds to form polynucleotides (Fig. 1.3). One acid group (negative oxygen) on each phosphate is left free by the diester linkage. This enables the polynucleotide to form bonds with positively charged molecules such as metal ions or histones. Histones are protein molecules rich in either argenine or lysine amino-acids and the combination of DNA + histone is called "Chromatin". Histones are found bound to DNA in units of eight molecules and each octomer plus its associated DNA is known as a nucleosome. Several nucleosomes together probably represent the basic genetic unit, or gene.

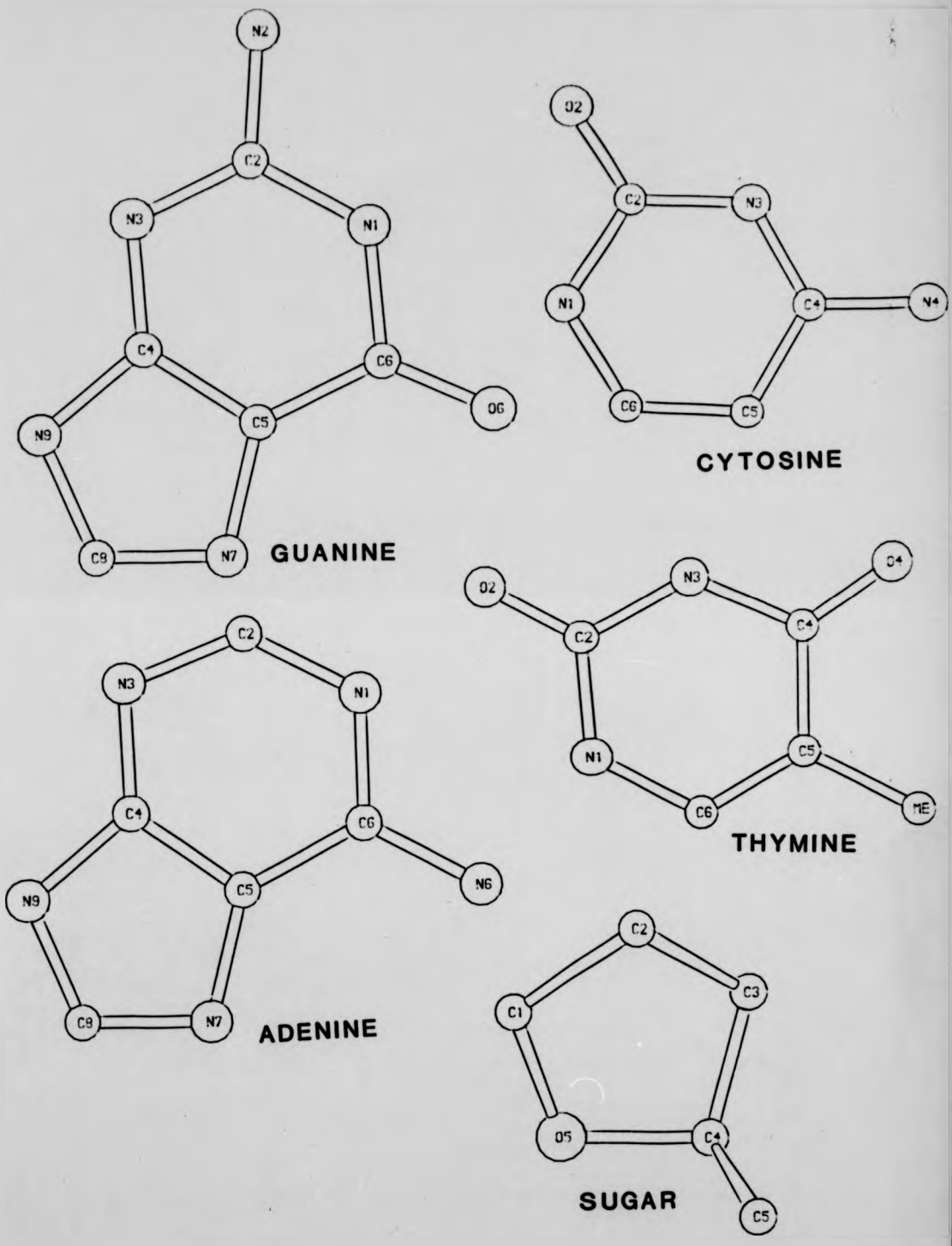


Fig. 1.1 ORTEP plots of the Purine and Pyrimidine Bases and Deoxyribose Sugar.

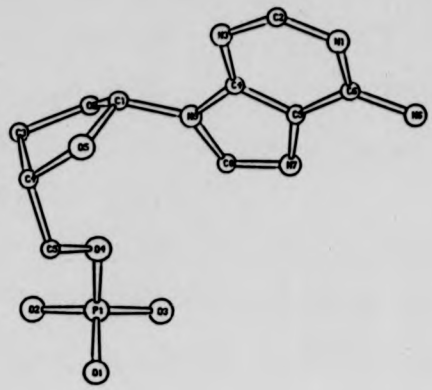

Fig. 1.2 A Nucleotide containing Adenine.

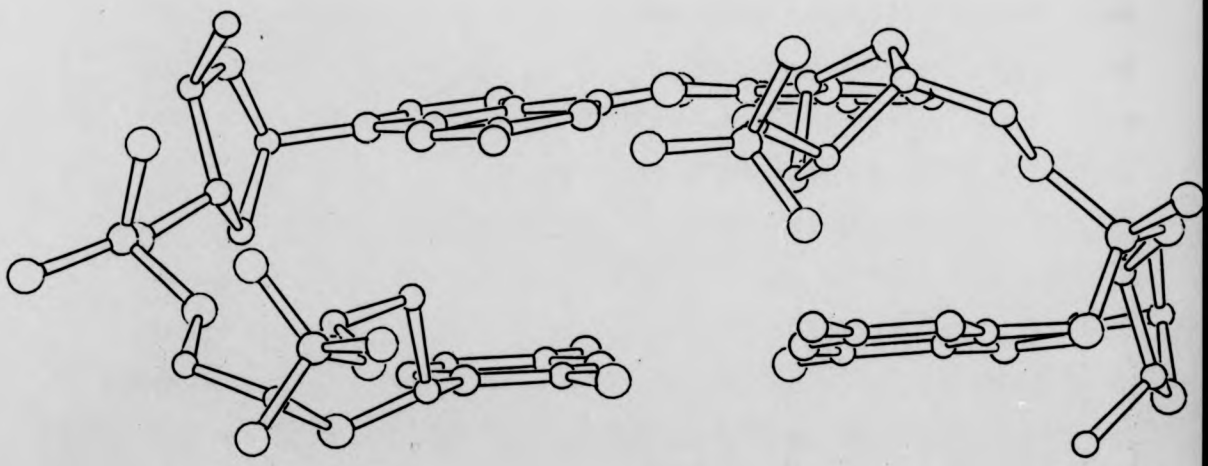

Fig. 1.3 A small section of a DNA helix showing base pairing.

In 1953 Watson and Crick, on the basis of results obtained from the fibre X-ray diffraction experiments of Wilkins et al. (1953) and Franklin and Gosling (1953) proposed their right-handed double helix model of DNA. This model represents the best available explanation of cell replication, protein synthesis and genetic variation.

The DNA double helix is formed from two polynucleotide chains, with their C3' - C5' diester linkages running anti-parallel and with the purine and pyrimidine bases pointing inside and stacked perpendicular to the helix axis. The formation of a regular helix requires specific pairing between the bases. Thus, adenine forms two hydrogen bond with thymine and cytosine forms three hydrogen bonds with guanine.

Because of the similar overall geometry of the AT and GC base pairs, the secondary structure adopted by the DNA duplex is identical whatever base pair sequence is present. In this pairing scheme there are always equal amounts of adenine with thymine and guanine with cytosine. However, the relative proportions of A + T and G + C depends upon the origin of the DNA.

During replication the hydrogen bonds are broken and the two polynucleotide chains unwind and separate. Each strand then acts as its own template on which a new DNA strand can be synthesised. The base pairing scheme compels the formation of a complementary base sequence in the new strand. Replication is therefore "semi-conservative" in that one "parent" polynucleotide strand is conserved in each replicate. The semi-conservative nature of DNA replication was confirmed by Meleson an Stahl in 1958.

Genetic information is coded by means of the base sequences along the polynucleotide chain. Only four bases are present in DNA but the massive size of each molecule (with molecular weights of $10^6$ to $10^9$) ensures that there will be billions of possible base sequences. During protein synthesis groups of three bases (called "codons") code for the

insertion of a particular amino-acid into a protein (Crick et al., 1961). The information, or code, is first transcribed into RNA in the nucleus; then, in the ribosomes, RNA translates the information into proteins (Davidson, 1976).

The stability of the double helix cannot be accounted for by base pair hydrogen bonding alone since the energy involved in such bonds (~16kJ) is too small. In fact, in solution base pairs will tend to stack up on each other rather than form hydrogen bonds and the hydrogen bonds are instead taken up by water molecules. The stacking mechanism arises out of the interactions between the $\pi$-electrons of the aromatic bases and accounts for the stability of single strand polynucleotides. Base pair stacking in DNA results in the exclusion of water. Hydrogen bonding between the base pairs is then a favourable interaction. A further stabilising influence on the double helix arises through the presence of small, positively charged salt ions, such as $Na^+$ and $K^+$, which tend to neutralise the electrostatic repulsions between the negative phosphate groups along the DNA backbone.

## 1.2 DNA Conformations in Fibres

Natural DNA in orientated fibres is known to be able to adopt any of three distinct conformations. These conformations are referred to as the A-, B- and C-forms. They are all adaptations of the same double helix structure but differ in the number of nucleotides per helix rotation, the pitch of the helix and the displacement of the base pairs from the helix axis (Table 1.1). The structures of the A- and B-forms are well documented (e.g. Fuller et al., 1965; Langridge et al., 1960; Arnott and Hukins, 1972). The C-form was first described by Marvin et al. (1961). These structures are all based upon X-ray fibre diffraction studies.

The A- and B-forms are most easily distinguished. In the B-form the bases lie close to the helix axis and the base tilt is small and negative (Fig. 1.4). In the A-form the bases are displaced by 4.25Å from

| | CONFORMATION | | |
|---|---|---|---|
| | A | B | C |
| Helix Sense | Right | Right | Right |
| Sugar Pucker | C3'-endo | C2'-endo | C2'-endo |
| Pitch (Å) | 28.2 | 33.8 | 31.0 |
| Bases per Turn | 11 | 10 | 9.3 |
| Rise per Base Pair (Å) | 2.56 | 3.40 | 3.30 |
| Base Tilt Angle | 19° | -6° | -8° |
| Groove Width (Å) | | | |
| Minor | 11 | 5.7 | 4.8 |
| Major | 2.7 | 11.7 | 10.5 |
| Groove Depth (Å) | | | |
| Minor | 2.8 | 7.5 | 7.9 |
| Major | 13.5 | 8.5 | 7.5 |
| Displacement 'D' (Å) | 4.72 | -0.16 | -2.13 |
| References: | 1 | 1 | 2 |

(1) Arnott and Hukins (1972); (2) Arnott and Sesling (1975)

Table 1.1 The Parameters Defining the Three Conformations of Native DNA in Fibres.

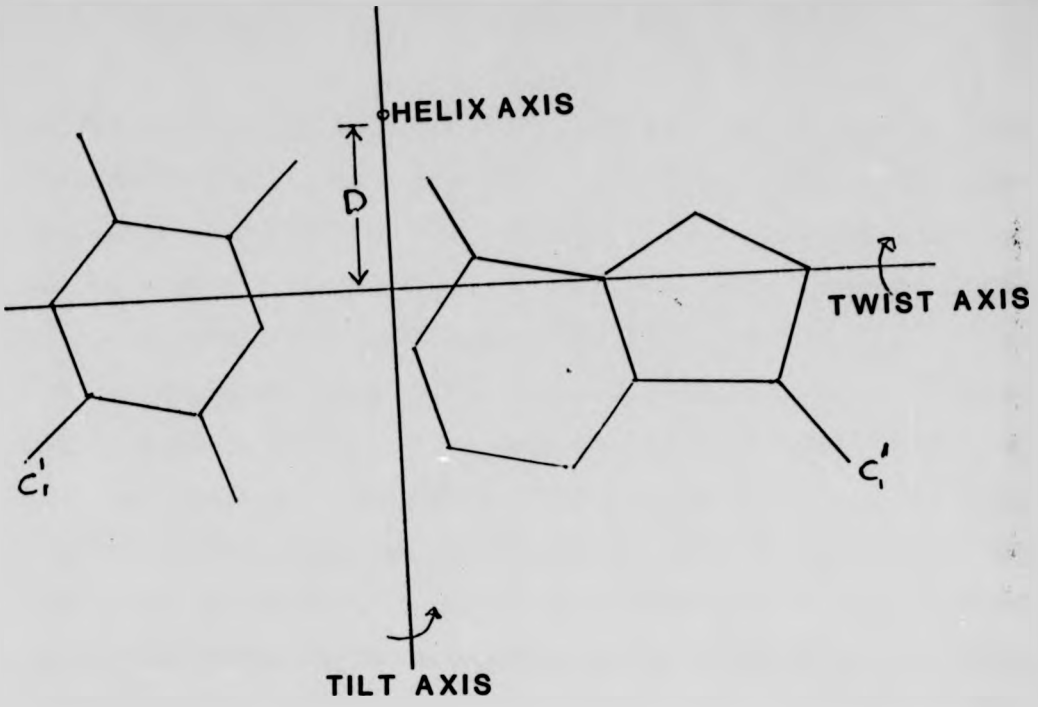


Fig. 1.4 The Parameters Defining the Position of a Base Pair relative to the Helix Axis.

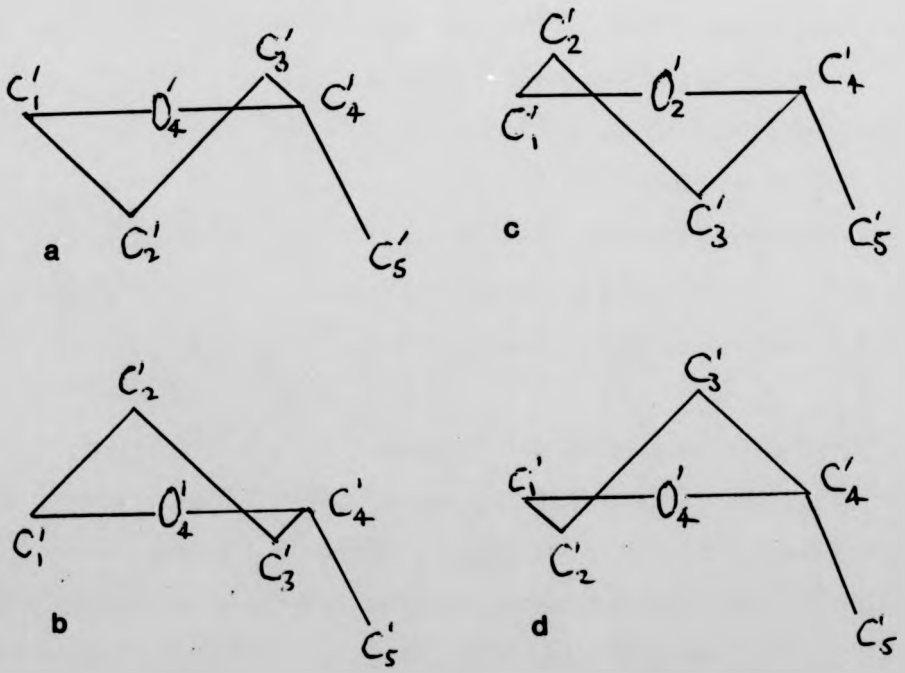


Fig. 1.5 The four possible Sugar Puckers: (a) C2'-endo (b) C2'-exo (c) C3'-endo (d) C3'-exo

the helix axis and the base tilt angle is large and positive. Sugar pucker also distinguishes the two conformations. The sugar pucker is given by the orientation of the C3' atom (or C2' atom) relative to the plane defined by the C1' - O5' - C4' atoms (Fig. 1.5). The conformation is "endo" if the out of plane atom lies on the same side as the C5' atom and "exo" if it lies on the opposite side to C5'. In B-DNA the sugar pucker is C2'-endo and in A-DNA it is C3'-endo. The B-form has a pitch of 33.8A and 10 base pairs per rotation of the helix. This conformation corresponds most closely to the original Watson-Crick model. The A-form has a pitch of 28.15A and approximately 11 base pairs are accommodated in one complete turn of the helix. The C-form is closely allied to the B-form: they share the same sugar pucker and nearly the same base pair conformation with respect to the helix axis. They differ, however, in the size of pitch and the number of residues per turn, which for the C-form are 31A and 9.33 respectively. The conformations are distinguished experimentally by their characteristic X-ray diffraction patterns. Three dimensionl computer drawings of the three conformations are shown in Figs. 1.6(a-c).

A recent attempt was made by Rodley et al. (1976) to account for the B-form structure by a "side-by-side" (SBS) model in which the two polynucleotide chains have alternating left- and right-handed helical sense at regular intervals. This model was examined by Greenall et al. (1979) and it was concluded that the conventional Watson-Crick model provided a better fit to the experimental data.

Early experiments established that the conformation adopted by the DNA depends crucially upon the condition of its local envioronment. The main factors are the degree of hydration of the fibre and the type and concentration of counterion present. Until recently it was believed that at low ionic strengths (< 5% excess salt) the A-form would be adopted up to 92% r. h. and occasionally at 98% r. h. and that at higher ionic strengths the B-form would be preferred at relative humidities above 75% (Cooper and

Hamilton, 1966). The C-form was usually observed at low humidities with lithium as the counterion. It was believed that a sodium salt C-form would be adopted at low humidities only rarely.

Recent work has modified this opinion considerably. Sodium salt fibres were observed to adopt the C-conformation readily under the appropriate conditions. These conditions represent a kind of balance between the two factors of salt concentration and relative humidity (Rhodes et al., 1982). At < 10mM salt concentration and between 30% and 75% r. h. Na-DNA was observed in the C-form; from 75% to 92% r. h. the A-form was observed and at relative humidities in excess of 92% the B-conformation was adopted. At higher salt concentrations the A-conformation was preferred and the C-conformation was prohibited. By keeping the salt concentration low, therefore, one may observe the three DNA conformations in turn, in the order C → A → B, simply by altering the relative humidity. Such a procedure was adopted in the present work. An alternative, though practically more awkward method, can be used in which the salt concentration is varied at a constant relative humidity.

The A-, B- and C-conformations are adopted by natural DNA's from a variety of sources but it is not yet known what significance can be attached to their existence. However, since the DNA secondary structure is intimately related to its function it is possible that each conformation has a function to perform.

Recent work, using synthetic polynucleotides and single crystals, has led to the identification of other DNA structures. Wang et al. (1979) found that, upon crystallisation, the oligomer d(CpGpCpGpCpG) adopted a left-handed helical conformation - the so called "Z-conformation". The name originates from the zig-zag path followed by the sugar-phosphate backbone as it rotates about the helix axis. The Z-conformation is stable **in vitro** at very high salt concentrations but its biological significance can be seen from the fact that, if the cytosine residues are replaced by

methyl-cytosine (a process which may occur **in vivo**), then the conformation is stabilised at much lower levels of salt concentration.

The possibility arises that different regions of the same DNA molecule may adopt different conformations. Kirkpatrick et al. (1984) have recently shown that fetal globin genes contain tracts of alternating purine-pyrimidine bases some 40-60 base pairs in length which adopt the left-handed Z-conformation. These base pair sequences are important for gene conversion and recombination and the presence of the left-handed structure may therefore be important in gene expression.

Recently, Arnott et al. (1980) observed the left-handed S-conformation in both Polyd(GC).Polyd(GC) and Polyd(AC).Polyd(TG) and Mahendrasingham et al. (1983a,b) have investigated the structure and dynamics of the B → S transition in Polyd(GC).Polyd(GC). This transition is especially interesting since it involves a change in the sense of the helix from right-handed to left-handed. The S-conformation is shown in Fig. 1.6d. The D-conformation, initially observed by Davis et al. (1963) in sodium fibres of Polyd(AT).Polyd(AT) and thought to be right-handed, has been re-examined by Mahendrasignham (1983) who claims that a left-handed structure is preferable. Synthetic polynucleotides and single crystals have also been known to adopt modified versions of the A-, B- and C-conformations (e.g. Shakked et al., 1983). None of these modified conformations has yet been observed in DNAs obtained from natural sources.

## 1.3 DNA-Drug Interactions

Many small, positively charged molecules are known to interact with DNA. These interactions are interesting not only from an analytical point of view: many of the molecules are drugs which have theraputic uses and their effect upon replication and protein synthesis is of great importance. Drug-DNA interactions are not as yet fully understood but data obtained from a variety of experimental techniques has led to definite

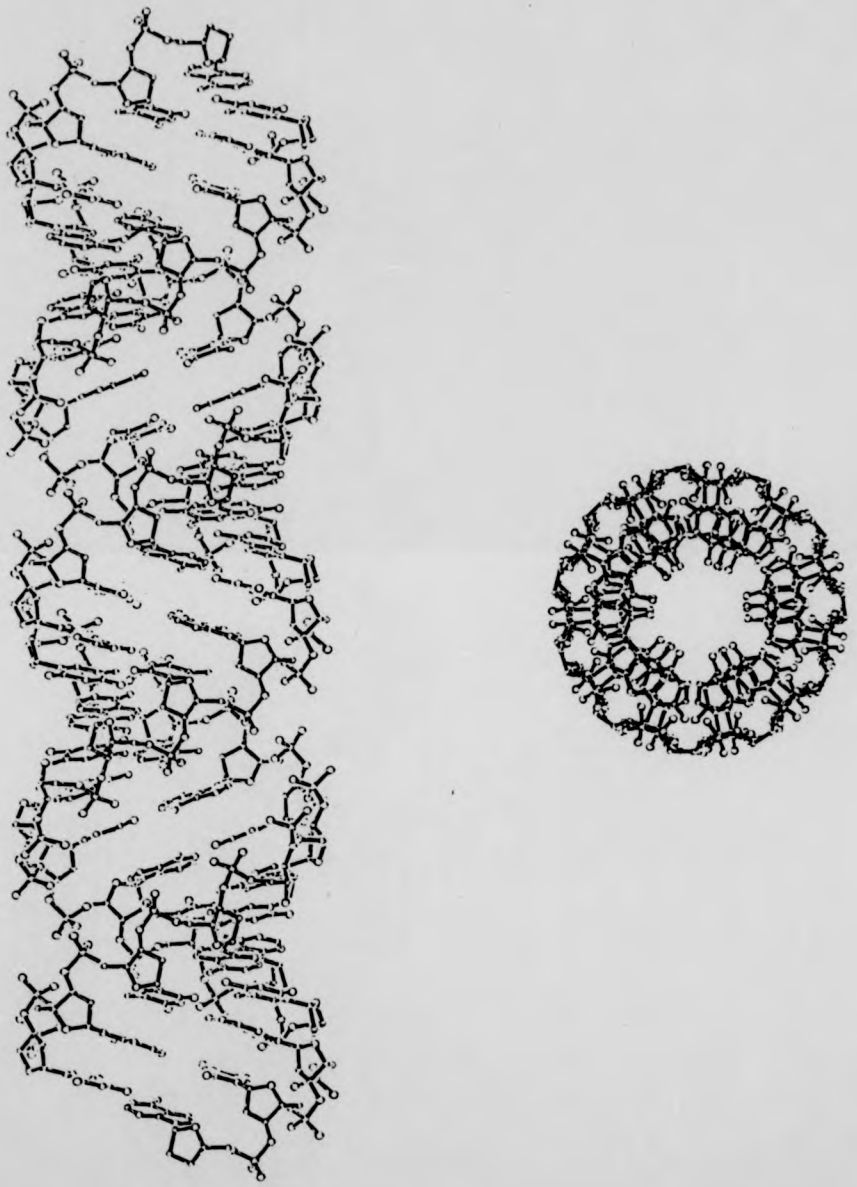

Fig. 1.6a A-form DNA.

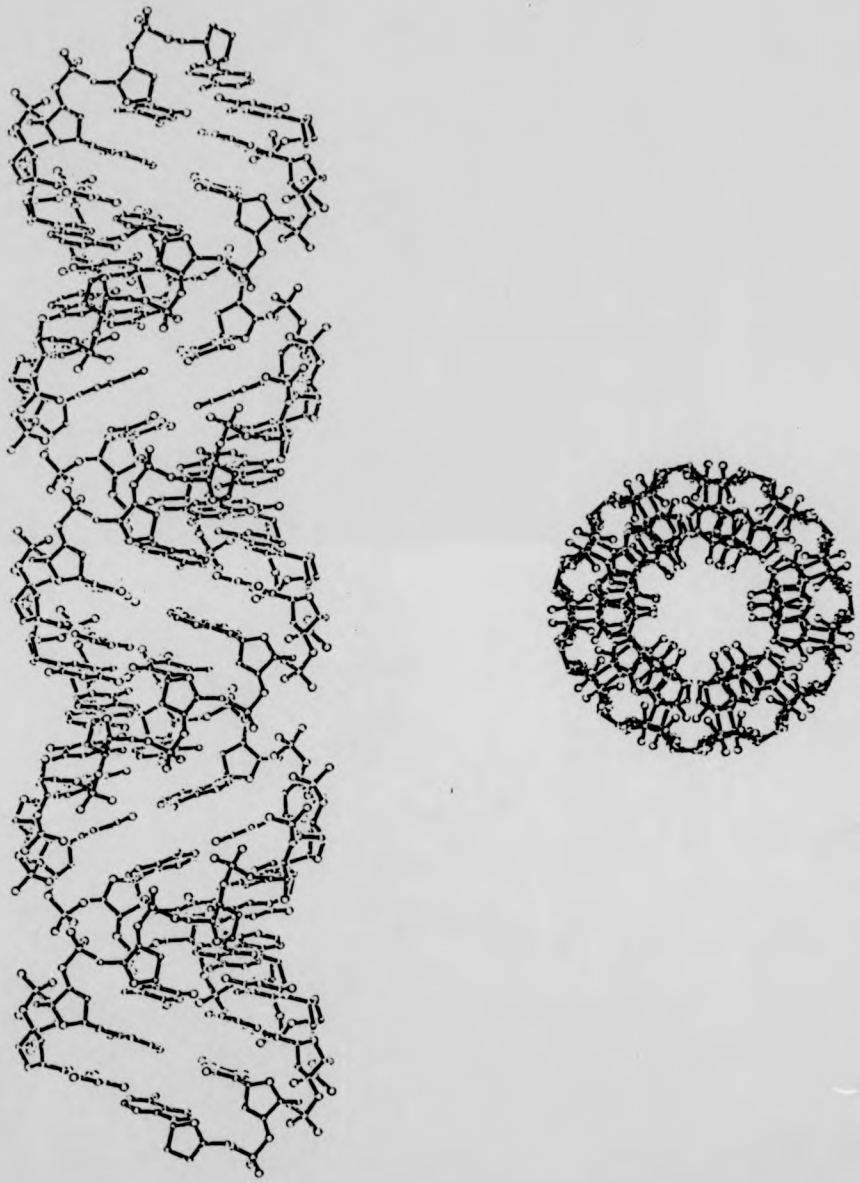

Fig. 1.6a A-form DNA.

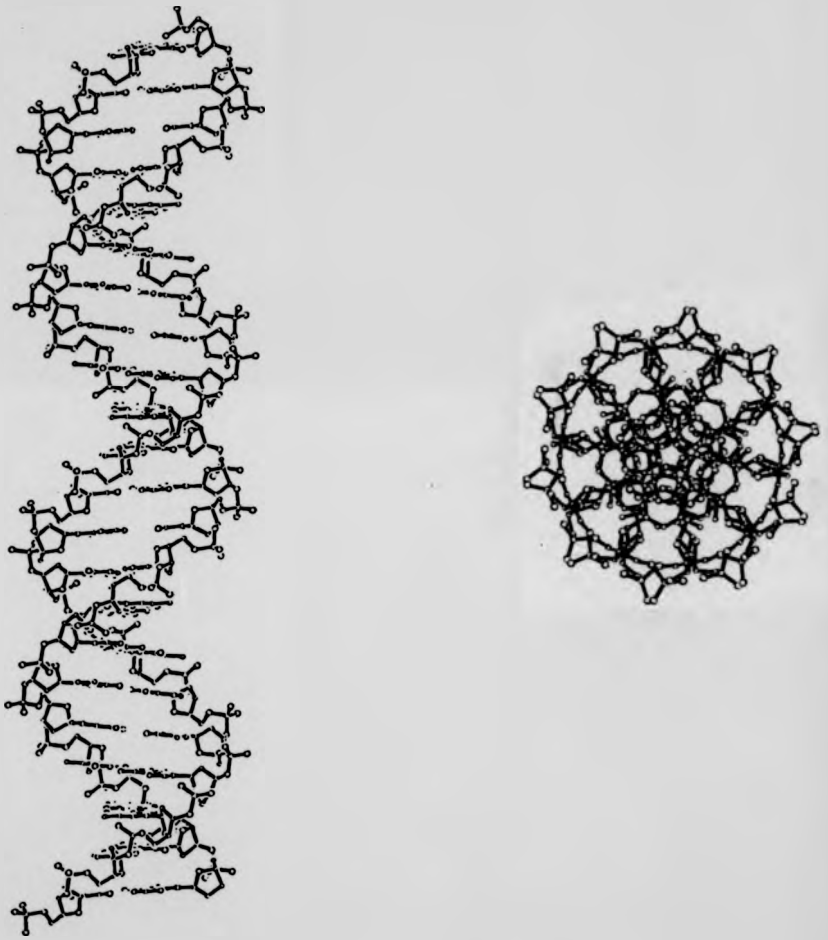

Fig. 1.6b B-form DNA.

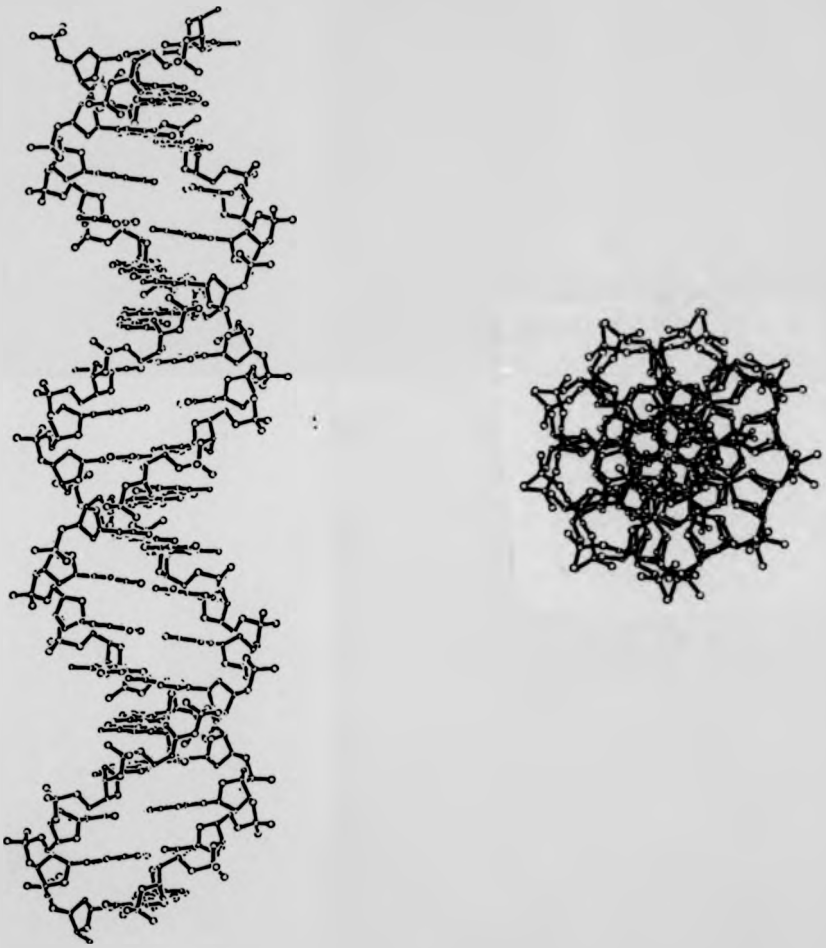

Fig. 1.6c C-form DNA.

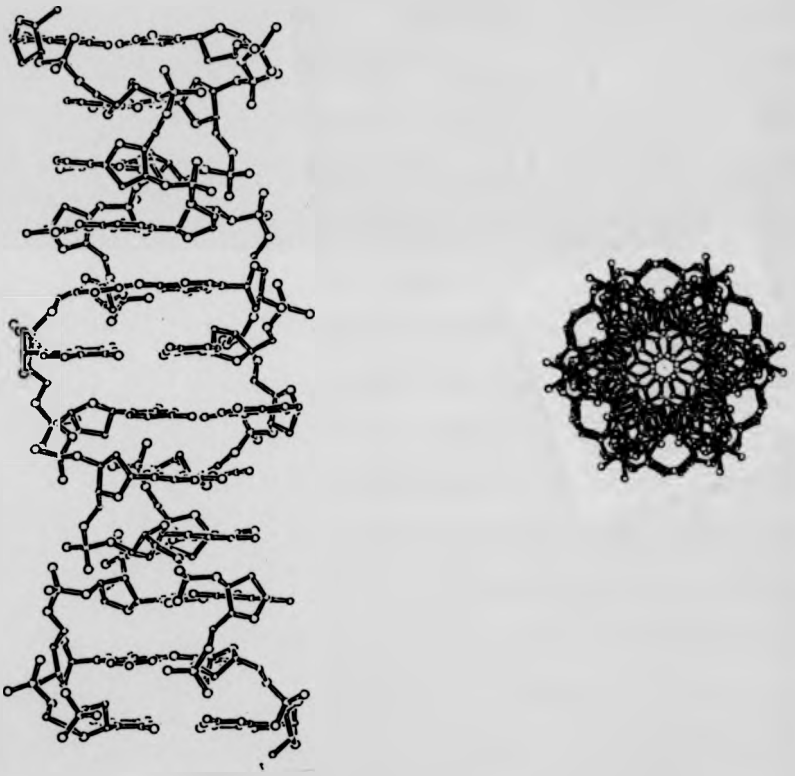

Fig. 1.6d S-form DNA.

ideas concerning the mechanisms involved. Probably the most important of these binding mechanisms is that of "intercalation".

Lerman (1961, 1963) studied the interactions of several acridine drugs with DNA. X-ray diffraction patterns of acridine-DNA fibres at high humidity showed that layer lines corresponding to helical repeats of the DNA were missing. However, the meridional repeat of 3.4Å was still observable (see Chapter 4). Furthermore, solutions of the complex showed an increased viscosity and a decreased sedimentation coefficient when compared with normal DNA solutions. These observations, which suggest that the binding of the acridine molecules results in a thinner and stiffer DNA helix, led Lerman to propose his intercalation model. On this model neighbouring base pairs are able to move apart in order to accommodate the drug molecule, which is then "sandwiched" between them. The base pairs remain perpendicular to the helix axis and in Van der Waal's contact with the drug molecule. The complex is stabilised by the overlap of the $\pi$-orbitals of the drug molecule and those of the pyrimidine or purine rings. For such a complex to be formed there must be a partial unwinding of the double helix at the site of the intercalated drug. The unwinding angle required for the intercalation of proflavine was estimated by Lerman (1964) at 36°. The unwinding disturbs the regularity of the DNA helix to such a degree that X-ray diffraction patterns for drug-DNA complexes in fibres are generally poorly resolved at even moderate concentrations of bound drug.

A substantial body of evidence now exists in support of the intercalation hypothesis. Fuller and Waring (1964) proposed a model for the intercalation of ethidium bromide in B-form DNA based upon fibre X-ray diffraction studies. Other work including low angle X-ray scattering experiments, flow dichroism, circular dichroism, and fluorescence polarisation techniques (King et al., 1982; Lerman, 1963; Le Pecq and Paoletti, 1967; H. Porumb, 1976) as well as optical spectroscopy

(Dougherty, 1979; Yielding et al., 1984) and NMR studies (Krugh and Reinhardt, 1975) on acridine or ethidium derivatives complexed with B-form DNA, suggests that the drug molecules are aligned with their chromophores parallel to the planes defined by the base pairs. Several models have also been proposed for the intercalation of these drugs in single crystals containing repeating base pair sequences (Aggarwal et al., 1984) and it has recently been reported that ethidium intercalates in Z-form Polyd(GC).Polyd(GC) (Shafer et al., 1984). Other drugs are also believed to intercalate in B-form DNA. These include the carcinogenic hydrocarbons (Hong and Piette, 1976; Nelson and Devoe et al., 1984; Meeham et al., 1982) and the anti-biotics daunomycin, andriamycin and nogalomycin and ecinomycin (Calendi et al., 1965; Wakelin and Waring, 1976 ).

The anti-biotic actinomycin D is known to cause a decreased viscosity and an increased sedimentation coefficient when bound to DNA. These effects are opposite to those expected if the drug molecules bind by intercalation. Hamilton et al. (1963) proposed a model in which actinomycin D binds externally in the minor groove of the helix, forming hydrogen bonds with a deoxyguanosine base via its amino and carboxylic groups. The complex would be stabilised further by the formation of hydrogen bonds between the secondary amino groups on the drug molecule and the DNA phosphate groups. On the other hand, Waring (1970) has shown that actinomycin D unwinds closed circular DNA in a way usually associated with intercalative binding.

It is clear that interactions between DNA and small drug molecules are more complicated than the early experiments of Lerman and coworkers would suggest. Whether or not a drug binds by intercalation would seem to depend upon many factors, e.g. DNA conformation, type of DNA, etc. Some of the possible factors are discussed below.

It has generally been accepted that, in order for intercalation to occur, the drug molecules must satisfy certain criteria. These criteria

are (a) that the drug chromophores have a geometry and size comparable to the polynucleotide base pairs and (b) that they intercalate such that their orientation in the DNA helix minimises contact with the aqueous envioronment. These criteria mean that unique and preferential binding sites should exist in the DNA molecules at which intercalation can occur. The drugs usually taken to be intercalators have at least two thing in common: they all possess at least three fused aromatic rings and contain a positive charge in at least one of the rings (usually centred on a nitrogen atom).

However, the work of Hong and Piette (1978) throws some doubt upon the size criterion. Using spin-labelled analogues of several nitrobenzene derivatives they were able to demonstrate that binding took place preferentially depending upon the number and position of the nitro-substitutes on the benzene ring. They suggested that the polarisation of the benzene ring is the important factor and argue that their ESR data is only consistent with an intercalation mechanism. Hong and Piette (1978) conclude that the nitroanilines should be classed apart from the polycyclic compounds, such as proflavine and ethidium bromide, in which substituted groups have little effect on the binding mechanism.

Nevertheless, the presence of substituted groups may give intercalating polycyclic drugs a specificity for certain base pairs (or base pair sequences) in the DNA by influencing the electronic properties of the chromophores. The direction of polarisation of the ring system depends upon the positions and types of substituted groups, whereas the dipole moment of a GC or AT base pair is fixed. If no steric hindrance exists one would expect a heteroaromatic ring, whose polarisation matches that of a GC base pair, to have a preference for GC rich regions of the DNA. This can be tested by examining the interactions of the polycyclic drug with DNAs of varying GC-content. Muller and Crothers (1975) have carried out such an examination using a series of heteroaromatic drugs and dyes.

Muller and Crothers (1975) found that the GC specificity of a heteroaromatic drug increases with its polarisability. This result is consistent with the fact that GC base pairs are more polar than AT base pairs and should therefore interact preferably with the more polarisable compounds. Many of the drugs examined by Muller and Crothers (1975) showed a GC specificity similar to that of actinomycin D and yet they lacked the hydrogen bonding capabilities of that molecule. This implies that the interaction between actinomycin D and DNA is primarily due to the polarisation of the chromophore.

In a recent study Newlin et al (1984) have demonstrated that the binding of daunomycin to DNA is not only base specific it is also base-sequence specific. Viz., daunomycin appears to bind preferably to a specific sequence of AT bases.

Base specific interactions are also believed to occur in the second mode of binding of drugs to DNA, although in this case the evidence is more scarce. The **external** binding mechanism involves both specific hydrogen bonding to sites on the DNA helix and electrostatic interactions between the positive drug molecules and the negatively charged oxygen atoms on the sugar-phosphate backbone. Muller et al. (1973) prepared an analogue of proflavine which is sterically hindered from binding by intercalation but instead forms hydrogen bonds to a combination of two AT base pairs and one GC pair.

Both intercalation and external binding of drugs can drastically alter the secondary structure of the DNA and this may have important consequences for replication and protein synthesis. For example, the ability of the aminoacridines to extend the polynucleotide chains of DNA is closely related to their ability to cause additions or deletions in the genetic code (Peacocke, 1970; Shearman et al., 1984; Topal, 1984). The acridine molecule, by intercalating in the polynucleotide chain, causes a mis-reading of the base pair sequence and therefore a mis-copying of a

single strand of DNA. In another case an intercalated acridine molecule could cause an insertion or deletion while it was undergoing recombination with a separate DNA double helix. Furthermore, if the deletion of a base at one site in the polynucleotide chain is followed by an insertion of a base further along the chain then the resulting amino-acid sequence might be altered only in the region between the two mutations. This may result in a "wild protein".

However, not all intercalating drugs are mutagenic. Many drugs possess a strong medicinal activity which is believed to increase with binding affinity (Wilson et al., 1982; King et al., 1982). Some simple derivatives of 9-Aminoacridine have been shown to possess a high anti-leukaemic activity (Denny and Cain, 1978) and several other drugs (e.g. Daunomycin) have been used to treat solid tumours in humans.

A recent approach in the development of chemotheraputic drugs has centred on the use of "bifunctional intercalators". These compounds consist of two intercalating moieties linked by a partially rigid molecular chain. Under favourable stereochemical conditions they bind to DNA with an affinity of the order of the square of that of the comparable mono-intercalators. The quinoxaline anti-biotics (e.g. quinomycin) are powerful anti-microbal and anti-tumour agents and their biological activity has been linked to their ability to act as bifunctional intercalators (e.g. Low et al., 1984). Several bifunctional derivatives of 9-aminoacrine have recently been prepared and their chemotheraputic activities investigated (Bernier et al., 1981; King et al., 1982).

Although most of the biological consequences of drug binding to DNA have been attributed to intercalation it has been recognised that external binding has a part to play. It is thought that the action of many platinum containing antitumour drugs lies in their interaction with DNA. A variety of studies suggest that cis-$[Pt(NH)_3]Cl_2$ ("platin") binds externally and covalently to DNA bases with the order of preference

G > A > C > T. In one possible binding model the Pt-drug forms interstrand covalent linkages to the N7 Guanine atoms in opposite polynucleotide chains (Segal et al., 1984). The conformational properties of several synthetic polynucleotides in the presence of bound platin have been investigated (e.g. Herman and Fazakerley, 1984).

The drugs used in the present study belong to the acridine and phenothiazine class of compounds. A detailed discussion of their relevant properties and structures will be found in the appropriate chapters, although some of the important features of acridine-DNA interactions have already been mentioned.

## 1.4 ESR Studies of DNA and DNA-Drug Interactions

Normal DNA is diamagnetic. The paramagnetism required for ESR (see Chapter 2) must therefore be artificially produced. Fortunately there are several methods available for introducing paramagnetic centres in nucleic acids. The chief ones are:

(a) The use of paramagnetic ions (or "Spin-Probes") such as $Cu^{2+}$, $Mn^{2+}$ and $Fe^{3+}$. These ions are substituted for the more normal $Na^{+}$ and $K^{+}$ ions found in the DNA and the information available from the ESR studies concerns the local envioronment of the paramagnet. For example, Shields et al. (1982) used ESR to determine the conformation and identity of the atoms bound to $Cu^{2+}$ in a copper-bleomycin complex bound to DNA in fibres.

(b) The creation of paramagnetic centres by irradiation of the DNA with X-ray, UV or $\lambda$-radiation. These studies have been carried out primarily to determine the extent and type of cellular damage caused by free radicals induced by irradiation (e.g. Gregoli et al., 1982).

(c) The use of nitroxide "spin-labels" and other free radicals. This method is employed in the present work.

The spin-label method was initiated by Stone et al. (1965) and developed by McConnell and co-workers (Griffith and McConnell, 1965;

G > A > C > T. In one possible binding model the Pt-drug forms interstrand covalent linkages to the N7 Guanine atoms in opposite polynucleotide chains (Segal et al., 1984). The conformational properties of several synthetic polynucleotides in the presence of bound platin have been investigated (e.g. Herman and Fazakerley, 1984).

The drugs used in the present study belong to the acridine and phenothiazine class of compounds. A detailed discussion of their relevant properties and structures will be found in the appropriate chapters, although some of the important features of acridine-DNA interactions have already been mentioned.

## 1.4 ESR Studies of DNA and DNA-Drug Interactions

Normal DNA is diamagnetic. The paramagnetism required for ESR (see Chapter 2) must therefore be artificially produced. Fortunately there are several methods available for introducing paramagnetic centres in nucleic acids. The chief ones are:

(a) The use of paramagnetic ions (or "Spin-Probes") such as $Cu^{2+}$, $Mn^{2+}$ and $Fe^{3+}$. These ions are substituted for the more normal $Na^{+}$ and $K^{+}$ ions found in the DNA and the information available from the ESR studies concerns the local envioronment of the paramagnet. For example, Shields et al. (1982) used ESR to determine the conformation and identity of the atoms bound to $Cu^{2+}$ in a copper-bleomycin complex bound to DNA in fibres.

(b) The creation of paramagnetic centres by irradiation of the DNA with X-ray, UV or λ-radiation. These studies have been carried out primarily to determine the extent and type of cellular damage caused by free radicals induced by irradiation (e.g. Gregoli et al., 1982).

(c) The use of nitroxide "spin-labels" and other free radicals. This method is employed in the present work.

The spin-label method was initiated by Stone et al. (1965) and developed by McConnell and co-workers (Griffith and McConnell, 1965;

Griffiths et al., 1965; Onishi et al., 1966).

A spin-label is a stable nitroxide free radical which exhibits a simple three line ESR spectrum with an isotropic hyperfine splitting of ~16G. The g- and A-tensors of the nitroxide are usually anisotropic and the ESR spectrum is therefore very sensitive to the rate of motion and degree of orientation of the molecule relative to the external magnetic field (see Chapter 2).

The spin-label method basically consists of attaching a nitroxide free radical to a macromolecule and using ESR to monitor the conformational behavior and interactions of the macromolecule. Changes in the ESR spectrum of the macromolecule (e.g. the hyperfine splittings) signify changes in the orientation and/or mobility of the spin-label or its immediate envioronment. By analysing the ESR spectra of the spin-labelled system one may therefore obtain important information concerning the structural and dynamic properties of the molecules. A detailed discussion of the sort of information available using spin-labels and ESR will be found in Chapters 2 and 4.

A spin-label may be attached to DNA either <u>directly</u> (i.e. covalently) or <u>indirectly</u>, via a secondary binding agent, such as a protein or drug molecule. In contrast to other techniques, such as X-ray diffraction or optical spectroscopy, the spin-label method is capable of providing information about specific or local sites in the DNA. Unfortunately, the complex chemical and structural properties of the nucleic acids often makes it extremely difficult to obtain the desired site-specific spin-labelling. The large majority of ESR studies on spin-labelled DNA have therefore been carried out using non site-specifically spin-labelled DNA. In this case the spin-labels are more or less randomly distributed.

Both Bobst (1979) and Kamzalova and Postnikova (1981) give details of the types of chemical modifications to the nucleic acids which

may take place. The labelling procedure often involves a modification of the nucleic acid bases. In general, spin-labels only react weakly with DNA. A typical non site-specific spin-labelling of calf thymus DNA may result in modifications to the extent of 3-10 labels per 1000 base pairs (Kamzalova and Postnikova, 1981). Because of the randomness of these modifications, non site-specific spin-labelling will provide information which relates to the properties of the DNA as a whole rather than to the local envioronment of the spin-labels. Nevertheless, many important studies have been carried out using this technique. For example, Bobst and co-workers have examined a series of different non site-specifically spin-labelled polynucleotides with a view to elucidating their conformational properties in solutions of varying viscocity, temperature, salt concentration and salt type (Pan and Bobst, 1973, 1974; Bobst, 1979; Bobst et al., 1979). Similar studies have been made by other workers (e.g. Petrov and Sukharokov, 1983).

In recent years site-specifically spin-labelled DNAs have been prepared. Zdhanov et al. (1979) have developed a method of spin-labelling the amino groups of nucleotides and nucleosides. Bobst et al. (1984) and Ozinskes et al. (1981) have also successfully obtained specific modifications to the DNA bases. These spin-labelled "fragments" are incorporated in the full DNA molecule by "enzymatic co-polymerisation" (Ozinskes et al., 1981; Bobst et al., 1984). Raikova et al. (1982, 1983) have used a guanine specific alkylating agent (containing a nitroxide) to investigate the conformational properties of DNAs of varying base pair composition. Other site-specific alkylating spin-labels suitable for use with DNA have been prepared by Ivanov et al. (1983).

One interesting application of spin-labelled DNAs in recent years has been their use to monitor the interactions of other small molecules (e.g. drugs) with DNA. (e.g. Chapman et al., 1983).

A simpler, and often more informative, method of applying ESR to

nucleic acid systems is to attach the spin-label to the DNA via an intermediate molecule. The intermediate molecule is usually much smaller and structurally simpler than DNA and this makes it easier to spin-label. As well as being easier it is also often the only way in which certain information may be obtained. Thus, the interactions of several histone proteins with DNA have been studied and the probable binding sites of these molecules have been determined (Chan and Piette, 1982; Lawrence et al., 1980). Several studies of drug binding to DNA have been reported where spin-labelled drug analogues have been used. Most of these studies have been carried out in aqueous media but some solid state (e.g. fibre) work has been done. The information available using the spin-labelled drug is varied and includes the possible specificity of the drug for certain base pair sequences, the binding affinity, the extent and type of motion of the drug or the region of the DNA to which it is bound, the orientation of the drug in the DNA, whether binding occurs in the major or minor grooves or by intercalation, and the ability of the drug to interfere with the actions of other molecules, such as histone proteins or carcinogens. Among the drugs which have been spin-labelled and used in such studies are the acridines (Bernier et al., 1981a, 1981b; Yamaoka and Noji, 1977; Sinha and Chignall, 1979; Robinson et al., 1980, 1982; Noji, 1980), the antibiotic Actinomycin D (Sinha et al., 1975, 1979, 1981a,b), ethidium bromide (Hong and Piette, 1976; Hurley et al., 1982), several aromatic carcinogens (Hong and Piette, 1976) and several nitrobenzene derivatives (Hong and Piette, 1978). In other ESR studies, free radical drug derivatives of the tranquiliser chlorpromazine (Porumb and Slade, 1976; Porumb, 1976; Onishi and McConnell, 1965) were used. The theraputic or carcinogenic activities of many of these compound are believed to be due to their interactions with nucleic acids. By providing information about such features as intercalation and binding specificity, ESR can lead to a better understanding of the nature of these interactions.

# CHAPTER 2

## BASIC ESR THEORY AND EXPERIMENTAL METHODS

In this chapter basic ESR theory is described which will later be of use in the analysis of the experimental work carried out in this thesis. The latter part of the chapter consists of a brief description of the main ESR experimental techniques.

### 2.1 The Zeeman Interaction

The existence of magnetic resonance is due to the fact that electrons and many nuclei possess an angular momentum J and magnetic moment $\mu$, related by the equation

$$\mu = -\gamma J \qquad (2.1)$$

where $\gamma$ is the "gyromagnetic ratio". The angular momentum may arise from orbital motion or from intrinsic spin.

Electrons always have a spin of one-half. Nuclei with odd mass number have spins which are odd integral multiples of one-half (e.g. for $^{1}H$, $^{13}C$ and $^{15}N$, I=1/2; $^{35}Cl$ has I = 3/2). Nuclei with an even mass number have either zero spin or integral spin (e.g. $^{14}N$ and $^{2}D$ have I = 1). Both $^{12}C$ and $^{16}O$, which are of great importance in chemistry, have zero spin.

The gyromagnetic ratio is given by

$$\gamma = g(e/2m) \qquad (2.2)$$

where e is electronic charge, m is the mass of the electron (or proton) and g is a number, called the "g-factor", whose magnitude depends upon the relative contributions of orbit and spin to the total angular momentum.

The **Zeeman interaction** is the fundamental interaction between a magnetic moment and a magnetic field. The Hamiltonian for the interaction is given by

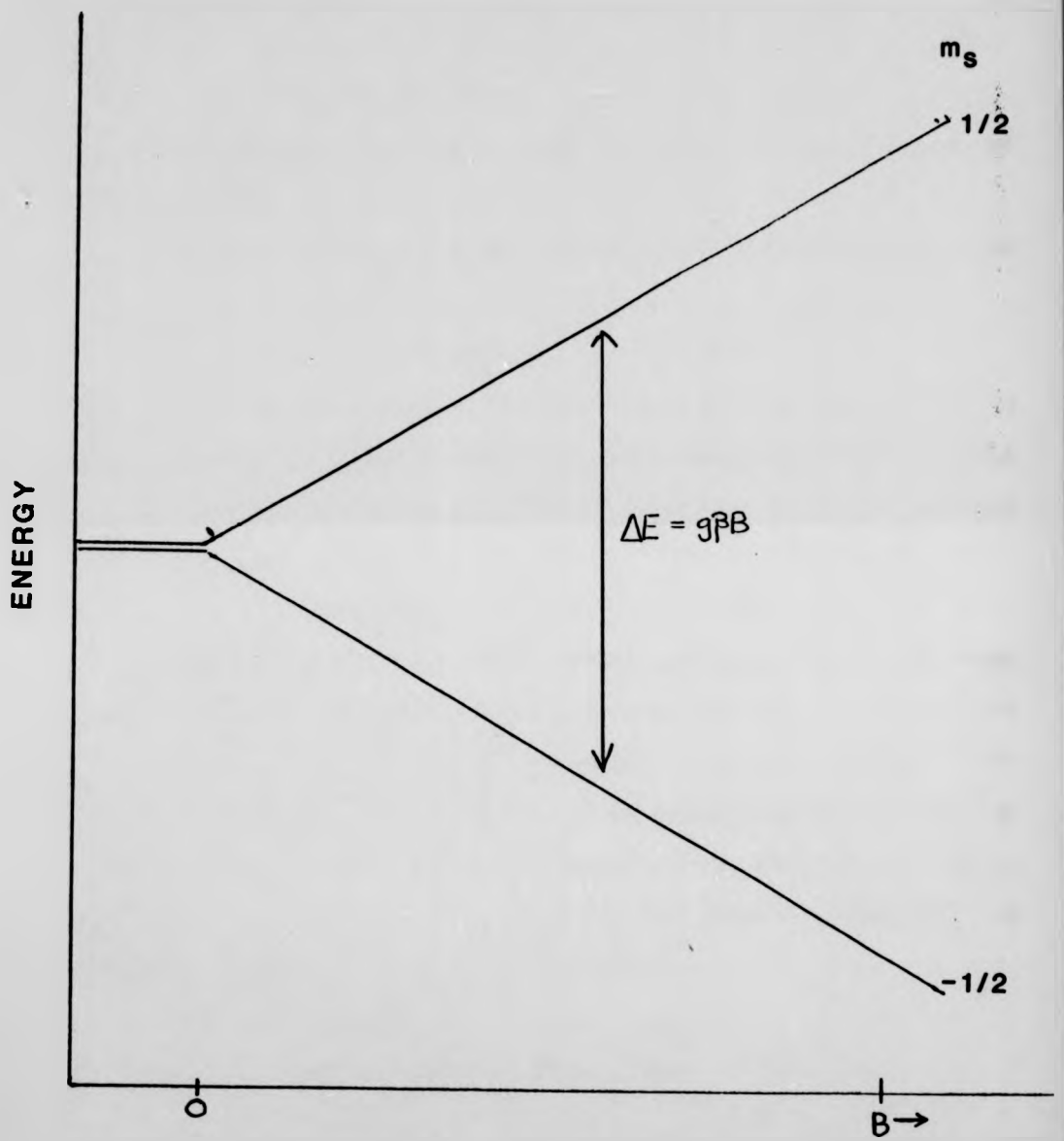


Fig. 2.1 Energy Level diagram representing the Splitting of two Zeeman States ($\Delta E = g\beta_e B$).

$$\hat{H} = -\boldsymbol{\mu}.\mathbf{B}_0 \qquad (2.3)$$

If the only contribution to the total angular momentum comes from the spin then

$$\mathbf{J} = \hbar\mathbf{S}$$

where $\hbar$ is Planck's constant divided by $2\pi$. It has a value of $1.05459 \times 10^{-34}$Js.

Assuming that $B_0$ is in the z-direction and substituting for $\gamma$ and $\boldsymbol{\mu}$

$$\hat{H} = g(e/2m)\hbar B_z S_z \qquad (2.4)$$

where $S_z$ is the z-component of the spin vector S. The term $(e\hbar/2m)$ is usually denoted by $\beta_e$ and is called the "Bohr magneton". It has a value for the electron of $9.2741 \times 10^{-24}Am^{-2}$. Equation (2.4) is therefore usually written as

$$\hat{H} = g\beta_e B_z S_z \qquad (2.5)$$

The vector S has (2S+1) values corresponding to different projections of its orientations along the direction of $B_0$. In the absence of a magnetic field the (2S+1) states have the same energy. This degeneracy is lifted by the application of an external magnetic field. For a single unpaired electron S = 1/2 and there are two possible spin states, characterised by $m_s = \pm\frac{1}{2}$, where $m_s$ is the quantum number for the z-component of the spin angular momentum. Thus

$$\hat{H} = \pm\tfrac{1}{2}g\beta_e B_z$$

The difference in energy between two Zeeman states is therefore

$$\Delta E = g\beta_e B_z \qquad (2.6)$$

An energy level diagram representing two Zeeman states is given in Fig. 2.1. Transitions between the two states can be stimulated by irradiating such a system with radiation of energy equal to $\Delta E$. By Planck's Law, $h\nu$ is the energy of a radiation quantum of frequency $\nu$. The condition for absorption of this quantum is therefore

$$h\nu = g\beta_e B_z \qquad (2.7)$$

Since $\beta_e$ is about three orders of magnitude larger than $\beta_n$ (the "Bohr nuclear magneton"), the resonant frequency for electrons is expected to be about $10^3$ larger than for protons. In practice ESR experiments are usually carried out at about $10^{10}$Hz and magnetic fields of 0.33 - 1.30 Tesla (1 Tesla = $10^4$G). Frequencies for nuclear magnetic resonence experiments are typically in the 100MHz range. This work is concerned with electron spin resonance. However, magnetic nuclei remain important due to their interactions with the resonant electrons.

The absorption of energy requires an excess of electrons in the lower energy state ($m_s = -\frac{1}{2}$). Boltzmann's law predicts that at thermal equilibrium such an excess will exist, thus enabling transitions to take place. Since the probability of stimulating the transition to a higher energy state is equal to the probability of the reverse transition, and since the rate at which the population of each energy level changes is proportional to the population, the two energy levels will eventually become equally populated. When this occurs further absorption of energy is impossible and the system is said to be "saturated". Fortunately, mechanisms exist whereby saturation is prevented from occurring too readily under normal conditions. These mechanisms involve the return of the excited electrons to the ground state via non-radiative processes. In this way the thermal equilibrium population distribution is maintained and absorption will continue. These "spin-lattice relaxation" effects are considered in the next section.

If orbital contributions to the total angular momentum are present the g-value may no longer isotropic and should be treated as a tensor whose elements are

$$\begin{bmatrix} g_{xx} & g_{xy} & g_{xz} \\ g_{yx} & g_{yy} & g_{yz} \\ g_{zx} & g_{zy} & g_{zz} \end{bmatrix}$$

The diagonal elements, $g_{xx}$, $g_{yy}$ and $g_{zz}$ are called the "principal g-values". The **general** form of the Zeeman interaction is therefore

$$\hat{H} = \beta_e \mathbf{B.g.S} \qquad (2.8)$$

In general the g-tensor is symmetric (i.e. $g_{xy} = g_{yx}$) and a matrix transformation to a coordinate system in which g is diagonal is always possible. In the diagonalized coordinate system the spin-Hamiltonian is written as

$$\hat{H} = \beta_e(g_{xx}S_xB_x + g_{yy}S_yB_y + g_{zz}S_zB_z) \qquad (2.9)$$

The general form of the Zeeman interaction is therefore **orientationally dependent** i.e. resonance is a function of the orientation of the spin system relative to the external magnetic field. In liquids, however, the rapid tumbling motions of the spins averages out the g-tensor anisotropy. This results in an isotropic g-value given by $g = (g_{xx} + g_{yy} + g_{zz})/3$.

## 2.2 Relaxation and the Bloch Equations

The Bloch equations describe the behavior of the spin system in terms of its bulk magnetisation (Bloch, 1948). Bloch's original treatment considered a system of nuclear magnetic dipoles but it may equally well be applied to electrons (Pake and Estle, 1973).

If **M** is the bulk magnetisation vector of a system of N non-interacting spins in a magnetic field $B_0$ then the equation of motion of the spins is

$$(d\mathbf{M}/dt) = \gamma \mathbf{M} \times B_0 \qquad (2.10)$$

where $\mathbf{M} = \sum \boldsymbol{\mu}_i$.

This equation may be solved in the usual way to show that M will precess about $B_0$ at an angular frequency $\omega_0 = \gamma B_0$, where $\omega_0$ is the "Larmor frequency".

The steady-state (or thermal equilibrium) magnetisation $M_0$ is given by $M_0 = \chi_0 B_0$, where $\chi_0 = g^2\beta_e^2 NS(S + 1)/3kT$.

The application of a small oscillating magnetic field $B_1$ perpendicular to $B_0$ will perturb the system and the distribution of spins between the Zeeman levels will change to a new value. This will result in a decrease of the net magnetisation from $M_0$ to $M_z$. The energy of the spin system ($E = -\mathbf{M_0}.\mathbf{B_0} = -M_z B_z$) depends upon $M_z$, which can only return to its ground state via processes in which excess spin energy is lost to the "lattice". The lattice represents all the degrees of freedom of the system other than the spin system e.g. the rotational and vibrational motions of the surrounding molecules. These "longitudinal" or "spin-lattice" relaxation effects are assumed to lead to an exponential decay of $M_z$ towards its thermal equilibrium value. This can be represented by

$$(dM_z/dt) = (M_0 - M_z)/T_1 + \gamma(\mathbf{M} \times \mathbf{B})_z \qquad (2.11)$$

where B is the vector sum of the static field $B_0$ and the microwave field $B_1$ and $T_1$ is the spin-lattice relaxation time, which is defined as the time required for the spin system to lose $e^{-1}$ of its excess energy. The first term in equation (2.11) is the relaxation term and the second accounts for the spin-angular momentum of the electron (i.e. the Larmor precession). Spin-lattice relaxation is in direct competition with resonant absorption due to $B_1$. To avoid saturation the relaxation term must be dominant.

At thermal equilibrium and in the absence of $B_1$ the x and y components of the magnetisation vector are equal to zero. When $B_1$ is applied, these components attain non-equilibrium values $M_x$ and $M_y$. These components of the magnetisation do not contribute to the spin-energy and return to their thermal equilibrium values in a "dephasing" time ($T_2$) without coupling to the lattice. $T_2$ is called the "spin-spin" or

"transverse" relaxation time. One cause of spin-spin relaxation is the magnetic dipolar interactions which exist between nearest neighbour spins. Since the magnetic field a distance r from a dipole is approximately $(\mu/r^3)$, the total field experienced by a particular spin is $\mathbf{B}_0 + B_1 + (\sum \mu/r^3)$. The Larmor frequency for this spin is $\omega_0 + \Delta\omega$, where $\Delta\omega$ corresponds to the local field contribution. In general, the local magnetic fields will fluctuate due to random molecular motions and this results in a spread of Larmor frequencies throughout the spin-system. This means an eventual loss of coherence of the precessing spins. If the decay of the x and y components of M is assumed to be exponential, then

$$(dM_x/dt) = \gamma(\mathbf{M} \times \mathbf{B})_x - (M_x/T_2) \qquad (2.12)$$

$$(dM_y/dt) = \gamma(\mathbf{M} \times \mathbf{B})_y - (M_y/T_2) \qquad (2.13)$$

Thus, while $M_z$ relaxes towards its equilibrium value $M_0$ in a time $T_1$, both $M_x$ and $M_y$ decay to zero in a characteristic time $T_2$.

Equations (2.11), (2.12) and (2.13) are the Bloch equations and their solution depends upon the experimental methods employed. Of particular importance is the relationship between the rate of change of $B_0$ and the relaxation times.

A <u>rapid passage</u> of $B_0$ through resonance is one which occurs in a time too short for relaxation to take place. In this case the magnetisation M will precess about $B_1$ several times before the spins have time to relax. Since $\omega = \gamma B_1$ is the period of this precession, rapid passage requires that $\gamma B_1 \gg T_1^{-1}$.

A <u>slow passage</u> through resonance is one in which the spins relax back to their equilibrium values in a time short compared to the precession of M about $B_1$. The condition for slow passage (or steady-state resonance) is $\gamma B_1 \ll T_1^{-1}$.

In ESR resonance is brought about at a fixed microwave frequency by sweeping the static magnetic field $B_0$ trough the appropriate range such that $(dB_0/dt) \ll \gamma B_1$. This method corresponds to the steady-state

condition outlined above.

## 2.3 The Steady-State Solution of the Bloch Equations

The Bloch equations are normally solved by transforming to a coordinate system $\sum(i', j', k')$ which is rotating with the microwave magnetic field at a frequency $\omega$. In the rotating frame the effective magnetic field at the electron, $B_{eff} = B_1 i' + (B_0 - [\omega/\gamma])k'$, is nearly constant (because $B_0$ changes only very slowly) and the solution of the Bloch equations is then independent of time. In this case the components of the magnetisation are given by

$$M_{x'} = M_0 \Gamma \gamma B_1 T_2^2 (\omega_0 - \omega) \qquad (2.14a)$$

$$M_{y'} = M_0 \Gamma \gamma B_1 T_2 \qquad (2.14b)$$

$$M_{z'} = M_0 \Gamma (1 + T_2^2 (\omega_0 - \omega)^2) \qquad (2.14c)$$

where $\Gamma = (1 + T_2^2(\omega_0 - \omega)^2 + \gamma^2 B_1^2 T_1 T_2)^{-1}$.

In the rotating frame (with $B_1$ along x') $M_{x'}$ will be in phase with $B_1$ and $M_{y'}$ will be 90° out of phase. Bloch introduced the idea of a complex susceptibility $\chi = \chi' - j\chi''$, where $\chi' = (M_{x'}/2B_1)$ and $\chi'' = (M_{y'}/2B_1)$. This leads to the following expressions for $\chi''$ and $\chi'$:

$$\chi' = \tfrac{1}{2}\chi_0 \omega_0 \Gamma T_2 (\omega_0 - \omega) \qquad (2.15a)$$

$$\chi'' = \tfrac{1}{2}\chi_0 \omega_0 \Gamma T_2 \qquad (2.15b)$$

where $\chi_0 = (M_0/B_0)$. The phase difference between $\chi'$ and $\chi''$ is $\theta = \tan^{-1}(\chi''/\chi')$. Experimentally one can detect either the dispersive component ($\chi'$) or the absorptive component ($\chi''$). It is usual to set the spectrometer to detect the latter component.

The average power absorbed by a sample is given by

$$P = B_1^2 \Gamma \omega_0 \omega \chi_0 T_2 \qquad (2.16)$$

This expression gives the "saturated lineshape". For an unsaturated system (i.e. $B_1$ is small) $\Gamma$ reduces to $(1 + T_2^2(\omega_0 - \omega)^2)^{-1}$ and the normalised lineshape is then "Lorentzian":

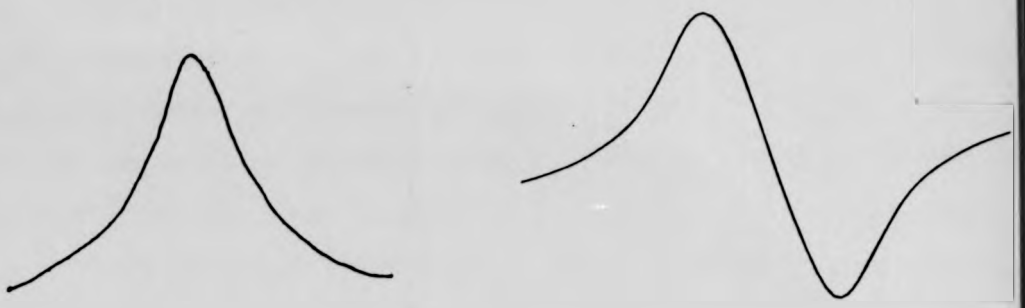

Fig. 2.2 The Lorentzian Lineshape (a) Absorption (b) Derivative.

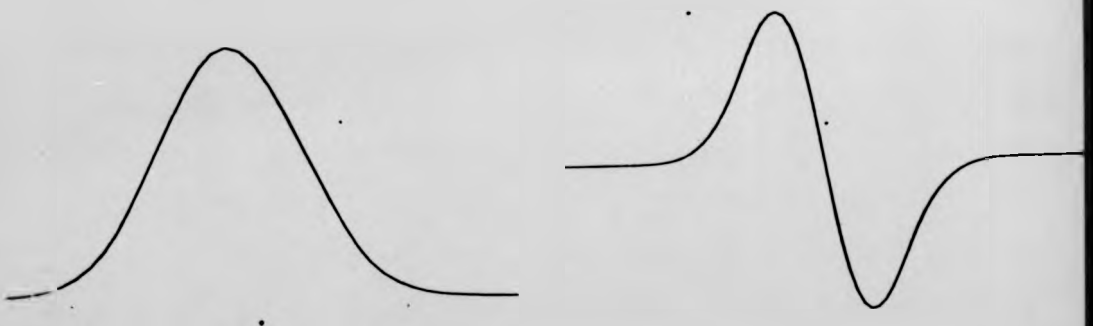

Fig. 2.3 The Gaussian Lineshape (a) Absorption (b) Derivative.

$$g(\omega) = (T_2/\pi[1 + T_2^2(\omega_0 - \omega)^2]) \qquad (2.17)$$

This lineshape is indicated in Fig. 2.2. Lorentzian lineshapes are commonly encountered in liquids where dipolar interactions between neighbouring spins are averaged to zero. In solids or concentrated solutions where dipolar interactions may be present the lineshape is often "Gaussian" (Fig. 2.3). This is given by

$$g(\omega) = T_2(2\pi)^{-\frac{1}{2}}\exp[\tfrac{1}{2}T_2^2(\omega_0 - \omega)^2] \qquad (2.18)$$

It is often the case that an experimental lineshape can be simulated by either one of these functions or by combination of both.

## 2.4 Nuclear Hyperfine Structure

The nuclear hyperfine structure present in the ESR spectrum of a free radical arises through the magnetic interaction between the unpaired electron spin magnetic moment and the nuclear spin magnetic moments. An analysis of the nuclear hyperfine interaction can provide important information on the electron spin density at various sites in the free radical and lead to an identification of the free radical species. Furthermore, in certain systems, such as in nitroxide single crystals, orientational information is present in the hyperfine structure from which it is possible to determine the shape and configuration of the free radical in a particular enviornment. If the free radical is undergoing some form of motion, say an oscillation or rotation, then this information can also often be determined. The general Hamiltonian for the hyperfine interaction is

$$\hat{H} = S.A.I \qquad (2.19)$$

where S and I are the electron and nuclear spin vectors and A is a tensor called the "hyperfine coupling tensor". Equation (2.19) may be split into two terms, the dipolar (or anisotropic) term and the isotropic (or contact) term. Thus,

$$\hat{H} = aS.I + S.A'.I \qquad (2.20)$$

where a is the isotropic coupling constant and A' is the dipolar hyperfine tensor, the terms of which are given by $A_{ij} = -g\beta_e g_n \beta_n \langle (r^2\delta_{ij} - 3x_i x_j) r^{-5} \rangle$. r is the separation of the spins (Nordio, 1976). The principal hyperfine terms are then given by $A_{xx} = A'_{xx} + a$, $A_{yy} = A'_{yy} + a$ and $A_{zz} = A'_{zz} + a$.

The dipolar hyperfine term arises through the interaction of the nuclear spin magnetic moment $\mu_n$ and the magnetic field at the nucleus due to the combined spin and orbital momentum of the unpaired electron. The dipolar term is often written as

$$g\beta_e g_n \beta_n \{(I.S/r^3) - (3/r^5)(I.r)(S.r)\} \qquad (2.21)$$

Because of the orbital motion of the electron this expression must be averaged over the probability distribution $\psi^2(r)$ of the electronic orbital. For a spherically symmetric orbital the dipolar term averages to zero. For p, d, f,... orbitals the electron charge distribution is not spherically symmetric and the dipolar term has a $\langle (1 - 3\cos^2\phi)/r^3 \rangle$ dependence, where $\phi$ is the angle between the direction of the applied field and the vector joining the electron and nucleus.

In liquids, where the free radicals are undergoing rapid twisting and tumbling motions, the angular dependence is averaged to zero and the hyperfine splitting is given by

$$a = (A_{xx} + A_{yy} + A_{zz})/3 \qquad (2.22)$$

In p-orbitals the hyperfine interaction is cylindrically symmetric and, since Trace{A'} = 0, it follows that $A'_{xx} = A'_{yy} = A'_{\perp}$ and $A'_{zz} = A'_{\parallel} = -2A'_{\perp}$. It can also be shown that $A'_{\parallel}$ is positive.

The isotropic hyperfine term arises through the interaction of the electron and nuclear spins at the position of the nucleus. The inteaction depends upon there being a finite unpaired spin density at the nucleus. This condition is satisfied in the case of s-orbital electrons but p, d, f,... orbitals all have a nodal point at the position of the nucleus and for these orbitals the isotropic term is zero. The isotropic

coupling constant is given by

$$a = -(8\pi/3)g\beta_e g_n \beta_n \psi^2(0) \qquad (2.23)$$

where $\psi^2(0)$ is the unpaired spin density at the nucleus (i.e. at r = 0).

The magnitude of the isotropic hyperfine term (and also the isotropic g-value) depends upon the polarity of the spin label's envioronment (Griffiths et al., 1965).

## 2.5 The Spin-Hamiltonian

The results of the previous sections can be combined to give the **spin-Hamiltonian** (e.g. Carrington and McLachan, 1967):

$$\hat{H} = \beta_e \mathbf{B}.\mathbf{g}.\mathbf{S} + \mathbf{S}.\mathbf{A}.\mathbf{I} \qquad (2.24)$$

The magnitudes of the Zeeman and hyperfine terms are $\sim 1 cm^{-1}$ and $10^{-2} - 10^{-3} cm^{-1}$ respectively.

It should be noted that the **nuclear** Zeeman interaction (i.e. $\beta_n \mathbf{B}.\mathbf{g}_n.\mathbf{S}$) and the **nuclear quadrupole** interaction (of the form **I.Q.I**) are missing. It can be shown that these terms make only a small correction to the spin-Hamiltonian.

The work presented in this thesis deals with only one type of paramagnetic species - the **free radical.** Free radicals are molecules which possess at least one unpaired electron. Most free radicals have their unpaired electron in a p-orbital (L = 1) which is three-fold degenerate ($m_L$ = +1, 0, -1). The orbital degeneracy is lifted by a crystalline electric field and the separation in energy between the ground state ($m_L$ = 0) and the excited (degenerate) states is $\sim 10^3 cm^{-1}$. The ground state will be the only one occupied under normal conditions and the unpaired electron will therefore have no orbital angular momentum. That is, it is a property of free radicals that the main contribution to their angular momentum, and therefore their g-values, comes from the electron spin. Free radical g-values should therefore be about equal to the free electron

g-value, $g_e = 2.002322$. Deviations from $g_e$ indicate the effects of orbital contributions to the total angular mometum.

Two species of free radical will be met in this work: stable **nitroxide** free radicals (Chapters 4 and 6) and **organic** free radicals (Chapter 5). The spin-Hamiltonian (Eq. 2.24) will be used to analyse the ESR spectra which result when these molecules are present in solutions or fibres containing DNA.

If the principal g- and A-tensor axes coincide, which will be assumed to be the case in the present work, the solution to Eq. 2.24 proceeds as follows.

In the molecular coordinate system $\sum(x, y, z)$ the g- and A-tensors are diagonal. The spin-Hamiltonian is invariant to an orthogonal transformation and in the laboratory coordinate system $\sum(X, Y, Z)$

$$\mathcal{H} = \beta_e \mathbf{B}'.\mathbf{g}'.\mathbf{S}' + \mathbf{S}'.\mathbf{A}'.\mathbf{I}' \qquad (2.25)$$

where $\mathbf{g}' = \mathbf{L}^{\tau}.\mathbf{g}.\mathbf{L}$ and $\mathbf{A}' = \mathbf{L}^{\tau}.\mathbf{A}.\mathbf{L}$ are the g- and A-tensors expressed in the laboratory system and $\mathbf{L}$ is the transformation matrix which rotates $\sum(x, y, z)$ into $\sum(X, Y, Z)$. (Libertini and Griffiths, 1970). In matrix form the g-tensor term transforms as:

$$\begin{bmatrix} g_{XX} & g_{XY} & g_{XZ} \\ g_{YX} & g_{YY} & g_{YZ} \\ g_{ZX} & g_{ZY} & g_{ZZ} \end{bmatrix} = \begin{bmatrix} l_{Xx} & l_{Xy} & l_{Xz} \\ m_{Yx} & m_{Yy} & m_{Yz} \\ n_{Zx} & m_{Zy} & m_{Zz} \end{bmatrix} \begin{bmatrix} A_{xx} & 0 & 0 \\ 0 & A_{yy} & 0 \\ 0 & 0 & A_{zz} \end{bmatrix} \begin{bmatrix} l_{Xx} & m_{Yx} & n_{Zx} \\ l_{Xy} & m_{Yy} & n_{Zy} \\ l_{Xz} & m_{Zy} & n_{Zz} \end{bmatrix}$$

where $l_{Xx}$, $m_{Xx}$,..etc, are the direction cosines relating the two coordinate systems. A similar term can be written for the A-tensor in the laboratory system.

If the laboratory magnetic field is directed along the Z-axis and the off diagonal terms in $S_X$ and $S_Y$ are neglected then Eq. (2.25) reduces to

$$\hat{H} = \beta_e g_{ZZ} B_Z S_Z + S_Z A_{ZZ} I_Z + S_Z A_{XZ} I_X + S_Z A_{YZ} I_Y \quad (2.26)$$

where,

$$A_{ZZ} = A_{zz} l_{Zx}^2 + A_{yy} m_{Zy}^2 + A_{zz} n_{Zz}^2$$

$$A_{XZ} = A_{xx} l_{Xx} l_{Zx} + A_{yy} m_{Xy} m_{Zy} + A_{zz} n_{Xz} n_{Zz}$$

$$A_{YZ} = A_{xx} l_{Yx} l_{Zx} + A_{yy} m_{Yy} m_{Zy} + A_{zz} n_{Yz} n_{Zz}$$

$$g_{ZZ} = g_{xx} l_{Zx}^2 + g_{yy} m_{Zy}^2 + g_{zz} n_{Zz}^2$$

Libertini and Griffiths (1970) have shown that Eq. (2.26) adequately accounts for the anisotropy of the g- and A-tensors in nitroxide free radicals. The matrix elements, eigenfunctions and eigenvalues of the Hamiltonian may be evaluated from the basis set of spin functions $|m_S m_I\rangle$.

The form of the spin-Hamiltonian (Eq. 2.26) corresponds to the so called "intermediate field treatment". In this treatment, the external magnetic field is not strong enough to decouple the electron and nuclear spins. The electron spins are therefore quantised along the direction of the external field while the nuclear spins are quantised along the direction of the "effective" magnetic field, that is, the magnetic field at the nucleus ue to the vector sum of the external field and the field set up by the unpaired electron. In this case it can be shown that

$$g' = g_{ZZ} = (g_{xx} l_{Zx}^2 + g_{yy} m_{Zy}^2 + g_{zz} n_{Zz}^2) \quad (2.27)$$

and

$$A' = (A_{XZ}^2 + A_{YZ}^2 + A_{ZZ}^2)^{1/2}$$

or

$$A' = (A_{xx}^2 l_{Zx}^2 + A_{yy}^2 m_{Zy}^2 + A_{zz}^2 n_{Zz}^2)^{1/2} \quad (2.28)$$

In the "high field treatment" the external magnetic field is assumed to decouple the spin vectors I and S which then precess independently about the direction of the applied field. In this case the terms involving $I_X$ and $I_Y$ in Eq. (2.26) can be neglected and

$$A' = A_{ZZ} = (A_{xx}l_{Zx}^2 + A_{yy}m_{Zy}^2 + A_{zz}n_{Zz}^2) \qquad (2.29)$$

The expression for g' is the same as in the intermediate field treatment. As mentioned above, in single crystal studies or in other orientated systems, the intermediate field treatment is usually preferred. In systems where there is only a limited g- or A-value anisotropy involved (e.g. organic radicals in solution) the high field approximation is also satisfactory.

## 2.6 Free Radical Solution Spectra

The ESR spectra of nitroxide and organic free radicals in liquids can be described by a spin-Hamiltonian which has isotropic g- and A-values, i.e.

$$\hat{H} = \beta_e g B_z S_z + a I_z S_z \qquad (2.30)$$

In this expression the laboratory field is along the Z-axis and $S_z$ has two spin components $m_s = \pm\frac{1}{2}$. For an $^{14}N$ nucleus (e.g. a nitroxide) I = 1 and $m_I$ = +1, 0 -1. The Zeeman interaction gives rise to two energy levels ($+\frac{1}{2}\beta_e g B_z$ and $-\frac{1}{2}\beta_e g B_z$) and the hyperfine interaction results in six further energy levels, three associated with each Zeeman levels: $|\frac{1}{2}\ 1\rangle$, $|\frac{1}{2}\ 0\rangle$, $|\frac{1}{2}\ -1\rangle$, $|-\frac{1}{2}\ 1\rangle$, $|-\frac{1}{2}\ 0\rangle$ and $|-\frac{1}{2}\ -1\rangle$. The energy levels for the six states are

$$E_1 = \tfrac{1}{2}\beta_e g B_z + \tfrac{1}{2}a \qquad E_4 = -\tfrac{1}{2}\beta_e g B_z + \tfrac{1}{2}a$$

$$E_2 = \tfrac{1}{2}\beta_e g B_z \qquad E_5 = -\tfrac{1}{2}\beta_e g B_z$$

$$E_3 = \tfrac{1}{2}\beta_e g B_z - \tfrac{1}{2}a \qquad E_6 = -\tfrac{1}{2}\beta_e g B_z - \tfrac{1}{2}a$$

The selection rules for transitions between these levels are $\Delta m_s = \pm 1$, $\Delta m_I = 0$. The transitions are induced by an oscillating microwave field applied perpendicular to the laboratory Z-axis. The three allowed transitions are shown in Fig. 2.4 (assuming a positive value for a).

When more than one magnetic nucleus interacts with the unpaired electron the spin-Hamiltonian will include a term $\sum a_n S_z I_{zn}$ where $a_n$ is the coupling constant associated with the $n^{th}$ nucleus of nuclear spin $I_{zn}$. The

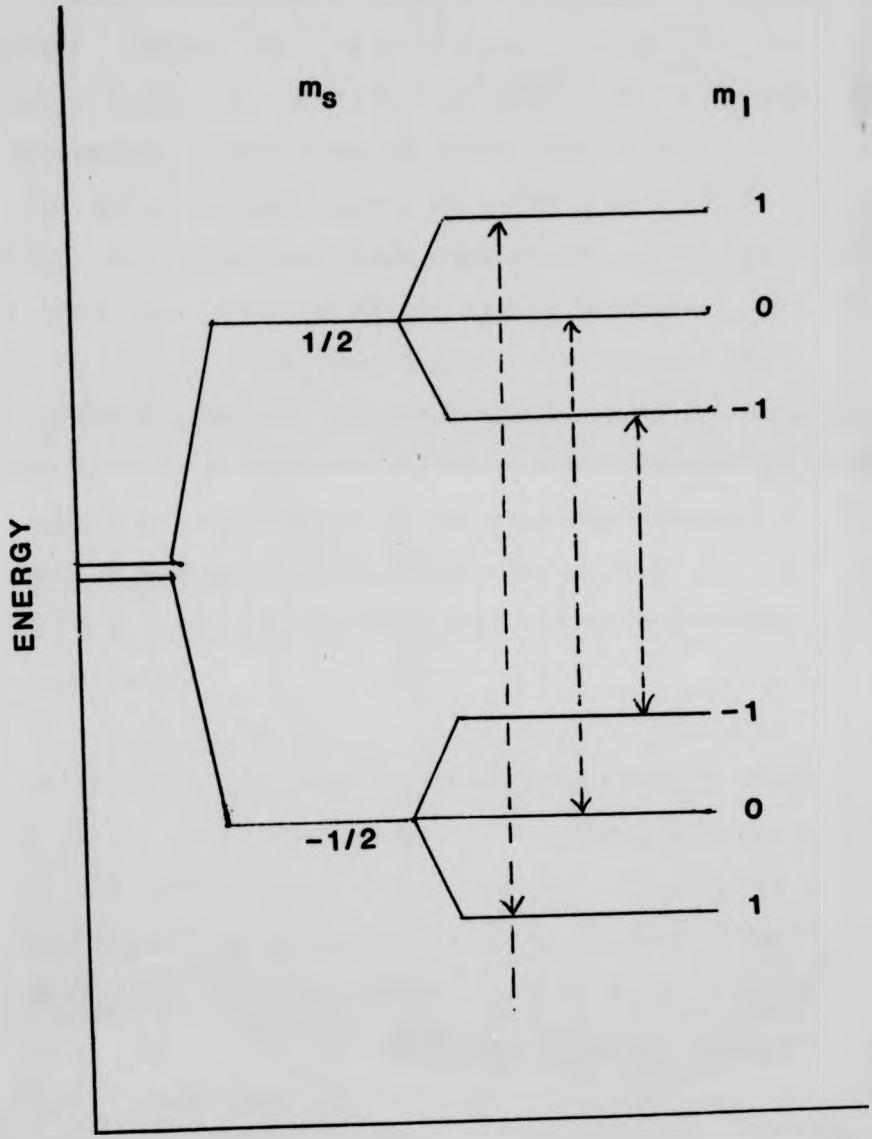


Fig. 2.4 The three allowed ESR transitions for a spin system with $S = \frac{1}{2}$ and $I = 1$.

above treatment can then be extended to account for a variety of spin systems, including n equivalent nuclei (giving rise to n + 1 hyperfine lines), n non-equivalent protons (giving $2^n$ hyperfine lines) and n non-equivalent nuclei of spins $I_{i,j,k...}$, giving rise to $(2I_i + 1)(2I_j + 1)(2I_k + 1)$...possible hyperfine lines. Simulated ESR spectra corresponding to these cases are shown in Fig. 2.5.

The above treatment ignores the terms in the spin-Hamiltonian involving $I_xS_x$, etc. When these **second order** effects are accounted for the hyperfine lines are found to be shifted slightly in frequency, but their separation is altered by only about 1 part in $10^5$ (Ayscough, 1967). For practical purposes, therefore, the first order treatment is acceptable. Incidentally, it might be noted that the second order treatment does enable certain transitions "forbidden" under the first order treatment to take place, namely those obeying the selection rules $\Delta m_S = \pm 1$, $\Delta m_I = \pm 1$. For these transitions to occur the microwave field must be directed parallel to the laboratory field.

In aromatic free radicals the unpaired electron occupies a $2p\pi$-orbital which has zero spin density at the nucleus, which is usually $^{14}N$ or $^{13}C$. Furthermore, the $2p\pi$-orbital also has a node in the plane of the aromatic molecule and the electron spin density should therefore be zero at all points in the plane. Contrary to these expectations, however, free radicals often exhibit ESR spectra possessing very rich hyperfine patterns due to the interaction of the unpaired electron with the ring protons. The existence of these splittings arises through a "delocalisation" of the unpaired spin density. The problem is how the electron spin finds its way into the 1s-orbitals of the ring protons.

One mechanism, called "polarisation", arises in the following way (Carrington and McLachan, 1967; Ayscough, 1967). In a C· - H "fragment" (found in both aromatic and aliphatic radicals) the C - H

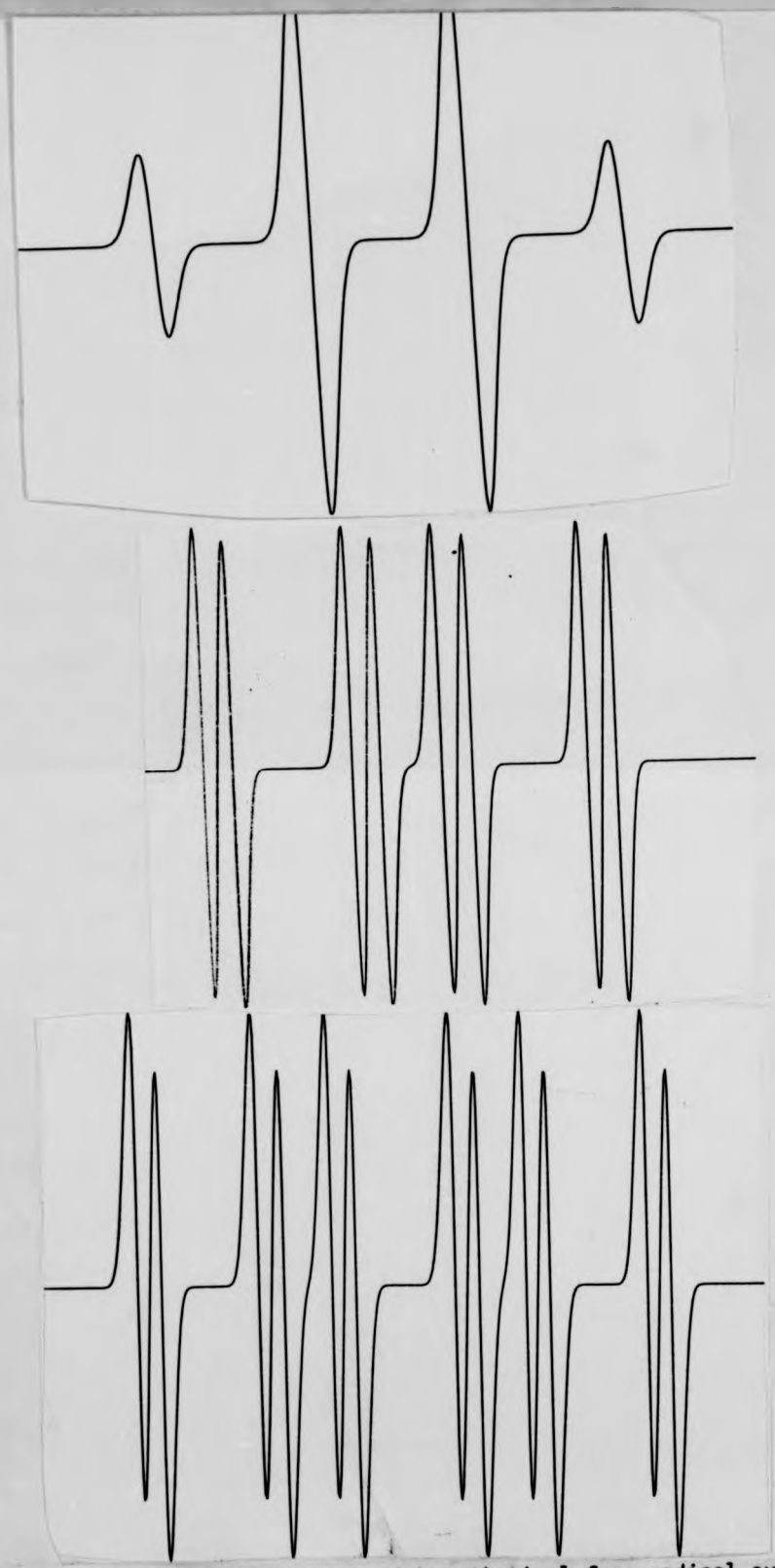

Fig. 2.5(a-c) Computer Simulations of hypothetical free radical systems with S = 1/2 consisting of:
(a) 3 equivalent protons ($a_1 = a_2 = a_3 = 0.25$mT)
(b) 3 non-equivalent protons ($a_1 = 0.8$mT; $a_2 = 0.5$mT; $a_3 = 0.1$mT).
(c) 3 nuclei with spins 1, 1/2, 1/2; ($a_1 = 0.8$mT; $a_2 = 0.5$mT; $a_3 = 0.1$mT)
In each of these simulations a Gaussian lineshape was used with a linewidth of 0.06mT.

σ-orbital electrons couple, via an exchange interaction, with the carbon 2pπ-orbital. This coupling results in a **polarisation** of the σ-orbital electrons through which the unpaired 2pπ electron spin induces a spin of opposite polarisation at the proton (Fig. 2.6a). The spin density at the proton ($\rho_H$) and the proton coupling constant are related by

$$a_H = -22.5\rho_H \qquad (2.31)$$

This expression is known as "McConnell's Relationship" and its importance lies in the fact that once the proton coupling constants are known (e.g. by simulation) the spin density over the protons at different sites in the ring system can be mapped out.

The mechanism of **hyperconjugation** may also lead to the existence of hyperfine coupling constants in aromatic radicals. This mechanism has been suggested as the cause of the "β-proton" coupling found in fragments such as $-HC^{\bullet}-CH_3$. The β-proton (i.e. methyl) couplings are often larger than the α-proton couplings. In crude terms the mechanism involves an overlap of the methyl proton 1s-orbitals with the 2pπ-orbital containing the unpaired electron. This situation is depicted in Fig. 2.6b. In the liquid state the methyl group will be freely rotating and the interaction will involve the 2pπ-orbital and three equivalent protons. In solids the couplings may be unequal. The mechanisms of hyperconjugation and spin polarisation have been presented by many authors (e.g. Carrington and McLachan, 1967; Atherton, 1973; Ayscough, 1967).

Because of the rapid motions of the free radicals in the liquid state no information can be obtained concerning the anisotropy of the electron-nuclear spin interaction. However, the isotropic interactions of the unpaired electron can usually be analysed and the various coupling constants determined. The detail observed in the hyperfine pattern depends upon several factors, one of which is the free radical concentration. Generally speaking concentrations in excess of about 1mM can lead to line broadening (Section 2.8). Since solution linewidths are of the order of

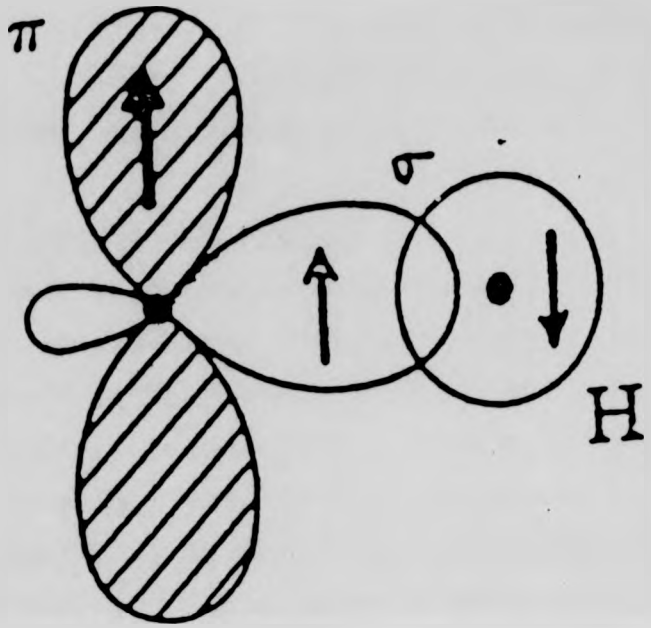


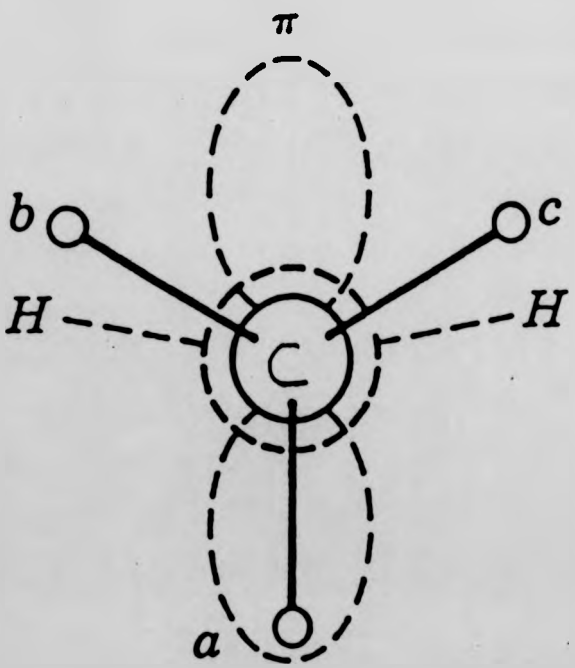


Fig. 2.6(a,b) (a) Spin-Polarisation mechanism for -C-H fragment.
(b) Hyperconjugation mechanism showing end-on view of a $HC-CH_3$ fragment (a, b and c are the methyl protons).

0.01 - 0.1 milli-Tesla (mT), the degree of broadening need not be too severe before the hyperfine structure becomes obscured. For this reason solution spectra are normally recorded at low concentrations.

## 2.7 ESR Spectra of Free Radicals in Solids

In **single crystal** samples all the free radical molecules have their molecular axes orientated in the same direction relative to the external magnetic field. By recording the ESR spectra of such samples at different orientations the principal g- and A-tensor values can be determined. The g- and A-tensor axes often coincide with the molecular axes and in the $^{14}N$ atom the principal $g_{zz}$ and $A_{zz}$ values are directly related to the direction of the $2p\pi$-orbital of the unpaired electron. The extent of the hyperfine splitting is correlated with the interaction between the electron and nuclear spins. This interaction is a maximum when the $2p\pi$-orbital z-axis is orientated parallel to the magnetic field and a minimum when orientated perpendicular to the field. $A_{zz}$ is therefore the largest hyperfine splitting and either $A_{xx}$ or $A_{yy}$ is the smallest. In many cases $A_{xx} \sim A_{yy}$. The three principal splittings are indicated in Fig. 2.7 for $A_{zz}$ = 3.2mT and $A_{yy} = A_{xx}$ =0.5mT. The principal g-values are located at the centres of these spectra. Intermediate values of g and A can be calculated from Eqs. 2.27 and 2.28. In spherical coordinates the direction cosines $l_{Zx}$, $m_{Zy}$ and $n_{Zz}$ of Eqs. 2.27, etc, are given by $Sin\theta Cos\psi$, $Sin\theta Sin\psi$ and $Cos\theta$ respectively, where $\theta$ and $\psi$ are the coordinates of the magnetic field relative to a right-handed molecular coordinate system. The ESR spectrum for any orientation of the crystal is obtained by application of Eq. 2.25.

If the ESR spectra calculated for possible orientations of the crystal are superimposed then a **powder** or **gel** spectrum is obtained. In a powder spectrum only the largest hyperfine splitting is normally resolved. The other principal values are usually obscured by an overlap of

absorptions in the centre of the spectrum. A typical nitroxide powder spectrum is shown in Fig. 2.8b. In nitroxides, as in many other free radicals, the g-values are slightly anisotropic, with $g_{zz}$ being smaller than $g_{xx}$ or $g_{yy}$, and the principal A-values are approximately axially symmetric, with $A_{xx} \sim A_{yy} < A_{zz}$. $A_{zz}$ may be estimated from the powder spectrum as shown in Fig. 2.28b.

In ESR experiments, any changes in the orientations of the free radicals which occur in a time longer than about $10^{-8}$ seconds will not be detected and the powder spectrum described above will be observed. The free radicals are therefore said to be immobilised if their **rotational correlation time**, $\tau_c$, is greater than or equal to $10^{-8}$ sec.

However, if $\tau_c < 10^{-8}$ sec, the changes of orientation will have an appreciable effect on the ESR spectrum due to an "averaging" of the hyperfine coupling constants. The magnitude of the averaging depends upon the type and rate of motion involved. If the motion consists of a simple, rapid (i.e. $\tau_c < 10^{-9}$ sec.) rotation about a principal axis (e.g. the x-axis) of a nitroxide the resulting "motion averaged" spectrum will look like Fig. 2.28a. In general, however, the analysis of a system which is undergoing some form of molecular motion can be very difficult.

Powder samples will often be encountered in this work (Chapters 4, 5 and 6). Partially oriented samples will also be examined. These samples, in the form of cylindrically symmetric fibres, are analysed using a computer programme described in Chapter 4.

Although the magnitudes of the principal hyperfine terms may be obtained either directly from single crystal studies or by computer simulation, the **signs** of these terms will be undetermined. To obtain the signs of $A_{xx}$, $A_{yy}$ and $A_{zz}$, the signs of the dipolar and isotropic terms are required. The sign of a can often be found from solution studies while the dipolar terms may be deduced from theoretical considerations (Atherton, 1973).

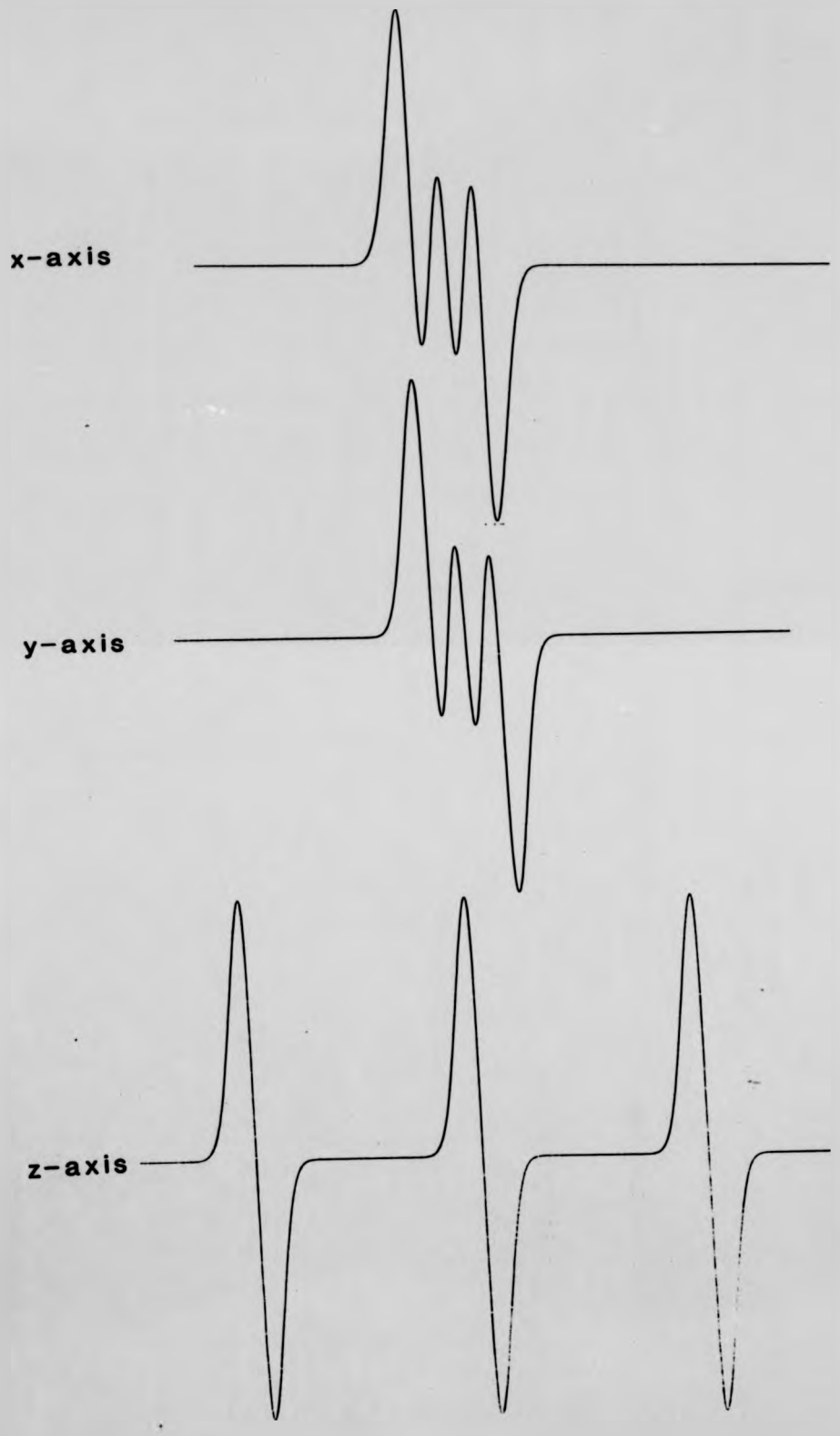


Fig. 2.7 Hyperfine Splittings for a single Nitroxide Crystal orientated along the principal x, y and z axes.

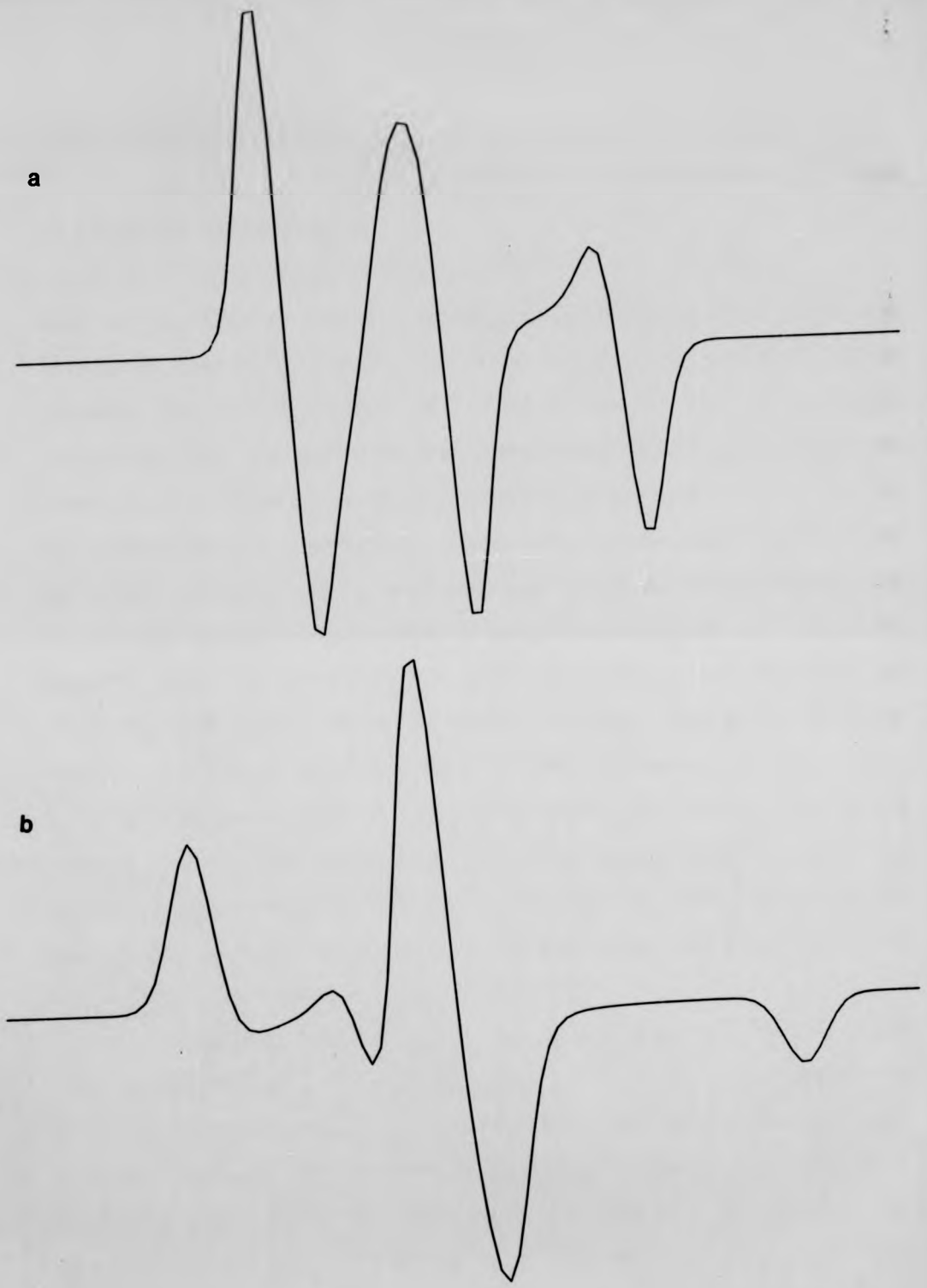


Fig. 2.8(a,b) ESR Powder Spectra for (a) a system undergoing a rapid rotation about the principal x-axis and (b) an immobilised spin-label.

## 2.8 The Linewidths of ESR Spectra

From the Bloch equations (Section 2.2) the normal ESR lineshape is Lorentzian and is given by

$$g(\omega) = (T_2/\pi[1 + T_2^2(\omega_0 - \omega)^2]) \qquad (2.17)$$

When $\omega = \omega_0$ (i.e. at resonance) $g(\omega)_{max} = 2T_2$ and the half-height of the absorption peak is $T_2^{-1} = (\omega_0 - \omega) = \Delta\omega_{1/2}$. That is, the half-width of the resonant line at half-height is a direct measure of the spin-spin relaxation time (it is assumed that **instrumental broadening** effects are absent). It follows that the more efficient the relaxation, the broader the absorption (or derivative) line. The processes which affect the spin-spin relaxation of a given unpaired electron arise through the fluctuating magnetic fields due to the molecular motions of the other magnetic electrons in the sample. $T_2$ therefore depends upon the extent to which the unpaired electron is exposed to these fluctuating magnetic fields. In solids, where the motions of the paramagnets are slow (i.e. $t_c >> 10^{-8}$sec) the unpaired electrons will spend a considerable time in the presence of the fluctuating fields and the spin-spin relaxation will be short. Line broadening will occur. In liquids, where the rapid molecular motions will mean an averaging of the fluctuating magnetic fields, $T_2$ will be long and narrow linewidths will be observed.

Linewidths may be broadened by **spin-lattice** relaxation via the Uncertainty Principle ($\Delta\nu \sim 1/T_1$). If $T_1$ is very short, as it may be in many transition metal ions, the linewidths may to broad to be observed. For free radicals in solids $T_1 >> T_2$ and the effects of spin-lattice relaxation can usually be neglected. In liquids, $T_1 \sim T_2$ and the spin-lattice relaxation could lead to a "lifetime broadening" of the ESR lines.

The major sources of relaxation and line broadening in solids are **exchange interactions** and **spin-spin dipolar interactions.** In liquids, exchange effects are negligible provided the free radical concentration is

kept low. The main contribution to line broadening in liquids is the process of **motional modulation.**

(a) Exchange Broadening

Exchange interactions occur when an overlap of nearest-neighbour spin-orbitals results in an exchange of spin orientations. For this effect to occur the interacting spins must be < 10A apart. If the free radicals approach to within Van der Waal's radii of each other the exchange is **strong** (i.e. stronger than the spin-spin dipolar interaction and the electron-nuclear hyperfine interaction). The exchange interaction is written as

$$JS_1.S_2 \qquad (2.32)$$

The width of the exchange broadened line is given by

$$\Delta\omega = (1/T_2) = (\omega_d^2/\omega_e) \qquad (2.33)$$

where $\omega_d$ is the dipolar interaction in frequency units (see below).

If the exchange is **slow** (i.e. $\omega_e << \omega_d$) the hyperfine structure is resolved but a lifetime broadening of the lines occurs. If the exchange is **fast** (i.e. $\omega_e >> a$ in frequency units) the hyperfine structure collapses and only a single narrow line is observed. At intermediate frequencies the hyperfine lines are shifted towards towards the centre of the resonant absorption.

(b) **The Dipolar Interaction**

If the separation of two adjacent spins is greater than about 10A the electron-electron dipolar interaction will be stronger than the exchange interaction. The dipolar interaction, which has the same form as the electron-nuclear dipolar coupling, is usually the most important source of line broadening and relaxation in solids. The lineshape of a dipolar broadened spectrum is Gaussian. Van Vleck (1948) showed that a polycrystalline sample containing n spins gives a dipolar broadened

linewidth of

$$\langle B_d^2 \rangle = (3/5)g^2\beta^2(1/n)S(S+1)\sum(1/r_{ij}) \qquad (2.34)$$

where $B_d$ is the linewidth and $r_{ij}$ is the distance between two nearest neighbour spins (i,j). In angular frequency units $B_d$ is replaced by $(h\omega_d/2\pi g\beta)$. If other, non-resonant spins are present in the sample these will also contribute to the dipolar broadening but the effect is reduced by a factor of 4/9.

(c) **Motional Modulation**

When a paramagnetic radical is present in a liquid medium the relaxation times and linewidths are affected by the Brownian motion of the solvent and solute molecules. The radicals move in a random fashion and adopt all orientations relative to the external magnetic field. Depending on the timescale of these random motions the anisotropy of the g- and A-tensors will be averaged away and the normal line broadening present in solids will be reduced. A measure of the motional time scale is really a measure of the frequencies of the random fluctuations compare with the frequencies of the interaction energies of the system (Ayscough, 1967; Carrington and McLachan, 1967). When the frequency of motion (or rate of tumbling) is greater than the maximum hyoperfine splitting in frequency units, the anisotropic terms in the spin-Hamiltonian are averaged and only the isotropic g- and A-values are observed. The linewidths are then said to be "motionally narrowed". The condition for motional narrowing is therefore $\tau_c << (A_{zz} - A_{xx})^{-1}$, assuming that $A_{zz}$ is the largest hyperfine term, or $\tau_c << h[(g_{xx} - g_{zz})\beta B]^{-1} \sim 10^{-8}$sec.

However, the rapid molecular tumbling makes the anisotropic terms a random function of time and this leads to a motional modulation of the anisotropic g- and A-values and therefore to a modulation of the energy levels and transition frequencies. This in turn leads to a broadening of the absorption lines (Nordio, 1976).

For the interaction of an unpaired electron with a single nucleus of spin I = 1 the linewidths can be shown to depend upon the nuclear spin quantum number as follows:

$$T_2^{-2} = A + Bm_I + Cm_I^2 \qquad (2.35)$$

Since A contains linewidth contributions which are not spin-dependent it is useful to write Eq. (2.35) as

$$T_2(0)/T_2(M) = 1 - BM - CM^2 \qquad (2.36)$$

where M = ±1 and

$$B = -(4\tau_c/15\hat{n})\beta_e[g_{zz} - \tfrac{1}{2}(g_{xx} + g_{yy})]bB_oT_2(0)$$

$$C = (\tau_c/8)b^2T_2(0)$$

and $b = (4\pi/3)(A_\parallel - A_\perp)$ where $A_\parallel$ and $A_\perp$ are in MHz units. $B_o$ is the central resonant field and $T_2^{-1}(M)$ and $T_2^{-1}(0)$ are the widths of the $m_I = \pm 1$ and $m_I = 0$ hyperfine lines. Eq. 2.36 is often used to calculate the correlation time $\tau_c$.

Exchange effects may also contribute to line broadening in liquids but only at high free radical concentrations. The linewidths of free radicals in solution may also be affected by structural or conformational transitions ring inversions and Cis-Trans isomer exchange. All of these processes are capable of causing a modulation of the isotropic hyperfine interaction at all or only a small group of magnetic nuclei. This type of motional modulation can lead to an alternating linewidth effect (Freed and Frankel, 1963; Anderson,1959).

## 2.9 Experimental Technique

To produce ESR signals basically all that is required is a static magnetic field B to cause the Zeeman splittings and a microwave frequency field, applied perpendicular to B, to cause transitions between the Zeeman levels.

For practical reasons resonance is obtained by sweeping the magnetic field rather than the microwave frequency. The magnetic field is

therefore supplied by an electromagnet which is controlled by an external sweep unit. Microwave radiation is supplied by a Klystron at a fixed frequency, either 9.5-GHz (X-band) or 35-GHz (Q-band). The power output from the Klystron is maintained by a stabilised power supply. The paramagnetic sample is placed between the poles of the magnet in a specially designed brass cavity which is coated with a conducting layer of gold or silver. The sample is placed so that it sits at the maximum of the magnetic component of the microwave field in the cavity. The performance of a cavity is given in terms of its "Q-factor". The "unloaded" Q-factor is given by

$$Q = \omega(\text{Energy stored in Cavity/Energy Dissipated}) \qquad (2.37)$$

Resonant cavities are designed to have very high unloaded Q values ($\sim 10^4$). It can be shown that the change of Q at resonance is

$$\Delta Q = 4\pi\chi'' Q_0^2 \xi \qquad (2.38)$$

where $\xi$ is the "filling factor", which is a measure of the fraction of microwave energy that is absorbed by the sample. $\Delta Q$ is observed as a change in the power reflected (or transmitted) from the cavity to the electronic detection system. The spectrometer system used in this work is described below.

The microwave power from the Klystron enters the waveguide via an isolator and attenuator. The isolator prevents microwave reflections passing back into the Klystron. The attenuator is used to control the power incident on the cavity. A fraction of microwave power is extracted from the waveguide via a **directional coupler** to the **bucking arm.** The bucking arm consists of an attenuator and phase shifter and by manipulating these controls the magnitude and phase of the microwaves can be varied to match those of the power reflected from the cavity. The output from the bucking arm is directed to the crystal detectors and is used to bias them at their optimum working power. In this way the power at the cavity may be varied without altering the crystal bias. When correctly biased the

crystals are very sensitive to the power absorbed in the cavity and resonance will be strongly detected.

Power is directed onto the sample in the cavity from the waveguide run via a **circulator.** In order to obtain resonance the cavity must be of a certain size and shape. A resonant mode is set up only if the length of the cavity is equal to a whole or half number of complete wavelengths. In the present work the X-band experiments were carried out using a Varian V-453 rectangular cavity whose dimensions could be slightly altered to achieve correct tuning (the cylindrical Q-band cavity had fixed dimensions). However, tuning is normally carried out by adjusting the Klystron until the power reflected to the crystals is a minimum. The power coupled to the cavity is finely adjusted by the use of a small iris-opening in the cavity wall. The microwave frequency is stabilised by an "automatic frequency control" (AFC), which uses a feed back loop to lock the Klystron frequency to that of the resonant cavity.

The sensitivity of the detection system is greatly improved by the use of phase sensitive detection (PSD). Two coils, one mounted each side of the cavity, are used to provide a 100-kHz modulation of the magnetic field as it is swept through resonance. This produces an AC signal at the crystal detectors which is easier to amplify than the DC signal which would be detected in the absence of any modulation. The amplitude of the 100-kHz modulation is kept smaller than the ESR linewidths otherwise "modulation broadening" of the ESR absorption occurs. In the PSD system a 100-kHz signal is compared with the 100-kHz modulated signal from the crystals. After the modulation frequency is filtered out the remaining signal is the first derivative of the ESR absorption. For a more detailed discussion of the experimental methods employed in ESR see Poole (1967).

# CHAPTER 3

# METHODS and MATERIALS

## 3.1 Materials

### 3.1.1 DNA Purification

Three types of commercially available natural DNA were used in this work: Calf Thymus (42% GC), Clostridium Perfringens (28% GC) and Micrococcus Lysodeikticus (70% GC). These materials were purchased from Sigma Chemicals Ltd. They were chosen because they covered a wide range of GC content. Synthetic polynucleotides, containing only GC (or AT) bases, were available but only at a much higher cost. For this reason only a few experiments were performed using synthetic polynucleotides (see Chapter 4). DNA from the bacteriophage ϕW-14, which is not commercially available, was obtained from Prof. R. A. J. Warren of the Department of Microbiology, University of British Columbia, Vancouver, Canada.

All DNA's, with the exception of ϕW-14, were purified before use in order to remove excess proteins and inorganic salts. Phenol has been reported as an effective reagent in the removal of protein from DNA samples (Massie and Zimm, 1965) and, in spite of the claims of Leng et al. (1973) that phenol can denature DNA, several workers have successfully included a phenol extraction stage in the purification of commercial DNA (e.g. Goodwin, 1977).

DNA solutions were initially prepared by dissolving 1-2mg of DNA in 2mM NaCl. This salt concentration is high enough to prevent denaturation but low enough to enable the DNA to dissolve rapidly. The samples were allowed to stand for several days at 4°C and the salt concentration was then brought up to 0.1M.

Anular grade phenol was distilled before use to remove oxidation products. The distillate was collected in 0.1M NaCl and after stirring

rapidly for 10 minutes the phenol/salt mixture was allowed to stand. The phenolic (lower) layer was collected and added to an equivalent volume of the DNA solution. The mixture was shaken for 15 minutes and the centrifuged for 15-minutes at 3,000 rpm. The aqueous (upper) layer was removed using a Pasteur pipette and centrifuged for a second time. The aqueous layer was again removed and the DNA was precipitated by the addition of two and a half volumes of cold propanol, producing a yield of ~80%. The precipitated DNA was collected on a glass rod and washed in 80% ethanol for 30 minutes (to remove excess salt), 95% ethanol for 15 minutes (to remove excess water) and acetone for 15 minutes (to remove the ethanol). The DNA was then dried over phosphorus pentoxide for several hours and finally stored at 4°C until required.

Solutions were made up at concentrations of 1-8mM DNA in either 1mM NaCl/pH = 6.5 or 100mM NaCl/pH = 6.5. After allowing several days for the DNA to dissolve fully the concentration of DNA in a solution was determined by measuring its absorbance at the wavelength of maximum absorptivity. The maximum absorptivity was taken to be the same for each DNA i.e. $E_\lambda = 6600 M^{-1} cm^{-1}$, where $E_\lambda$ is the maximum absorptivity at wavelength $\lambda$. For Calf Thymus $\lambda = 258nm$; for Clostridium Perfringens $\lambda = 256nm$ and for Micrococcus Lysodeiktus $\lambda = 255nm$.

### 3.1.2 The Drugs and Spin-Labels

Proflavine Hemisulphate was obtained from the BDH Chemical Company Ltd and the phenothiazine derivatives were purchased from Squibb and Son Ltd. All the compounds were in powder form and were stored in a dessicator at 4°C. The spin-labels, 2,2,5,5-tetramethylpyrroline-1-oxyl and "Spin Imidate" were obtained from the Aldrich Chemical Company Ltd and Eastman Kodak Ltd respectively. Other reagent used in the spin-labelling experiments were obtained from either BDH or Aldrich. The structural formulae of the drugs and spin-labels are given in the appropriate

chapters.

Solutions of the phenothiazines were made up without purification in 1mM NaCl. For most purposes a concentration of 0.01M drug was adequate. The solutions were stored at 4°C and covered with foil to prevent photolytic degradation. Concentrations were calculated from the known molecular weights of these compounds.

Proflavine Hemisulphate, the starting material for the spin-labelling experiments was converted to its free base and dissolved in tetrahydrofuran immediately prior to use. The spin-labelling experiments and the treatment of spin-labelled proflavine are described in Chapter 4.

## 3.2 Methods

### 3.2.1 The Preparation of DNA-Drug Complexes and Fibres

DNA-drug complexes were prepared by adding an appropriate volume of a dilute drug solution dropwise, with stirring, to a stock solution of DNA. In the case of the phenothiazines, the drugs were converted to their free radical forms by acidic oxidation before adding to the DNA solution. The rate of decay of the free radicals was quite rapid and for this reason they were prepared at 4°C. Precipitation of the DNA due to its interaction with the positively charged drug molecules was easily provoked at room temperature. The DNA-drug complexes were therefore also prepared at 4°C.

Gels were obtained by sedimentation of the complex in an MSE 50 ultracentrifuge. The complex was distributed in a 3 x $3cm^3$ rotor and centrifuged at 40,000rpm for 8-12 hours. Care was taken to ensure that all the supernatent was removed from the resulting gel otherwise it redissolved. A Pasteur pipette was used for this task which was performed as quickly as possible. Gels were usually used immediately but some were stored for future use and kept at 4°C.

An estimate was made of the P/D of the gels and fibres by a spectrophotometric analysis of the initial solution and the supernatent

(see Section 3.2.2).

Fibres were prepared using the method described by Fuller (1967). Two small glass rods with rounded ends were mounted in plasticine and placed about 1mm apart. A drop of gel was placed on and between the glass rods and allowed to dry. As the gel dried the DNA helices tended to align themselves along the fibre axis. The degree of orientation of the DNA in the fibre was found to depend upon the initial consistency of the gel, the rate of drying and the thickness of the fibre. Thick fibres (diameter > 0.5mm) tended to dry too quickly on the outside, leaving the internal distribution of DNA poorly orientated. This problem was overcome by stretching the fibres whilst they dried. However, thin fibres, which were less than about 0.2mm in diameter, usually buckled during the drying process. In practice a reasonable degree of orientation was achieved from fibres of 1-4mm in length and 0.2-0.5mm in diameter.

ESR spectra were recorded up to a P/D of 70 for a single fibre containing spin-labelled proflavine. The instability of the phenothiazine free radicals, on the other hand, meant that a good ESR spectrum was only obtained for these complexes using 8-12 fibres.

### 3.2.2 Visible and Ultraviolet Spectroscopy

(a) **Spin-labelled proflavine-DNA complexes.** Visible and UV spectra of these complexes were obtained in order to estimate the P/D ratios present in the gels and fibres. The method relies on the fact that the drug molecules have characteristic visible absorption spectra while the DNA absorbs only in the UV region. The ratio between the amounts of DNA and drug sedimented by centrifugation can be calculated from

$$P/D = (P_0 - P_1)/(D_0 - D_1)$$

where $P_0$ = the initial DNA concentration

$P_1$ = the concentration of DNA in the supernatent

$D_0$ = the initial drug concentration

$D_1$ = the concentration of drug in the supernatent

The term $P_0$ was estimated from the volume of the DNA stock solution used and the concentration of this stock solution was obtained by measuring its maximum UV absorbance (assuming $E_\lambda = 6600 M^{-1}cm^{-1}$).

The term $D_1$ was measured at the maximum visible absorption peak of the supernatent. In practice, this term was often small enough to be neglected.

The concentrations, $P_1$ and $D_1$, were calculated using the Beer Lambert law:

$$A = E_\lambda cl$$

where A is the measured absorbance, l is the optical path in cm, $E_\lambda$ is the molar extinction coefficient in $M^{-1}cm^{-1}$ and c is the unknown concentration in moles per litre.

Spin-labelled proflavine was found to obey this law for concentrations less than $10^{-5}M$. However, the concentration of spin-labelled proflavine used in the initial mixing stage was typically an order of magnitude larger than this. For this reason initial concentrations of drug were calculated on the basis of the amount of drug dissolved per unit volume of solution.

(b)**Phenothiazine free radical-DNA complexes** The above method was not used in the case of complexes containing phenothiazine free radicals because of the quite considerable decay of these specimens during the interval between the preparation of a complex and the formation of a gel. However, a rough estimate of the amount of drug present in a gel was made by crushing a piece of gel between two quartz glass plates and comparing its UV absorption (due to the DNA) with its visible absorption

(due to the drug). The P/D ratio is then calculated from

$$P/D = A(DNA)/A(\text{Free Radical}) \times E_1(DNA)/E_1(\text{Free Radical})$$

where $E_1$(DNA) and $E_1$(Free Radical) are the extinction coefficients of the DNA and free radical solutions. This method assumes that the extinction coefficient of the free radical in solution is the same as that of the bound free radical species, an assumption for which no evidence has been produced. The figures obtained from this method should therefore be accepted as no more than a rough guide to the true P/D ratios in the gels. The extinction coefficients of several phenothiazine free radicals have been estimated by Rieder (1960) and Thierry (1968). The values all lie in the range 6000-8000$M^{-1}cm^{-1}$. Wherever possible the published values were used. In other cases a value of 7000$M^{-1}cm^{-1}$ was adopted. Using the above procedure it was estimated that only about 10% of the original free radical concentration was present in the gels. As mentioned before, several phenothiazine free radical-DNA fibres were required to give a signal strength comparable to that for a single fibre containing spin-labelled proflavine. Although account must be taken of the differences in the linewidths and lineshapes of these spectra this last fact does suggest that some 80-90% of the original free radical concentration decays by the time a fibre is made. All spectrophotometric measurements were taken using a Cary 118C operating in its auto gain mode in the absorbance range 0.5-1.0. As well as obtaining the drug concentrations the Cary was also used to monitor changes in the UV and visible spectra of the phenothiazine free radicals as they decayed.

### 3.2.3 The Control of Relative Humidity

The degree of hydration of the DNA-drug fibres and gels was controlled by passing compressed air into the ESR cavity via a saturated salt solution. The humidification system consisted of three glass jars, the first of which contained distilled water, the second held a saturated

salt solution and the last was empty. The relative humidity produced in the cavity depe depended on the type of salt used. Viz,

| | |
|---|---|
| Calcium Chloride | RH = 33% |
| Potassium Carbonate | RH = 44% |
| Sodium Bromide | RH = 57% |
| Sodium Nitrite | RH = 66% |
| Sodium Chlorate | RH = 75% |
| Potassium Chloride | RH = 86% |
| Sodium Sulphite | RH = 92% |
| Potassium Chlorate | RH = 98% |

(Reference: CA Handbook, 1976).

The empty glass jar was present in order to capture any water droplets which might be carried along in the air-flow. The rate of flow was kept to a minimum because the ESR cavity easily became saturated at even moderate rates of flow. The flow-rate was estimated by observing the rate of bubbling of the compressed air through the saturated salt solutions.

### 3.2.4 Digitised Spectra

Experimental ESR spectra were originally recorded on an analogue XY plotter. They were then digitised using a "CETEC Digitiser", which was operated in its continuous stream mode. The digitised data was stored on magnetic tape on a GEC 4090 computer and computer programmes for converting the digitised information into standard format were available through the system library KEELE (written by members of the computer Centre). Scaling and least-squares curve smoothing routines were written by the author with the aid of the GINO and NAG software libraries. Interactive computer graphics were available on an IMLAC refreshed screen display, a tektronix T4010 paged graphics terminal and a Sigma T5000 colour graphics display. Hardcopies were obtained on a CALCOMP plotter.

# CHAPTER 4

## Interactions between DNA and Spin-Labelled Proflavine

### 4.1 Introduction

This chapter is largely concerned with presenting the results of an ESR investigation into the nature of complexes formed, in solutions and fibres, between DNA and a spin-labelled analogue of proflavine. This section describes the sort of information which can be obtained from such an investigation.

By attaching small paramagnetic nitroxide molecules or spin-labels (see Chapter 1) to drug molecules, such as proflavine, the interactions of these drugs are readily monitored. When bound to DNA in fibres the spin-labelled molecules exhibit ESR spectra whose hyperfine splittings are dependent upon the orientation of the DNA helix axis with respect to the external magnetic field. If the spin-labelled molecules are randomly bound to the DNA each orientation of the fibre in the magnetic field will give the same ESR spectrum. However, if the spin-labelled molecules bind systematically, either externally on the helix or by intercalation, then orientation-dependent spectra will be observed. Since intercalation in particular implies a certain geometrical relationship between the DNA helix axis and the spin-orbital of the nitroxide this relationship will show up in the fibres in the anisotropy of the hyperfine splittings. If the geometry of the spin-labelled drug system is known, the orientation of the drug molecule itself can then be deduced. In this way the possibility of intercalation for the spin-labelled molecules can be examined. In particular, the possibility that intercalation occurs for each of the three conformations adopted by DNA in fibres can be investigated.

Conformational transitions of DNA in fibres can be induced by alterations in the ambient relative humidity (see Chapter 1). For a fibre at a given orientation with respect to the external magnetic field, any change in its ESR spectrum as the relative humidity is altered will indicate that the mode of binding of the spin-labelled molecules, or their orientation in the DNA, has changed. A change in the binding geometry of the molecules is unlikely to be brought about merely by increasing or decreasing the water content of the fibre. Conformational transitions of the DNA molecules can, however, be expected to bring about such a change. By analysing the ESR spectra obtained from oriented fibres over a range of relative humidities, the nature of the binding of the spin-labelled molecules to different DNA conformations can be examined. Futhermore, once the effects of the conformational transitions on the ESR spectra have been recognised, this information can then be used to study the influence on these transitions of varying concentrations of bound spin-labelled molecules.

In solutions, since the DNA molecules will be randomly aligned in the external magnetic field, any preferential binding geometry will be obscured. However, on binding to DNA the spin-labelled molecules are likely to be highly immobilised. As will be seen in section 4.3, the extent of this immobilisation under a variety of conditions (e.g. temperature) can provide important information on the nature of the binding in these complexes.

## 4.2 Spin-Labelled Proflavine

### 4.2.1 Description

Proflavine is a planar, tricyclic heterocycle (Fig. 4.1). It was chosen for this study for several reasons. Firstly, its interactions with DNA have been previously investigated (see Chapter 1) and the results of

this work will be relevant to the analysis of the results of the present study. Secondly, the possession of two amino groups on the heterocyclic ring means that proflavine can be easily modified (i.e. spin-labelled). Thirdly, in virtue of its structural simplicity, spin-labelled proflavine should bind in such a way that the helical symmetry of the DNA molecules is not perturbed. This is important because if the binding is not regular, analysis of the resultant ESR spectra may prove to be very difficult (i.e. too many spectral components may be present).

In section 4.1 it was implicitly assumed that the nitroxide moiety is attached to the drug molecule (i.e. proflavine) so that its mobility is highly restricted. That this feature of the spin-labelled system is a desirable one can be seen with reference to Chapter 2. Let us suppose that the spin-label is free to undergo some form of motion when bound, via proflavine, to DNA. If the motion is slow (i.e. $t_c > 10^{-8}$sec.), any orientational preferences of the spin-labelled proflavine molecules will show up in the ESR spectra. However, if the motion is rapid and **isotropic** ($t_c < 10^{-8}$sec.), the hyperfine anisotropy will be averaged out to a single value and no orientational information will be detected. If the motion is rapid and **anisotropic** the spin hamiltonian parameters will be averaged out in a more complex fashion. Since, in the general case, all the possible types of motion and orientation of the spin-labels will have to be included, a quantitative analysis of the ESR spectra obtained from such samples will be extremely difficult. Only in certain cases, for example a rapid rotation of the spin-label about a principal axis, can the effects of motion and orientation be easily distinguished. Such a case will be examined later. Clearly, the immobilisation of the spin-label attached to the proflavine is not only a desirable, it is also an essential feature of this work.

It was realised that in order to achieve complete immobilisation, the nitroxide moiety would need to be attached to the proflavine ring by

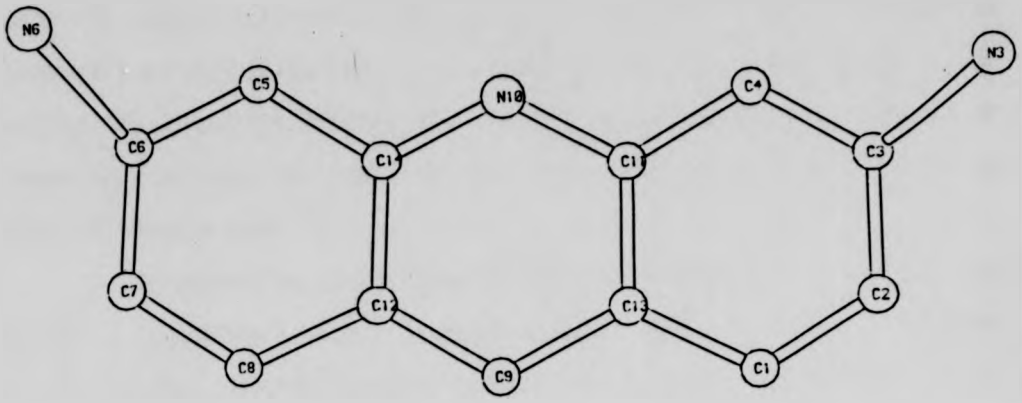


Fig. 4.1 Proflavine.

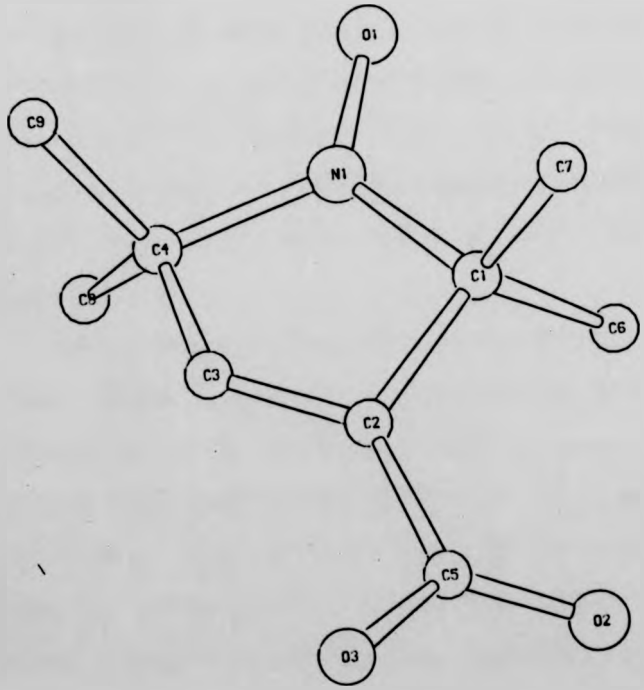


Fig. 4.2 3-Carboxy-2,2,5,5-tetramethylpyrroline-1-oxyl

several bonds, or at least by a double bond. Unfortunately, in view of the difficult and time-consuming chemical procedures that would be involved in synthesizing such a compound, these possibilities had to be rejected. It was decided that the easiest means of obtaining at least some degree of immobilisation was to link the nitroxide to the proflavine ring by a "partial" double bond.

In molecules containing the amide group (-NHCO-), e.g.Urea, a resonance condition exists in which a double bond is "shared" between several atoms. Crystallographic studies of many such compounds have shown that the amide group is always planar and that rotations about the partial double bonds are highly constrained.

Only a few spin-labels possess the structural means of forming such bonds, such as nitroxides which contain the carboxyl group (-COOH). These compounds can easily be converted to their acid-chlorides (-COCl) and then reacted with an amino group to form an amide bond. In view of this it was decided that a suitable spin label to use in this work would be 3-Carboxy-2,2,5,5-tetramethylpyrroline 1-oxyl (Fig. 4.2). This molecule possesses a planar ring structure and thus possible inversions of the nitroxide ring, which would show up as motion in the ESR spectra, are eliminated.

The spin-labelling procedure carried out in this work consisted of three stages. Firstly, Rozantsev's method (1970) was used to prepare the acid-chloride of the chosen nitroxide radical. Secondly, proflavine hemisulphate was converted to its free-base which was then reacted with the acid-chloride. Finally, the product of the reaction was examined and purified by chromatographic methods. The various reactions involved are presented schematically in Fig. 4.3. Experimental details are given below (Rozantsev's method is included for completeness). Yamaoka (1977) and Robinson et al. (1980) have used a similar method to obtain several spin-labelled derivatives of ethidium bromide and aminoacridine.

The following experiments were carried out with the invaluable aid of Dr. D. V. Griffiths of the Chemistry Department at Keele University.

4.2.2 Spin-Labelling Experiments

(a) **Preparation of 3-Chloroformyl-2,2,5,5-tetramethylpyrroline-1-oxyl**

A suspension of 0.75g of 3-Carboxy-2,2,5,5-tetramethylpyrroline 1-oxyl in 30cm$^3$ of dry benzene was treated with 0.4cm$^3$ of dry pyridine and with cooling and stirring, 0.38cm$^3$ of thionyl chloride was added dropwise to the resulting solution. After stirring for 1 hour at room temperature the precipitate was filtered off and washed (on the filter) with dry benzene. The solvent was then evaporated under pressure.

(b) **Preparation of Spin-Labelled Proflavine**

1g of proflavine hemisulphate was dissolved in 250cm$^3$ of warm distilled water. 10g of sodium hydroxide pellets were added and the mixture was stirred. After several minutes the precipitate (i.e. proflavine free base) was filtered off and washed with distilled water. Excess water was removed by flushing through with acetone, and the free base was then dried under vacuum at 70°C.

0.65g of free base was dissolved in 50cm$^3$ of tetrahydrofuran (THF) and 24cm$^3$ of 3-Chloroformyl-2,2,5,5-tetramethylpyrroline-1-oxyl in dry benzene was added. The mixture was refluxed at 50°C for 1 hour under anhydrous conditions. After this time the solid was filtered off, washed with distilled water and then dried under vacuum at 80°C.

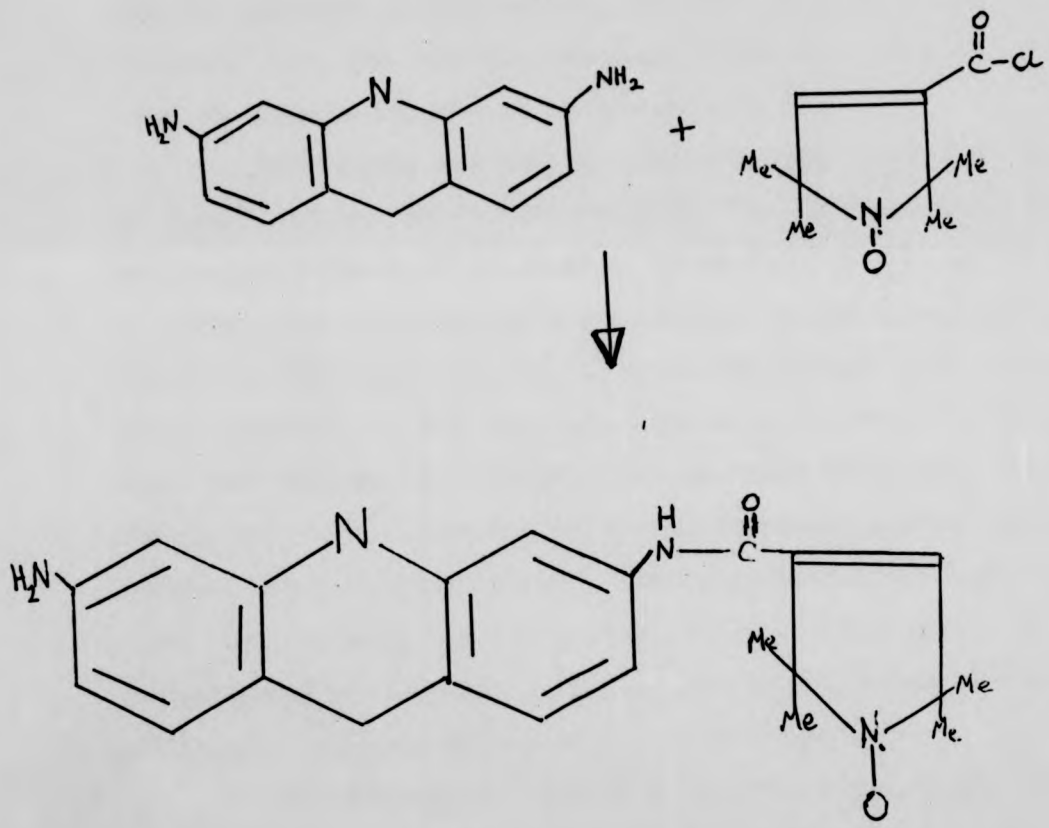


Fig. 4.3 Schematic representation of the Spin-Labelling experiments.

(c) **Purification**

The crude product of the reaction consisted of a mixture of free base, free spin-label (the acid chloride having been hydrolysed), several solvents and spin-labelled proflavine. It was found to be very insoluble in methanol, quite soluble in a 50:50 mixture of dimethylformamide (DMF) and ethyl acetate (EtAc), and very soluble in DMF alone. Preliminary work using thin layer chromatography (TLC) showed that free spin-label was rapidly extracted by EtAc, and that spin-labelled proflavine was nicely separated from the remaining components by DMF or a DMF/EtAc mixture. Final purification was achieved using a chromatatron.

Purification was begun by dissolving 200mg of the crude material in $80cm^3$ of EtAc. $20cm^3$ of DMF was added. Insoluble components in the mixture were filtered off and $10cm^3$ of the remaining solution was placed on a chromatatron disc which had previously been flushed through with EtAc. Elution was then begun using EtAc to remove the free-spin label components, which showed up as a dark band under short-wave UV. After 3 hours no more free label was detected. Meanwhile two more bands had begun to separate. The solvent was changed to a 50:50 DMF/EtAc mixture and the separation between the two bands increased. Both bands were collected and an ESR signal was detected from a sample of the first (yellow) band. This was assumed to be spin-labelled proflavine. The second (orange) band gave no ESR signal. This component was proflavine free base.

The spin-labelled component was dried under vacuum and the resulting yellow residue was re-crystallised from methanol. TLC, using methanol as solvent, exhibited only a single spot. Stock solutions of $10^{-3}M$ spin-labelled proflavine were prepared by carefully weighing appropriate quantities of the solid in $10cm^3$ volumetric flasks and dissolving in dry methanol or deionised water. The samples were covered with aluminium foil and stored at 4°C. Concentrations were calculated assuming a molecular weight of 374.

## 4.3 Solution Studies

### 4.3.1 Optical Spectroscopy

#### 4.3.1 (a) Method

Absorption spectra were recorded using the method described in Chapter 3. Stock solutions of $5 \times 10^{-5}$M spin-labelled proflavine and $2.6 \times 10^{-3}$M DNA were used. The ionic strength of each solution was adjusted to 0.1M NaCl.

#### 4.3.1 (b) Results

The visible absorption spectra of proflavine and spin-labelled proflavine are quite different (Fig. 4.4). Proflavine gives an absorption peak at 440nm whereas two absorption maxima are observed for spin-labelled proflavine. These occur at 372nm and 448nm.

On binding to DNA, the absorption spectrum of the spin-labelled compound is shifted to longer wavelengths (Bathochromic or "red-shift") and the maximum absoptivity is reduced (Hyperchromism). The red shift of the spectra with increasing amounts of DNA is shown in Fig. 4.4. It is significant that as the binding ratio r increases, so the red shift becomes less pronounced. For example for r = 0.005 (moles of spin-labelled proflavine per mole of DNA base pairs) the peak at 382nm is shifted by nearly +20nm whereas for r = 0.15 the same peak is shifted by only +1nm. At sufficiently high concentrations of bound drug the absorption spectrum actually becomes blue shifted with respect to the free drug spectrum.

#### 4.3.1 (c) Discussion

These spectral changes are similar to those observed for proflavine and other acridine drugs and are believed to be associated with the different modes of binding of the molecules to the DNA (see Chapter 1). In particular, the red shift is believed to be caused by intercalation of

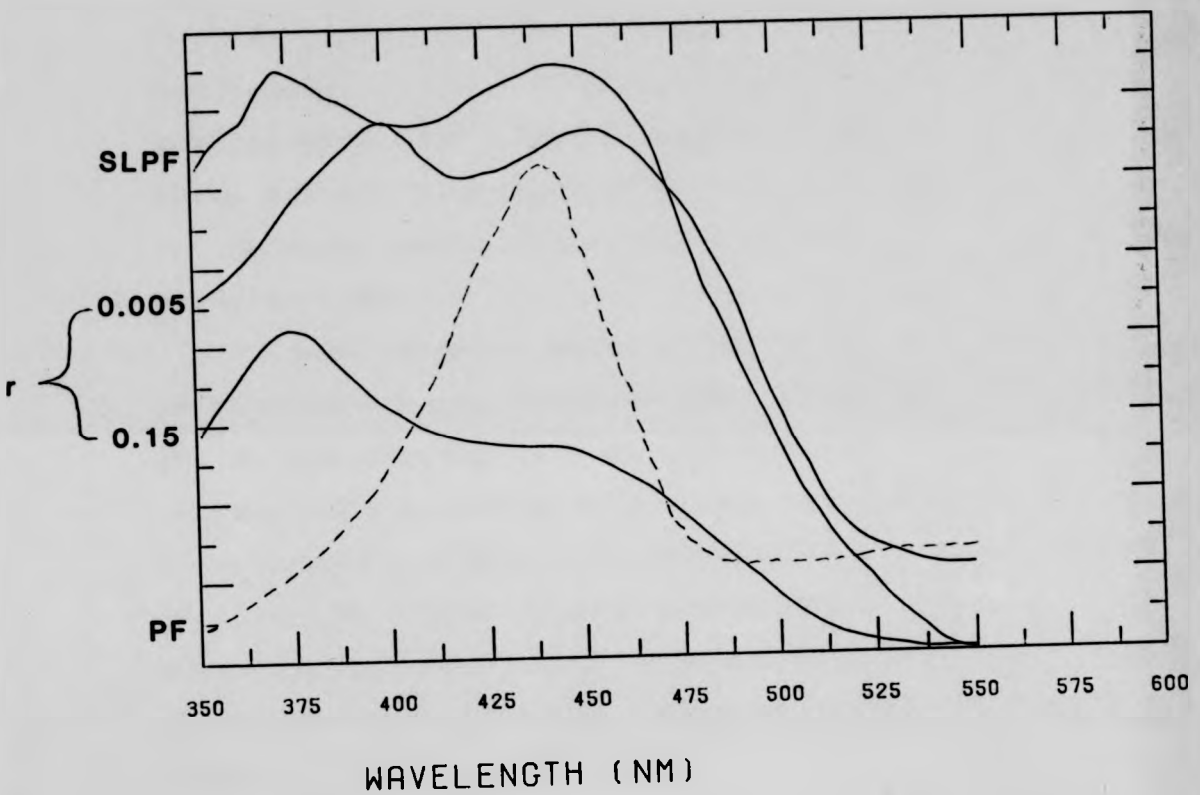


Fig. 4.4 Absorption Spectra of Proflavine, Spin-labelled Proflavine and Spin-Labelled Proflavine-DNA Complexes.

the drug molecules in the DNA. This is the dominant mode of binding at low drug concentrations. The blue shift begins when the drug concentration is high enough for all the possible intercalation sites to be used up. This occurs for the acridines at about r = 0.2. A similar figure was recorded for spin-labelled proflavine (see Section 4.3.4). At even higher concentrations the proflavine molecules are prone to self-aggregation and these aggregates bind externally to the DNA molecules. This causes a further blue shift in the absorption spectrum until a point is reached when all the external binding sites are used up and the DNA precipitates (Blake and Peacocke, 1968).

Since the optical results obtained for spin-labelled proflavine are consistent with those obtained for other acridine drugs, it is probable that its interaction with DNA is not significantly affected by the presence of the nitroxide group on the acridine ring. This conclusion is supported by the observations of Blake and Peacocke (1968) who note that the presence of a long and bulky side group on 9-aminoacridine does not destroy its ability to intercalate and may even enhance its binding affinity. The binding affinity for DNA of spin-labelled proflavine will be examined in section 4.3.4.

### 4.3.2 The ESR Spectrum of Spin-Labelled Proflavine

The 9.5-GHz ESR spectrum of spin-labelled proflavine in dry methanol is is shown in Fig. 4.5a. The spectrum was recorded using a concentration of $2 \times 10^{-5}$M and a modulation amplitude of 0.05mT. The three line spectrum is typical of nitroxide radicals tumbling freely in solution. The separation between the lines is 1.59mT. Using the method described in Chapter 2 the rotational correlation time of the molecules was estimated to be 0.1nsec.

In the presence of DNA the ESR spectrum indicates the existence of two species of spin-labelled proflavine (Fig. 4.5b). In addition to the

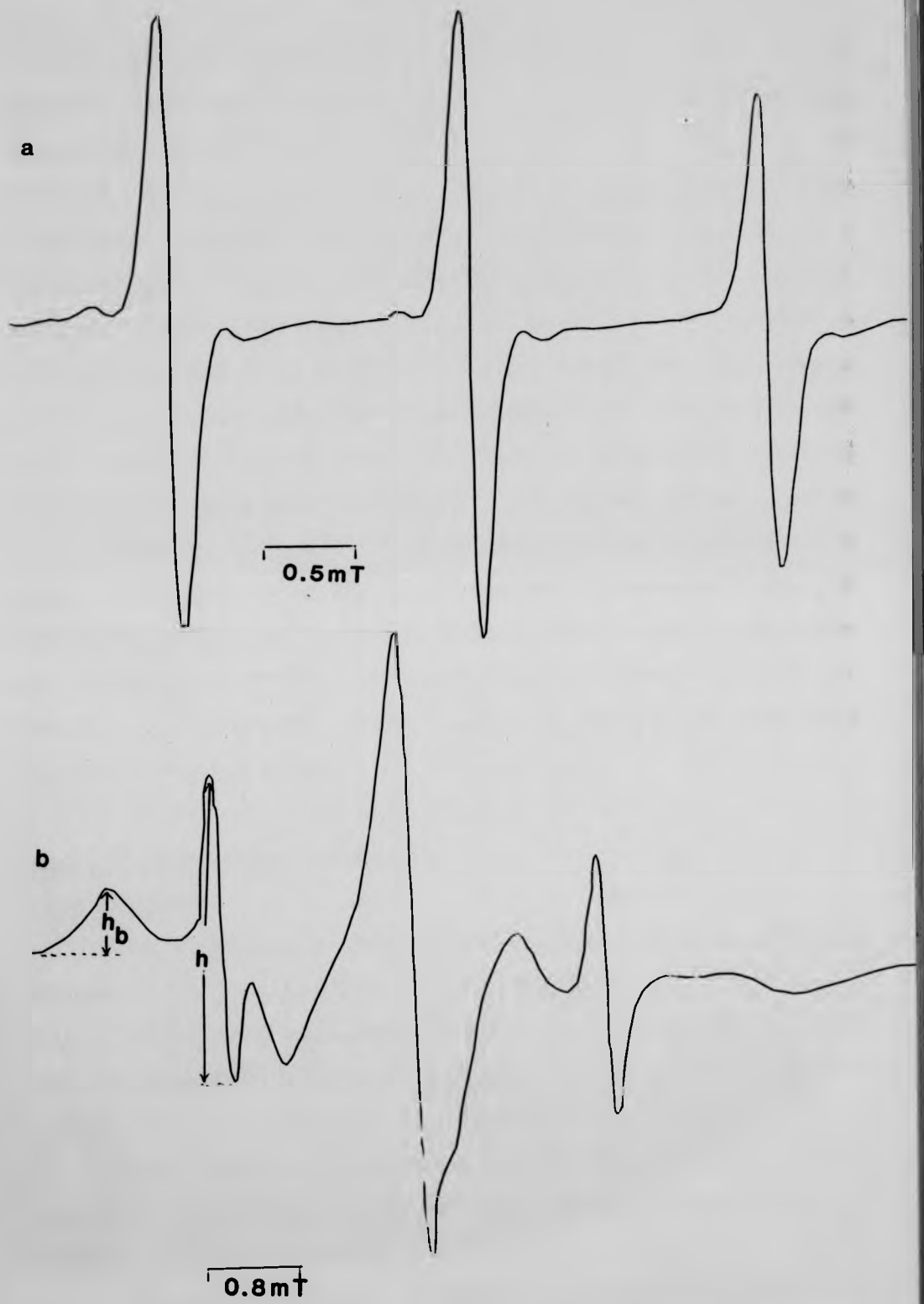


Fig. 4.5 (a) 9.5-GHz ESR Spectrum of Spin-Labelled Proflavine.
(b) 9.5-GHz ESR Spectrum of a Spin-Labelled Proflavine DNA complex (P/D = 20; 1mM NaCl).

original three line spectrum there is now a broad component with a maximum hyperfine splitting of 5.6mT. This component arises from the interaction between the DNA and the spin-labelled molecules. The large hyperfine splitting suggests that the spin-labelled molecules become highly immobilised on binding to the DNA. The probable cause of this immobilisation is the intercalation of the molecules in the DNA. Several arguments support this claim. Firstly, the optical results presented in section 4.3.1 (i.e. the bathochromic shifts) suggest that spin-labelled proflavine, in common with other acridine drugs, binds to DNA at high P/D values predominantly by intercalation. Secondly, the hyperfine splitting of the bound spectrum is comparable to the values quoted by Sinha et al. (1979) for two intercalating derivatives of 9-aminoacridine. In addition it is worth noting that, as deduced from CPK molecular models, the bulk of the nitroxide group attached to the proflavine ring does not hinder the structural possibility of intercalation. Further evidence for intercalation is provided by the results of the melting temperature experiments described below.

## 4.3.3 Melting Temperature Experiments

### 4.3.3 (a) Method

An examination of the binding of spin-labelled proflavine to DNA was made for P/D values of 20 and 50 in the temperature range 20°C to 90°C. Drug-DNA complexes were prepared by adding appropriate quantities of $5 \times 10^{-4}$M of spin-labelled proflavine dropwise into a $50cm^3$ flask containing $10cm^3$ of $2.6 \times 10^{-3}$M DNA. The ionic strength of the mixture was 0.001M NaCl. Since there were no facilities available for variable temperature experiments to be performed whilst the sample remained in the ESR cavity, a relatively crude but effective alternative was used.

A "Stuart" hotplate with magnetic stirrer was used to heat the drug DNA solutions to the required temperature. The solution was

maintained at the set temperature for 5 minutes with stirring. After this time a sample was removed (about $1cm^3$) and allowed to cool to room temperature. Meanwhile, the remaining solution was raised to a higher temperature, stirred for 5 minutes and another sample was taken. This cycle was repeated until several samples had been collected and allowed to cool. The ESR spectrum of each sample was then recorded.

4.3.3 (b) Results

With increasing temperature the proportion of bound molecules decreased. This was evident from the changes in the relative heights of the bound and free spectral components. Taking the ratio of the heights of the low field absorption lines of the free and bound components (denoted by $h(+1)$ and $h_b(+1)$ in Fig. 4.5a) a plot was made of the release of the bound drug molecules as a function of temperature (Fig. 4.6a). Each point on the plot represents the average of three separate measurements.

Also shown in Fig. 4.6a is a thermal denaturation curve for DNA alone. This was determined by monitoring the change in the UV absorption of the DNA at 260nm as the temperature was raised.

The UV absorption of the DNA was constant between 20°C and 50°C (curve C in Fig. 4.6a). Over the same temperature interval and up to 65°C the ESR signal intensity (defined as $h(+1)/h_b(+1)$ ) gradually increased (curves A and B). Between 65°C and 80°C there was a large increase in the number of unbound molecules. In a similar 15° interval (i.e. between 50°C and 65°C) a large increase in the UV absorption of DNA was observed. The temperature of the mid-point of this range (the "melting temperature") was 61°C. The melting temperatures of the drug-DNA complexes are dependent upon the initial drug concentrations. This can be seen by comparing curves A (P/D=20) and B (P/D=50) which give melting temperatures of 74°C and 71°C respectively. The melting curves are somewhat broader than those previously reported for DNA-drug complexes (Hong and Piette, 1978). This

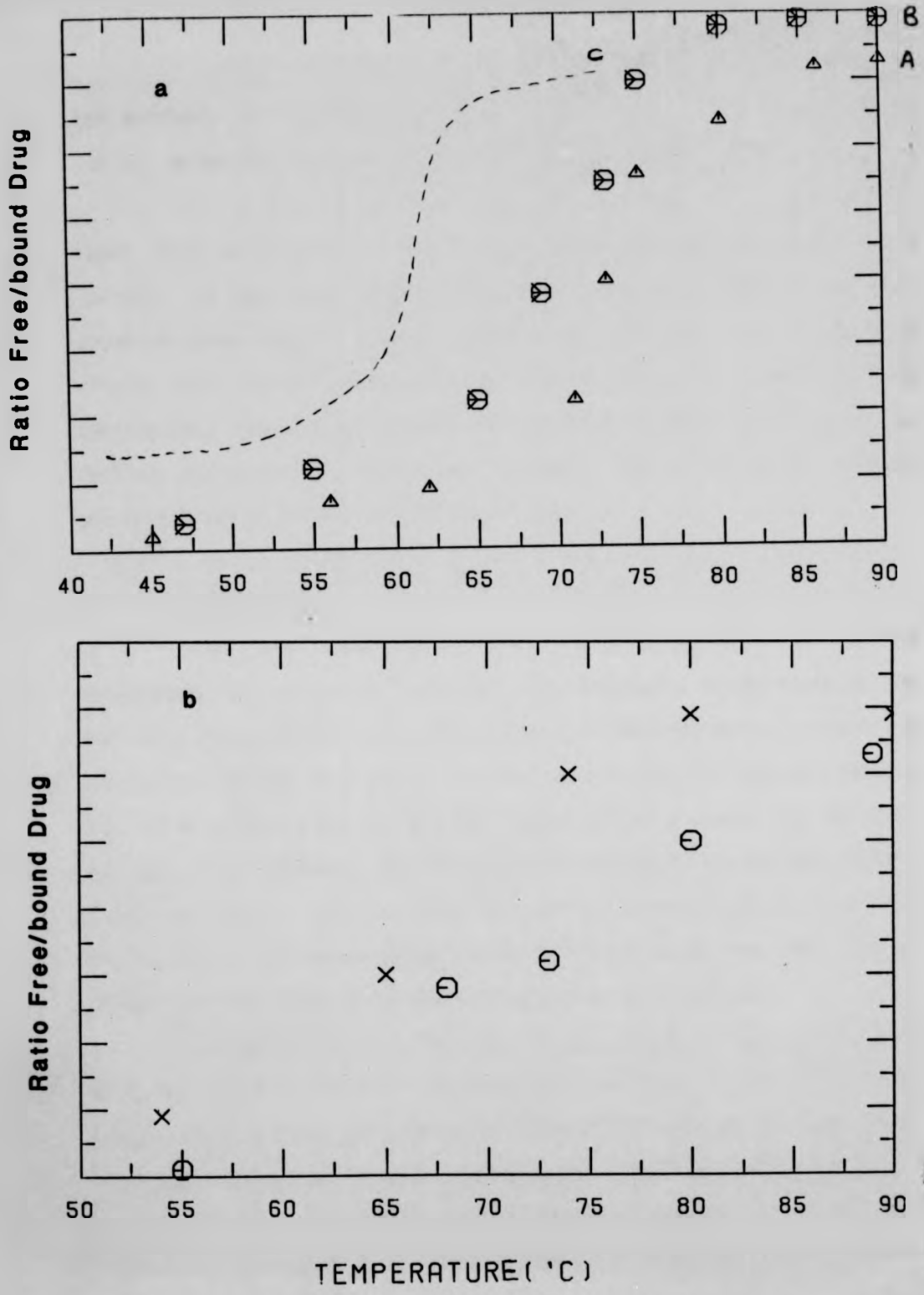


Fig. 4.6 (a) Thermal Denaturation of Spin-Labelled Proflavine DNA Complexes (A) P/D = 20; (B) P/D = 50; (C) UV Meltng Curve of DNA.
(b) Melting Temperature Curve using Denatured DNA.

can probably be attributed to the method used here which allows for a partial recombination of the double helix as the sample cools.

In a similar experiment using denatured DNA the release of the bound drug occurred over a much broader temperature range and the sharp increase in the number of free components between 65°C and 80°C was not observed (Fig. 4.6b). Similar behavior was also seen when a DNA-drug complex was initially taken up to 90°C and then allowed to cool to room temperature. Samples were removed at intermediate temperatures during the cooling period and ESR spectra were recorded. The melting curve obtained was very broad as can be seen in Fig. 4.6b.

4.3.3 (c) Discussion

The total absorbance of DNA at 260nm is due to the sum of the absorbances of its component bases. This absorbance is depressed in the DNA molecule because of the close stacking of the base pairs. However, on subjecting the DNA molecules to extreme temperatures the hydrogen bonds in the helix are ruptured and the DNA collapses into a random coil in which the bases are exposed. This "helix-coil" transition takes place over a narrow temperature range and produces a sharp increase in the UV absorption of the DNA. The sharp change in the melting curve of the DNA observed between 50°C and 65°C can be identified with this transition.

By comparing the melting curves obtained for the drug-DNA complexes with that for DNA it is clear that the rapid release of the bound drug molecules between 65°C and 80°C is associated with the collapse of the secondary structure of the DNA. On the other hand, the gradual increase in the ESR signal intensity between 20°C and 65°C suggests that, in this temperature interval, the release of the bound molecules occurs without disruption of the DNA secondary structure. This observation is best explained by a model in which the drug molecules bind by intercalation. Only by binding in this way will the drug molecules be intimately connected

with the secondary structure of the DNA. The absence of a well defined melting temperature for complexes containing denatured DNA confirms this conclusion.

The differences between the melting temperatures of native DNA and the drug-DNA complexes are accounted for by supposing that the DNA secondary structure is strengthened by the presence of the bound molecules. This possibility is supported by the observation that the melting temperatures increase with increasing drug concentration.

In conclusion, these results strongly imply that at low concentrations the spin-labelled molecules bind to DNA predominantly by intercalation, and that this binding results in an increase in the stability of the DNA helix.

### 4.3.4 Binding Parameters of Spin-Labelled Proflavine

The ESR spectra of a series of spin-labelled proflavine-DNA complexes were recorded and the concentrations of free and bound drug were determined. This data was then used to determine the binding parameters of the interaction (i.e. the association constant and the number of binding sites per base pair). A comparison was made with the binding characteristics of other acridine drugs.

#### 4.3.4 (a) Theory

Assuming that there is only one species of bound drug (e.g. intercalated) then, if n is the number of binding sites per base pair, r is the number of drug molecules bound per base pair and c is the concentration of free drug :

$$r/c = k(n-r)$$

where k is the "association constant". The association constant is related to the standard free energy ($\Delta G$) of the binding by

$$k = \exp(-\Delta G/RT)$$

where R is the gas constant and T is the temperature.

For a single species of bound drug a plot of r/c against r will be a straight line of gradient -k and intercept nk (Fig. 4.7a). This is called a "Scatchard Plot" (Scatchard, 1949). If there is more than one species of bound drug present the Scatchard plot will be curved (Fig. 4.7b). Often the curve can be analysed in terms of two bound species, each with its own association constant. Peacocke and Skerrett (1956) found this to be the case for the binding of proflavine to DNA. They obtained two association constants, one at $r < 0.22$ ($k_I = 1.3 \times 10^6 M^{-1}$) and another at $r > 0.22$ ($k_{II} = 4.92 \times 10^4 M^{-1}$). The stronger binding ($\Delta G = -9$kCal.) was identified with the intercalation of the proflavine molecules in the DNA; the weaker interaction ($\Delta G = -5$kCal.) was identified with some form of external binding.

The number of binding sites can also be estimated from a plot of r against c. For single species binding the plot asymptotically approaches r = n (Fig. 4.7c). If two binding modes are present the plot has the characteristic curve shown in Fig. 4.7d.

4.3.4 (b) Method

The total ESR absorption of the drug-DNA complex consists of the sum of the absorptions of the free and bound spin-labelled molecules. The total area of the absorption spectrum is proportional to the spin-label concentration. By measuring this area and estimating the fraction due to the free drug component, the concentrations of the free and bound molecules can be determined.

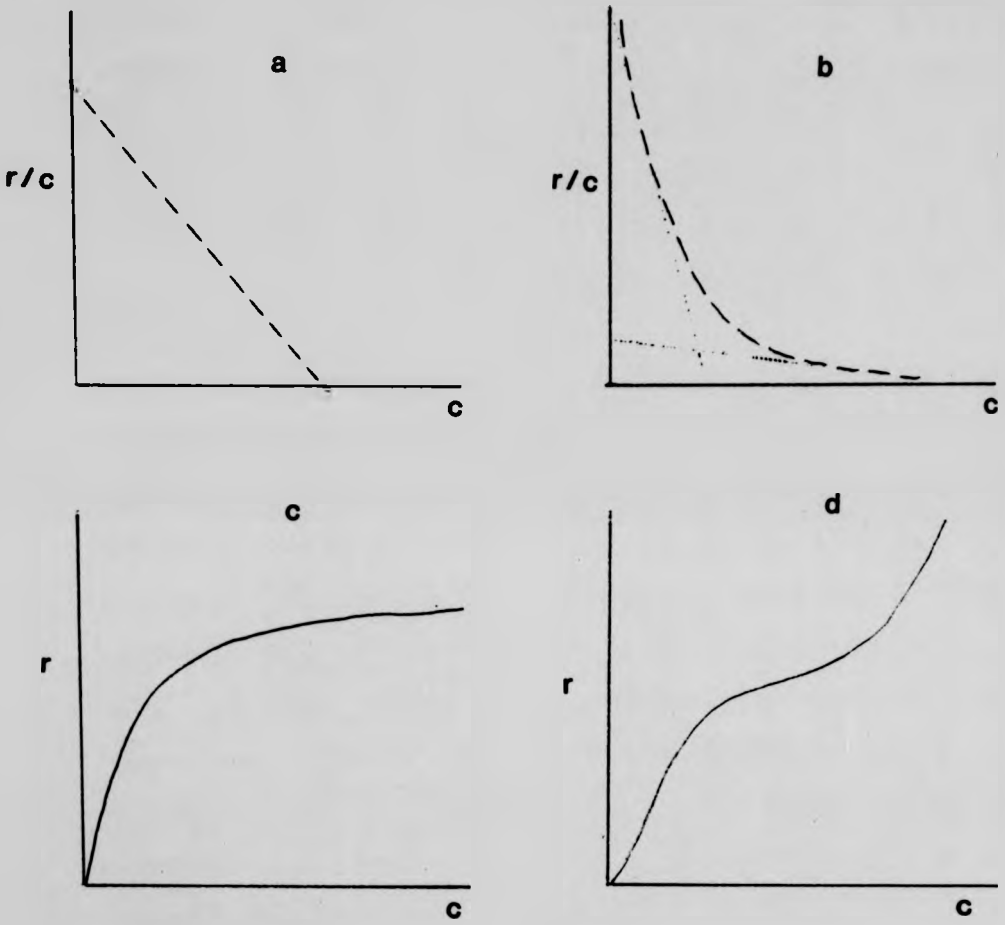


Fig. 4.7 Drug-DNA Binding Curves
(a) Single-Species Scatchard Plot.
(b) Several-Species Binding Scatchard Plot.
(c) Single-Species r v c plot.
(d) Several-Species r v c plot.

To estimate the total area of the ESR absorption a spectrum was first digitised as described in Chapter 3. The digitised spectrum usually consisted of between 150 and 250 (field, intensity) data pairs. A continuous representation of this data was obtained by a cubic splines interpolation (using NAG Library routines E02BAF and E02BBF) and the fitted spectrum was divided along the x-axis (magnetic field) into 600 equal segments. After correcting for base-line drift and setting the base-line at zero, the area of this spectrum was calculated by integrating twice using Simpson's Rule.

As can be seen in Fig. 4.5b the spectral components of the free and bound molecules were well resolved. This meant that an estimate of the area of the free drug component could be obtained by isolating the high-field absorption line and integrating over the appropriate limits. At low drug concentrations it was necessary to extrapolate the wings of the high-field line until they reached the base-line. In the worst case, the areas calculated before and after extrapolation differed by 3.2%. The total area of the free drug component was obtained by assuming that the high-field line contributes 33% of this area. Given the area of the ESR spectrum and the area of the free drug component the concentrations of free and bound drug were easily calculated.

4.3.4 (c) Results

The r against c binding curve obtained from these calculations is shown in Fig. 4.8a. The curve rises sharply at low values of r and c but r approaches a constant value at high concentrations of free drug. This is consistent with there being only one species of bound drug (see Fig. 4.7c). A Scatchard plot of the data is shown in Fig. 4.8b. A linear least squares fit (regression coefficient = 0.97) gives an association constant of 1.5 x $10^4 M^{-1}$ and a maximum binding capacity of 0.21 drug molecules per base pair.

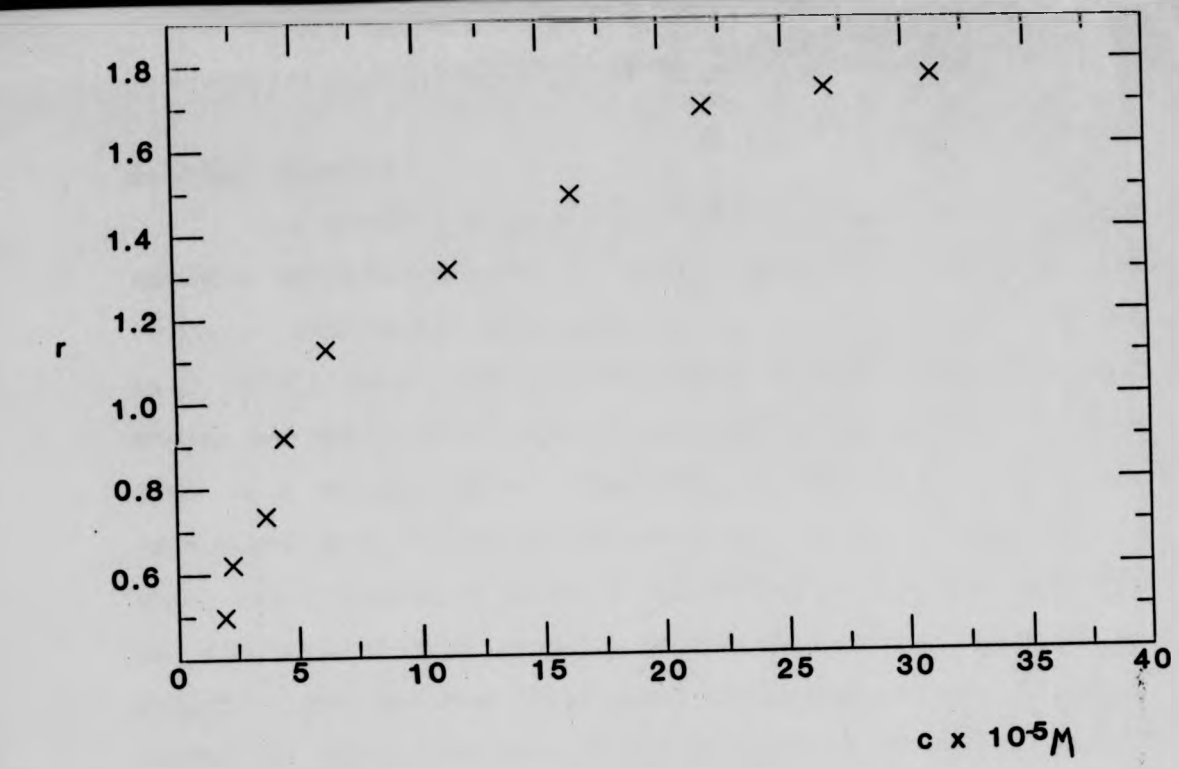


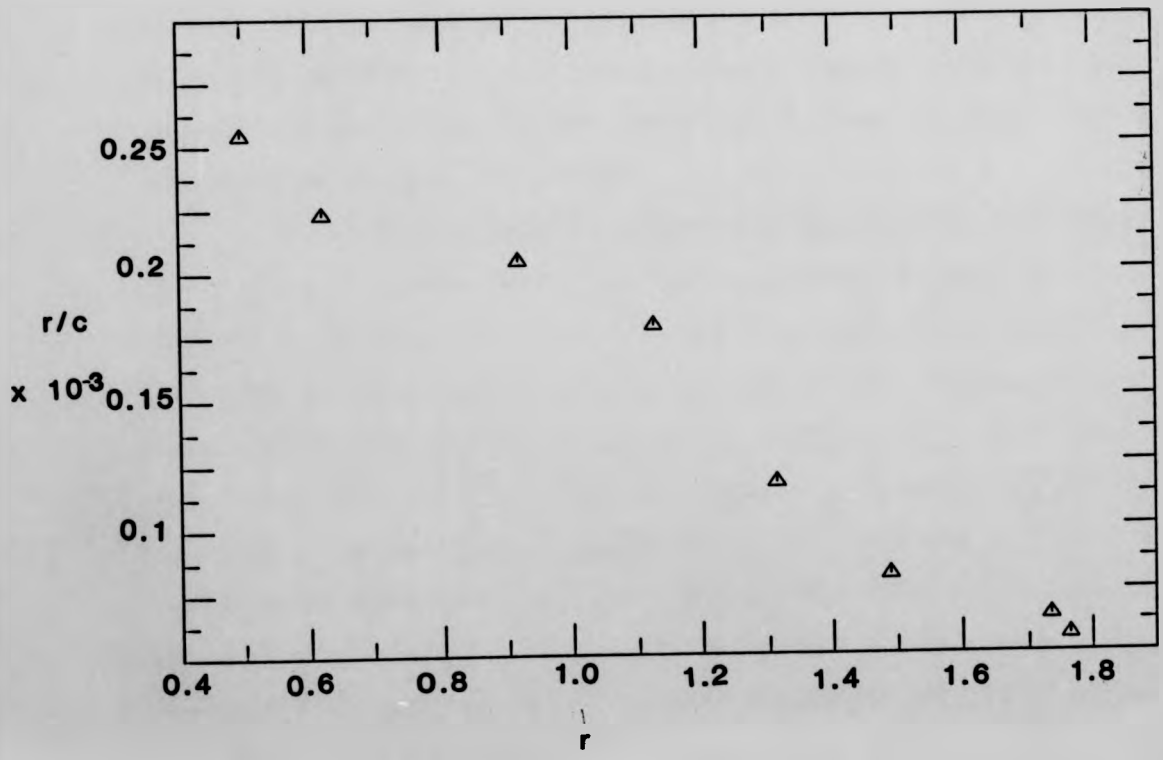


Fig. 4.8 (a) Experimental r v c Binding Curve for binding of Spin Labelled Proflavine to DNA ($r_{max}$ = 0.21).
(b) Experimental Scatchard Plot indicating the presence of a Single Species of Bound Drug.

4.3.4 (d) Discussion

The binding studies carried out here suggest that at high ionic strengths spin-labelled proflavine interacts with DNA by a single mode of binding. This result agrees with the studies performed by Armstrong et al. (1970), Peacocke and Skerrett (1956), Blake and Peacocke (1968) and Bradley and Wolf (1959) on the binding of proflavine and other acridine drugs to a variety of DNAs. Bernier et al. (1981) also analysed the interactions of a spin-labelled 9-aminoacridine in terms of one species of bound drug. However, it should be realised that a linear Scatchard plot can also arise if there are several species of bound drug simultaneously present. This can occur if the association constants of the different species are nearly identical. In such circumstances the various binding modes will be indistinguishable on a Scatchard plot. The association constant obtained here for spin-labelled proflavine is nearly equal to the association constant ($k_{II}$) of the weak binding mode of proflavine. This suggests that the analysis of the binding data in terms of a single binding mode should be accepted with caution.

The association constant obtained for spin-labelled proflavine is two orders of magnitude smaller than the values quoted by Armstrong et al. (1970) and Peacocke and Skerrett (1956) for the strong binding of proflavine to DNA. This reduction in the binding affinity of the spin-labelled compound may be caused by the modification of the primary amino group on the proflavine ring. Wakelin and Waring (1980) have observed a similar decrease in the binding affinities of a series of 8-substituted phenanthridiums. They attribute the effect to a decreased enthalpy of the binding associated with the loss of a primary amino group. An alternative explanation, or perhaps a related one, is that the specificity of the spin-labelled molecules for particular base pairs, or sequences of base pairs (e.g. A:T clusters) is enhanced (or diminished) compared to that of proflavine. Proflavine is believed to have a

preference for A-T rich regions of DNA (Peacocke, 1970; Glesch and Jordan, 1966). It is possible to investigate the binding preferences (if any) of spin-labelled proflavine by using DNAs of varying base pair composition, such as **Clostridium Perfringens** (70% AT content) and **Micrococcus Lysodeikticus** (28% AT content). Such an investigation was not carried out here, but it is suggested as being worthy of further study.

As can be seen from the Scatchard plot (Fig. 4.8b) the binding is saturated at about r = 0.2. A possible explanation of this is as follows. It might be expected that the binding would continue one drug molecule bound per base pair. In the excluded site model (McGhee and Von Hippel, 1974) the intercalation of a drug molecule between two base pairs distorts the DNA secondary structure sufficiently enough to prevent further intercalation of drug molecules in closely adjacent sites. A further restriction is imposed on the extent of the intercalative binding by the limit to which the DNA may unwind in order to accommodate the drug molecules. This may further restrict the number of intercalated binding sites to about r = 0.2 - 0.24. In addition, if there are any base specific interactions occurring these may further reduce the number of available binding sites.

At the ionic strength used (0.1M NaCl) it is likely that the spin-labelled molecules bind predominantly by intercalation. At the pH of these experiments the nitrogen in the proflavine ring is positively charged. The $Na^+$ ions, which reduce the electrostatic repulsions between the negative phosphoryl groups along the DNA backbone, also reduce the electrostatic attraction between the phosphoryl groups and the spin-labelled molecules. This effectively limits the number of external binding sites available to the spin-labelled molecules. The extent of the quenching of the external binding modes by the $Na^+$ ions can be investigated by constructing binding curves for a series of salt concentrations. With this in mind attempts were made to repeat the binding experiments at low

ionic strength (i.e. 0.001M NaCl). At this ionic strength proflavine molecules are liable to stack up along the phosphate groups of the DNA, or in the helical grooves, until r = 1.0 (Peacocke and Skerrett, 1956). It was thought that spin-labelled proflavine would behave in the same fashion. Unfortunately, precipitation of the complex at this ionic strength at even moderate values of r precluded the possibility of obtaining any useful information. The precipitation of the complex was probably a result of the increase in the association constant due to the decreased electrostatic repulsion between the $Na^+$ ions and the spin-labelled molecules. Even a very slow and careful mixing of the spin-labelled drug with the DNA solution resulted in the formation of small precipitates. A similar problem was encountered by Dougherty (1979) in a spectrophotometric study of the binding characteristics of prothidium di-bromide at low ionic strengths. At moderate ionic strengths equilibrium dialysis can be used to bring the complexes up to large values of r. Unfortunately, at low ionic strengths the method becomes suspect because of the "Donnan Effect" (Peacocke and Skerrett, 1956).

Due to the problem of precipitation, the only reliable results obtained were from the binding experiments at high ionic strength. Only the results of these experiments are presented here.

## 4.4 Fibre Studies

In the next section previous ESR and X-ray diffraction studies of proflavine-DNA complexes in fibres are reported. The aims of the present study are then outlined in section 4.4.2. Section 4.4.3 describes a general model for use in the analysis of ESR spectra obtained from oriented spin-labels in fibres and the followng section describes a computer programme based upon this model. In section 4.4.5 the results of orientational studies performed with spin-labelled proflavine-DNA fibres are presented. The rest of the chapter is largely taken up with the analysis of these results using the computer programme described in section 4.4.4. Other sections are concerned with presenting some general remarks on the ESR results and section 4.4.7 discusses the results of the present X-ray diffraction study.

### 4.4.1 Previous Studies

**X-Ray Studies**

The process of intercalation has been previously described (Chapter 1). Molecular models based upon the intercalation of drugs in B-form DNA have been proposed (e.g. Lerman, 1961; Fuller and Waring, 1964; Pigram et al., 1972; Sobell and Jain, 1972; Goodwin, 1977). Although some crystallographic studies of drug-dinucleotide crystalline complexes have been reported (e.g. Sobell, 1979), these models have been based primarily on the results of X-ray diffraction studies of orientated DNA-drug complexes in fibres.

Neville and Davies (1966) examined a series of fibre diffraction patterns obtained from proflavine-DNA complexes. They observed that the layer line spacing varied with relative humidity. At high relative humidity ( > 98%) the diffraction patterns resembled the B-form of sodium DNA in having a meridional reflection at 3.4A. However, the patterns were more diffuse and gave a reduced layer line spacing compared with normal

B-form DNA. Depending on the P/D value this indicated an increase of helical pitch of between 37 and 48Å. When the relative humidity was lowered to between 92% and 98% the layer lines became sharper and their separation increased. The patterns were then identical to that of B-form DNA with a pitch of 34Å. Neville and Davis found that the patterns recorded below 92% were very diffuse, giving meridional and equitorial reflections only. These patterns were not studied in detail. The changes in helical pitch at high humidity were attributed to an unwinding of the helix caused by either intercalation or some form of external binding. Although both binding models could account for the X-ray data only intercalation was consistent with the results of Luzzatti et al. (1961). The increased separation of the layer lines with decreasing hydration to give B-form difraction patterns was explained by Neville and Davies (1966) in terms of a change in the number of intercalated molecules. Viz., for fibres at 100% humidity virtually all the proflavine molecules ( P/D = 6 ) were intercalated. As the degree of hydration was reduced to below 98% the molecules were released from their binding sites until, at 92% relative humidity, only a small fraction of the drug was intercalated. The larger fraction of drug was assumed to be either free in the fibre or bound externally to the helix. Unfortunately, it was not possible to distinguish between these structures from the X-ray data.

In the present work, X-ray diffraction patterns were recorded from spin-labelled proflavine-DNA fibres at several P/D ratios. The X-ray data were used, firstly, to distinguish between the various DNA conformations and, secondly, to investigate the changes of helical pitch and intermolecular separation with relative humidity. From these studies information was obtained concerning the possibility of intercalation. The details are presented in Section 4.4.7.

**ESR Studies of Fibres**

Previous ESR studies using spin-labelled acridines have concentrated upon the nature of their interactions with nucleic acids in solution (e.g. Bernier, 1981a,b; Sinha, 1979, 1981a,b). However, Robinson et. al (1980) have reported on a study of fully hydrated fibres of spin-labelled proflavine complexed with DNA. These fibres, which were prepared by a method different to the one used here, were equilibrated with a concentrated salt solution containing the spin-labelled compound. Under such circumstances the DNA in the fibre was probably in the B-conformation, although this was not explicitely stated. Robinson et. al assumed that the drug molecules were intercalated in the DNA and found that they possessed a considerable degree of freedom in the plane of the base pairs. They estimated that the drug molecules rotated about the DNA helix axis (either fully or partially) in a time of 0.2nsec. Other spin-labelled acridine derivatives were found to have correlation times of up to 10nsec. The motion followed by the spin-labelled probes was considered to be a free rotation of the acridine ring in the plane of the base pairs, indicating that the probes were only weakly coupled to the DNA. A more successful indicator of DNA dynamics was found in a spin-labelled prothidium probe which coupled more tightly to the base pairs. A correlation time of 30nsec was estimated for this probe. Hurley et al. (1982) reported the same value for a spin-labelled derivative of ethidium. A model of DNA motion was suggested in which the base pairs are represented by discs connected by coaxial torsional springs. The random thermal oscillations of each disk are coupled to its nearest neighbours and the spin-labelled probes are assumed to act as normal base pairs. The motional and elastic properties of DNA inferred from this model have been shown to be consistent with the results of other techniques (e.g. Millar et al., 1980).

To date there have been no other ESR studies of proflavine-DNA interactions in fibres. However, an orientational study of ethidium

bromide bound to DNA has been reported by Hong and Piette (1976) and this work was followed up with a study of the interactions of several spin-labelled nitrobenzene derivatives with DNA (Hong and Piette, 1978). In these experiments the DNA-drug complexes were orientated by brushing a gel onto the surface of a flat tissue cell. The conformation adopted by the DNA in these complexes was not reported. However, ESR measurements were carried out at room humidity and at high salt concentration and, from the remarks made in Chapter 1 concerning the influence of salt concentration on DNA conformation, one may conjecture that the results of Hong and Piette (1976) relate to B-form DNA. In any case, Hong and Piette (1976, 1978) concluded that the drug molecules were intercalated in the DNA. Unfortunately, Hong and Piette did not carry a quantitative analysis of their ESR data and their conclusions remain open to doubt.

As may be seen from the outline given above, previous work has tended to neglect or ignore the possibility of drug-binding to A- or C-form DNA. However, as described in the next section, the present work is an attempt to examine the orientational nature of the interactions of proflavine with DNA in fibres under conditions in which the DNA adopts each of the three normal conformations.

### 4.4.2 Aims of Present Work

By measuring the intensities of certain diffraction spots it should be possible to distinguish from the X-ray data between between the various structures in which the drug molecules are not intercalated. For example, if the drug molecules were to bind specifically in the major grooves of the helix, this would reduce the groove size and alter the intensities of certain reflections compared to identical reflections for normal DNA. In order to observe these effects high concentrations of drug are required. Unfortunately, at such concentrations the diffraction patterns become very diffuse, making accurate measurements of intensity

impossible. In fact the patterns are often too diffuse for accurate measurement of the layer line separations. Under such conditions the X-ray technique is quite uninformative. On the other hand, ESR spectroscopy can provide a clear answer to the problem of the fate of the drug at any humidity. At low humidities the ESR spectra will reveal whether the drug molecules (in this case spin-labelled proflavine) are free in the fibre or bound externally to the DNA. Furthermore, in the latter case it will be possible to distinguish between randomly bound molecules and those which adopt specific orientations (see Section 4.1). The mobility of the drug molecules and the degree of alignment of the DNA in the fibre can also be determined. In the present study, in order to evaluate these parameters, computer simulations of the ESR spectra were obtained. The computer program used and the model on which it is based are described in sections 4.4.3 and 4.4.4.

Since the earlier X-ray diffraction studies were made much has been learned about the effects of salt concentration and humidity on the conformational properties of DNA in fibres (Rhodes et al., 1982). By strictly controlling the ionic strength and degree of hydration of the fibres conformational transitions can be regularly induced. In this way the binding of spin-labelled proflavine to the A-, B-, and C-forms of DNA can be examined. In particular, the nature of the binding to the low humidity (A and C) conformations can be investigated. Previous studies have suggested that intercalation occurs only in B-form DNA. It will be particularly interesting to study the possibility of intercalation for C-form DNA. The helical structure of the C conformation is closely akin to that of the B-form (see Chapter 1) and yet the C-form is present at low humidities. Hence there is here a contrast between the two factors which have been shown to have an important bearing on the process of intercalation viz., DNA conformation and relative humidity.

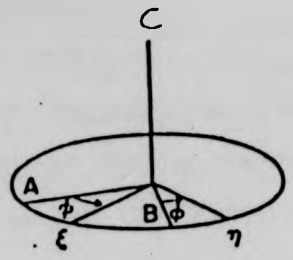


$$L^{\phi} = \begin{pmatrix} \cos\phi & \sin\phi & 0 \\ -\sin\phi & \cos\phi & 0 \\ 0 & 0 & 1 \end{pmatrix}$$

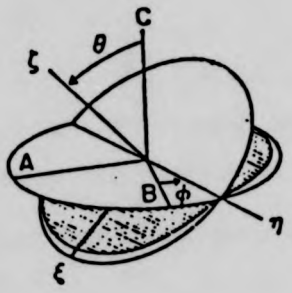


$$L^{\theta} = \begin{pmatrix} \cos\theta & 0 & -\sin\theta \\ 0 & 1 & 0 \\ \sin\theta & 0 & \cos\theta \end{pmatrix}$$

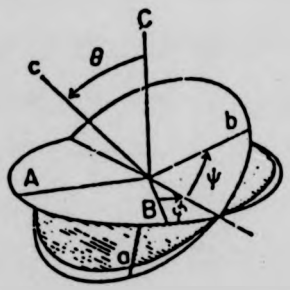


$$L^{\psi} = \begin{pmatrix} \cos\psi & \sin\psi & 0 \\ -\sin\psi & \cos\psi & 0 \\ 0 & 0 & 1 \end{pmatrix}$$

TRANSFORMATION MATRIX OF DIRECTION COSINES

$(L = L^{\psi} L^{\theta} L^{\phi})$

| | A | B | C |
|---|---|---|---|
| a | $\cos\theta\cos\phi\cos\psi - \sin\phi\sin\psi$ | $\cos\theta\sin\phi\cos\psi + \cos\phi\sin\psi$ | $-\sin\theta\cos\psi$ |
| b | $-\cos\theta\cos\phi\sin\psi - \sin\phi\cos\psi$ | $-\cos\theta\sin\phi\sin\psi + \cos\phi\cos\psi$ | $\sin\theta\sin\psi$ |
| c | $\sin\theta\cos\phi$ | $\sin\theta\sin\phi$ | $\cos\theta$ |

(After Van et al., 1974)

Fig. 4.9 Definition of the Eulerian Angles used in the Co-ordinate Transformations described in the text.

4.4.3 The Fibre Model

A theoretical treatment of the orientational nature of spin-labelled drug-DNA interactions will now be developed for later use in the analysis of the experimental results. The treatment is based upon those given by Jost and Griffiths (1976) and Porumb and Slade (1976).

The spin-Hamiltonian of a nitroxide free radical is described by (see Chapter 2)

$$H = \beta_e \mathbf{B}.\mathbf{g}.\mathbf{S} + \mathbf{S}.\mathbf{A}.\mathbf{I} \qquad (4.1)$$

where $\beta_e$ etc. have their usual meanings. The g and A tensors are diagonal in the nitroxide frame of reference, with principal values $g_{xx}$, $g_{yy}$, $g_{zz}$, and $A_{xx}$, $A_{yy}$, $A_{zz}$. It is more convenient to express H in the laboratory frame of reference. This is easily accomplished using the formalism set up by Van et al. (1974). Four coordinate systems are involved in the transformation to the laboratory frame - the nitroxide/drug frame $\sum(x, y, z)$, the DNA frame $\sum(x_2, y_2, z_2)$, the fibre frame $\sum(X_1, Y_1, Z_1)$ and the laboratory frame $\sum(X, Y, Z)$. The static magnetic field is assumed to be along the laboratory Z-axis. In the laboratory frame the **g** and **A** tensors are no longer diagonal. The transformation from one Cartesian reference frame to another is accomplished by successive rotations about each of the three coordinate axes. The transformation matrices $L_0$, $L_1$ and $L_2$ which rotate the reference frames into one another are defined in terms of the three rotation angles ("Eulerian angles") $\theta$, $\psi$ and $\phi$ (Fig. 4.9).

Assuming that the nitroxide group is rigidly attached to the proflavine molecule and taking the $2p_\pi$ orbital to be along the nitroxide z-axis then the transformation which sends $\sum(x, y, z)$ into $\sum(x_2, y_2, z_2)$ is given by

$$L_2 = L^{\psi} L^{\theta} L^{\phi} \qquad (4.2)$$

where

$$\mathbf{L}^{\phi} = \begin{bmatrix} \cos\phi_2 & \sin\phi_2 & 0 \\ -\sin\phi_2 & \cos\phi_2 & 0 \\ 0 & 0 & 1 \end{bmatrix}$$

$$L^{\psi} = \begin{bmatrix} \cos\psi_2 & \sin\psi_2 & 0 \\ -\sin\psi_2 & \cos\psi_2 & 0 \\ 0 & 0 & 1 \end{bmatrix}$$

and

$$L^{\theta} = \begin{bmatrix} \cos\theta_2 & 0 & -\sin\theta_2 \\ 0 & 1 & 0 \\ \sin\theta_2 & 0 & \cos\theta_2 \end{bmatrix}$$

The angle $\phi_2$ is a positive rotation of the nitroxide about the DNA $z_2$-axis (Fig. 4.10a); $\theta_2$ is the angle of tilt of the nitroxide z-axis relative to the DNA $z_2$-axis and $\psi_2$ is the angle of twist of the nitroxide about its own z-axis. The full form of the matrix is therefore:

$$L_2 = L^{\psi}L^{\theta}L^{\phi} = \begin{bmatrix} A_{11} & A_{12} & A_{13} \\ A_{21} & A_{22} & A_{23} \\ A_{31} & A_{32} & A_{33} \end{bmatrix}$$

where,

$A_{11} = \cos\theta_2\cos\phi_2\cos\psi_2 - \sin\phi_2\sin\psi_2$

$A_{12} = \cos\theta_2\sin\phi_2\cos\psi_2 + \cos\phi_2\sin\psi_2$

$A_{13} = -\sin\theta_2\cos\psi_2$

$A_{21} = -\cos\theta_2\cos\phi_2\cos\psi_2 - \sin\phi_2\cos\psi_2$

$A_{22} = -\cos\theta_2\sin\phi_2\sin\psi_2 + \cos\psi_2\cos\phi_2$

$A_{23} = \sin\theta_2\sin\psi_2$

$A_{31} = \sin\theta_2\sin\phi_2$

$A_{32} = \sin\theta_2\sin\phi_2$

$A_{33} = \cos\theta_2$

The transformation from the DNA helix to the fibre reference frame involves the angles shown in Fig. 4.10b. In this case $\theta_1$ is the angle of tilt of the DNA $z_2$-axis with respect to the fibre $Z_1$-axis, $\phi_1$ is a rotation about the fibre $Z_1$-axis and $\psi_1$ is the angle of twist about the DNA $z_2$-axis. The rotation $\psi_1$ can be set to zero since it has been accounted for by the rotation $\psi_2$ of the previous transformation. Therefore, the transformation

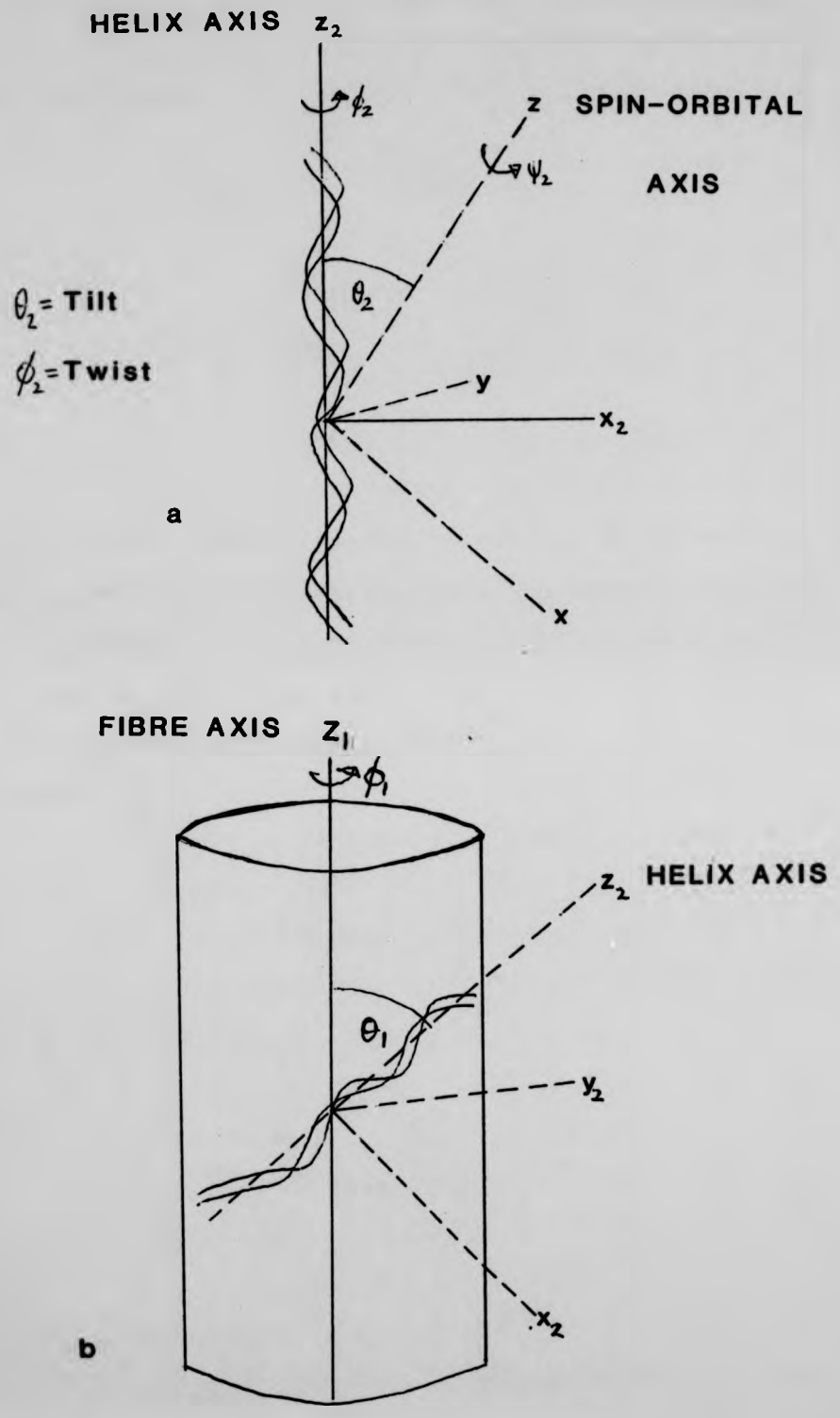


Fig. 4.10 (a) Angles involved in the Nitroxide-DNA transformation.
(b) Angles involved in the DNA-Fibre Transformation.

matrix which rotates $\sum(x_2, y_2, z_2)$ into $\sum(X_1, Y_1, Z_1)$ is

$$L_1 = L^{\theta}L^{\phi} \qquad (4.3)$$

or

$$L_1 = \begin{bmatrix} \mathrm{Cos}\theta_1\mathrm{Cos}\phi_1 & \mathrm{Cos}\theta_1\mathrm{Sin}\phi_1 & -\mathrm{Sin}\theta_1 \\ \mathrm{Sin}\phi_1 & \mathrm{Cos}\phi_1 & 0 \\ \mathrm{Sin}\theta_1\mathrm{Cos}\phi_1 & \mathrm{Sin}\theta_1\mathrm{Sin}\theta_1 & \mathrm{Cos}\theta_1 \end{bmatrix}$$

In the final transformation from the fibre to the laboratory frame the angles involved are $\theta_0$, $\psi_0$ and $\phi_0$. Since H is invariant to rotations about the laboratory Z-axis (i.e. the magnetic field), $\phi_0$ can be set to zero. $\psi_0$ can also be set to zero since rotations about the fibre $Z_1$-axis were accounted for by the previous transformation.

Therefore,

$$L = L_0^{\theta} = \begin{bmatrix} \mathrm{Cos}\theta_0 & 0 & -\mathrm{Sin}\theta_0 \\ 0 & 1 & 0 \\ \mathrm{Sin}\theta_0 & 0 & \mathrm{Cos}\theta_0 \end{bmatrix}$$

Thus, the coordinates of the nitroxide reference frame are given in the laboratory frame by

$$\begin{bmatrix} X \\ Y \\ Z \end{bmatrix} = L_0^{T}L_1^{T}L_2^{T} \begin{bmatrix} x \\ y \\ z \end{bmatrix}$$

where $L_0^T$ is the transpose of $L_0$ etc.

Using this transformation matrix the spin-Hamiltonian is expressed in the laboratory frame by

$$H = \beta_e B'.g'.S' + S'.A'.I' \qquad (4.4)$$

where the primes denote the laboratory frame and

$$g' = L^{\tau}.g.L = (L_0^I L_1^I L_2^I).g_{xyz}.(L_0 L_1 L_2)$$

$$A' = L^{\tau}.A.L = (L_0^I L_1^I L_2^I).A_{xyz}.(L_0 L_1 L_2)$$

These equations are formally identical to those presented in Section 2.5, Chapter 2. In the intermediate field approximation $g'$ and $A'$ are reduced to

$$g' = g_{xx}l^2 + g_{yy}m^2 + g_{zz}n^2 \qquad (4.5)$$

and

$$A' = (A_{xx}l^2 + A_{yy}m^2 + A_{zz}n^2)^{1/2} \qquad (4.6)$$

where l, m and n are the direction cosines between the nitroxide axes and the laboratory axes. In the fibre model the direction cosines are complex arguments of the nine Eulerian angles involved in the transformation between the two frames.

For an ideal fibre the DNA will be perfectly aligned. In practice the DNA molecules are arranged with their long axes only nearly parallel to the fibre $Z_1$-axis. That some degree of disorder is present is clear from the arcing of the spots of diffraction patterns of the DNA fibres. Several models of the packing of DNA in the fibres are possible. The model adopted here assumes that there is a Gaussian distribution of orientations of the DNA about the fibre $Z_1$-axis. A similar model was proposed by Libertini et al. (1969, 1974) to account for the ordering of lipid molecules in phospholipid bilayers. Provision is also made in the present model for the possibility that a fraction of the DNA may be randomly orientated in the fibre.

The angle $\theta_1$ gives the tilt of the DNA helix axis relative to the fibre $Z_1$-axis and the distribution function

$$P(\theta_1) = N^{-1}\mathrm{Sin}(\theta_1)\exp[-(\theta_1)^2/2\delta^2] \quad (4.7)$$

is such that $P(\theta_1)d\theta_1$ gives the fraction of DNA molecules lying within a cone of semi-angle $\theta_1$. N is a normalising constant and $\delta$ is the half-width of the distribution (standard deviation). For $\delta = 0$ there is perfect alignment of the DNA in the fibre; for $\delta = \infty$ there is complete misalignment (i.e. the DNA is randomly distributed). The term $\mathrm{Sin}(\theta_1)$ arises from the use of spherical coordinates .

The model presented thus far assumes that there is no motion of the spin-label system on the ESR timescale (i.e. $t_c > 10^{-8}$sec.). Modifications to the model to include the effects of rapid anisotropic motion are described later in this chapter.

A computer programme based upon the above model was used to obtain theoretical simulations of the fibre ESR spectra. The programme was based upon those described by Libertini et al. (1974) and Porumb and Slade (1976).

### 4.4.4 Computer Programmes

The programmes described below were written in Fortran IV and were run interactively on the GEC 4190 series computer at the University of Keele Computer Centre. They have also been adapted to run on the more powerful CDC 7600/Amdahl machines at Manchester. Facilities exist at Keele for directing output to VDU terminals, line printer, an "IMLAC" high resolution graphics terminal and a "Calcomp" plotter. Experimental spectra were input using the method given in Chapter 3.

Two main programmes are involved:

(a)**FIBRE**, which deals with the input of data (see below) and sets up the angular limits for generating the spin-label orientations.

(b)**SPCTR**, which calculates, for each orientation, the ESR absorption and derivative spectra.

The initial input parameters to **FIBRE** are:

1. The microwave frequency
2. The principal A- and g-values
3. The nuclear spin
4. The linewidth (or linewidths)
5. The lineshape (either Gaussian or Lorentzian)
6. The angle of tilt ($\theta_2$) of the drug/nitroxide to the DNA $z_2$-axis.
7. The degree of misalignment of the DNA in the fibre ($\delta$)
8. The angle of twist of the nitroxide about its own z-axis ($\psi_2$)
9. The orientation of the fibre in the magnetic field ($\theta_0$)
10. The angle of tilt ($\theta_1$) of the DNA in the fibre
11. The angle of rotation of the drug/nitroxide about the DNA axis ($\phi_2$)
12. The angle of rotation of the DNA about the fibre axis ($\phi_1$)
13. The initial field value and sweep range

There are provisions in the **FIBRE** programme for selective alteration of any of these parameters so that each one only needs to be entered once (i.e. at the first run).

The DNA molecules can be considered to be cylindrically symmetric. Therefore, once the tilt and twist angles ($\theta_2$ and $\psi_2$) of the drug relative to the DNA are defined, all other orientations of the drug can be obtained by rotations about the DNA $z_2$-axis. This is then followed by a further averaging about the fibre $Z_1$-axis. The rotation angles $\phi_2$ ($0 < \phi_2 < 360°$), $\phi_1$ ($0 < \phi_1 < 360°$) and $\theta_1$ ($0 < \theta_1 < 180°$) are therefore set to automatically pass through their allowed ranges in the desired increments. The direction cosines l, n and m are calculated for each orientation and

the resulting g- and A-values then calculated and passed to the subroutine **SPCTR**. This programme calculates the positions of the ESR absorption lines for each orientation of the nuclear spin. The line positions are obtained from

$$B_I = h\nu/g\beta - \sum m_I A \qquad (4.8)$$

where A is in milli-Tesla and $m_I$ = -1, 0, +1. A lineshape is then attached to the absorption (see Equations 2.17and 2.18 of Chapter 2). The result is then weighted by the distribution function $P(\theta_1)$ and added to the accumulator. The absorption is then calculated for the next orientation. This process is repeated until all orientations ($\theta_1$, $\phi_1$ and $\phi_2$) have been sampled. The accumulated spectrum is normalised by division by the sum of the weights. The derivative spectrum is then calculated and either stored or plotted for comparison with an experimental spectrum.

In the programme allowance is made for the possibility of the linewidths being field-dependent (see Chapter 2). Provision is also made for varying the tilt and/or twist angles automatically from within the programme. This is useful for obtaining simulations of spectra which consist of absorptions due to more than one bound component.

**Powder spectra** are calculated by setting the angles $\theta_2$, $\psi_2$ and $\delta$ to zero and redefining $\theta_1$ and $\phi_1$ to be the coordinates of the spin-labelled drug in the laboratory frame of reference. Since a gel produces a powder spectrum, the $Z_1$-axis (i.e. the gel axis) can be taken to be parallel to the DNA $z_2$-axis. The direction cosines l, n and m are then given by $\mathrm{Sin}\theta_1\mathrm{Cos}\phi_1$, $\mathrm{Sin}\theta_1\mathrm{Sin}\phi_1$ and $\mathrm{Cos}\theta_1$ respectively. The angles $\theta_1$ and $\phi_1$ are swept through their allowed ranges in the desired intervals ($0 < \theta_1 < 90'$ and $0 < \phi_1 < 180'$ unless the g- and A-tensors are symmetric about the z-axis, in which case $\phi_1 = 0$). The ESR absorption is calculated as before and then weighted by $P(\theta_1) = \mathrm{Sin}\theta_1$. After summing over all orientations the final derivative spectrum is calculated as for the fibre case.

In view of the large number of adjustable parameters involved in

the simulations no attempt was made to obtain a "goodness of fit" parameter by the least squares method. Acceptable simulations were instead obtained by a visual comparison of the simulated and experimental lineshapes.

The **FIBRE** and **SPCTR** programmes are listed in an appendix, together with subroutines which were used for scaling and plotting the simulated and experimental results.

### 4.4.5 Experimental Fibre Studies

In this section experimental studies of spin-labelled proflavine-DNA gels (powders) and fibres are presented. The experiments were carried out for several P/D values between 6 and 70 and at several values of relative humidity between 33% and 100%r. h. Fibres were prepared at 1mM and 100mM NaCl concentration.

Orientational information was obtained from the fibres from the anisotropy of the ESR spectra. Computer simulations were used to determine the parameters of the fibre model (e.g. the angle of tilt of the drug and the degree of misalignment of the DNA).

### 4.4.5 (a) Method

Stock solutions of $8 \times 10^{-3}$M DNA in 1mM (or 100mM) NaCl were prepared and appropriate quantities of $2.6 \times 10^{-3}$M spin-labelled proflavine were added dropwise by pipette. Extreme care was exercised in this task since precipitation of the DNA at low ionic strengths was easily provoked. Complexes were best prepared by mixing the solutions cold (at 4°C). After centrifuging for 8-12 hours at 40,000 rpm, the resulting gel was used to prepare fibres by the method described in Chapter 3. Each gel produced some 4-6 fibres whose dimensions varied between 2-4mm in length and 0.1-0.3mm in diameter. The degree of orientation of the DNA in the fibre was quickly estimated by measuring its birefringence. Thin fibres were generally better orientated since large fibres (diameter > 0.2mm) tended to

dry unevenly at room temperature. However, large fibres showed an improved orientation when allowed to dry in a cold atmosphere.

After removing from the glass rods a fibre was placed on the sticky side of a piece of selotape (3mm x 3mm) and mounted on either a Varian tissue cell or on a home-made quartz-rod and goniometer device. In both cases the fibre could be easily aligned in the magnetic field. Further orientations of the fibre were obtained by rotating the sample-holder.

The usual spectrometer settings were: microwave frequency 9.5-GHz, 100-KHz modulation frequency amplitude 0.05 - 0.125mT, microwave power 15mW, filter time constants (PSD) 0.1 - 0.3secs., sensitivity (PSD) 10$\mu$V cm$^{-1}$, scan speed (magnet) 1.5mT min$^{-1}$ and scan speed (XY-plotter) 20sec. cm$^{-1}$. All experiments were carried out at room temperature (18° - 20°C).

Two fibres resulting from each gel were selected. One was examined by ESR spectroscopy, the other by X-ray diffraction. In both cases the full range of humidities was used. In this way the various ESR spectra were identified with particular DNA conformations. Humidification of the fibres in the ESR experiments was achieved by the method describred in Chapter 3. In the X-ray diffraction experiments helium was used instead of compressed air. In both cases the volume being humidified was quite small (i.e. the ESR cavity and the X-ray camera). At high rates of flow the ESR cavity became saturated whatever salt solution was used. This easily led to erroneous identifications being made of the ESR spectra with particular DNA conformations. Therefore, unless complete saturation of the fibres was required, the rate of flow was reduced to a minimum. To obtain virtually 100% saturation the following procedure was adopted. A fibre was first placed in a cold room at 4°C for several hours (or days) after which time it had absorbed enough water to become visibly swollen. The fibre was then quickly placed in the ESR cavity and humidified at 98% r. h. (at

maximum flow rate). Under this condition the fibres remained wet for up to 1 hour.

In the general case a systematic procedure was adopted in which a fibre was first examined at low relative humidity and then at several intermediate humidities up to 98% r. h. At each humidity the ESR spectrum at each orientation of the fibre to the magnetic field was recorded.

4.4.5 (b) Results

ESR spectra were recorded several times during the humidification process. Humidification was considered to be complete when no further changes in a spectrum were observed. This procedure often took a considerable time. It was found that, although the ESR cavity quickly attained the set humidity, conformational transitions of the DNA took considerably longer. Two factors were involved here: the rate at which the fibre absorbed water and the rate at which the DNA changed its conformation.

The rate at which a fibre absorbed water (at a given air-flow rate) depended upon the size of the fibre, the salt concentration and the final relative humidity. In this case the salt concentration was fixed at 1mM NaCl and as might be expected, humidification was quickly completed for any fibre between 58% and 75% r. h. At higher or lower humidities small fibres reached equilibrium more quickly, although this often took more than 1 hour. Conformational transitions of the DNA accompanied the rise and fall in the level of hydration of the fibres, and these transitions usually occurred quite rapidly. Some specific examples will now be given.

It is convenient to define a splitting (or coupling) constant $\Delta A$ which gives the distance in Gauss between the high-field and low-field peaks of a derivative ESR spectrum. The following notation shall be used: $\Delta A_{\parallel}^{i}$ and $\Delta A_{\perp}^{i}$ will refer to the splittings of the parallel and perpendicular orientations of a fibre in the magnetic field, where i = a, b or c will

denote the DNA conformation. Thus, $\Delta A_{\parallel}^{C}$ will refer to the splitting of the parallel orientation of a fibre for C-form DNA. In this notation $\Delta A_{g}^{i}$ will refer to the splitting for a gel spectrum. The measured splittings are accurate to at least 0.1 milli-Tesla.

The DNA of a fibre of P/D = 70 was found to adopt an A-type conformation at 44% r. h. (Fig. 4.28). The gel and fibre ESR spectra associated with this conformation are given in Figs. 4.11(a-d). The apparent coupling constants for the parallel and perpendicular orientations of the fibre are $\Delta A_{\parallel}^{a} = \Delta A_{\perp}^{a} = 7.0$mT. A certain degree of anisotropy is visible in the lineshapes although the spectrum for the 45° orientation of the fibre is virtually identical to that for the parallel orientation. These spectra remained unchanged for all humidities up to 98% r. h. At this humidity the fibre gave a B-type diffraction pattern (Fig. 4.28). The spectra associated with this conformation are shown in Figs. 4.12(a-d). The spectrum recorded with the fibre parallel to the magnetic field is little altered in shape from the spectrum obtained at the lower humidities, although there is a reduction of the coupling constant of approximately 0.8mT ($\Delta A_{\parallel}^{b} = \Delta A_{45}^{b} = 6.2$mT). A more drastic change in the spectrum is apparent for the perpendicular orientation of the fibre. The lineshape is now completely altered compared with the A-form spectrum and the coupling constant is reduced by approximately 2.8mT to $\Delta A_{\perp}^{b} = 4.2$mT. The gel spectrum for this fibre has a splitting of about 5.5mT. The A → B transition observed here was monitored over a period of a few minutes and this transition, as depicted by changes in the ESR spectra at 92% r h., is shown in Fig. 4.13. The corresponding A/B mixture diffraction pattern recorded at the same humidity is shown in Fig. 4.29. It was reversed upon lowering the humidity to below 98% r. h. It was expected that the low salt concentration in the fibre would enable the DNA to go into the C-conformation at low humidity. However, the C-conformation was only observed as an A/C mixture after prolonged exposure (~40hrs) at 33%

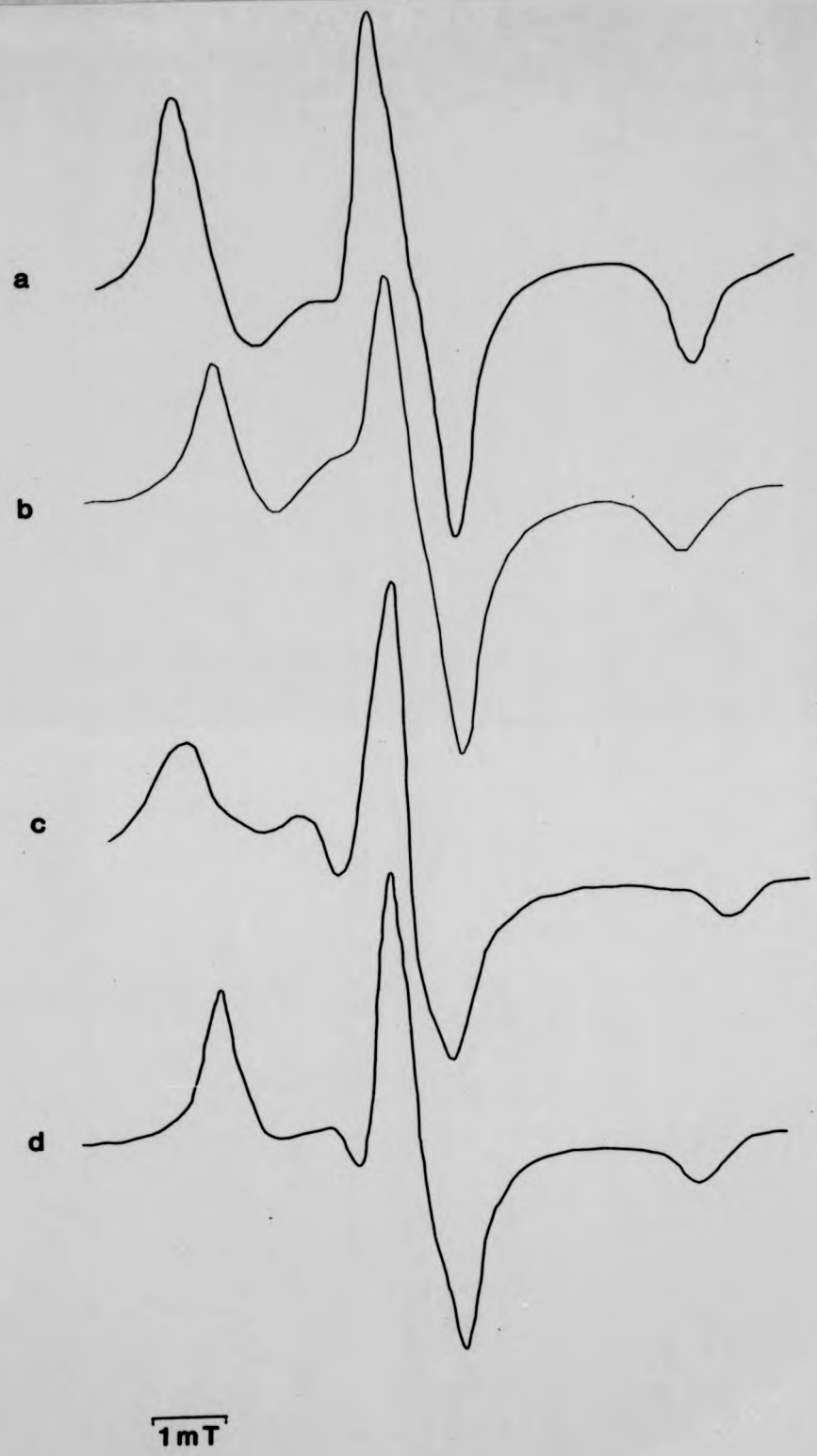


Fig. 4.11(a-d) Experimental A-Form Gel and Fibre Spectra (P/D = 70) recorded at 44% relative humidity: (a) 0° (b) 45° (c) 90° (d) gel.

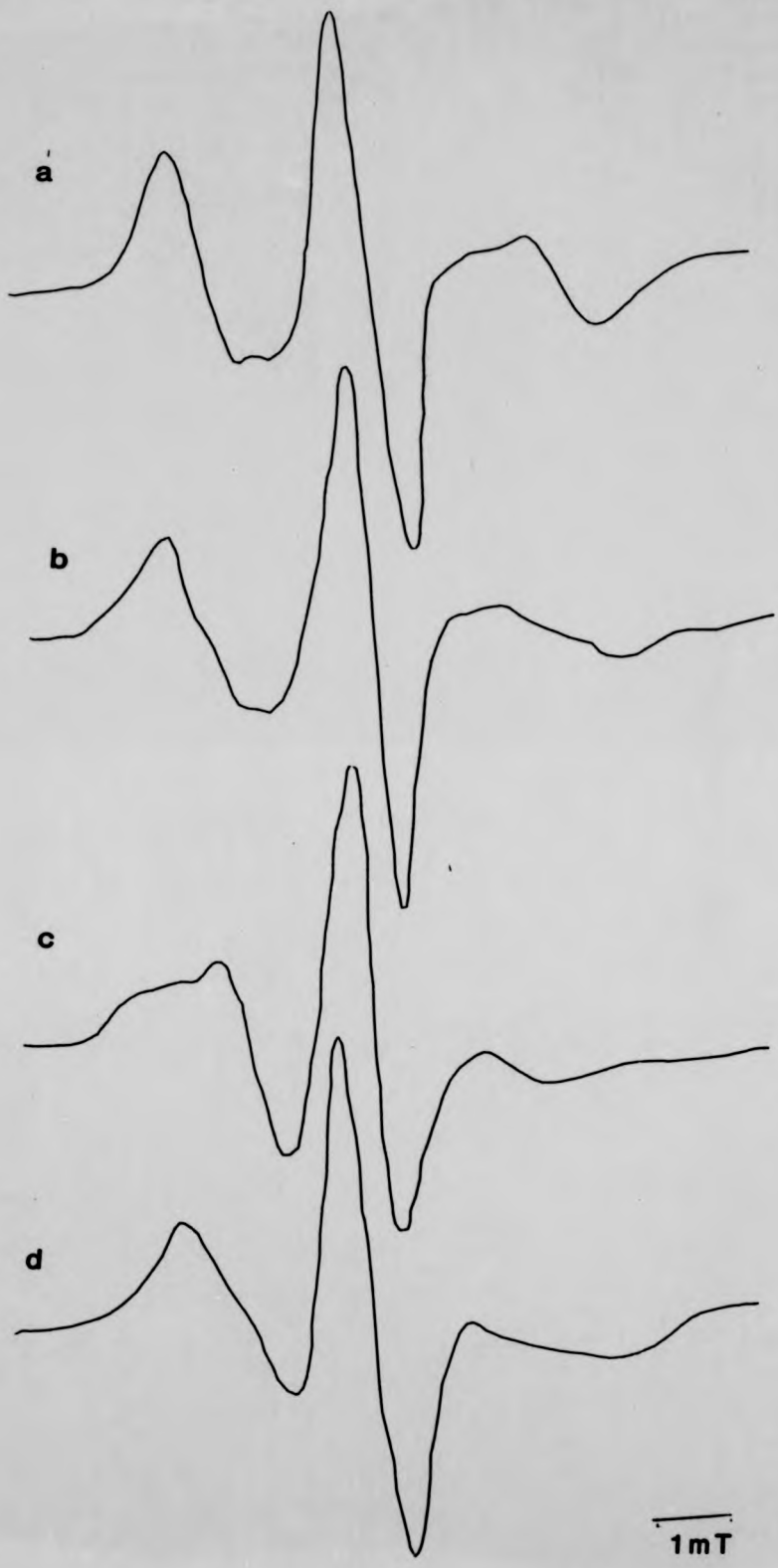


Fig. 4.12(a-d) Experimental B-Form Gel and Fibre Spectra (P/D = 70) recorded at 98% relative humidity: (a) 0° (b) 45° (c) 90° (d) gel.

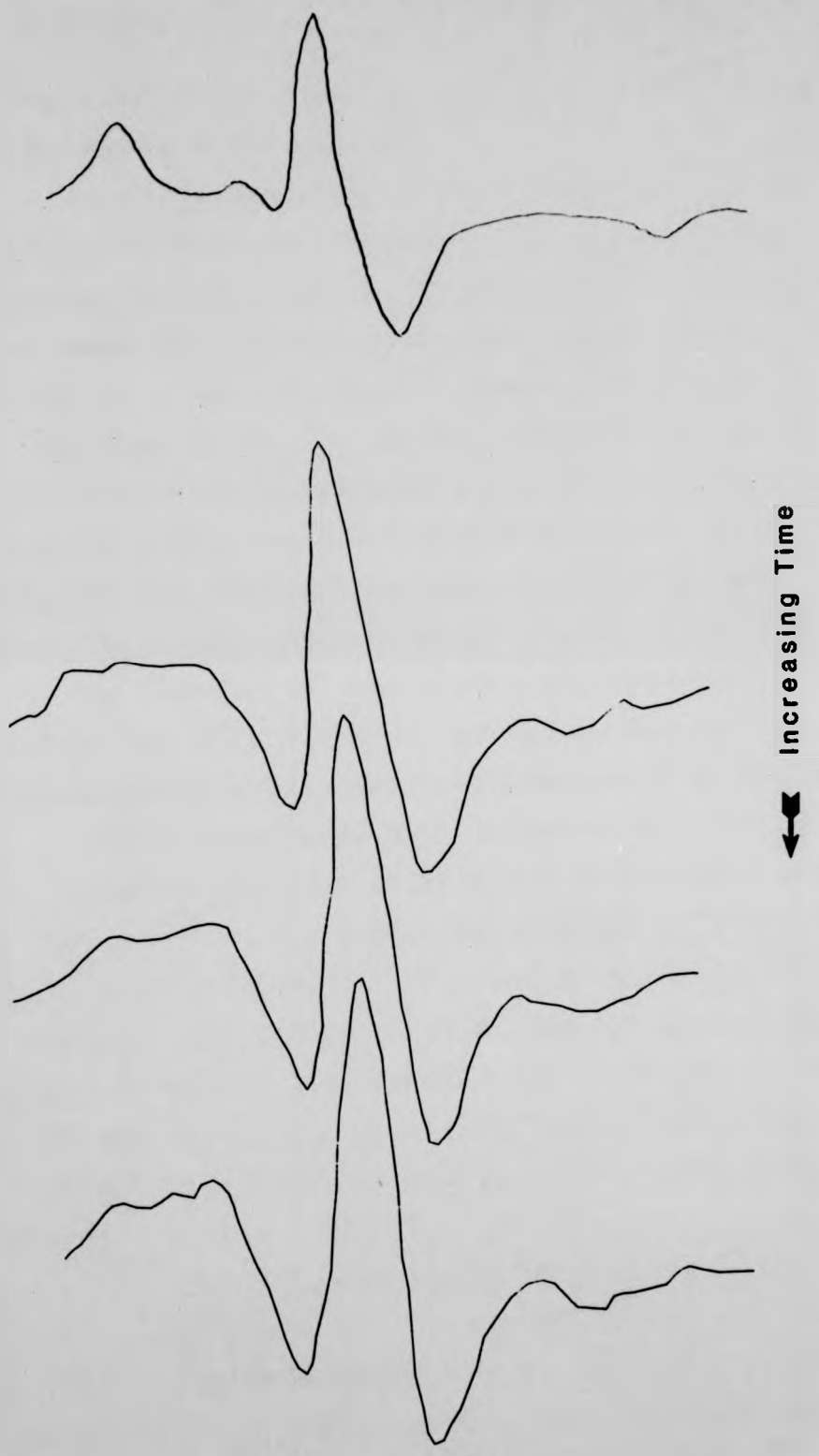


Fig. 4.13 The A → B Transition monitored by changes in the the Fibre ESR Spectra at 92% relative humidity.

r h. (Fig. 4.29). Similar results were obtained from a fibre prepared at a P/D of 50, although no C-form was seen.

The results obtained for a fibre of P/D = 6 were quite different. At 33% r. h. the fibre gave a C-type diffraction pattern (Fig. 4.30). The corresponding ESR spectra are given in Figs. 4.14(a-d). X-ray diffraction studies showed that the fibre retained the C-type conformation at all humidities up to 98% r. h. The ESR lineshapes were also constant over these humidities. At 98% r. h. the fibre adopted a B-type conformation, and the ESR spectra for this conformation are shown in Figs. 4.15(a-d). On lowering the relative humidity to below 98% the C-form was recovered. However, for this fibre no A-type spectra or diffraction patterns were observed. The diffraction patterns recorded are shown in Figs. 4.30.

The lineshapes at this P/D are considerably broadened at all orientations and at all humidities. Nevertheless, there are some clear differences between the B-form spectra and those recorded at low humidity.

The splittings for the B-form spectra are $\Delta A_{\parallel}^{b}$ = 6.2mT and $\Delta A_{\perp}^{b}$ = 4.2mT. These splittings are identical to those of the B-form spectra for the fibre of P/D = 70. However, the lineshapes in this case are dramatically broadened compared with the previous fibre and the presence of two components is indicated. The C-form spectra on the other hand are completely different to any previous results: although the coupling constants are equal to those of the A-form spectra of the previous fibre the lineshapes are considerably altered, particularly for the perpendicular orientation.

This is more clearly seen in the results obtained from a fibre of P/D = 30. The C- and B-form ESR spectra obtained are given in Fig. 4.16(a-c). The DNA conformations for this fibre were first identified on the basis of the ESR results and these identifications were then later confirmed by X-ray diffraction. At this concentration of spin-labelled drug the spectra show some evidence of broadening but it is easy to see

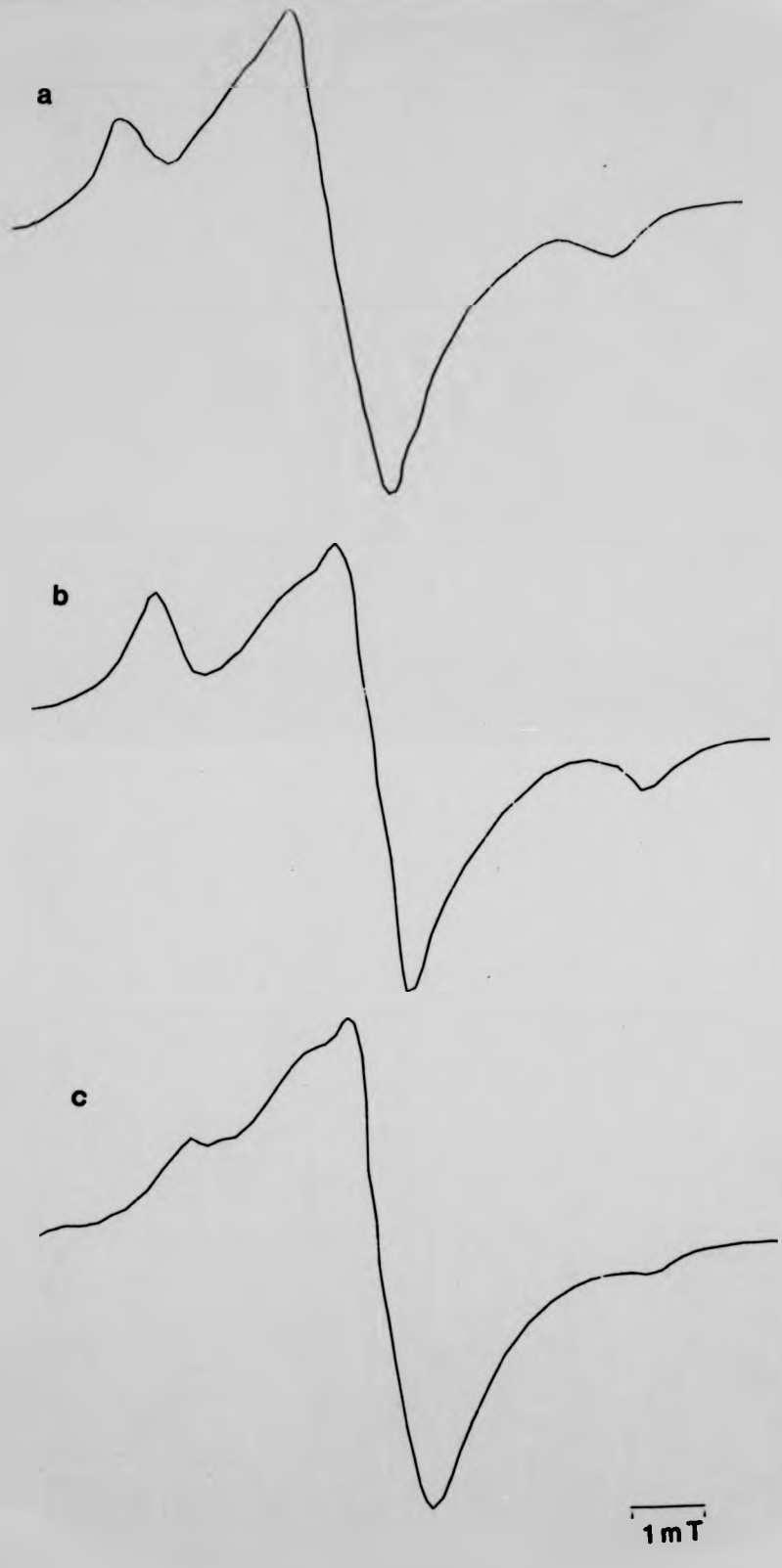


Fig. 4.14(a-c) Experimental Fibre Spectra (P/D = 6) recorded at 33% relative humidity: (a) 0° (b) 45° (c) 90° (C-Form DNA).

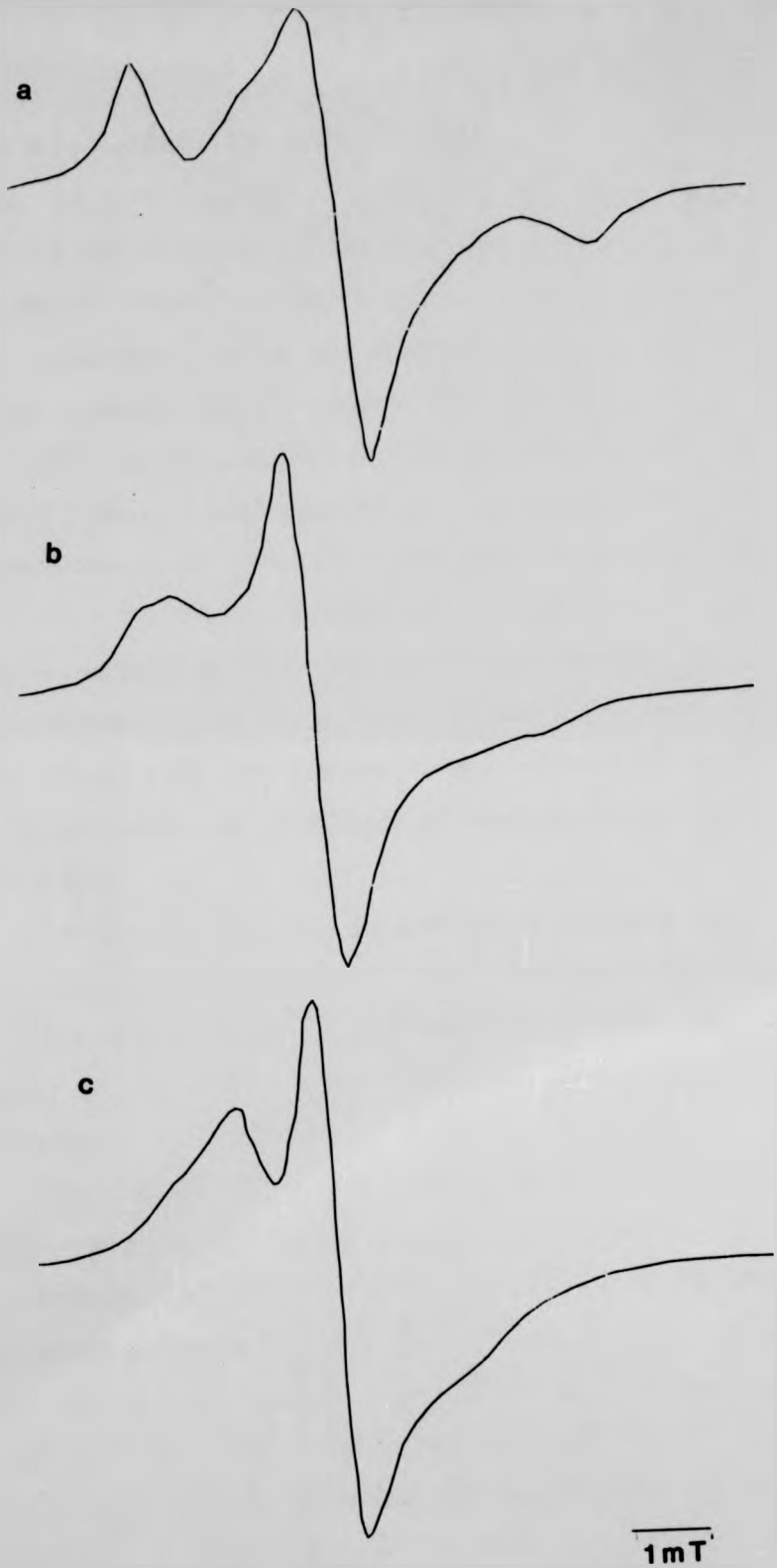


Fig. 4.15(a-c) Experimental Fibre Spectra (P/D = 6) recorded at 98% relative Humidity: (a) 0° (b) 45° (c) 90° (B-Form DNA).

that the B-form spectra are similar to those previously obtained (i.e. at P/D = 70). The C-form spectra still have the same coupling constants as at this P/D, but the lineshapes are now more clearly defined. The spectra for parallel and 45° orientations of the fibre give lineshapes similar to those of the A-form spectra at the same orientation. However, there are some differences apparent in the shapes of the central ($m_I$ = 0) absorption lines. This is more obvious in the spectrum for the perpendiclar orientation, where a peak occurs between the low-field and centre lines. The possible reasons for this will be discussed later in the chapter.

All the fibres examined at ~ 100% r. h. gave B-type diffraction patterns and their ESR spectra were identical in all respects to those recorded at 98% r. h. It is interesting to note, however, that all the fibres which were examined at this humidity had a tendency to remain in the B-form when re-examined at lower humidities, even after long exposure at 33%.

The fibres used in the experiments performed thus far were prepared from Calf Thymus DNA. Interesting results were also obtained from fibres containing Miccroccocus Lysodiekticus (GC-rich) and Clostridium Perfringens (AT-rich) DNAs. These fibres were prepared at a P/D of 25 and a salt concentration of 1mM NaCl.

The GC-rich fibre gave an A-type diffraction pattern at all humidities up to 98% and at this humidity a B-type pattern was observed. The corresponding ESR spectra are not shown here since they were closely similar to those obtained for Calf Thymus DNA.

The AT-rich fibre on the other hand produced some quite unexpected results. The C-form ESR spectra at 33% r. h. were very broad and only a small degree of anisotropy was noticeable between the parallel and perpendicular orientations of the fibre (Figs. 4.17(a, b)). The broadening was similar to that observed at high concentrations of spin-labelled proflavine (e.g. at P/D = 6). At 98% r h. a transition to

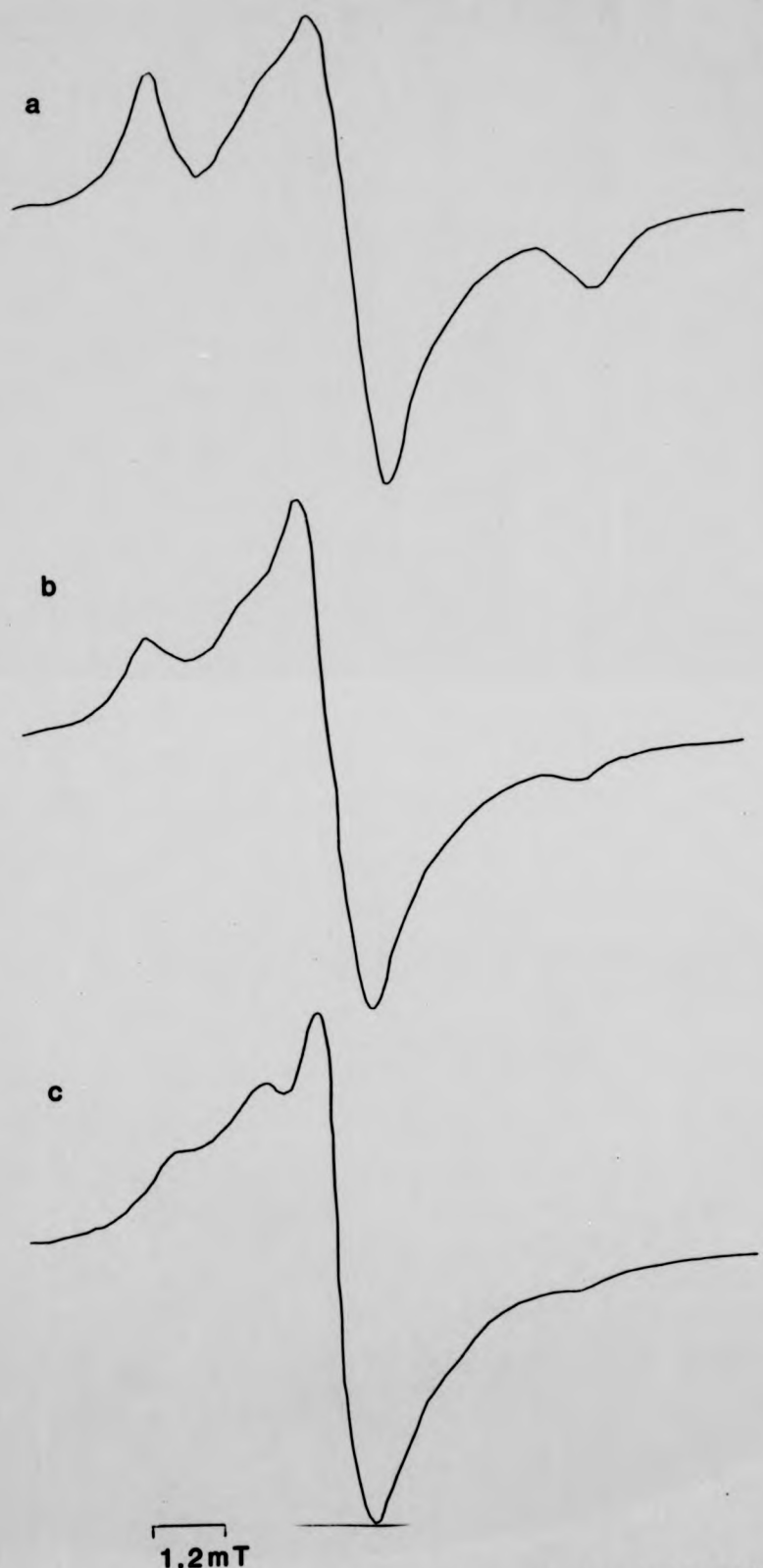


Fig. 4.16(a-d) Experimental C-Form Gel and Fibre Spectra (P/D = 25) recorded at 33% relative humidity: (a)0° (b) 45° (c) 90°

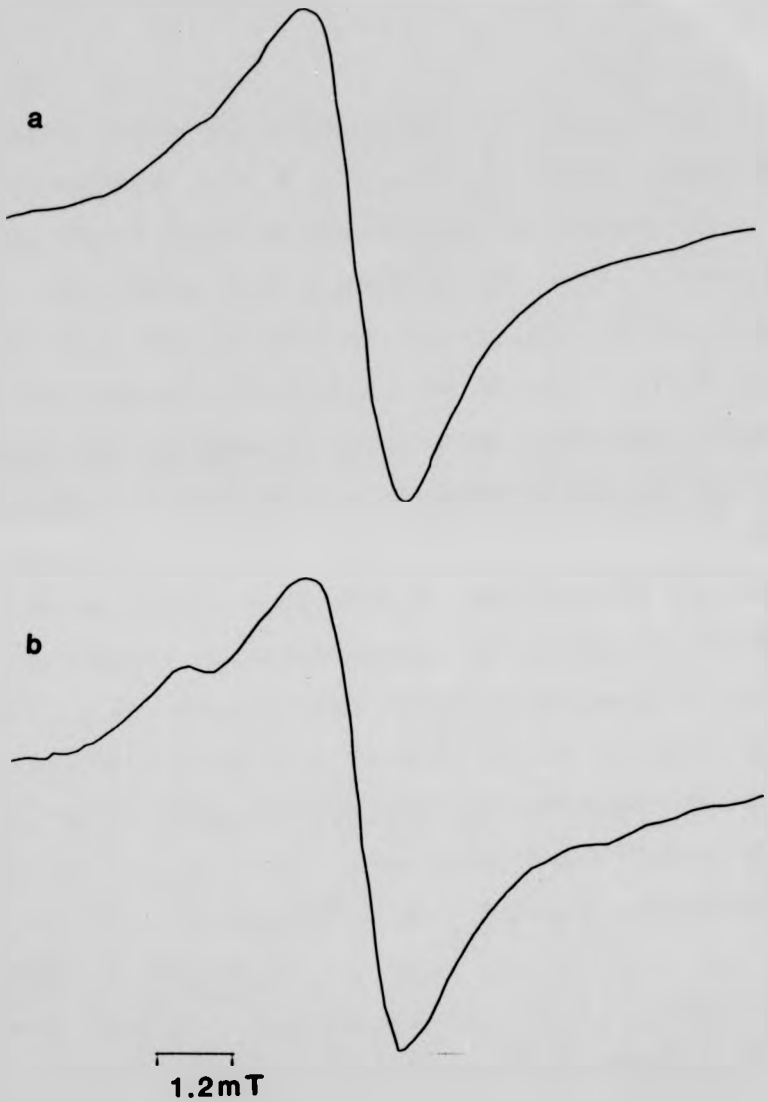


Fig. 4.17(a,b) AT-Rich DNA Fibre Spectra (P/D = 20) recorded at 66% relative humidity: (a) 0° (b) 90° (C-Form DNA).

the B-form was observed in the X-ray patterns but the ESR spectra remained unchanged.

4.4.5 (c) Discussion

These results clearly show that conformational transitions of the DNA complexed with proflavine occur at high humidities and that changes in the ESR spectra take place almost simultaneously with these transitions.

Although the amount of water present in the fibres increases exponentially with the level of hydration, the influence of water in determining the ESR linshapes is negligible. The following observations support this claim. Although there is large increase in the water content of a fibre between 33% r. h. and 92% r. h. no changes in the ESR spectra were observed during this interval. The lineshapes only changed at 98% r.h. and the X-ray studies showed that at this humidity the DNA molecules made a transition to the B-conformation. Of course, even between 92% r. h. and 98% r. h. there is as a large increase in the amount of water present in a fibre. If this fact alone accounted for the changes in the ESR spectra then further changes should have been observed when the relative humidity was raised to ~ 100%. However, no further changes were observed at this humidity. In the analysis of the ESR results the effects of water can therefore be neglected.

The results given in the previous section indicate that there are two possible conformations for DNA in the complexes below 98% r. h. At high concentrations of bound spin-labelled proflavine the DNA adopts a C-type conformation; at lower levels of drug an A-type conformation is preferred. In both cases a transition to the B-form occurs at 98% r. h.

The anisotropy exhibited in the spectral lineshapes at a given relative humidity for various orientations of a fibre in the magnetic field indicates that the spin-labelled proflavine molecules adopt specific orientations in the DNA.

In order to carry out a quantitative analysis of the experimental results it is convenient to treat the results for each of the DNA conformations separately.

**A-form Spectra and their Simulations**

The following discussion considers as a specific case the ESR spectra obtained from a fibre and its corresponding gel at 33% r. h. and a P/D of 70. These spectra are shown in Figs. 4.11(a-d).

The large hyperfine maxima of 7.0mT observed for all orientations of the fibre to the magnetic field are indicative of a lack of motion of the spin-labelled molecules about any direction. The drug molecules are therefore either rigidly bound to the DNA or are constrained by some other feature of the interaction, for example by some form of steric hindrance. The spin-label itself is assumed to have no motion independent of the proflavine molecule to which it is bound. This assumption - the justification for which has previously been mentioned (Section 4.2) - will be considered more fully in due course.

A gel represents a state in which the DNA molecules are randomly distributed in all directions. The gel spectrum (Fig. 4.11d) therefore consists of a superposition of the spectra from all orientations of the spin-labelled drug. The lineshape of the gel spectrum ($\Delta A_g^a$ = 7.0mT) is similar in many respects to the lineshapes recorded at several orientations of the fibre. This fact, together with the limited anisotropy exhibited by the fibre spectra suggests that there may be a fraction of randomly bound drug molecules present in the fibre. Whether or not this is the case can only be determined by a quantitative examination of the orientational nature of the binding of the spin-labelled molecules.

In the following discussion a theoretical calculation of the gel spectrum is carried out and the magnetic parameters obtained are then used to aid the more complex calculations involved in simulating the fibre

spectra.

**Gel Simulation**

In order to simulate the gel spectrum the only variables required were the principal g- and A-values and the linewidths. As a starting point in the calculation the principal g-values used were those published in Berliner (1976) for 3-Carboxy-2,2,5,5-tetramethylpyrroline-1-oxyl: $g_{xx}$ = 2.0088, $g_{yy}$ = 2.0066 and $g_{zz}$ = 2.0032.

The linewidths and hyperfine values were varied within the powder programme until a reasonable fit to the experimental spectrum was obtained. The angles $\theta_1$ and $\phi_1$ were stepped through their allowed ranges in 4° and 12° intervals respectively. Larger intervals than these produced powder spectra which were not adequately sampled over all orientations; smaller intervals of $\theta_1$ and $\phi_1$ were adequate but the calculations were then more time-consuming. With the given intervals each spectrum consisted of the sum of 315 components.

A good fit to the experimental spectrum was obtained with the following set of parameters:

| | | |
|---|---|---|
| | $g_{xx}$ = 2.0088 | $A_{xx}$ = 0.64mT |
| | $g_{yy}$ = 2.0066 | $A_{yy}$ = 0.64mT |
| | $g_{zz}$ = 2.0027 | $A_{zz}$ = 3.49mT |
| Linewidths: | $m_I(-1)$ = 0.44mT | |
| | $m_I(0)$ = 0.38mT | |
| | $m_I(+1)$ = 0.38mT | |

Lineshape: Lorentzian.

A small change in the z-component of the g tensor was required in order to improve the fit to the high-field part of the spectrum. The x- and y-components of the g tensor could be altered slightly without making too much difference to the calculated fit. The maximum hyperfine component, $A_{zz}$, was obtained from the experimental spectrum. $A_{xx}$ and $A_{yy}$

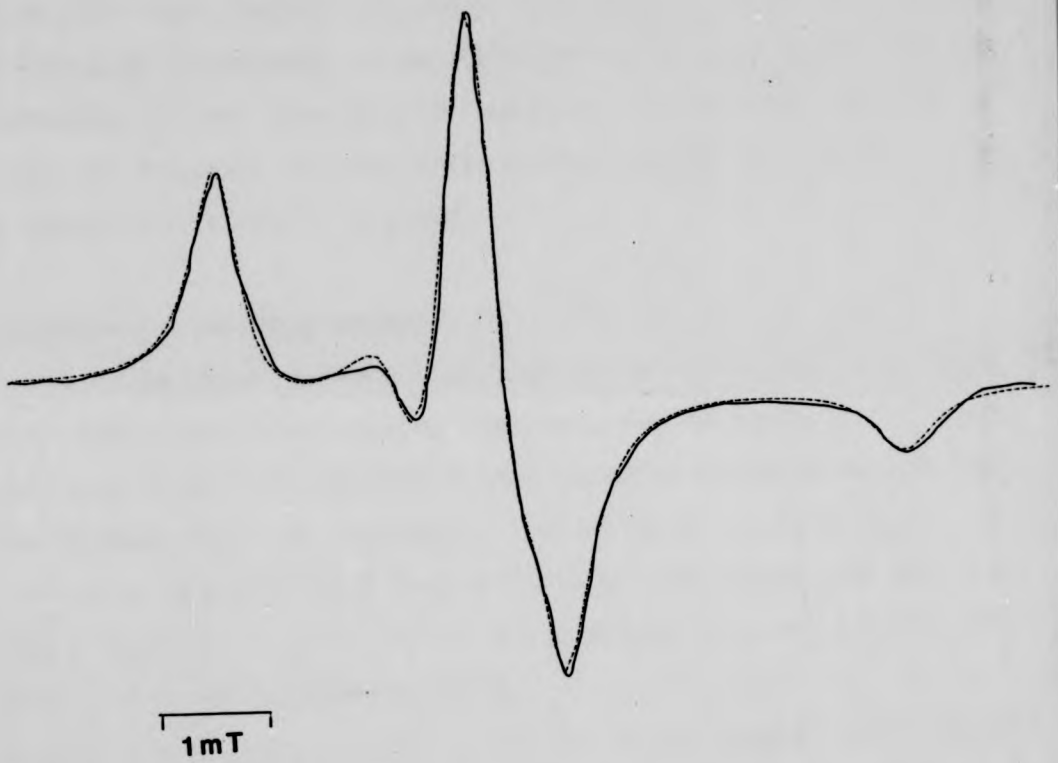


Fig. 4.18 Computer Simulation of the A-Form Gel Spectrum.

could also be varied within small limits. A Gaussian lineshape was also tried but this did not fit the high-field part of the spectrum quite as well as the Lorentzian. However, a mixture of both lineshapes, weighted about 50:50, gave a good fit. The best fit was obtained by broadening the high-field line relative to the other components. The origin of the differential linewidths, in the absence of molecular motion, lies in the anisotropy of the g-values (see Chapter 2). The simulated spectrum is shown in Fig. 4.18, together with its experimental counterpart. The calculated fit is clearly very good.

**Simulations of the Fibre Spectra**

The input parameters required for the fibre simulations, aside from the g- and A-values and the linewidths, were the angles of tilt ($\theta_2$) and twist ($\psi_2$) of the spin-orbital with respect to the DNA helix axis and the maximum angle of misalignment ($\delta$) of the DNA in the fibre. In calculating the theoretical spectra it was initially assumed that all the drug molecules are bound to the DNA in the same way (i.e. there is only one angle of tilt and one angle of twist).

The angles $\theta_1$, $\phi_2$ and $\phi_1$ were set to sweep through their allowed ranges in 4°, 15° and 15° intervals respectively. With these intervals a simulated spectrum would consist of more than 25000 components. In practice, however, the weighting function $P(\theta_1)$ (Section 4.4.4) operates so as to reduce the number of significant components to less than 2500.

The g- and A-values used in the following calculations were those estimated from the gel simulation. The tilt and twist angles and the angle of misalignment were varied until a set of parameters was obtained which simulated the experimental spectra for all orientations of the fibre to the magnetic field. In determining these parameters the angle of twist was initially set to zero and only the tilt and misalignment were varied. The linewidths were initially considered to be equal and were given a value of

0.45mT. A Lorentzian lineshape was assumed. By altering the value of tilt and misalignment concurrently a set of spectra was obtained from which an estimate was made of the probable values of these parameters. Some examples of these simulations are shown in Figs. 4.19 and 4.20.

In Fig. 4.19 the angle of tilt was set to zero and a series of spectra corresponding to the parallel and perpendicular orientations of the fibre are shown for several angles of misalignment between 0° and 70°. In Fig. 4.20 the angle of tilt was varied and simulations are shown for a misalignment of 50°.

In both sets of simulations only those combinations of tilt and misalignment which gave the experimentally observed maximum hyperfine splitting ($\Delta A_{\parallel}^{a}$ =7.0mT) were considered. An examination of the simulated lineshapes indicates that the best fit to the experimental spectra occurs with a zero tilt angle and a misalignment of between 40° and 50°.

The next step in the simulation consisted of a refinement of the calculated fit. This was accomplished by first evaluating the effects on the simulated lineshapes of variations in the angle of twist. The introduction of a non-zero angle of twist considerably improved the calculated fit, particularly to the spectrum for the perpendicular orientation of the fibre. The fit was also improved by broadening the outer lines relative to the central line. With these refinements the final parameters used in the simulations were:

$g_{xx}$ = 2.0088 $A_{xx}$ = 0.64mT

$g_{yy}$ = 2.0066 $A_{yy}$ = 0.64mT

$g_{zz}$ = 2.0027 $A_{zz}$ = 3.49mT

The angle of tilt of the spin-orbital, $\theta_2$ = 0° ± 5°

The angle of twist of the spin-label about its z-axis, $\psi_2$ = 50° ± 5°

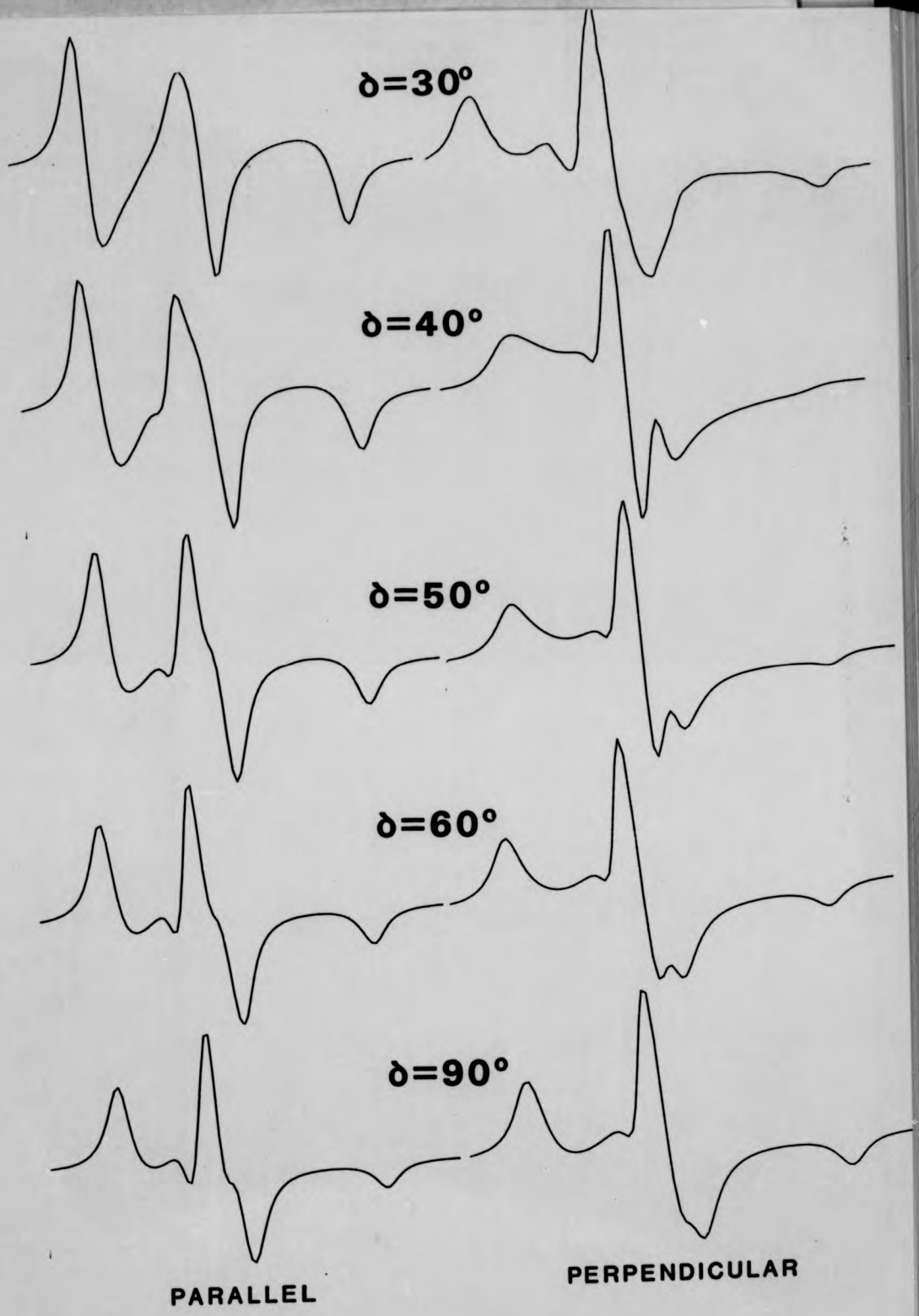


Fig. 4.19 Computer Simulations of the Fibre Spectra for several angles of misalignment (Tilt = 0°).

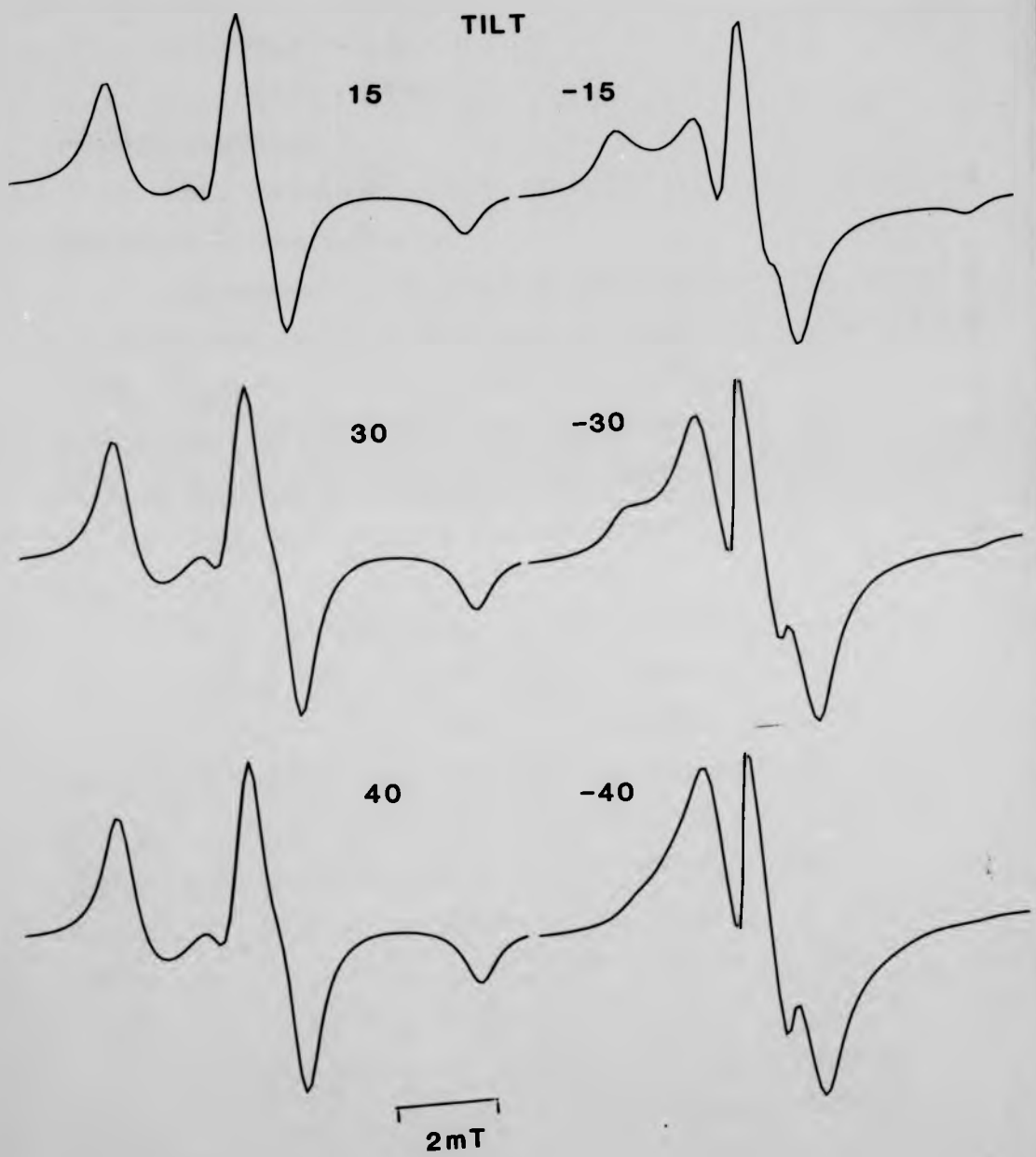


Fig. 4.20 Computer Simulations of the Fibre Spectra for several angles of tilt (Misalignment = 50°).

The angle of misalignment of the DNA in the fibre, $\delta$ = 45° - 50°

The linewidths, $m_I(-1)$ = 0.48mT

$m_I(0)$ = 0.44mT

$m_I(+1)$ = 0.48mT

Lineshape: Lorentzian.

The theoretical spectra are shown with their experimental counterparts in Figs. 4.21(a,b).

The agreement in the splittings and lineshapes of the theoretical and experimental spectra is quite good, particularly for the low-field and central absorption lines. The fluctuations which appear in the high-field line of the simulated spectrum for the perpendicular orientation of the fibre can be eliminated by increasing the high-field linewidth. However, the fit to the spectrum of the parallel orientation of the fibre is then spoilt.

It was earlier suggested that the lack of anisotropy of the fibre spectra (except at extreme orientations) was indicative of a certain degree of randomness in either the binding of the drug molecules to the DNA or in the orientations of the DNA within the fibre. However, these simulations show that the experimental spectra can be successfully reproduced without explicitely including in the calculations a fraction of randomly orientated drug or DNA molecules. Nevertheless, a good fit to the experimental spectra was only obtained by allowing for a large spread in the orientations of the DNA in the fibre.

At high concentrations of bound drug the regular geometry of the DNA helices would be disrupted and this may be expected to produce a fairly high degree of misorientation of the DNA within the fibre. In the present case, however, the drug concentration was low (P/D = 70) and the estimated angle of misalignment is therefore surprisingly high. On the other hand, a reduction in the angle of misalignment to 20° or 30°, in combination with various angles of tilt, proved to be fruitless. For example, although a

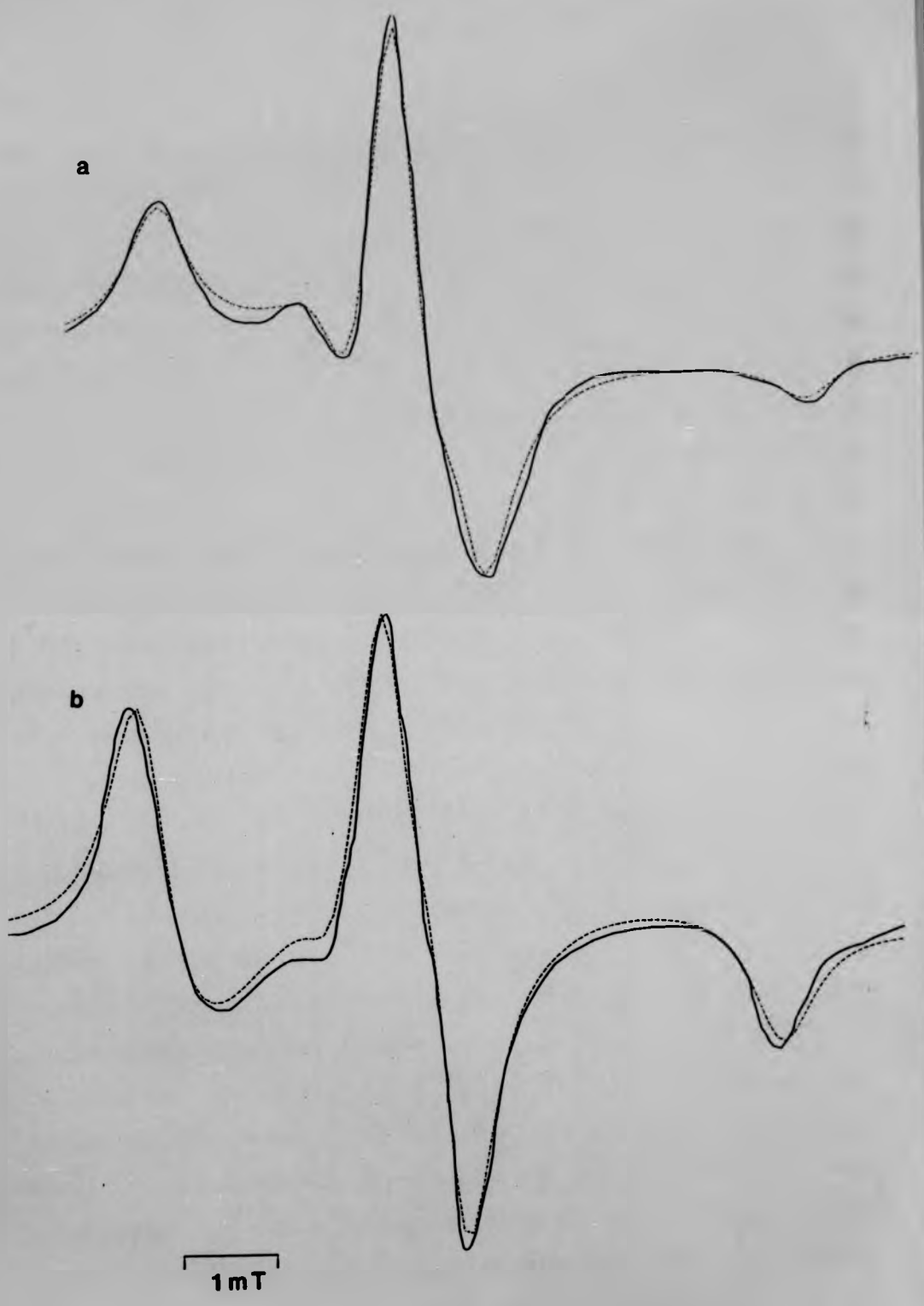


Fig. 4.21(a,b) Computer Simulations of the A-Form Fibre Spectra: (a) 0° (b) 90°.

tilt of 30° and a misalignment of 30° produced a reasonable simulation of the perpendicular spectrum, the corresponding simulation of the parallel spectrum gave a hyperfine splitting which was 1mT too small.

It has hitherto been assumed that all the drug molecules are bound to the DNA in the same way. However, by allowing for a spread in the orientations of the drug molecules, the degree of misorientation of the DNA could be reduced. This "spread" could take the form of a Gaussian distribution of orientations of the drug molecules about a preferred angle of tilt. Two types of misalignment would then be present: the misalignment of the DNA molecules about the fibre $Z_1$-axis and the misalignment of the drug molecules about their preferred angle of tilt to the DNA helix axis. In the present simulations the preferred angle of tilt puts the nitroxide z-axis approximately parallel to the helix axis. A combination of the two distributions may well account for the total misalignment, estimated in this case at between 45° and 50°.

In practice, to avoid further increasing the number of variables involved in the theoretical calculation, it is assumed that the total misalignment is due only to the misorientation of the DNA.

In order to estimate the orientation of the proflavine molecule relative to the DNA helix axis, CPK and wire frame models of the proflavine-nitroxide system were studied. These models show that the plane of the nitroxide ring is orientated at an angle of between 30° and 40° to the plane of the acridine ring. This angle is also the angle of tilt between the $2p\pi$-orbital of the spin-label and the perpendicular to the acridine ring. A planar configuration of the proflavine-nitroxide system is prohibited due to a close contact between the carbonyl oxygen of the nitroxide and the acridine ring protons at positions 5 and 7. The angle of tilt estimated from these models is in agreement with the values reported by Hurley et al. (1980) and Robinson et al. (1980) for the same compound and with the value of 35° given by Yamaoka and Noji (1977) for a similar

spin-labelled compound.

Since the $2p\pi$-orbital is calculated to have a tilt of between 0° and ± 5° to the DNA helix axis, it follows , from the geometry of the spin-labelled molecule, that the plane of the proflavine ring is orientated at between 45° and 65° to the helix axis.

In A-form DNA the base pairs are tilted at approximately 71° to the helix axis. The maximum angle of tilt of the acridine ring inferred from the ESR results is some 6° smaller than this and an intercalative mode of binding therefore seems unlikely. An examination of the A-form diffraction patterns provides support for this conclusion. Viz., all the A-form diffraction patterns, including those recorded at higher concentrations of drug, exhibited pitch values close to that of a control A-form pattern obtained at the same humidity. The secondary structure of the DNA is therefore hardly affected by the presence of the drug molecules, contrary to what would be expected in the event of intercalative binding. An external mode of binding is therefore indicated.

In the A-form the minor groove is shallow while the major groove is narrow and very deep (Fig. 1.6a, Chapter 1). The "hollow core" of the A-form helix extends to a depth of 6-7Å from the sugar-phosphate backbone. There is therefore a large space available in the major groove in which to accommodate the spin-labelled molecules.

External binding of the spin-labelled molecules is envisaged as being primarily due to a strong electrostatic interaction along the sugar-phosphate backbone, with the positively charged ring nitrogens directed towards the negatively charged phosphate groups and hydrogen bonding occurring between adjacent phosphates and the 3-amino groups on the proflavine ring. (The amide groups would be expected to form only weak hydrogen bonds). Such a binding scheme would be likely to greatly restrict the mobility of the spin-labelled drug.

A possible model of this structure is shown in Fig. 4.22. The

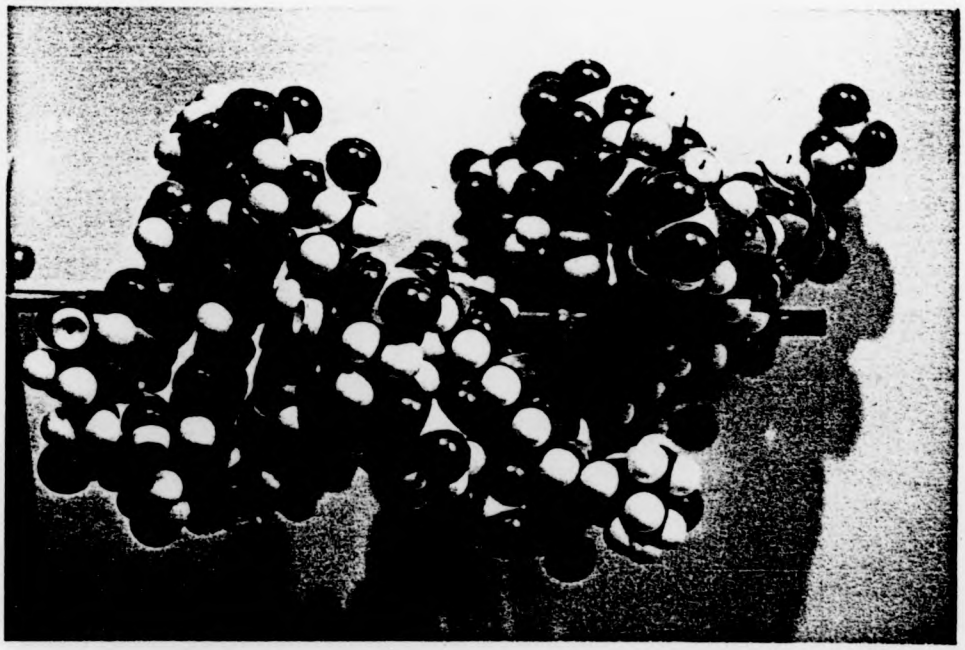

Fig. 4.22 CPK model of Spin-Labelled Proflavine-A-form DNA Structure.

Fig. 4.22 CPK model of Spin-Labelled Proflavine-A-form DNA Structure.

acridine ring lies in the major groove at an angle of approximately 60° to the helix axis. In this arrangement the nitroxide moiety lies across the sugar-phosphate chain, with the N-O group itself protruding outside the major groove. As expected, motion of the drug about any direction is highly constrained. The major groove is large enough to allow the binding of several drug molecules in close proximity to one another, resulting in a dipolar broadening of the ESR spectra. Such a broadening was observed at high concentrations of bound drug (e.g. P/D = 6). Stacking of the drug molecules is also possible in this model and this may lead to exchange broadening of the spectral lines .

**B-form Spectra and their Simulations**

At high humidities a transition to the B-form occurs. The maximum hyperfine splittings and lineshapes of the B-form ESR spectra clearly indicate that the orientation and mobility of the drug (or nitroxide) has altered during this transition. An examination of the gel spectrum in particular (Fig. 4.12d) shows that motional effects are present. i.e. the 1.5mT decrease in the maximum hyperfine splitting compared with the A-form gel spectrum and the increased broadening of the high and low-field lines.

At high humidities proflavine is known to bind to DNA by intercalation. Although spin-labelled proflavine has a much lower binding affinity for DNA than proflavine (Section 4.3.4), there is no evidence that its mode of binding is altered by the presence of the nitroxide moiety. Indeed, there is strong evidence from the X-ray diffraction results that spin-labelled proflavine does bind to B-form DNA by intercalation. The diffraction patterns, which shall be discussed later in the chapter, exhibited a decrease in layer line spacing compared with normal B-form patterns. This effect is characteristic of the intercalative mode of

binding.

Given that spin-labelled proflavine binds by intercalation then the most likely configuration of the drug is as follows. The planar acridine ring will be "sandwiched" between two base pairs while the nitroxide moiety, because of its shape and thickness, will not be accommodated between the base pairs but will protrude into the major groove of the helix. By virtue of the partial double bond character of the amide linkage which joins them, a rotation of the nitroxide moiety relative to the acridine ring is severely prohibited. Motion is further restricted due to steric hindrance resulting from the bulkiness of the nitroxide methyl groups and the close contact between the carbonyl oxygen and the acridine ring protons.

It is reasonable to assume, therefore, that the nitroxide moiety is fixed in orientation with respect to the acridine ring. The observed motional effects can, therefore, only be attributed to a rotation of the acridine ring itself. The only plausible motion in this case is a rotation, or oscillation, of the acridine ring in the plane of the base pairs.

At first sight it seems unlikely that a rotation of the spin-labelled molecules about the helix axis could be rapid enough, on the ESR time scale, to produce any detectable averaging of the magnetic parameters. However, recent work, using fully hydrated fibres, has shown that intercalated drug molecules which are weakly coupled to adjacent base pairs possess a considerable degree of motion in the plane of the base pairs (Section 4.4.5). Correlation times of between 0.2nsec and 10nsec have been estimated for these motions for several spin-labelled acridine derivatives (Robinson et al. 1980; Hurley et al. 1982; Hurley et al. 1979). It is thus quite plausible to suppose that the motion followed by the spin-labelled molecules is a rotation of the acridine ring about the helix axis.

**The Gel Spectrum**

As before (Section 4.3.4) the DNA $z_2$-axis is taken to be parallel to the gel $Z_1$-axis. Since all orientations of the spin-orbital relative to the magnetic field are included in the gel (or powder) spectrum, a change in the orientation of the spin-orbital relative to the DNA helix axis will not, by itself, result in any changes in the spectrum. Only an increase in the mobility of the drug can account for the observed reduction of the gel hyperfine splitting.

A rotation of the spin-labelled drug about an arbitrary axis $\xi$ will result in a spectrum whose maximum hyperfine splitting and linewidths depend upon the direction of $\xi$ relative to the spin-orbital axis and on the rate of rotation.

If the rate of rotation is slow ($\tau_c > 10^{-8}$sec) a spectrum identical to the A-form gel spectrum (Fig. 4.11d) will be obtained whatever the direction of $\xi$.

For a rapid rotation about $\xi$ the g and A tensors are averaged and the resulting g- and A-values are axially symmetric. For example, for a rotation about the direction of the nitroxide x-axis (the N-O bond) averaging of $A_{zz}$ and $A_{yy}$ and of $g_{zz}$ and $g_{yy}$ occurs and one observes a spectrum characterised by $A_{\parallel} = A_{xx}$ and $A_{\perp} = (A_{zz} + A_{yy})/2$ and the g-values $g_{\parallel} = g_{xx}$ and $g_{\perp} = (g_{zz} + g_{yy})/2$.

If the rate of rotation is intermediate ($10^{-9} < \tau_c < 10^{-9}$sec) the g- and A-values are incompletely averaged and line broadening occurs as described in Chapter 2.

The equations relating the motion averaged g- and A-values to the principal nitroxide values for a rapid rotation about an axis tilted at $\theta_2$ to the nitroxide principal z-axis are (Griffith and Jost, 1976):

$$A_{\parallel} = A_{zz}\,\mathrm{Cos}^2\theta_2 + A_{yy}(1-\mathrm{Cos}^2\theta_2) + (A_{xx}-A_{yy})\mathrm{Sin}^2\theta_2\mathrm{Cos}^2\psi_2$$

$$A_{\perp} = 0.5[A_{zz}(1-\mathrm{Cos}^2\theta_2) + A_{yy}(1+\mathrm{Cos}^2\theta_2) + (A_{xx}-A_{yy})(1-\mathrm{Sin}^2\theta_2\mathrm{Cos}^2\psi_2)]$$

$$g_{\parallel} = g_{zz}\mathrm{Cos}^2\theta_2 + g_{yy}(1-\mathrm{Cos}^2\theta_2) + (g_{xx}-g_{yy})\,\mathrm{Sin}^2\theta_2\mathrm{Cos}^2\psi_2$$

$$g_{\perp} = 0.5[g_{zz}(1-\mathrm{Cos}^2\theta_2) + g_{yy}(1+\mathrm{Cos}^2\theta_2) + (g_{xx}-g_{yy})(1-\mathrm{Sin}^2\theta_2\mathrm{Cos}^2\psi_2)] \qquad (4.9)$$

The angles $\theta_2$ and $\psi_2$ are the tilt and "twist" angles of the nitroxide z-axis respectively (Section 4.4.5).

For $\theta_2 = 0°$, the rotation axis is parallel to the nitroxide z-axis. By substituting for $g_{zz}$, etc. one finds that the maximum hyperfine splitting is unaltered by a rotation about the direction of the nitroxide z-axis. Since the x and y components of the principal g- and A-values are (for nitroxides) nearly symmetric about the z-axis, the motion averaging results in only a small change in their magnitudes. The resulting spectrum is therefore virtually identical to the powder spectrum obtained in the absence of molecular motion.

On the other hand, for a rapid rotation of the nitroxide about the direction of the principal x (or y) axis, the motional averaging results in a reduction of the maximum hyperfine splitting and a significant change in the g-values. For example, a rapid rotation about the direction of the nitroxide x-axis results in a maximum hyperfine splitting $\Delta A_g^b$ of about 4.1mT. The corresponding g-values are $g_{\parallel} = 2.0088$ and $g_{\perp} = 2.0046$. The resulting spectrum will therefore exhibit a different lineshape and a maximum splitting of some 3.0mT smaller than the rigid limit spectrum.

Equations 4.9 were incorporated in the FIBRE programme and powder spectra were calculated for various angles of $\theta_2$ ($\psi_2 = 0°$ or $90°$) by substituting $A_{\parallel}$ and $A_{\perp}$ for $A_{zz}$ and $A_{xx}$, $A_{yy}$ and $g_{\parallel}$ and $g_{\perp}$ for $g_{zz}$ and $g_{xx}$, $g_{yy}$ respectively. Some of these simulations are shown in Fig. 4.23(a-h).

By comparing Fig. 4.11d with Fig. 4.23a it can be seen that the effects on the gel spectrum of a rapid rotation about the direction of the

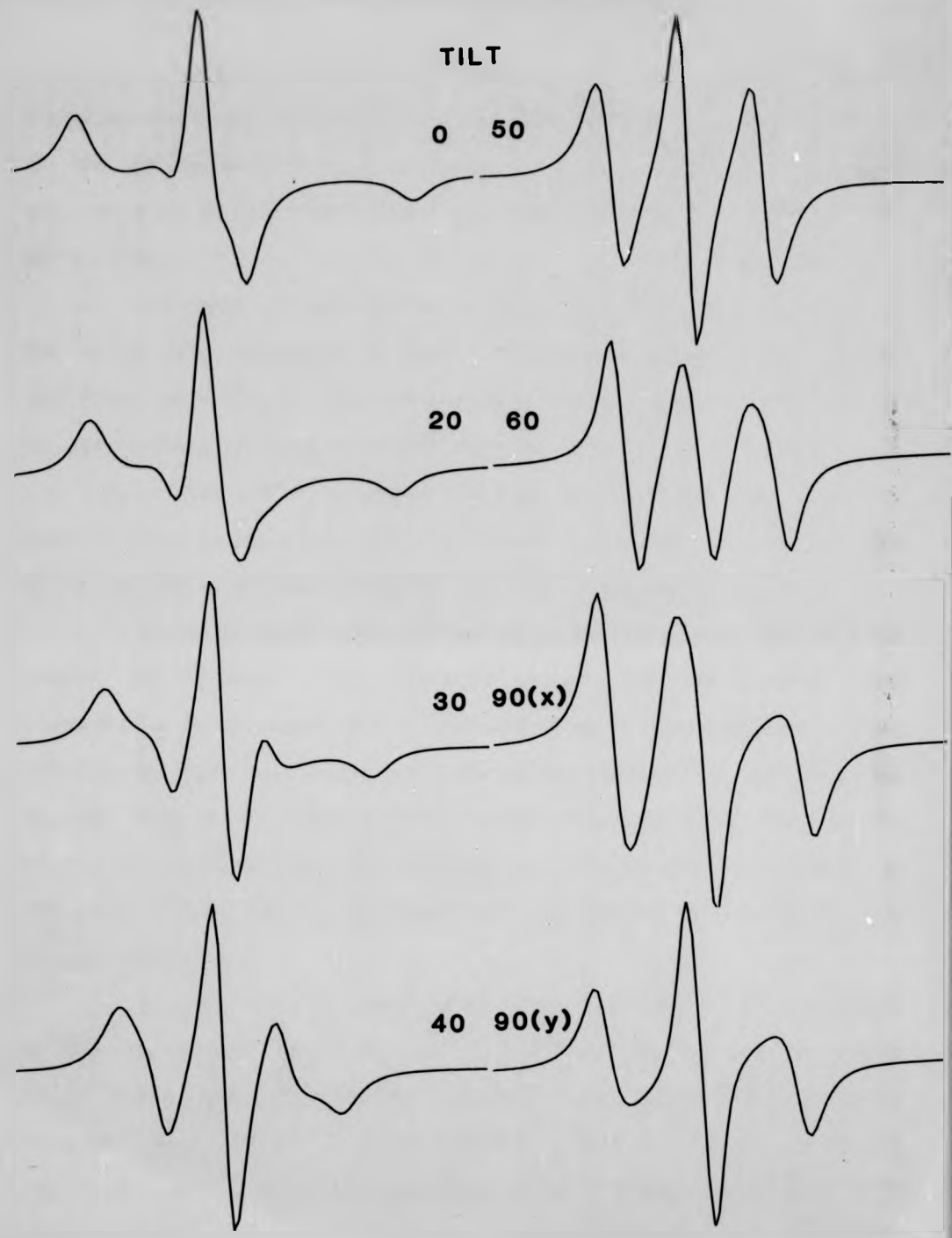


Fig. 4.23(a-h) Computer Simulations of the Gel Spectra for a rapid rotation about the DNA Helix Axis for several angles of tilt.

nitroxide z-axis are negligible. One concludes from this observation that, if the gel spectrum is to be accounted for by a rotation about a single axis, an angle of tilt must exist between the nitroxide z-axis and the axis of rotation.

The axis of rotation is assumed, at least initially, to be the DNA helix axis and space filling models of intercalated spin-labelled proflavine show that the spin-orbital is orientated at between 30° and 40° to the helix axis. The simulated spectrum for a tilt of 30° is shown in Fig. 4.23c. The splitting between the high and low-field lines is ~5.5mT, which is close to the value of the experimental spectrum. By contrast, the splittings for x- or y-axis rotation are clearly too small.

At this point some preliminary calculations were made of the B-form ESR spectra. The simulated spectra for the parallel and perpendicular orientations of the fibre are shown in Fig. 4.24(a-h). These calculations were performed using the motion averaged g- and A-values obtained from the gel simulations for several values of tilt. The best fit to the experimental hyperfine splittings was obtained for a tilt angle of about 30°. This result is consistent with the angle of tilt estimated from the gel simulations.

In view of the complexity of the fibre model the agreement between the calculated and experimental hyperfine splittings is not likely to be merely fortuitous. One may therefore regard the motional averaging treatment presented here as being essentially correct. However, although the lineshapes of the calculated spectra are in general agreement with their experimental counterparts, there is considerable room for improvement. This is also true with regard to the gel simulations.

One may expect the fit to be improved by treating the motion as a partial (or restricted) rotation about the helix axis rather than as a complete rotation. In this case the g- and A-values will be only incompletely averaged and their resulting anisotropy should contribute to

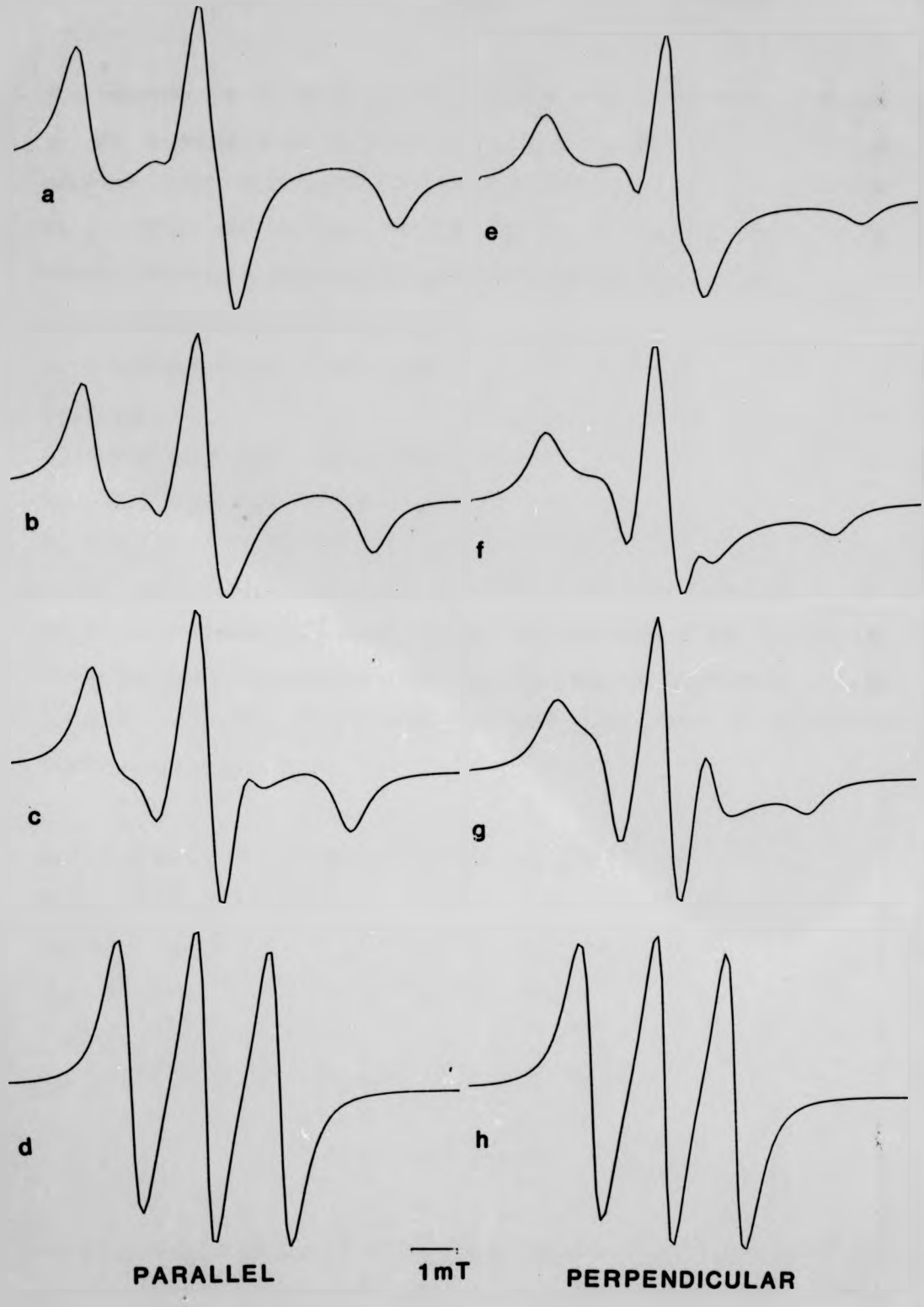


Fig. 4.24(a-h) Computer Simulations of the Fibre Spectra using the motion averaged principal values obtained from the gel simulations.

the observed line broadening. The equations relating the motion averaged g- and A-values to the principal nitroxide values for a rapid restricted rotation about the direction af a principal axis have been derived by Van et al. (1974) and Griffith and Jost (1976). The equations for a rapid restricted rotation about an arbitrary axis ($\theta_2$) are given below:

$$
\begin{aligned}
g_{x1} &= 0.5[(g_{x2} + g_{y2}) + \sigma(g_{x2} - g_{yy})] \\
g_{y1} &= 0.5[(g_{x2} + g_{y2}) - \sigma(g_{x2} - g_{y2})] \\
g_{z1} &= g_{z2} \\
A_{x1} &= 0.5[(A_{x2} + A_{y2}) + \sigma(A_{x2} - A_{y2})] \\
A_{y1} &= 0.5[(A_{x2} + A_{y2}) - \sigma(A_{x2} - A_{y2})] \\
A_{z1} &= A_{z2}
\end{aligned}
\qquad (4.10)
$$

where $\sigma = (\sin\alpha\cos\alpha)/\alpha$, where $\alpha$ is the half amplitude of the oscillation about the axis of rotation. $A_{x2}$, $A_{y2}$ etc. are the coordinates of the principal nitroxide values in the molecular (DNA) frame of reference. These are given by:

$$
\begin{aligned}
g_{x2} &= g_{xx}\cos^2\theta_2\cos^2\psi_2 + g_{yy}\cos^2\theta_2\sin^2\psi_2 + g_{zz}\sin^2\theta_2 \\
g_{y2} &= g_{xx}\sin^2\psi_2 + g_{yy}\cos^2\psi_2 \\
g_{z2} &= g_{xx}\sin^2\theta_2\cos^2\psi_2 + g_{yy}\sin^2\theta_2\sin^2\psi_2 + g_{zz}\cos^2\theta_2 \\
A_{x2} &= A_{xx}\cos^2\theta_2\cos^2\psi_2 + A_{yy}\cos^2\theta_2\sin^2\psi_2 + A_{zz}\sin^2\theta_2 \\
A_{y2} &= A_{xx}\sin^2\psi_2 + A_{yy}\cos^2\psi_2 \\
A_{z2} &= A_{xx}\sin^2\theta_2\cos^2\psi_2 + A_{yy}\sin^2\theta_2\sin^2\psi_2 + A_{zz}\cos^2\theta_2
\end{aligned}
\qquad (4.11)
$$

These equations are derived following the method of Van et al. (1974). They reduce to the equations given by Van et al. and Griffith and Jost (1976) for $\theta_2 = 0°$ (z-axis motion), $\theta_2 = 90°$, $\psi_2 = 0°$ (x-axis motion) and $\theta_2 = 90°$, $\psi_2 = 90°$ (y-axis motion).

The input parameters to the powder programme now include, in addition to those previously mentioned (Section 4.4.4), the angle of tilt ($\theta_2$) of the nitroxide z-axis to the axis of rotation, the half angle of oscillation ($\alpha$) of the nitroxide about the axis of rotation and the angle of twist ($\psi_2$) of the nitroxide about its own z-axis. The programme first calculates the coordinates of the nitroxide principal values ($g_{xx}$, etc) in the DNA frame of reference ($g_{x2}$, etc). The motion averaged g- and A-values ($g_{x1}$, etc) are then calculated using equations 4.10. To calculate the powder spectrum, the motion averaged principal values are substituted for $g_{xx}$, etc. in equations 4.5 and 4.6.

There are two limiting cases in the restricted rotation model:
(a)No motion: In this case the rotation axis is undefined and $\theta_2 = \psi_2 = \alpha = 0°$. Therefore, $g_{x1} = g_{xx}$, $g_{y1} = g_{yy}$, etc.
(b)Complete axial rotation: In this case, $\alpha = 90°$ and $\sigma = 0$. The motion averaged values are then given by equations 4.9.

As seen from Fig. 4.12d the high-field ($m_I = -1$) and low-field ($m_I = +1$) lines of the experimental spectrum are much broader than the central ($m_I = 0$) line. This effect is assumed to arise from the "modulation broadening" of the three ESR lines which results from the rotational motion of the nitroxide. For nitroxides this broadening is predicted to be greater for the high-field line than for the other components (see Chapter 2). The fit to the experimental spectrum should therefore be improved by including contributions to the linewidths from motional modulation effects. This is achieved in practice by giving the three lines different intrinsic widths

In order to obtain the "best-fit" values of $\theta_2$, $\psi_2$, $\alpha$ and the linewidths, the following procedure was adopted.

The three linewidths were initially kept constant at 0.45mT each and the angle $\psi_2$ was set equal to zero. $\theta_2$ and $\alpha$ were then altered concurrently until the correct hyperfine splitting and general lineshape

features were obtained. At this point the linewidths were varied, with the high-field and low-field components being increased relative to the central line. The fit was finally improved by making small adjustments of $\psi_2$, $\alpha$ and $\theta_2$. As before (Section 4.4.5) the calculated spectrum was generated by stepping the angles $\theta_1$ and $\phi_1$ through 4° and 8° intervals respectively.

The best fit to the experimental spectrum was finally obtained with the following set of parameters:

$g_{xx}$ = 2.0088 $A_{xx}$ = 0.64mT

$g_{yy}$ = 2.0066 $A_{yy}$ = 0.64mT

$g_{zz}$ = 2.0027 $A_{zz}$ = 3.49mT

Tilt of nitroxide z-axis to axis of rotation, $\theta_2$ = 30° ± 2°

Twist of nitroxide about its z-axis, $\psi_2$ = 30° - 90°

Half-amplitude of rotation of nitroxide, $\alpha$ = 20° - 90°

Linewidths: $m_I(-1)$ = 0.68mT

$m_I(0)$ = 0.48mT

$m_I(+1)$ = 0.61mT

Lineshape: Lorentzian.

As may be seen from Fig. 4.25 the main features of the gel spectrum are accounted for by the "rapid motion model". The largest discrepancy between the experimental and simulated lineshapes occurs at the high-field region of the spectrum. As mentioned earlier, the phenomenon of motional modulation has its most significant effect on this region of the spectrum. However, in view of the simple line-broadening treatment used in these simulations a better fit to the experimental spectrum should not be expected. In any case, further changes in the linewidth parameters, such as the introduction of orientation-dependent linewidths, only results in a "cosmetic refinement" of the calculated fit (Jost et al., 1971).

The determining factor in the overall best-fit was the angle of tilt parameter ($\theta_2$), which was clearly restricted to the indicated range.

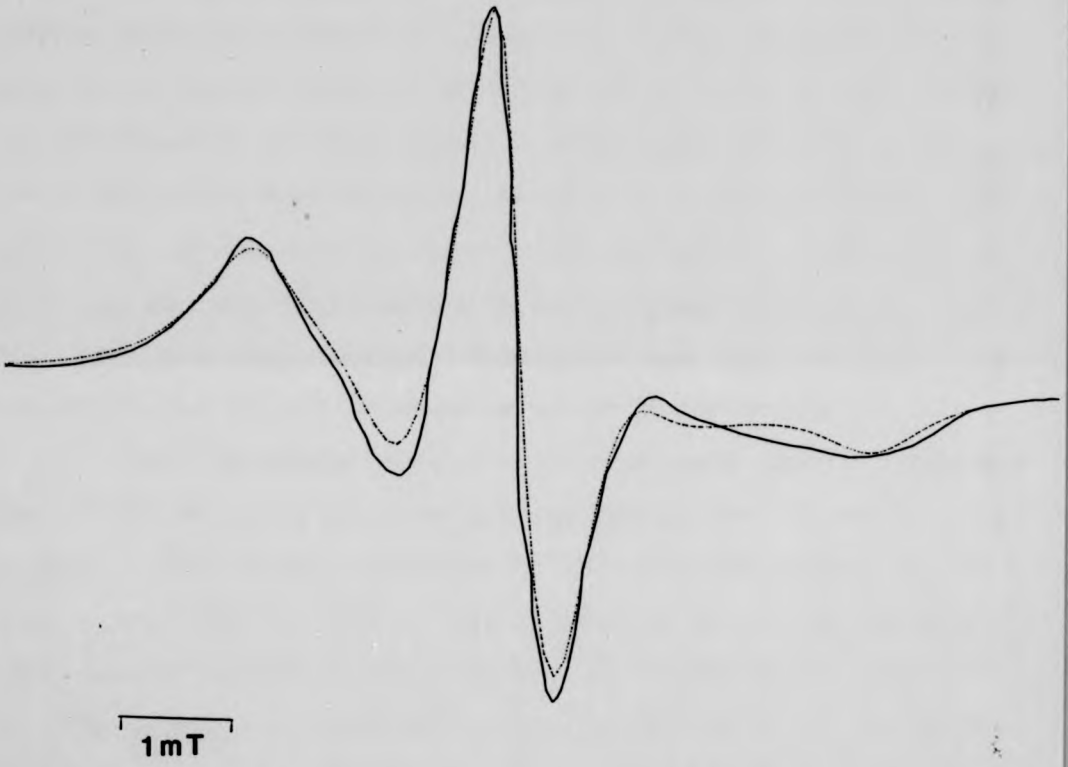


Fig. 4.25 The B-Form Gel Simulation.

Values of $\theta_2$ outside this range resulted in a spectrum whose hyperfine splitting was either too small ($\theta_2 > 30°$) or too large ($\theta_2 < 30°$).

**The Fibre Simulations**

In the fibre simulations, the Gaussian misalignment was initially assumed to be equal to its "A-form value" (i.e. ~45°) and simulations were obtained using a procedure similar to that adopted in the gel case. That is, the linewidths were held constant at 0.45mT, while the values of $\theta_2$, $\phi 2$ and $\alpha$ were varied about the limits prescribed by the gel simulation. The coordinates of the principal values in the DNA frame of reference (i.e. $g_{x2}$, $g_{y2}$, etc) were calculated and the motion averaged values (i.e. $g_{x1}$, $g_{y1}$, etc) were then obtained. These values were then substituted in Eqs. 4.5 and 4.6 and the ESR absorption was calculated from Eq. 4.8.

Once the general features of the experimental spectra appeared, the values of $\theta_2$, $\phi 2$ and $\alpha$ were kept constant and the linewidths were altered. As in the gel simulation, the linewidths were broadened in the order $m_I(-1) > m_I(0) > m_I(+1)$. Small alterations of all the parameters were made and the best-fit was found for a misalignment of 40°. Like the gel simulation, the lineshape which best approximated the experimental lineshape was a 1:1 mixture of Gaussian and Lorentzian. The final parameters were therefore:

Angle of misalignment = ~40°

Angle of tilt, $\theta_2$ = 145 - 150°

Angle of twist, $\psi_2$ = 40 - 55°

Half-angle of rotation, $\alpha$ = 40 - 50°.

Linewidths: $m_I(-1)$ = 0.68mT, $m_I(0)$ = 0.48mT, $m_I(+1)$ = 0.62mT

Lineshape: Lorentzian + Gaussian.

The simulations are shown in Figs. 4.26(a,b).

Whereas the fit to the parallel spectrum is good, the fit to the perpendicular spectrum is rather poor, particularly at the hyperfine extrema. This may be due to a combination of several factors.

The above treatment assumes that the intercalated molecules are undergoing a rapid rotation about a single axis, i.e. the DNA helix axis. It is quite possible, however, that there is also a component of motion (e.g. "wobble") about the perpendicular to the helix axis. This motion, if present, would considerably complicate the analysis and the simple model of "one-axis rotation" would no longer be satisfactory. If such a wobbling motion exists it would most likely take the form of a partial rotation of the nitroxide relative to the proflavine ring. This motion should, however, be quite restricted due to the presence of the amide linkage and the steric hindrance which results from the geometry of intercalation. In fact, the presence of an orientational dependence in the ESR spectra suggests that motion of the spin-label perpendicular to the helix axis must be limited: otherwise it is difficult to see how any orientational information could arise.

An additional complication in the B-form spectra is the possibility of there being more than one component of drug present in the fibre. Although it has been assumed that all the drug is intercalated, the A → B transition sequence shown in Fig. 4.13 certainly suggests that there is more than one bound component present in the final spectrum (viz. the broad outer lines). The second drug component, which may well account for the poor fit to the perpendicular spectrum, is probably due to the presence of spin-labelled drug which is externally bound to the DNA. Earlier work by Muller and Crothers (1973) and Neville and Davies (1966) indicated that the extent of intercalation of proflavine in DNA was a function of the the degree of hydration of the fibre and that even at high humidity a considerable fraction of the drug remained externally bound. In the

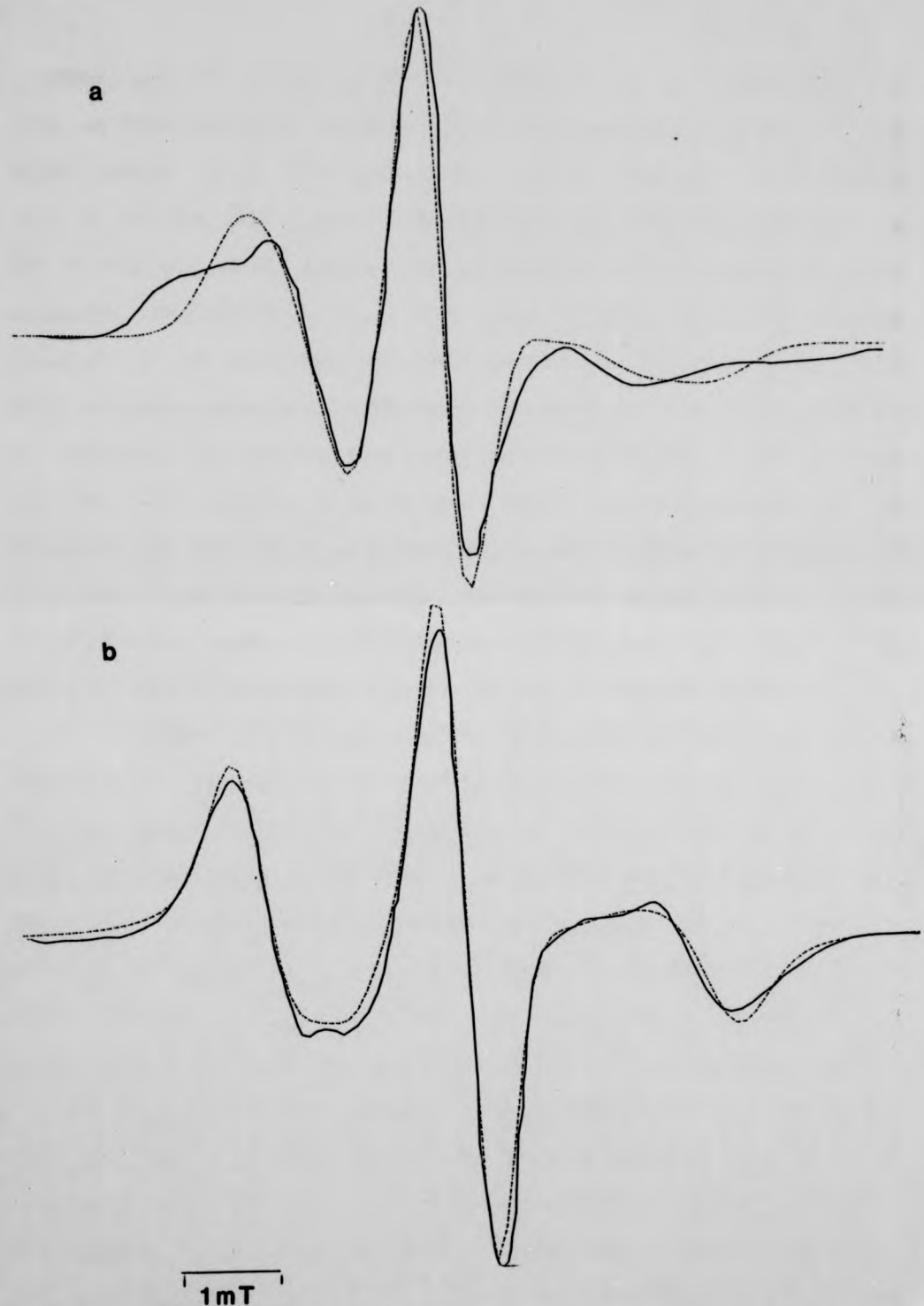


Fig. 4.26(a,b) B-Form Fibre Simulations (a) 90° (b) 0°.

previous section it was shown that, when bound to A-form DNA, the spin-labelled molecules adopted a preferred orientation, probably in the major groove, with their spin-orbital z-axes orientated approximately parallel to the DNA $z_2$-axes. The major groove is shallower and wider in the B-form than in the A-form. The angle of tilt of the externally bound molecules, assuming that they bind in the major groove, would therefore be expected to be different from its A-form value. The contribution that these molecules would make to the total ESR spectrum is therefore difficult to estimate, but judging from the quite reasonable fits to the gel and parallel fibre spectra, it may be quite small. Simulations show that the perpendicular spectrum is more sensitive to small changes in the angle of tilt than is the parallel spectrum. The presence of even a small fraction of externally bound drug would therefore have a more significant effect when the fibre is orientated perpendicular to the magnetic field.

Another interesting feature of the B-form simulations is the finding that the best-fit was obtained for a smaller misalignment angle than was used for the A-form simulations. X-ray diffraction studies have shown that the degree of misalignment of the DNA does not alter much with changes of humidity (Mahendrasingham, private communication). The most probable explanation of the reduced misalignment is, therefore, that the spread in the orientations of the bound drug has been reduced. This explanation fits in well with the model of intercalative binding, whereby all the drug molecules will have the same orientation relative to the DNA. Only the small fraction of externally bound molecules will be able to contribute to the spread of orientations which leads to a large degree of misalignment. The B-form simulations furnish some evidence, therefore, that the large misalignment angle required for the A-form simulations was due to the existence of a spread of drug orientations. One may expect a similarly large misalignment to be present in the C-form fibres in which the external binding mode is expected to predominate.

**C-Form Spectra and their Simulations**

The C-form gel and fibre spectra were recorded for a fibre of P/D = 20 at 33% r h. They are shown in Fig. 4.16(a-c). The lineshapes are clearly broader than in the A- or B-form spectra and this is no doubt due to the much higher loading of spin-labelled drug present. Attempts were made to obtain C-type conformations and ESR spectra at higher P/D values but without success. An A/C mixture diffraction pattern was recorded at a P/D of 70 at low humidity, but the ESR spectra were little different from the normal A-form spectra.

Drug binding to C-form DNA is interesting because of the structural similarities of the C- and B-conformations (see Chapter 1). Before embarking on a quantitative analysis of the ESR results some general remarks may be relevant.

(i) The C-form gel spectrum has a maximum hyperfine splitting of about 7.0mT. This is comparable to the splitting of the A-form gel spectrum and it indicates that the spin-labelled molecules are strongly bound to the DNA (i.e. $\tau_c > 10^{-8}$ sec.)

(ii) The large maximum hyperfine splittings for all orientations of the fibre suggest, by analogy to the A-form fibre spectra, that the spin-labels are orientated with their $2p\pi$-orbital z-axes nearly parallel to the DNA helix axis. However, the tilt angle must be somewhat larger than that present in the A-form, otherwise A-form type spectra would be obtained.

(iii) If the spin-labelled molecules were intercalated then, because of the geometrical constraints that this imposes on the molecules, one would expect to see ESR spectra which exhibit hyperfine splittings and lineshapes similar to the B-form spectra. The fact that the water content of the fibre is greatly reduced at 33% r h. compared to 98% r h. should not significantly effect the ESR results : as previously noted, significant changes in the ESR spectra only came about as a result of changes in DNA

conformation. The actual hyperfine splittings and lineshapes are, in fact, more comparable to the A-form spectra, suggesting that an external binding mode is present. Unfortunately, the C-type diffraction patterns (Fig. 4.30) were too diffuse for layer-line measurements to reveal whether intercalation had occurred or not.

Bearing the above points in mind, and referring to Fig. 4.20, it may be seen that the overall shape of the perpendicular C-form spectrum (Fig. 4.16c) is given by a tilt angle of about -15° and a misalignment of about 50°. The linewidths of the experimental spectra are much broader than those used in the simulations in Fig. 4.20, but when allowance is made for this a reasonable simulation of the perpendicular spectrum is obtained using:

Angle of tilt, $\theta_2 = -15° \pm 3°$

Angle of misalignment, $\lambda = 50 - 55°$

Angle of twist, $\psi = 40 - 60°$

Lineshape: Lorentzian

Linewidths: $m_I(-1) = 0.88mT$, $m_I(0) = 0.78mT$, $m_I(+1) = 0.82mT$

The usual principal g- and A-values were used.

These parameters also give a reasonable fit to the other orientations of the fibre (Fig. 4.27(a,b)).

The angle of misalignment is again quite large, indicating a spread of drug orientations.

Since the spin-orbital z-axis is orientated at between 30 and 40° to the plane of the proflavine ring, the calculated angle of tilt (i.e. ~-15°) means that the plane of drug must be orientated at between 62 and 78° to the helix axis. This estimate of the angle of tilt rules out the possibility of intercalation. It is probable, therefore, that the B → C transition occurs with a redistribution of the bound drug from intercalated to external binding sites and that the external binding occurs not randomly but with a specific geometry. A CPK model of C-form DNA shows that the

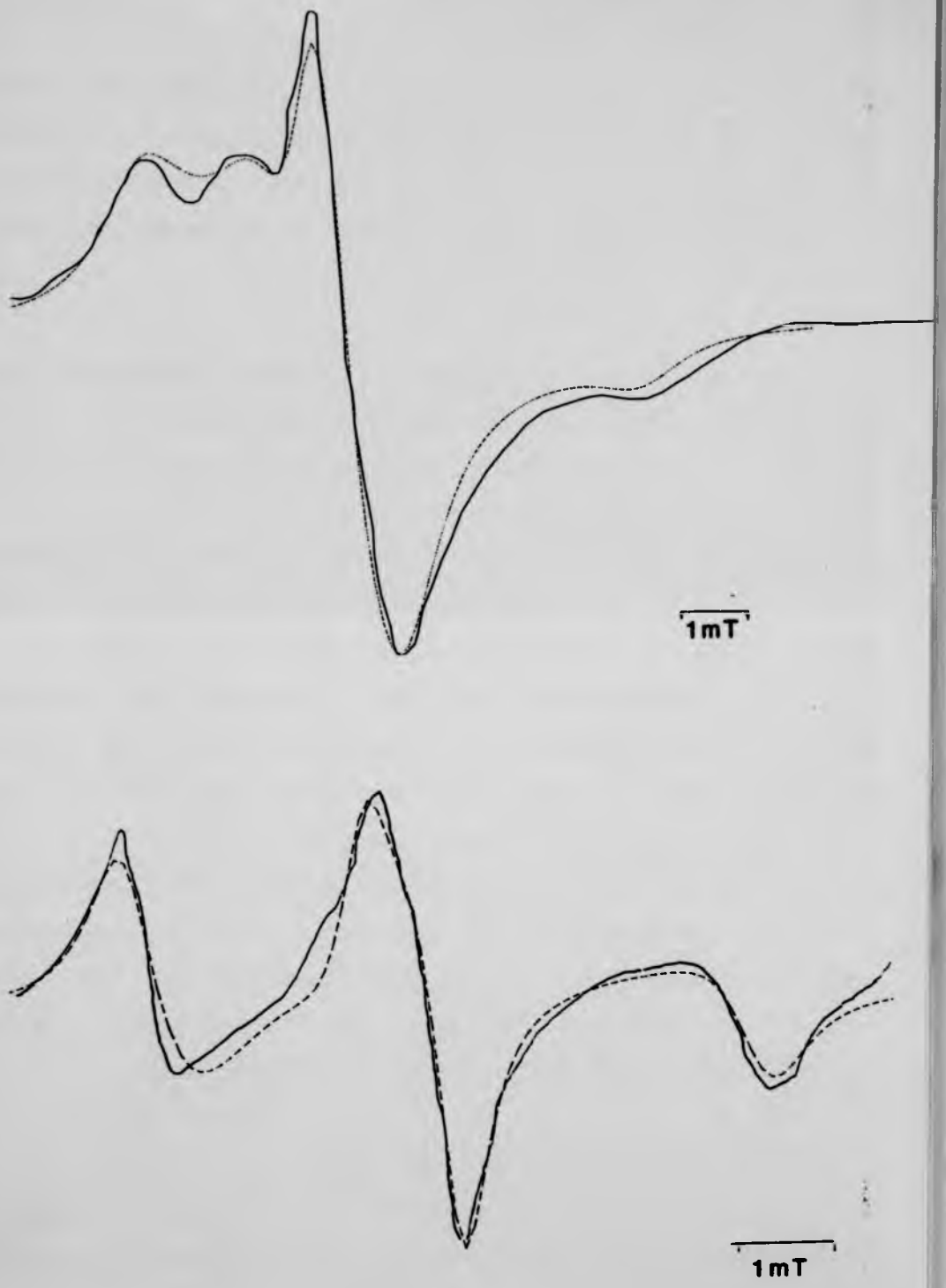


Fig. 4.27 Computer Simulations of the C-Form Fibre Spectra (a) 90° (b) 0°.

proposed structure agrees with a binding scheme in which the drug molecules interact electrostatically with the phosphate groups in the major groove. A strengthening of the structure is possible due to a "hydrophobic contact" between the drug and the exposed areas of the bases in the major groove.

4.4.6 DNA Conformation and Drug Concentration

The conformational behavior of the drug-DNA complexes clearly depended upon the concentration of drug present in the fibre. At high P/D values the A- and B-forms were observed and the C-form was only seen as an A/C mixture at low humidity. At low P/D values the A-form was not observed but a B → C transition occurred at about 92% r h.

When large amounts of drug are present in the fibre at high humidities the B-form will be stabilised. With a reduction in relative humidity the intercalated molecules will be released from their binding sites and will adopt external orientations, possibly by binding along the sugar-phosphate backbone in the major groove. The release of intercalated drug will be a function of the relative humidity and it is probable that a considerable fraction of the drug is redistributed to the external binding sites before a conformational transition takes place. It is the presence of these externally bound molecules which seems to determine the nature of the conformational change, i.e. whether the DNA goes from the B-form to the A- or C-conformation.

In pure, low salt, calf thymus DNA fibres the transition normally observed is B → A → C; the transition B → Ψ has never been observed. The existence of this transition in DNA-drug fibres at high drug concentrations is therefore unexpected. Nevertheless, the results clearly show that, provided the drug concentration is high enough (P/D ~ 20 for 1mM NaCl fibres) the A-form will be prohibited and the C-form will be favoured instead.

To explain this observation it may be relevant to consider the results of some recent studies on the hydration-structure of single crystals of DNA (Drew and Dickerson, 1981). These studies have suggested that the B-type conformation in crystals is stabilised by the formation of a network of water-$Na^+$ ion "bridges" which spread along the **minor** groove of the helix. Destruction of this bridging structure is believed to bring about the transition to the A-conformation. The A-conformation is itself thought to be stabilised by a network of water-$Na^+$ ion bridges which form across the **major** groove of the helix.

If it is assumed that the results of the single crystal studies can be applied in the fibre case (i.e. at the polynucleotide level) then one is led to the following possibility, that the externally bound drug molecules interfere with and disrupt the formation of the water-$Na^+$ ion bridges. The drug molecules would, in effect, displace the $Na^+$ ions from their usual binding sites along the sugar-phosphate backbone and thus limit the extent of the build up of water across the major groove. In such a situation a B-type structure may be preferred. Since the B- and C-forms are structurally very similar (see Chapter 1) their water-structures would be expected to be similar. At low levels of hydration the water structure may lead to a favourable B → C transition. The reappearance of the A-form at higher P/D values arises on this model because the drug concentration has become too low to affect the build up of water-$Na^+$ ion bridges in the major groove.

The absence of a pure C-form at high P/D and low humidity may be due to the drug molecules behaving rather like salt ions. It is known that the conformational states of DNA in fibres are strongly dependent upon the type and concentration of salt ion present (Rhodes, 1982). In particular, the C-form is prohibited at high salt concentrations. It is possible that drug concentrations which are too low to prohibit the A-form are, on the other hand, sufficiently high to prohibit the C-form.

Whilst being purely speculative the above comments are consistent with the experimental results presented here and by other workers. It might be noted, in support of these remarks, that the A-form is also prohibited in certain bacteriophage DNAs possessing modified bases which project into the major groove (e.g. SP15 DNA, Prof. Warren, private communication). It has been speculated that the presence of these bulky modifications interferes with the water structure in the major groove and prevents the A-form from occurring (Mahendrasingham, 1983).

4.4.7 AT and GC Rich DNAs

The linewidths of the ESR spectra recorded from fibre containing spin-labelled proflavine bound to AT-rich DNA (at P/D = 25) were considerably broadened compared with the linewidths found at the same P/D for both calf thymus and GC-rich DNA-drug fibres. The broadening arises from electron spin-spin dipolar interactions and its existence signifies that the spin-labels are closer together in the AT-rich complexes. This suggests that the binding of the spin-labelled drug is specific to the AT-rich regions of the DNA. Furthermore, a second fibre prepared at P/D = 25 using the synthetic polynucleotide Polyd(AT).Polyd(AT) also exhibited a very broad ESR spectrum. The "clustering together" of the drug in the pure AT fibre may signify more than the preference for AT bases: it could suggest the presence of a "co-operative binding effect". That is, the binding of one spin-labelled drug molecule may induce the binding of a second drug in a closely adjacent site. There is some evidence that native proflavine binds co-operatively (Peacocke and Skerrett, 1956). Co-operativity may arise when the Van der Waal's forces between molecules at adjacent sites overcome the electrostatic repulsions between them (Dougherty, 1979). Co-operative binding is more likely to occur for externally bound molecules and diffraction patterns of the Polyd(AT).Polyd(AT) fibres show them to be in the C-form up to 98% r h., a

conformation in which the drug is largely externally bound. At 98% r h., but only after prolonged exposure, the AT-rich fibres gave B-type diffraction patterns. However, the ESR spectra remained unchanged. If there were any alterations of the drug orientations they were obscured by the broadness of the hyperfine lines. The problems of base pair specificity and co-operativity are interesting and are suggested as suitable for further study.

4.4.8 X-Ray Diffraction Patterns

The X-ray diffraction patterns shown in Figs. 4.28-4.30 were recorded on flat film from fibres which had been lightly dusted with calcite powder. Calcite powder gives a diffraction ring at 3.029A and this was used as a calibration from which the specimen (i.e. fibre) to film distance could be measured. A set of conversion tables was used to translate the specimen to film distance and the coordinates of the diffraction spots (measured using a travelling microscope) into reciprocal (and real) space coordinates, from whoich the layer line spacings and intermolecular separations could be calculated. The details have been given elsewhere (e.g. Dougherty, 1979).

The X-ray diffraction pattern obtained from a DNA fibre consists of a series of spots arranged in layer lines, as may be seen from Fig. 4.28. The separation between the layer lines is a function of the pitch of the helix. The meridional reflections are the layer lines at the furthest extremes of the diffraction pattern above and below the equator. The separation between the meridional reflections is related to the distance between two adjacent base pairs in the helix. The equitorial reflections, found on each side of the centre of the pattern along the equator in B-form DNA, can be used to obtain the separation between two adjacent DNA molecules in the fibre (Wilson, 1966).

The pitch and intermolecular separation can provide information about the possibility of intercalation. As mentioned in section 5.4.4, a

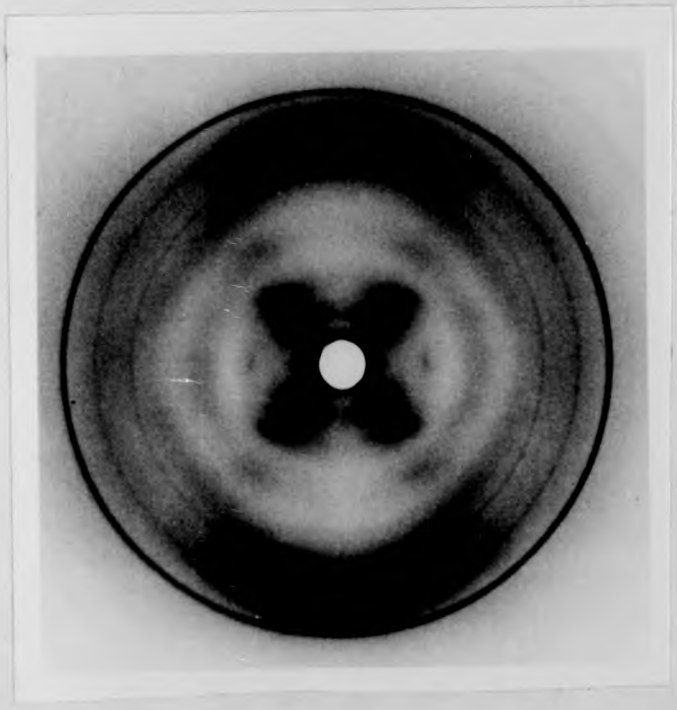

Fig. 4.28 A- and B-form X-ray fibre diffraction patterns for P/D = 70.

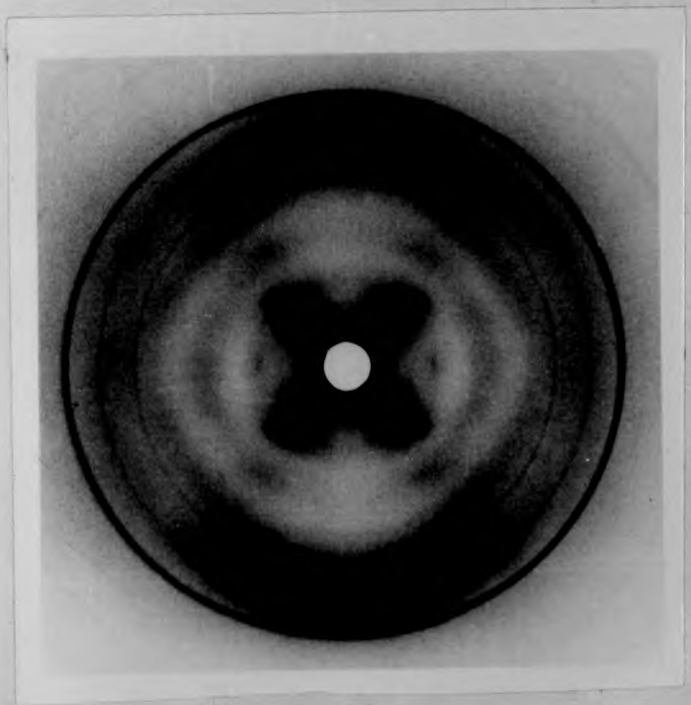

Fig. 4.28 A- and B-form X-ray fibre diffraction patterns for P/D = 70.

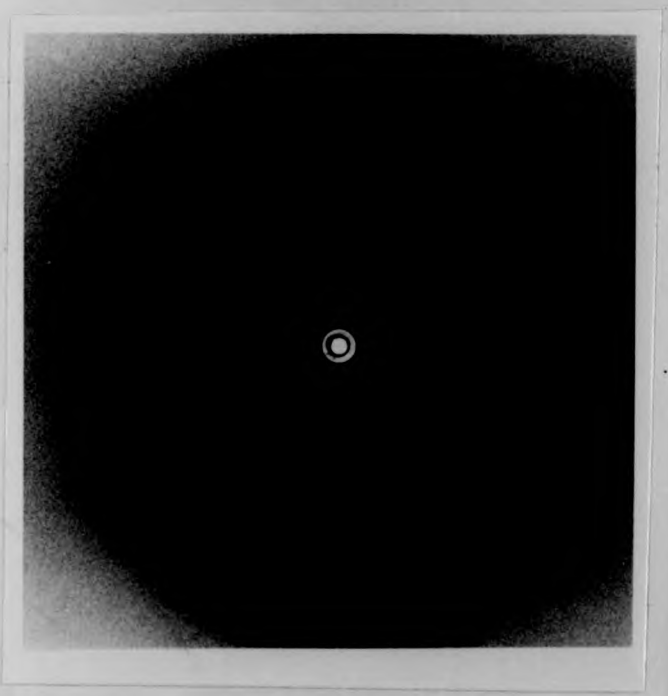

Fig. 4.29 A/B and A/C Mixture diffraction patterns (P/D = 70).

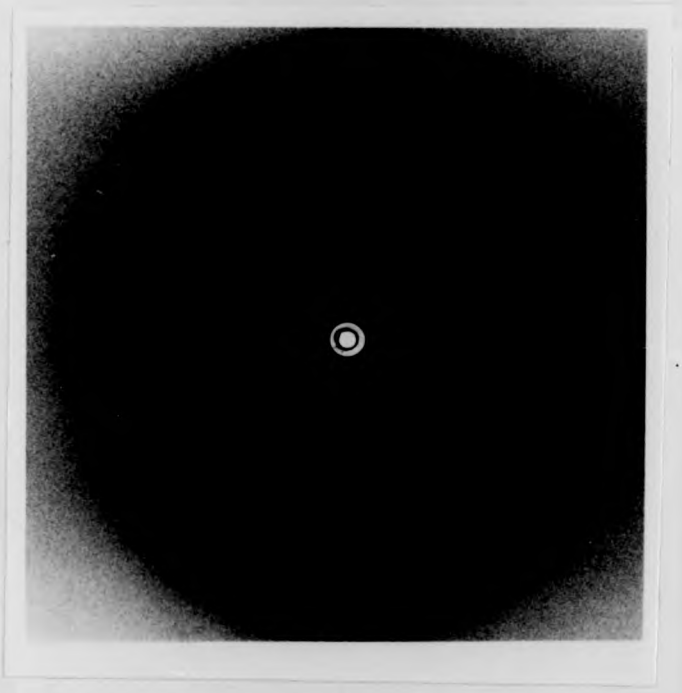

Fig. 4.29 A/B and A/C Mixture diffraction patterns (P/D = 70).

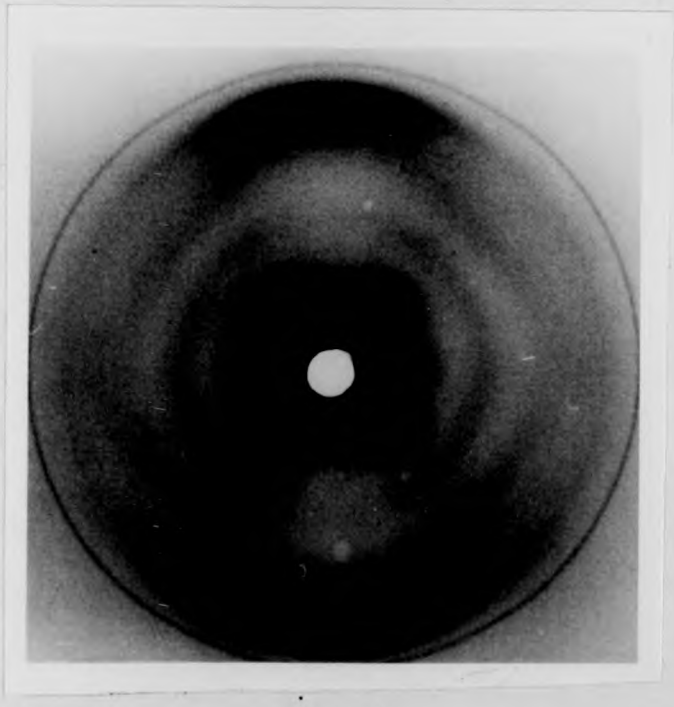

Fig. 4.30 C-form and B-form fibre diffraction patterns (P/D = 6).

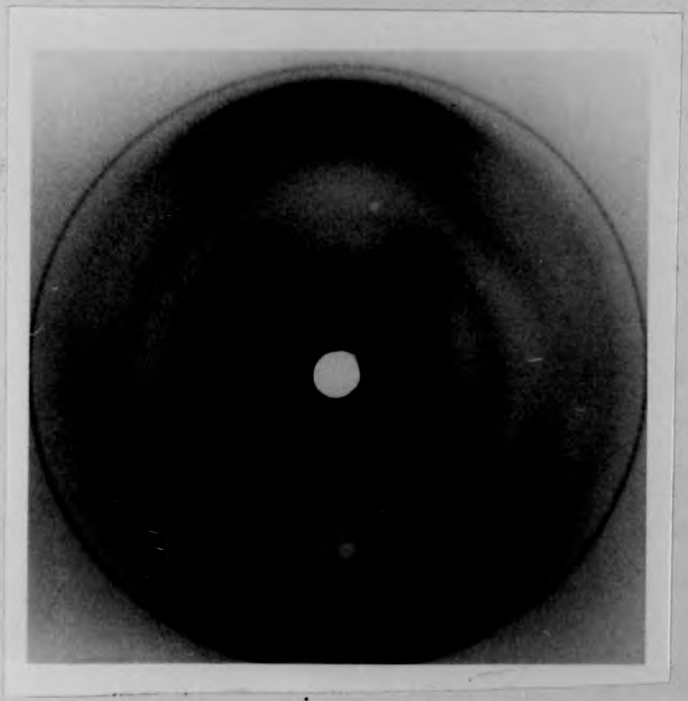

Fig. 4.30 C-form and B-form fibre diffraction patterns (P/D = 6).

decrease in the layer line separation of a drug-DNA diffraction pattern compared with a normal DNA diffraction pattern signifies an increase in helical pitch and the liklihood of an intercalative mode of binding.

In the present work, X-ray diffraction patterns were recorded for normal, low salt, fibres at the same relative humidities used for the spin-labelled proflavine-DNA fibres. The patterns obtained at low humidity ( < 44%) were of the semi-crystalline C-form and between 44 and 92% r h. crystalline A-form patterns were observed. Between 92 and 98% r h. the semi-crystalline B-form appeared. The A-form patterns gave a pitch of 28.1A. The layer line separation in the B-form corresponded to a pitch of 34.1A (at 98% r h.) and the intermolecular separation was 26A. The C-form patterns had a pitch of 30.8A at 33% r h.

Fibres which contained only small amounts of spin-labelled drug (i.e. P/D = 70 or 50) gave A-type and B-type diffraction patterns which were well defined and similar to the normal A- and B-form patterns (Figs. 4.28 and 4.29). The pitch measurements yielded 34.3A for the B-type pattern and 28.3A for the A-type pattern. These values are not significantly different from the normal values.

However, with increasing amounts of bound drug the layer line separations of the B-type patterns steadily increased. At P/D = 6 a wet B-form fibre gave a pitch of 40.1A - an increase of 6A on the normal value. The intermolecular separation for this fibre was 23A and the meridional reflection at 3.4A was still strong. No A-type patterns were found at this P/D but a C-type pattern was recorded at 33% r h. (Fig. 4.30). The layer line spacing of this pattern was difficult to measure because of the diffuseness of the reflections. However, the meridional reflection gave a base pair separation of 3.3A, which is normal for a C-form.

The increased pitch of the B-form at high humidities clearly indicates that the drug molecules are intercalated. An increase of pitch does not actually <u>prove</u> that intercalation has taken place, since an

external binding mechanism could coceivably bring about the same effect. However, the presence of a number of externally bound molecules (at a high enough concentration) would probably result in an increased intermolecular separation rather than the decrease which is observed. Furthermore, it must be remembered that "native" proflavine also causes an increase in pitch and a decrease in intermolecular separation.

**Summary**

Previous studies have not reported on the orientational nature of drug binding to A-form or C-form DNA. It has often been assumed that the drug molecules bind randomly to the outside of the helix. The orientational study performed here using spin-labelled proflavine has demonstrated that the drug molecules are preferentially aligned when bound to both A-form and C-form DNA. The plane of the drug chromophore is probably orientated at 55° ± 10° to the helix axis (in the A-form) and at 70° ± 8° (in the C-form). A tentative space-filling model of the A-form structure shows that the acridine ring can easily be accommodated in the major groove at an angle of ~30° to the helix axis, in agreement with the calculated angle of tilt. The C-form structure can likewise be built with space-filling models. In both models the observed line broadening at high drug concentrations can be accounted for.

The B-form ESR spectra have been simulated by assuming a binding model in which the acridine ring is intercalated and free to rotate about its own z-axis. The simulation predicts a rapid rotation of the intercalated drug within a half-angle of ~40° about the DNA helix axis. The model does not take into account complications introduced by the possibility of rapid off-axial motion, but the main features of the experimental spectra have nevertheless been reproduced. The results are found to be in agreement with the work of Robinson et. al. (1980) and Hurley et al. (1982).

The simulations showed that the angle of misalignment parameter was a good indicator of the mode of binding, viz. intercalation resulted in a reduction of the Gaussian spread of drug orientations. External binding may therefore be identified with a large angle of misalignment.

# CHAPTER 5

## Interactions Between DNA and Several Phenothiazine Derivatives

### 5.1 Introduction

In this chapter interactions between DNA and several members of a class of tranquiliser are examined. The tranquilising drugs used are Chlorpromazine (CPZ), Prochlorperazine (PCPZ), Trifluopromazine (FPRZ), Promazine (PRZ), Promethazine (PRTZ) and Trifluoperazine (FPEZ). They are all derivatives of the three membered heterocyclic molecule Phenothiazine. The basic structure of the phenothiazines is shown in Fig. 5.1.

The pharmacological effects of many phenothiazines are well documented, for example in the treatment of schizophrenia (e.g. Hollister, 1982), and the interactions of phenothiazines with many and varied biologically active compounds, both in vivo and in vitro, have been studied. Chlorpromazine, the most extensively used of the drugs, has been shown to have an inhibiting effect on the actions of certain enzymes, such as the membrane-bound amines (Ziemsen, 1983). Promazine and Chlorpromazine are known to inhibit certain functions of the visual cortex in both schizophrenic and normal patients (Harris et al., 1983). The action of phenothiazines on Escherichia-Coli biochemical reactions in the human gut has been examined (Roland, 1981). Several phenothiazines show potent anti-sickling properties when bound to erythrocyte membranes (Jones, 1980). And it is well known that phenothiazines can form complexes with transition-metal ions, such as $Fe^{2+}$ or $Mn^{3+}$. These complexes may be important in vivo via their effects on metal ion binding to enzymes or proteins (Borg, 1961; Borg and Cotzias, 1962).

In spite of the vast catalogue of data available on the varied biochemical interactions and properties of the phenothiazines, of which the

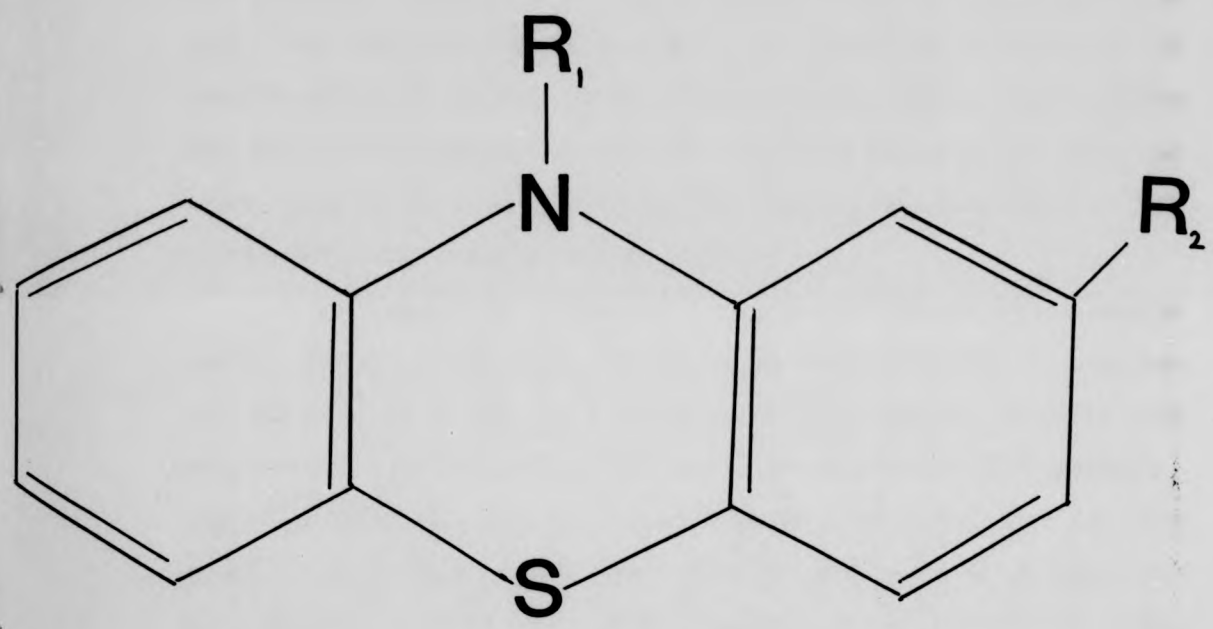


Fig. 5.1 The Phenothiazine Nucleus

above examples are only a few, a satisfactory description of their actions at a molecular level is lacking. However, since Forrest et al.(1958) found that phenothiazine free radicals were present in the urine of patients soon after ingestion of the corresponding drug, the importance of free radicals as reactive intermediates in the biochemical action of phenothiazines has been realised (Fenner, 1974). For example, in a recent study it was shown that the chlorpromazine free radical is an effective inhibitor of dopamine-activated enzymes in rats (Sweatt et al., 1982). Free radicals and their decay products have been detected in several types of mammalian organ, such as the liver. In cells, free radicals have been found in the mitrochondria and in nuclei (Forrest, 1974).

The superficial structural similarity between the chlorpromazine radical and the acridine dyes led Onishi and McConnell (1965) to consider the possibility of its binding to DNA. Using ESR to determine the orientation of the free radical in flowing solutions of DNA-$CPZ^+$ complexes, they concluded that the chlorpromazine radical intercalates in the DNA helix. Later work on solid DNA-$CPZ^+$ fibres showed that, although the chlorpromazine radical adopts a preferred orientation when bound to DNA, the possibility of external binding is not ruled out (Slade and Porumb, 1976; Porumb, 1976).

The form of binding of small molecules to DNA is dependent upon the structural and electronic properties of the molecules (see Chapter 1). In the phenothiazines the substituents at positions C2 and N10 in the heterocyclic ring (see Fig. 5.1) are known to have a profound influence on the tranquilising effectiveness of these drugs (e.g. McDowell, 1974). In the present study the effects of the substituents on the binding of phenothiazines to DNA are investigated. In most of these experiments DNA-drug fibres are used to obtain information concerning the orientations of the free radicals, and it is hoped that a clear answer can be given to the question of intercalation for these molecules. In the course of the

work the influence of the substituents on the formation and stability of the free radicals is considered.

## 5.2 Some properties of the phenothiazines

Crystallographic studies of several phenothiazines have been made (e.g. McDowell, 1974; Malmstrom and Cordes, 1972; Marsau, 1971). Nuclear magnetic resonance analyses of some phenothiazines have also been reported (Fronza et al., 1976, and refs.therein), and quantum mechanical methods have been used to determine the possible low energy conformations of many drugs (Kauffman and Kerman, 1974). The main results of these studies are reviewed here.

The phenothiazine ring system consists of a series of conjugated double bonds, with extensive delocalisation of the π-electrons over the ring, and lone pair electrons on the nitrogen and sulphur atoms (Fig. 5.1). A notable feature of the structure is the folding of the ring along the N-S axis, forming a dihedral angle of between 139° and 154° between the outer planes ( 139.4° for chlorpromazine, see Fig. 5.2). This folding is characteristic of other heterocyclic compounds which possess S in the central ring (Hosoya, 1964). The folding is thought to be due to the participation of the 3-d orbitals of the S atom in the ring structure.

Malrieu and Pullman (1964) used theoretical arguments to show that there are two distinct electronic configurations of the side group at the N10 position. If the side chain is directed towards the dihedral angle (the 'quasiequitorial' position), the lone pairs on the N can contribute to the π-system. If the side chain is directed away from the dihedral angle (the 'quasiaxial' position), the participation of the N lone pairs in the ring system is reduced. These possibilities are shown in Fig. 5.3. In solution there can be transitions between the two configurations, and these take place via an intermediate state in which the phenothiazine ring is planar (Fenner, 1974). This intermediate conformation may have important

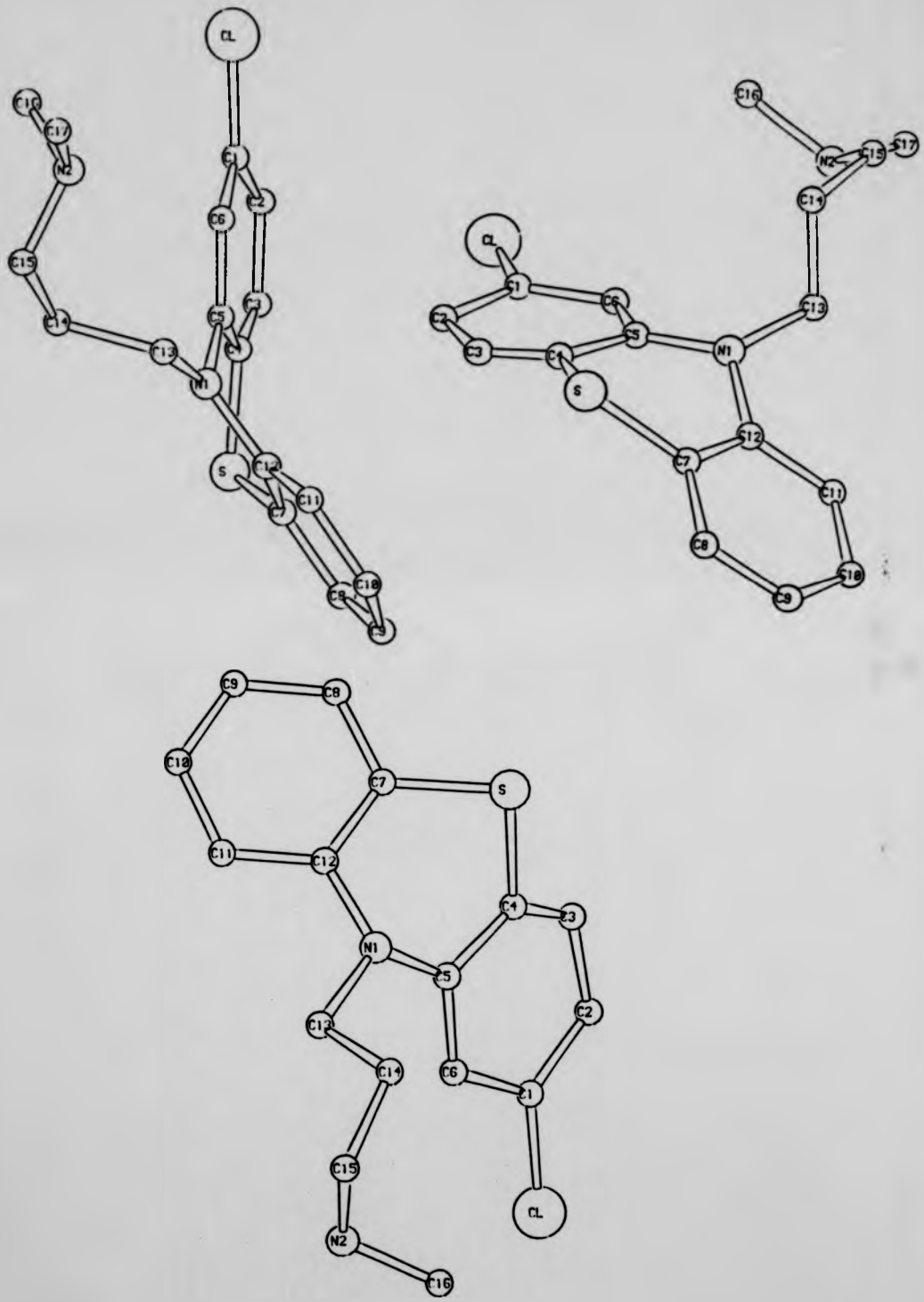


Fig. 5.2 ORTEP plots of CPZ demonstrating the folding of the Heterocyclic ring along the nitrogen-sulphur axis.

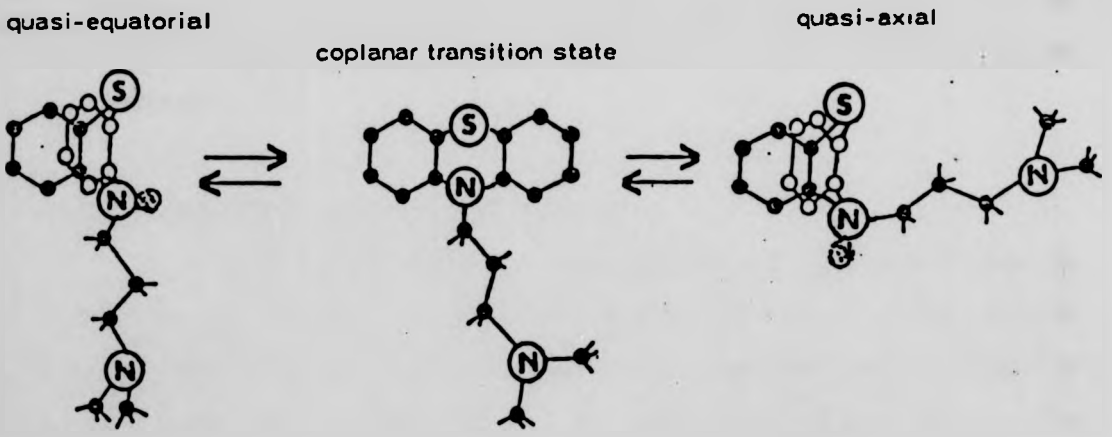


(After Fenner, 1974)

Fig. 5.3 The two possible Configurations of the N10 sidechain in the Phenothiazine Derivative.

biological consequences.

The drugs used in this study are distinguished by the types of substituents present at the N10 and C2 positions in the ring system. Thus, derivatives with the N10 substituent $(CH_2)_3N(CH_3)_2$ are generally classified as **promazines** and derivatives with the sidechain $(CH_2)_3N$ 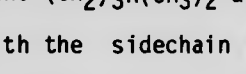 $N(CH_3)_2$ belong to the **perazine** "family". Several of the phenothiazine derivatives have branched N10 sidechains, such as promethazine: $CH_2(CHCH_3)N(CH_3)_2$. Within each "family" the various derivatives are distinguished by their C2 substituents, which in this case are either Cl, H or $CF_3$. Table 5.1 gives a full list of the phenothiazine derivatives used in this work. All of these compounds readily form free radicals under the appropriate conditions.

## 5.3 Free Radicals: Formation and Stability

Free radical forms of the phenothiazine derivatives may be obtained by a variety of methods including electrolytic oxidation (Piette and Forrest, 1962), enzymic oxidation (Piette, 1964) and chemical oxidation (Borg and Cotzias, 1962; Hanson et al., 1973; Langercrantz, 1961). The latter method is preferred here. Oxidation was achieved using either concentrated sulphuric acid or sodium persulphate as oxidising agents and the conditions for maximum radical yield and stability were investigated.

### 5.3 (a) Method

10mM and 1mM stock solutions of the phenothiazine derivatives (PRZ, PCPZ, CPZ, FPEZ, FPRZ and PRTZ) were prepared using their known molecular weights. All solutions were colourless and dissolution was improved by using warm distilled water. Stock solutions of sodium persulphate and sulphuric acid were also prepared.

Free radicals were obtained by adding a small volume of the

| NAME | R1 | R2 |
|---|---|---|
| Promazine | -H | $(CH_2)_3N(CH_3)_2$ |
| Chlorpromazine | -Cl | $(CH_2)_3N(CH_3)_2$ |
| Triflupromazine | $-CF_3$ | $(CH_2)_3N(CH_3)_2$ |
| Prochloroperazine | -Cl | $(CH_2)_3N$$N(CH_3)$ |
| Trifluperazine | $-CF_3$ | $(CH_2)_3N$  $N(CH_3)$ |
| Promethazine | -H | $CH_2(CHCH_3)N(CH_3)_2$ |

Table 5.1 The Phenothiazine Derivatives used in this work

oxidising reagent to an equal volume of a drug solution and allowing the mixture to stand. After only a few seconds the colour of the mixture changed and then progressively deepened until, after 1-2 minutes, maximum free radical yield was achieved. To slow down the free radical decay rate the mixing stage was accomplished at 4°C and in subdued lighting.

5.3 (b) Results and Discussion

It was found that, when prepared from 1mM solutions, the free radical decay rate exceeded the rate of formation. This resulted in very weakly concentrated solutions. On the other hand, when drug and oxidising reagents were used at concentrations in excess of about 5-10mM solid free radical precipitates were formed in the mixture. These precipitates were stable for weeks and could not be removed by dilution. The optimum concentration for free radical preparation for both drug and oxidising solutions was about 10mM.

The colour changes accompanying the formation of the free radicals were characteristic of the substituted groups present. Thus, solutions containing free radicals with a chlorine atom at C2 ($PCPZ^+$ and $CPZ^+$) were red, whereas those with a $CF_3$ substituent at C2 ($FPEZ^+$ and $FPRZ^+$) were orange/brown. The $PRZ^+$ radical, which has a hydrogen at C2, gave pink solutions and $PRTZ^+$, which has a branched N10 sidechain, gave solutions which were deep blue/mauve. These colour changes were obtained with both sulphuric acid and sodium persulphate.

Quantitative estimates of the rates of decay of the free radicals were not made but it was clear that

(i) The formation and decay of the radicals in sodium persulphate occurred rapidly i.e. within 1 hour at room temperature and 3-4 hours at 4°C.

(ii) Free radicals were formed more slowly in dilute sulphuric acid but remained stable for several hours at room temperature and for several days at 4°C.

(iii) The stability of the radicals in both sulphuric acid and sodium persulphate depended upon the C2 substituent in the order: H ~ Cl > $CF_3$.

(iv) The $PRTZ^+$ radical was considerably more stable than $PRZ^+$.

The capacity of the phenothiazine free radicals to form different oxidised species in sulphuric acid has been noted by several workers (Shine and Mach, 1965; Tozer and Tuck, 1965; Hanson and Norman, 1973). Under the conditions used here the free radical formed is the cationic free radical, which has the structure shown in Fig. 5.4a. This species ultimately decays to its sulphoxide form through a series of complex reactions which are enhanced by the presence of water (Borg and Cotzias, 1962; Bodea and Silberg, 1968).

In general the stability of a free radical depends upon three important factors: the extent of the delocalisation of the unpaired spin density, steric hindrance and polarity (Nonhebel et al., 1979). Since the samples used in this work all possess similar N10 substituents any steric influences this substituent has on free radical stability should also be similar. On the other hand, the electron-donating (or withdrawing) capacity of the C2 substituent will have a strong influence on the unpaired electron density distribution in the ring system. For example, the fluorine atoms of the $CF_3$ substituent are strongly electronegative and the $CF_3$ group is therefore expected to be electron-donating. The unpaired spin density on the ring nitrogen should therefore be increased relative to its value for the H-substituent. The Cl substituent will, however, be electron-withdrawing and this should result in an increased delocalisation of the unpaired spin. These possibilities are shown schematically in Fig. 5.4b. Since the stability of a free radical increases with the extent of spin delocalisation, the above remarks suggest that the order of

a

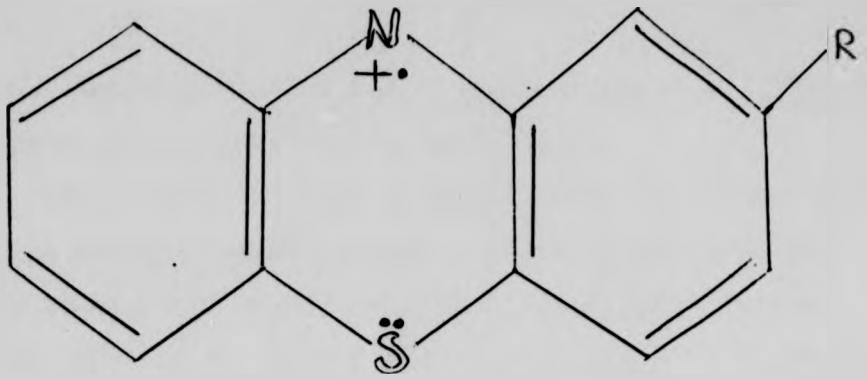


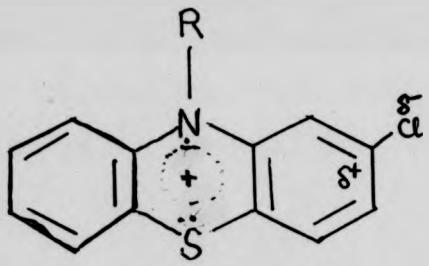


b

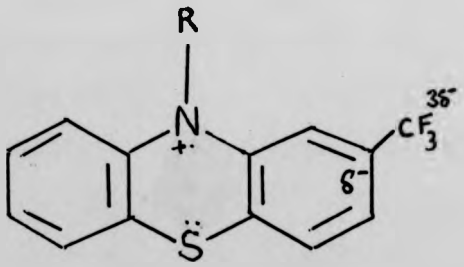


Fig. 5.4 (a) The Cationic Phenothiazine Derivative Free Radical.
(b) A schematic representation of the effects of the C2 substituents on the distribution of spin-density α electronic charge density over the ring system.

stability should be Cl > H > $CF_3$. It can be seen that the experimental observations are consistent with this interpretation.

The greater stability of the $PRTZ^+$ radical relative to $PRZ^+$ may be due to steric influences introduced by the closer proximity of the ring and N10 nitrogen atoms and the branching of the sidechain. Differences in the polarisability of the two N10 substituents may also be important. Hanson et al. (1981) and Clarke et al. (1978) studied the effects of different N10 substituents for a series of phenothiazine radicals and they were led to the conclusion that a close relationship exists between the spin density on the ring nitrogen and the length and polarity of the substituent: the spin density was found to increase with both length and polarity. If this result is applied to the present case then one would expect the localisation of the unpaired electron to be greater for $PRZ^+$ than for $PRTZ^+$. The $PRTZ^+$ radical should therefore, as observed, be more stable.

Visible and UV absorption spectra of several of the free radical species were recorded and those obtained from $FPRZ^+$ are shown in Fig. 5.5. The spectra exhibit several **isosbestic points**, which suggests the existence of a single decay mechanism. The decay curves are similar to those previously obtained for $CPZ^+$, whose final decay product is CPZ-Sulphoxide (Borg and Cotzias, 1962; Shine and Mach, 1965). The pH of the free radical solutions decreases rapidly during the decay process. For the radicals used in this work the pH stabilised in the range 3.7 - 4.3. The pH was not important for work which did not involve the use of DNA. However, since DNA denatures at pH values close to 3.7 some care was required in preparing the DNA-free radical complexes. An attempt to buffer the DNA solutions at about pH = 7 failed because it resulted in a very rapid quenching of the cationic free radicals. It might be noted at this point that, for

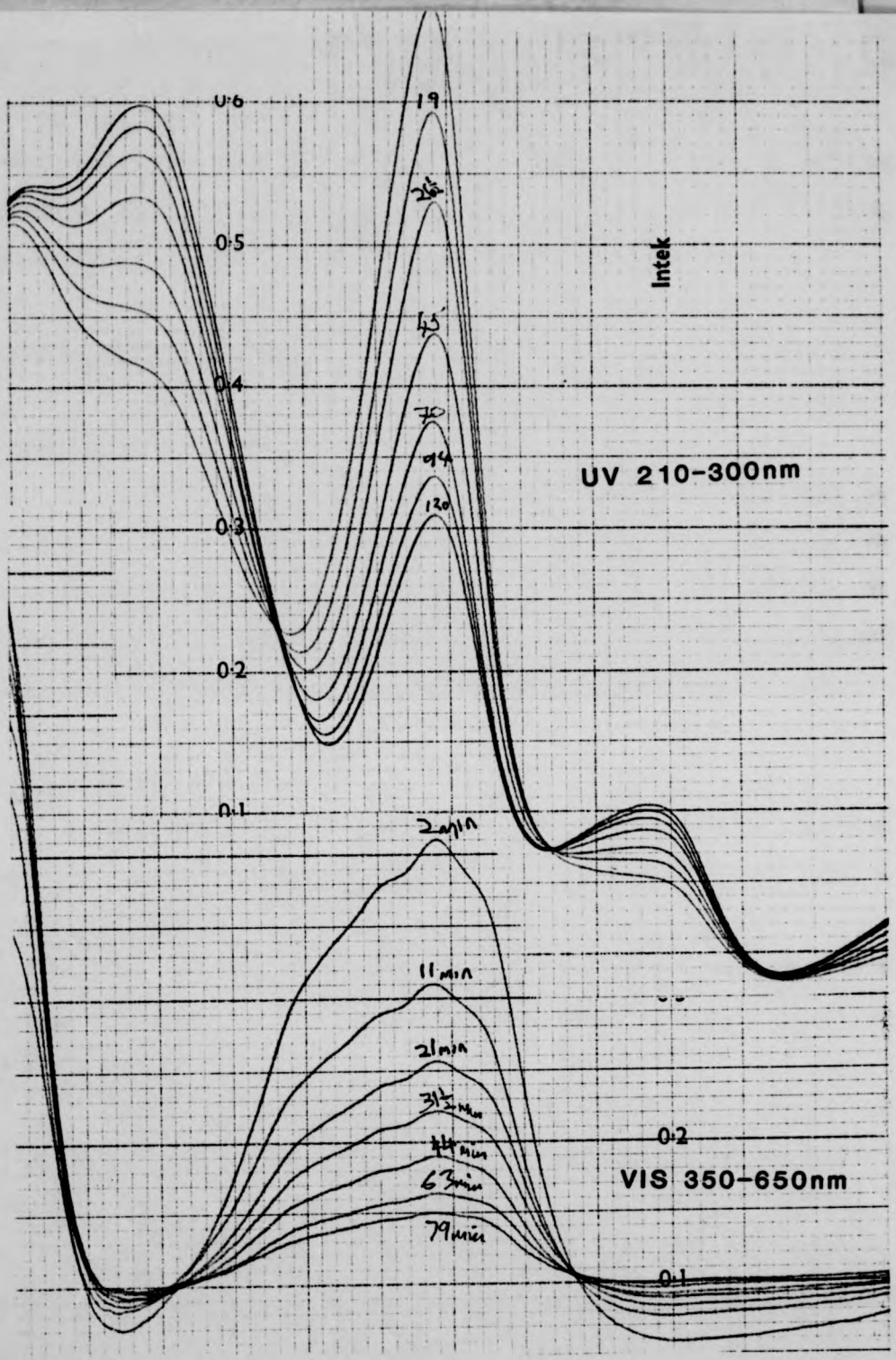


Fig. 5.5 Absorption spectra in the UV and visible regions of the $FPRZ^{+}$ free radical.

experiments involving DNA, sodium persulphate was preferred as the oxidising agent. This was because the resulting pH was slightly more favourable for continued polynucleotide stability.

## 5.4 Free Radical ESR Spectra

### 5.4(a) Method

Free radicals were prepared from 10mM solutions as described in section 5.4(a) using sulphuric acid as the oxidising agent. ESR spectra were recorded at 10mW microwave power and at a modulation amplitude of 0.01mT pK-pK. The magnetic field was swept through resonance at a rate of 0.6mT $min^{-1}$. All spectra were recorded at room temperature.

### 5.4(b) Results

The fluorine containing free radicals, $FPRZ^+$ and $FPEZ^+$, yielded identical ESR spectra consisting of about 23 lines superimposed upon a background lineshape of ~2.5mT width (Fig. 5.6a).

The chlorine containing free radicals, $PCPZ^+$ and $CPZ^+$, also gave similar lineshapes, this time consisting of about 16 resolved hyperfine lines (Fig. 5.7a).

The spectrum of the $PRZ^+$ radical is shown in Fig. 5.7b. It has an overall width and background lineshape similar to the $PCPZ^+$ and $CPZ^+$ spectra.

The promethazine free radical has a distinctly different background lineshape, as can be seen form Fig. 5.6b. For this spectrum about 18 hyperfine lines are resolved.

All the spectra were centred on $g = 2.0053 \pm 0.0003$.

### 5.4(c) Analysis and Discussion

It is not the aim of this section to analyse in great detail the

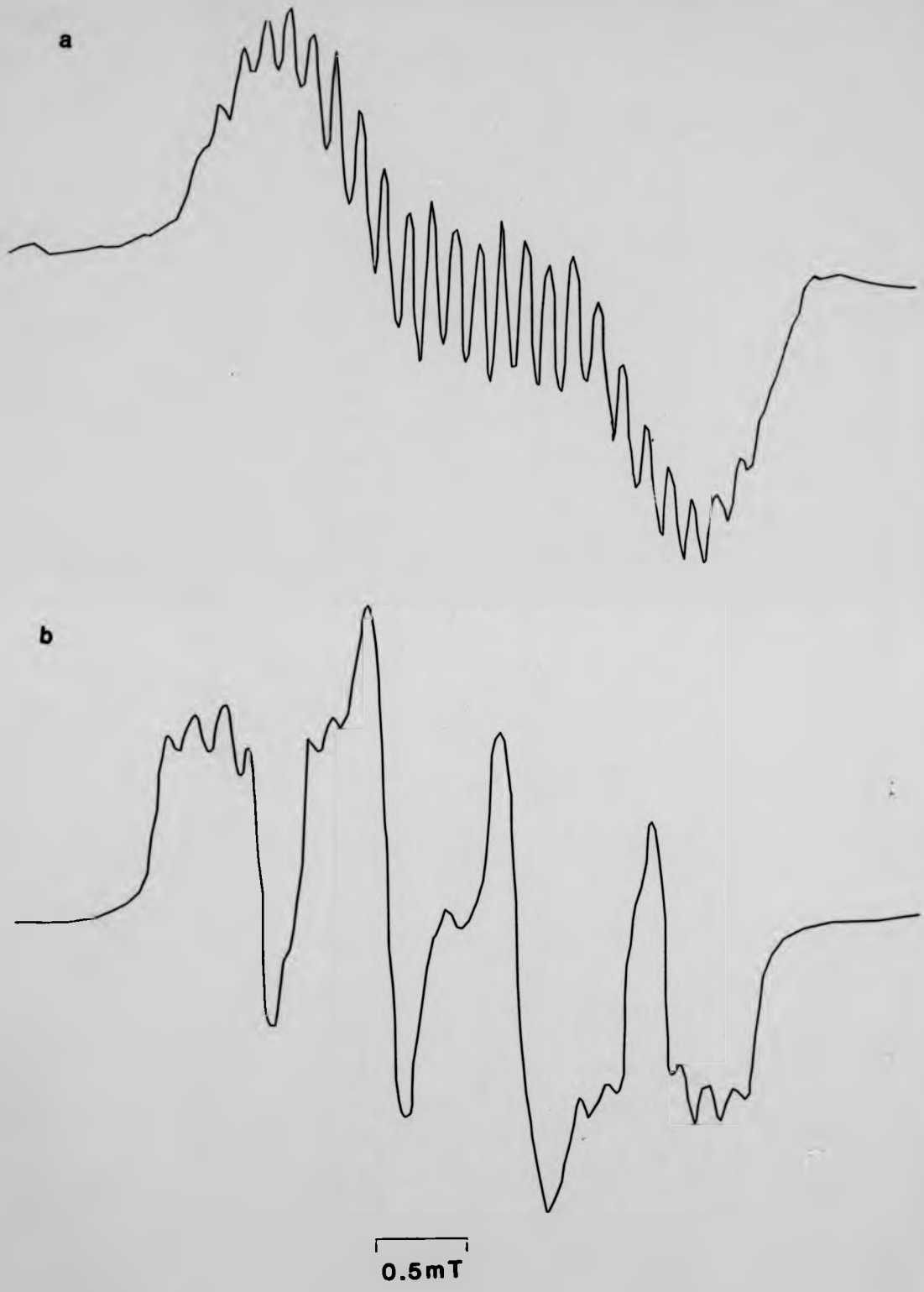


Fig. 5.6 (a) The $FPRZ^+$ radical ESR spectrum.
(b) The $PRTZ^+$ radical ESR spectrum.

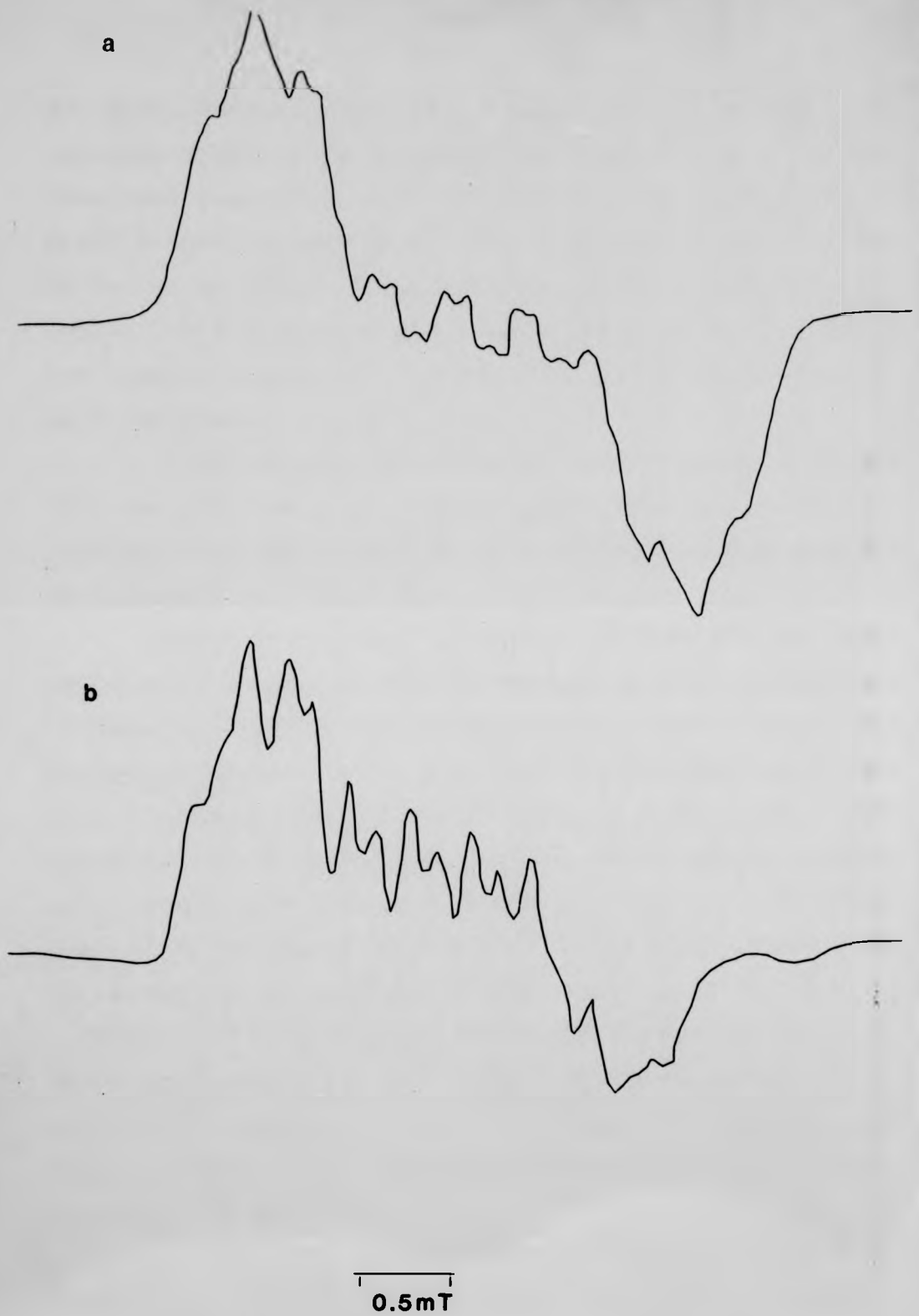


Fig. 5.7 (a) The $PRZ^+$ radical ESR spectrum.
(b) The $PCPZ^+$ radical ESR spectrum.

ESR solution spectra mentioned above. However, the various sidechains and substituted groups do have an important influence on the electronic and psychotropic properties of the different derivatives and it is important, as well as useful, to determine what relative contributions the $^{14}N$ nucleus and the ring and sidechain protons make to the hyperfine structure of these spectra. In order to aid this task computer simulations of the spectra were attempted. Before discussing these simulations some general comments may be appropriate.

Firstly, the equivalence of the $PCPZ^+$ and $CPZ^+$ spectra and of the $FPEZ^+$ and $FPRZ^+$ spectra shows that the magnetic influences of the N10 substituent do not extend further than at most the third methylene group in the sidechain.

Secondly, the overall similarity of the $PCPZ^+$, $CPZ^+$ and $PRZ^+$ spectra (e.g. the undulating series of peaks superimposed on the background lineshape) is significant for the following reason. The $PRZ^+$ radical is structurally identical to $CPZ^+$ (and to $PCPZ^+$ if the sidechain beyond the third methylene is neglected) but it lacks the C2 chlorine atom. The experimental results strongly imply, therefore, that the chlorine nuclear spin ($I = 3/2$) makes only a small contribution to the $PCPZ^+$ (or $CPZ^+$) spectrum. This contribution may be due to either the direct interaction of the unpaired electron with the Cl nuclear spin, or to the indirect influence of the electronegative Cl atom on the distribution of spin density and cationic charge density in the ring system. As will be seen in the following simulations, even very small changes in the coupling constants assigned to the ring protons can produce significant changes in the resulting ESR spectrum.

Thirdly, as may be seen from Table 5.1, except for the presence of the $CF_3$ group, the $PRZ^+$ and $FPRZ^+$ radicals are structurally identical. By comparing Fig. 5.6a, Fig. 5.7a and Fig. 5.7b it is clear that the $CF_3$ substituent has a greater effect on the ESR spectrum than does the Cl

substituent. This may be due to the interaction of the three fluorine nuclear spins (I = 1/2) with the unpaired electron. Alternatively, or additionally, the electron-donating tendency of the $CF_3$ group may be responsible for the contrasting effects of the Cl and $CF_3$ substituents.

Fourthly, the $PRZ^+$ and $PRTZ^+$ radicals differ only in their N10 substituents: the sidechain is branched in $PRTZ^+$ and "linear" in $PRZ^+$ and the ring and sidechain nitrogens are closer in $PRTZ^+$ than in $PRZ^+$. These differences account for the quite different background lineshapes of the $PRTZ^+$ spectrum and the spectra of the $PRZ^+$ "family", comprising $PRZ^+$, $PCPZ^+$, $CPZ^+$, $FPRZ^+$ and $FPEZ^+$.

**Simulations**

Computer simulations of the ESR spectrum of the $PRZ^+$ radical have not previously been reported. However, molecular orbital calculations of the unpaired spin density distribution in the phenothiazine and 10-methylphenothiazine free radicals indicates that all the ring protons make some contribution to the observed hyperfine structure (Sullivan and Bolton, 1969; Clarke, 1978). The computer simulations obtained by Ruperez et al. (1982) for the trimeprazine free radical shows that the ring protons can be assigned coupling constants close to the values predicted for this derivative by the molecular orbital calculations.

In the $PRZ^+$ radical there are four pairs of equivalent protons in the ring, i.e. H(1,9), H(2,8), H(3,7), H(4,6) (see Fig. 5.1). In addition, there are six protons in the three methylene groups in the sidechain. If it is assumed that the unpaired spin density is centred near the heterocyclic ring then only the first two methylene protons need to be considered. These protons, labelled $\beta_1H$ and $\beta_2H$ for convenience, are assumed to have the same

coupling constant. Fenner (1970) has argued, without doing any simulations, that the β-protons should be assigned coupling constants given by

$$a_\beta = \tfrac{1}{2} a_{N10}$$

With this proposition in mind computer simulations of the $PRZ^+$ radical were made.

The ring $^{14}N$ coupling constant was first varied until the overall background lineshape and splitting were obtained. The β proton coupling constants were then assigned. The ring coupling constants, originally derived from molecular orbital theory for the 10-methylphenothiazine radical, were taken from Ruperez et al. (1982). Adjustments of these values were required to obtain the best fit, which is shown in Fig. 5.8a, and the full set of coupling constants is

$a_{N10}$ = 0.71mT $\quad$ $a_\beta$ = 0.35mT

$a_H(1,9)$ = 0.098mT $\quad$ $a_H(2,8)$ = 0.088mT

$a_H(3,7)$ = 0.195mT $\quad$ $a_H(4,6)$ = 0.004mT

Linewidths: 0.12mT

Lineshape: Gaussian.

When compared with Fig. 5.7b it can be seen that the experimental spectrum is not quite symmetrical: there is an overall slope to the spectrum and the high-field region is broadened. The broadening probably arises from the motional modulation effects described in Chapter 2 (Section 2.7). The overall slope of the spectrum may be due to an "alternating linewidth effect" (Frankel, 1967; Hudson and Luckhurst, 1968). This effect can arise in several ways. As mentioned in section 5.2, depending on the configuration of the N10 sidechain, the phenothiazine ring can exist in at least two distinct conformations. Inversions between these conformations can occur in solution (Fenner, 1974) and this may lead to a modulation of certain isotropic hyperfine coupling constants. This in turn may lead to a broadening of certain of the hyperfine lines in the spectrum (Hudson and

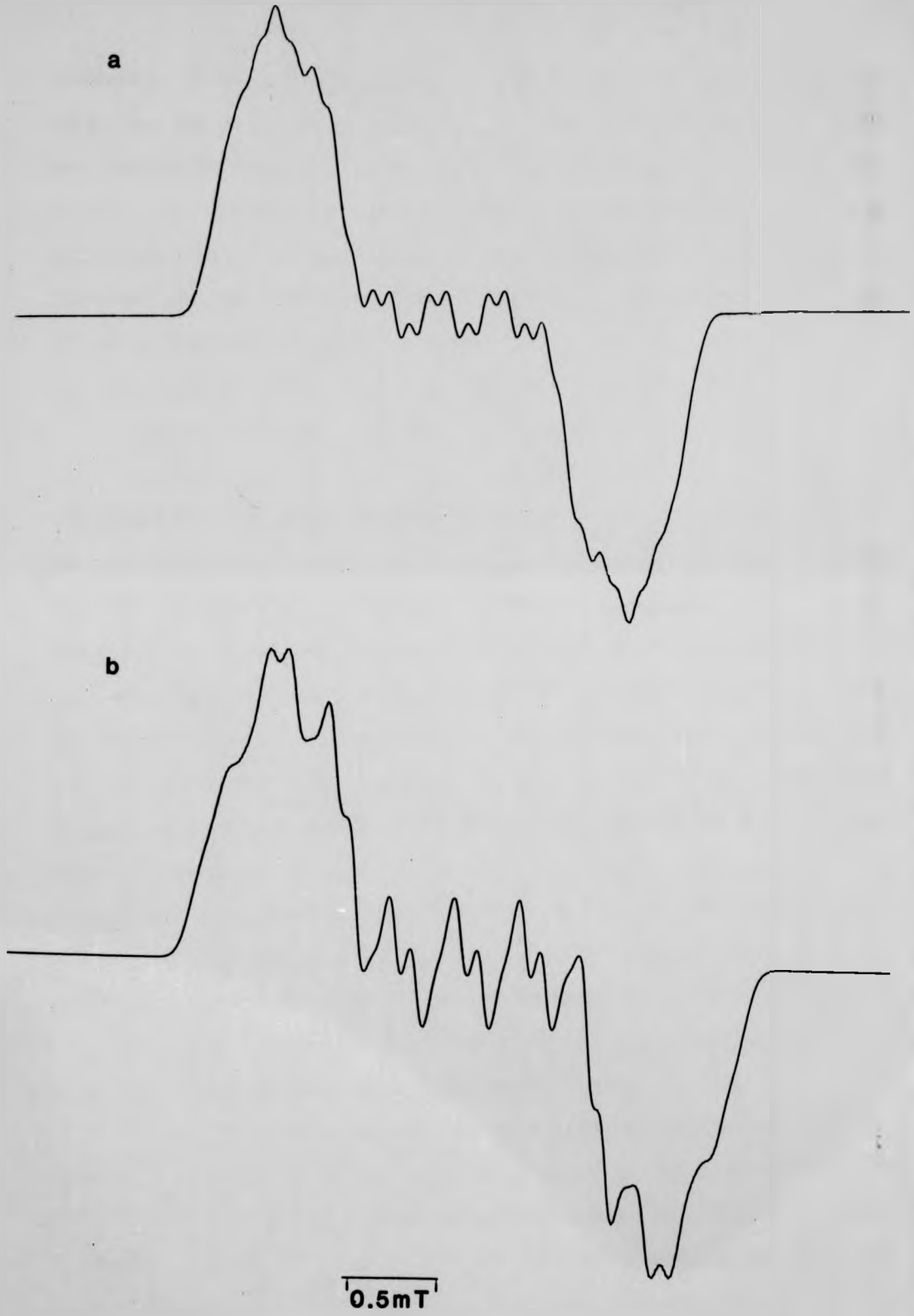


Fig. 5.8 (a) Computer simulation of the $PRZ^+$ spectrum.
(b) Computer simulation of the $PCPZ^+$ spectrum.

Luckhurst, 1968). It is not possible to test this idea using the present data, but the work of Ruperez et al. (1982) indicates that ring inversions are responsible for the sloping effect in the ESR spectrum of trimeprazine.

An attempt was made to simulate the $PCPZ^+$ spectrum by first neglecting the Cl nuclear spin. Only seven ring protons were therefore involved and the spectrum shown in Fig. 5.8b was obtained with the following coupling constants

$a_{N10}$ = 0.66mT $a_\beta$ = 0.33mT

$a_H(1,9)$ = 0.098mT $a_H(3,7)$ = 0.195mT

$a_H(4,6)$ = 0.003mT $a_H(8)$ = 0.095mT

and linewidths of 0.115mT (Gaussian lineshape).

The simulation reproduces the main features of the $PCPZ^+$ spectrum, although the fit to the high- and low-field regions is quite poor. The 0.05mT reduction of the $^{14}N$ coupling constant of $PCPZ^+$ compared with the coupling constant for $PRZ^+$ demonstrates the "delocalising" influence of the electron-withdrawing Cl substituent. Simulations were also attempted with the Cl spin present, but, although the spectrum retained its background shape, the hyperfine structure could not be reproduced. These simulations were by no means exhaustive but they do suggest that the Cl spin contribution can indeed be neglected. The physical reason for the absence of any Cl hyperfine structure may be due to the presence of relaxation processes caused by the electric quadrupole moment ($Q \sim 0.08 \times 10^{-24} cm^2$) of the Cl nucleus. The relaxation effects will cause a broadening of the Cl hyperfine contribution which may not then be resolved.

A complete simulation of the $FPEZ^+$ spectrum was difficult because of the large number of nuclear spins involved. Viz, including the fluorine nuclei (which do not possess quadrupole moments) a total of 13 nuclei were involved. The computation time required for the simulation was huge (in excess of 700 CPU). For this reason only 11 nuclei were used, as in the $PRZ^+$ case. This time, however, the C2 and C8 substituents were not

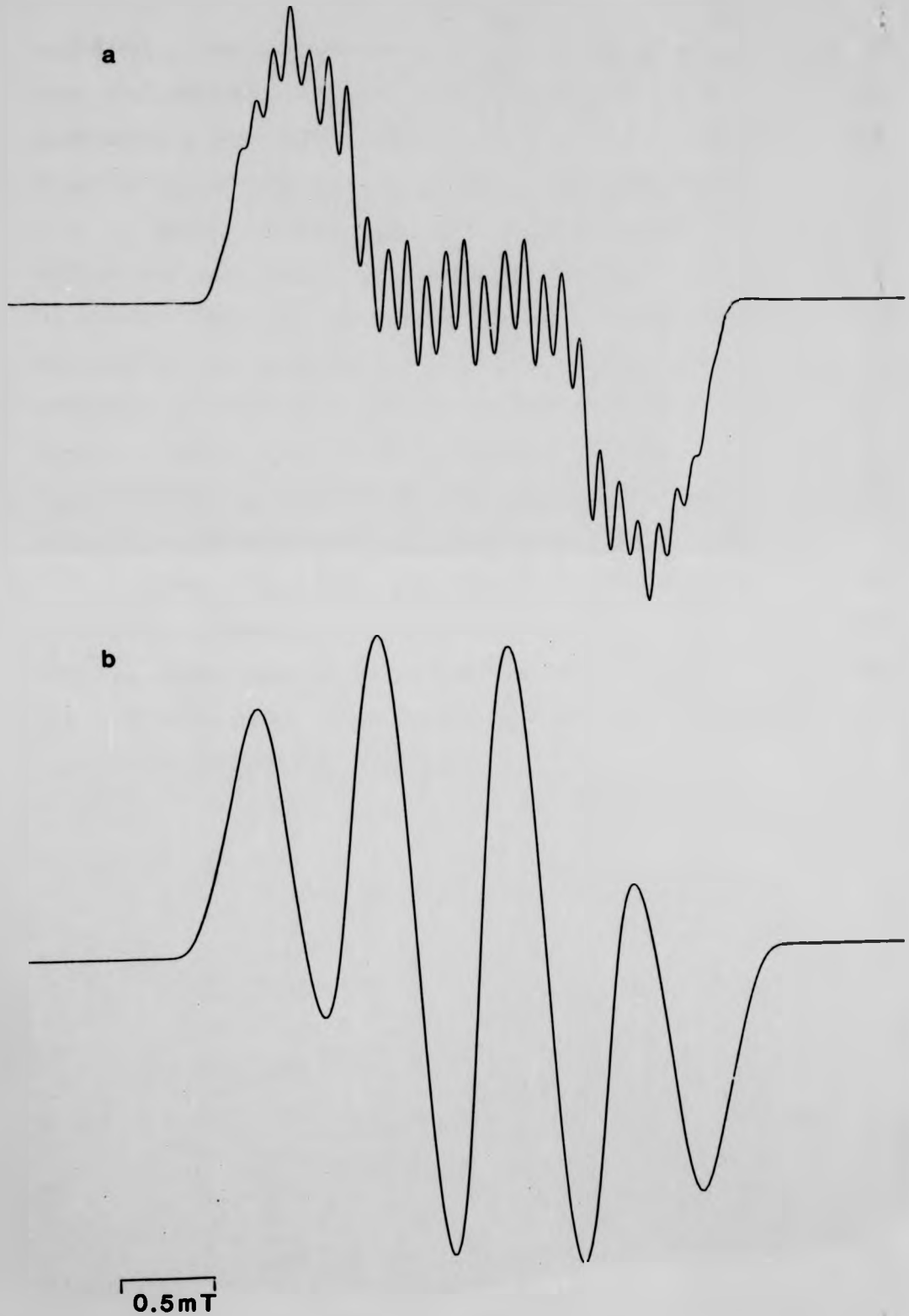


Fig. 5.9 (a) Computer simulation of the $FPRZ^+$ spectrum.
(b) Computer simulation of the $PRTZ^+$ spectrum.

equivalent. The one parameter which could be reasonably well estimated from the simulation (Fig. 5.9a) was the $^{14}N$ coupling constant, which was expected to be about equal to the $PRZ^+$ $^{14}N$ coupling. The simulation gave a value for $a_{N10}$ of 0.59mT, which is close to the expected value.

Several attempts were made to simulate the $PRTZ^+$ spectrum, without too much success. However, it was clear that the overall background lineshape was reproducible only if the β-protons were magnetically not equivalent (Fig. 5.9b). The non-equivalence may be explained in terms of the chirality of the N10 sidechain (Clarke, 1978; Ruperez, 1982). The coupling constants used for Fig. 5.9b were $a_{N10}$ = 0.585mT, $a_{\beta 1}$ = 0.17mT and $a_{\beta 2}$ = 0.56mT. As expected, the $^{14}N$ splitting is smaller than the value recorded for the $PRZ^+$ radical.

These simulations show that the unpaired spin density is principally concentrated in the $^{14}N$ nucleus and that changes in the $^{14}N$ coupling can be accounted for by variations in the electronegativities of the ring substituents. A considerable spin density was also found on the β-protons of the methylene sidechain.

## 5.5 Fibre Studies

### 5.5 (a) Method

The following stock solutions were prepared:
10mM Sodium Persulphate ($Na_2S_2O_8$) in de-ionised water, 10mM drug solutions in 0.1 - 0.5M NaCl and 3 - 8mM Calf Thymus DNA in 5mM NaCl.

The phenothiazine derivatives were converted to their cationic forms in concentrations suitable for binding to DNA by the following method.

$2cm^3$ of Sodium Persulphate was added to an equivalent volume of the stock drug solution and the mixture was allowed to stand for 1 - 2 minutes until a good yield of free radical was obtained. After this time, the mixture was diluted ten times by the addition of de-ionised water. An appropriate volume of the resulting solution was then added dropwise to $5cm^3$ of the 3mM DNA solution (or to an appropriate volume of another DNA solution). The mixing of the free radical and DNA solutions was accomplished in the dark at 4°C to reduce precipitation. Precipitation was more easily accomplished using one of the fluorine compounds. The final pH of the resulting complex varied between 3.9 (for $FPRZ^+$) and 4.7 (for $PRZ^+$).

The complex was distributed in either a 3 x $3cm^3$ or a 10 x $10cm^3$ rotor and then centrifuged as usual. Gels and fibres were then prepared as before (see Chapter 3). The salt concentration in the fibres varied between 5 and 25mM NaCl.

Several fibres (between 8 and 12) were mounted together and orientated on the sticky side of a small piece of Selotape. A small blob of silicon grease was used to attach the Selotape to the flat surface of a Varian Tissue Cell, which was then mounted in the spectrometer cavity.

As before, the relative humidity of the fibre envioronment was varied between 33 and 98% and ESR spectra were recorded over a range of fibre orientations. The microwave power was normally set at 15mW and the

100-kHz modulation was set at 0.125mT.

X-ray diffraction patterns were recorded to determine the DNA conformations.

5.5 (b) Results

The P/D ratios of the original complexes varied between 6 and 10. These were the nominal values, calculated assuming that maximum radical yield was present prior to dilution with de-ionised water. However, the decay of the free radicals meant that the true P/D was much larger. Estimates based upon the method outlined in Chapter 4 put the true P/D ratios at about 60 to 100 or more per fibre.

All the fibres examined at relative humidities between 33 and 92% gave A-type diffraction patterns (Fig. 5.10). B-type diffraction patterns were seen at > 92% r h. (Fig. 5.10). C-type patterns were never observed.

The most striking features of the ESR results were:

(i) All the ESR spectra showed the same orientational dependence and were otherwise identical, regardless of which free radical was present, and

(ii) The spectra associated with the A- and B-conformations were identical at all orientations.

The A-form (or B-form) spectra for three orientations of a bunch of eight $FPRZ^+$ - DNA fibres are shown in Fig. 5.11(a-c). The corresponding gel spectrum is shown in Fig. 5.11d. The gel spectrum has a maximum splitting of $\Delta A_g$ = 3.35mT. The spectrum corresponding to the parallel orientation of the fibre exhibits three hyperfine lines with a maximum separation $\Delta A_{\parallel}^{a,b}$ = 4.14mT. The perpendicular spectrum shows a single line of width ~0.9mT. Within experimental error the same splittings and field cross-over values were recorded for the ESR spectra of the other free radical - DNA fibres.

Fig. 5.10 A- and B-form X-ray diffraction patterns for a FPRZ$^{+}$-DNA fibre recorded at 33% and 98% relative humidities.

Fig. 5.10 A- and B-form X-ray diffraction patterns for a FPRZ$^{+}$-DNA fibre recorded at 33% and 98% relative humidities.

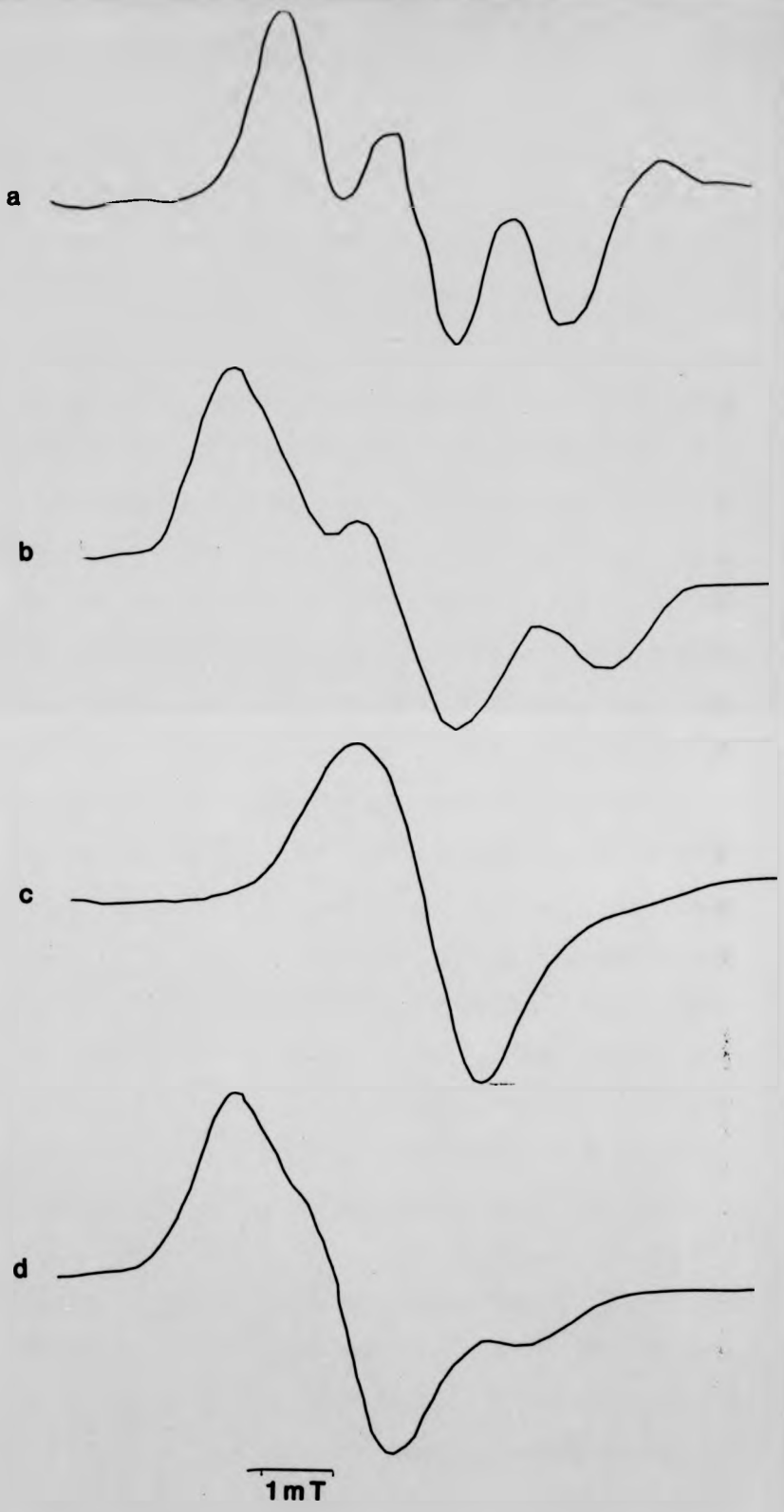


Fig. 5.11(a-d) Experimental ESR Spectra of $TFPZ^{+}$-DNA Fibres and Gel (a) 0° (b) 45° (c) 90° (d) Gel.

Fig 5.11

5.5 (c) Analysis and Discussion

**The Gel Simulation.**

The proton hyperfine couplings which are present in the ESR solution spectra of the free radicals are not resolved in the gel and fibre spectra. Computer simulations of the solution spectra (Section 5.4) make it clear that the unpaired electron spin density is principally concentrated in the $2p\pi$ orbital of the $^{14}N$ atom in the phenothiazine ring. It will initially be assumed, therefore, that the principal hyperfine values are axially symmetric (i.e. $A_{zz} = A_{\parallel}$ and $A_{xx} = A_{yy} = A_{\perp}$). Furthermore, the gel spectrum (Fig. 5.11d) has a splitting and lineshape similar to that of a frozen (~200°K) solution spectrum of the $CPZ^{+}$ radical (recorded by Porumb, 1976). This observation suggests that the free radicals are strongly immobilised on binding to the DNA. The magnitude of the largest hyperfine component is therefore taken as $A_{\parallel} = \frac{1}{2}\Delta A_g = 1.67mT$.

The principal g-values are also initially taken to be axially symmetric (to speed up the calculations), with $g_{\parallel} = g_{zz}$, etc. For many aromatic $\pi$-electron free radicals, $g_{\perp} > g_{\parallel}$ and $g_{\parallel} \sim g_e$ (McConnell and Robertson, 1957; Ayscough, 1967). $g_{\parallel}$ is therefore initially set at 2.0023.

Using these starting values for $A_{\parallel}$ and $g_{\parallel}$ and setting the linewidths at 0.85mT each, simulations were obtained by stepping $\theta_1$ through 4° intervals. $g_{\perp}$, $g_{\parallel}$ and $A_{\parallel}$ were varied until the correct field positions and general lineshapes were obtained. It was quickly established that a Gaussian lineshape provided the better fit - a Lorentzian was too broad in the wings of the spectrum. The linewidths were then varied and eventually increased to 0.95mT each. At this point small adjustments of $g_{\perp}$ were required and it was found that the fit could be considerably improved by dropping the assumption of axial symmetry. The final parameters were:

$g_{xx}$ = 2.0070 $A_{xx} = A_{\perp}$ = (0.3 ± 0.03)mT

$g_{yy}$ = 2.0061 $A_{yy} = A_{\perp}$ = (0.3 ± 0.03)mT

$g_{zz}$ = 2.0025 $A_{zz} = A_{\parallel}$ = 1.67mT

Linewidths: 0.95mT

Lineshape: Gaussian.

The fit given by these parameters is good, as may be seen from Fig. 5.12. As noted above, the $FPRZ^{+}$ - DNA gel spectrum was used as a model spectrum for the simulation. However, the above set of parameters also gives a good fit to the other gel spectra obtained using the other free radical species. The only difference between these spectra was a small variation in their linewidths. This effect may be attributable to a variation of the free radical concentration in the different gel preparations. This in turn is probably a consequence of the different rates of decay of the various free radical species.

**The Fibre Simulations**

If the free radical unpaired electron is localised entirely in the $2p\pi$-orbital of the $^{14}N$ atom then the interaction between the unpaired electron and the nitrogen nuclear spin should result in a characteristic three-line hyperfine splitting in the ESR spectrum. Such a "triplet" splitting was observed when the fibres were orientated parallel to the external magnetic field (Fig. 5.11a). The triplet remained visible with the fibre at 45° to the field (Fig. 5.11b) but only a single (broad) line was observed with the sample at 90° to the field (Fig. 5.11c). The strength of the electron - nitrogen nuclear hyperfine coupling can be correlated with the relative orientations of the long axis of the $^{14}N$ $2p\pi$-orbital and the external magnetic field (see Chapter 2). The hyperfine interaction is a maximum when the $2p\pi$-orbital z-axis and the external field are parallel and a mimimum when they are at 90° to each other. It is therefore natural to suppose that the observed maximum in the hyperfine

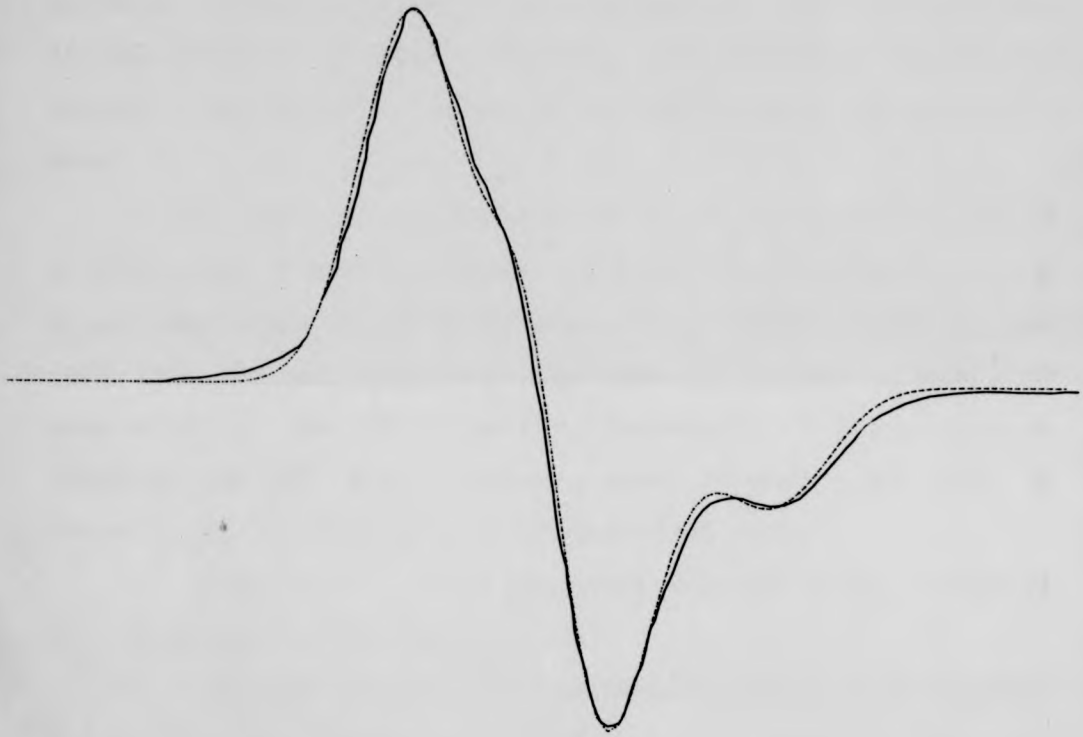

Fig. 5.12 Computer simulation of the $FPRZ^{+}$-DNA gel ESR spectrum.

splittings corresponds to a parallel arrangement of the 2p$\pi$-orbital z-axis and the external magnetic field. If the DNA molecules were perfectly orientated in the fibre it would then follow that the free radicals are orientated with their chromophores perpendicular to the DNA helix axis. In practice, of course, a spread in the orientations of the DNA in the fibre is more likely. An estimate of the degree of misalignment of the DNA was obtained from computer simulations in which the following assumptions were made.

The angles of tilt and twist were set to zero and the linewidths at 0.95mT each. A gaussian lineshape was assumed and the angles $\theta_1$, $\phi_1$ and $\psi_2$ were swept throgh 4°, 8° and 15° respectively. The g- and A-values were taken from the gel simulation. Simulations for several of angles of misalignment of the DNA in the fibre from between 0° (i.e. perfect alignment) and 90° (i.e. virtually random alignment) are shown in Fig. 5.13, with the fibre parallel to the magnetic field.

The assymmetry of the experimental spectrum is best reproduced for a misalignment angle of about 40°.

Simulations were then obtained for various angles of tilt between 0° and 180°. These calculations proceeded as above except that this time the angle of misalignment was fixed at 40°. The results of these calculations are shown in Fig. 5.14. Simulations for both the parallel and perpendicular orientations of the fibre are shown and it is clear that the observed anisotropy is reproduced by tilt angles other than zero degrees. Simulated spectra having tilt angles in the range 160 - 180° (i.e. -20° to 0° to the helix axis) and those centred about 110° (-70°) all follow the observed pattern in the hyperfine splittings and a comparison with the experimental results shows that any one of these possible angles of tilt gives an acceptable fit at all orientations of the fibre (Fig. 5.15(a-c)).

Because of the near equality of the x and y components of the principal g-values, variations in the angle of twist only produced minimal

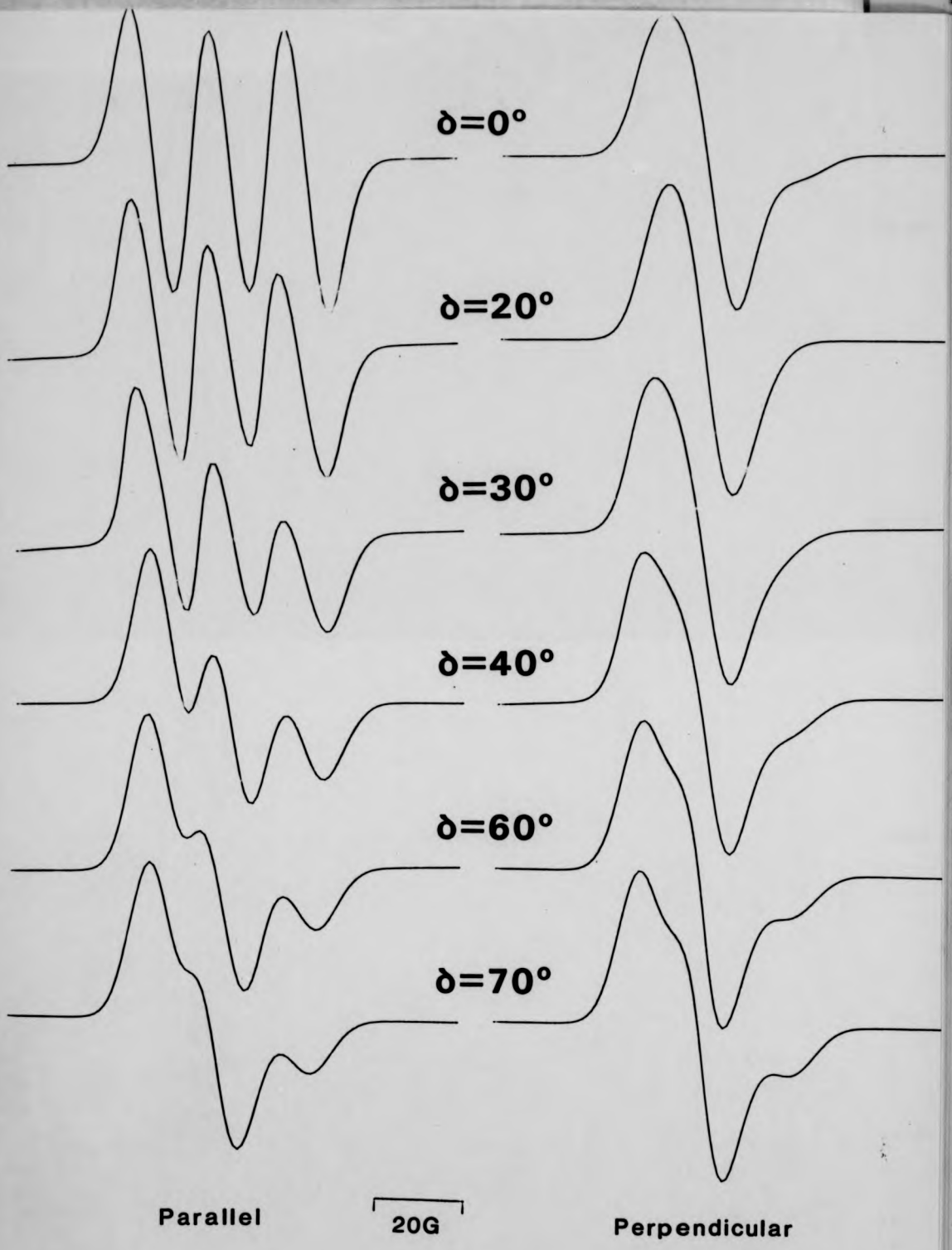


Fig. 5.13 Computer simulations for a fibre for several angles of misalignment (Tilt = 0°).

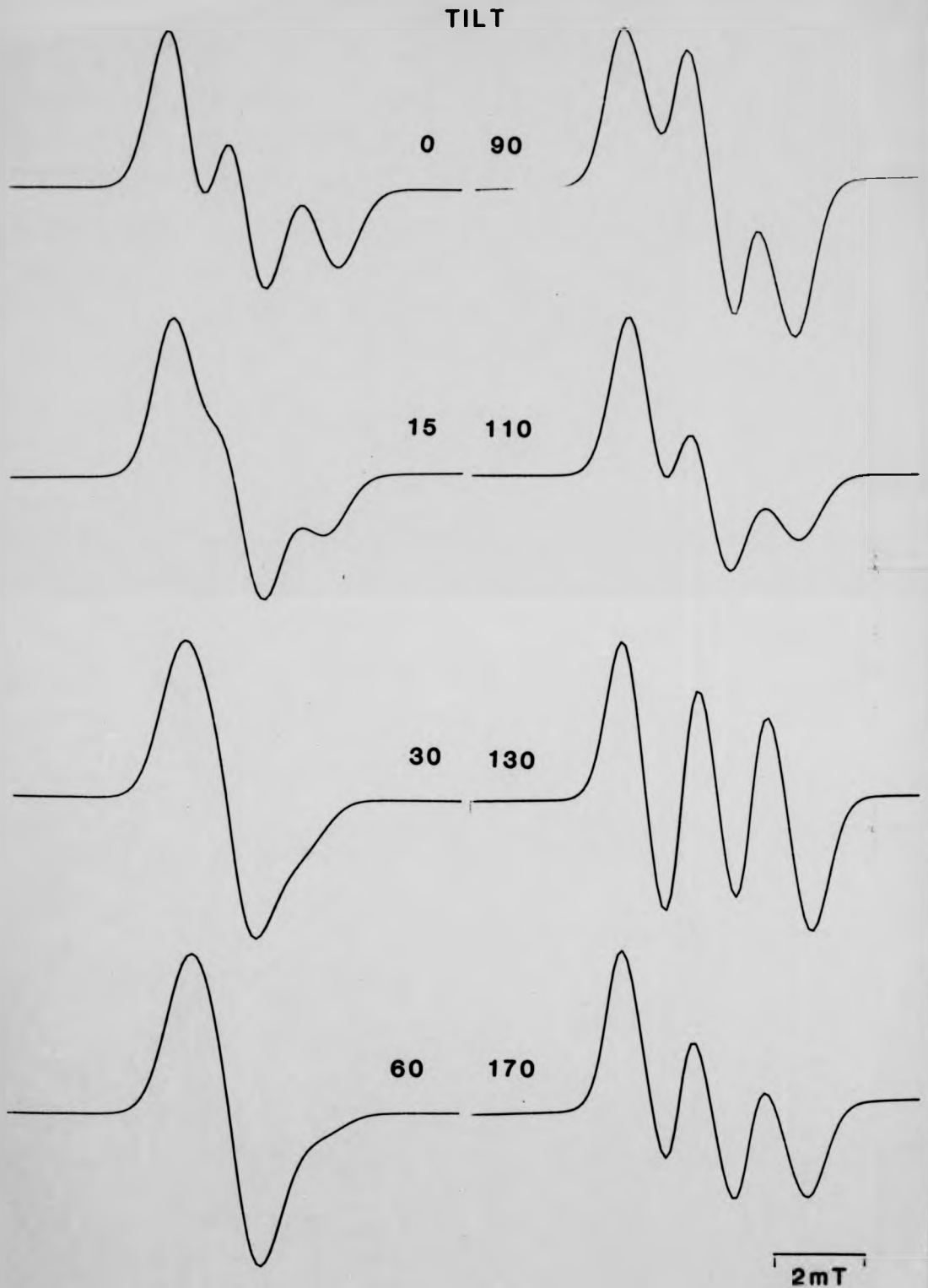


Fig. 5.14a Computer Simulations of the Parallel Fibre Spectra for several angles of tilt using a misalignment of 40°.

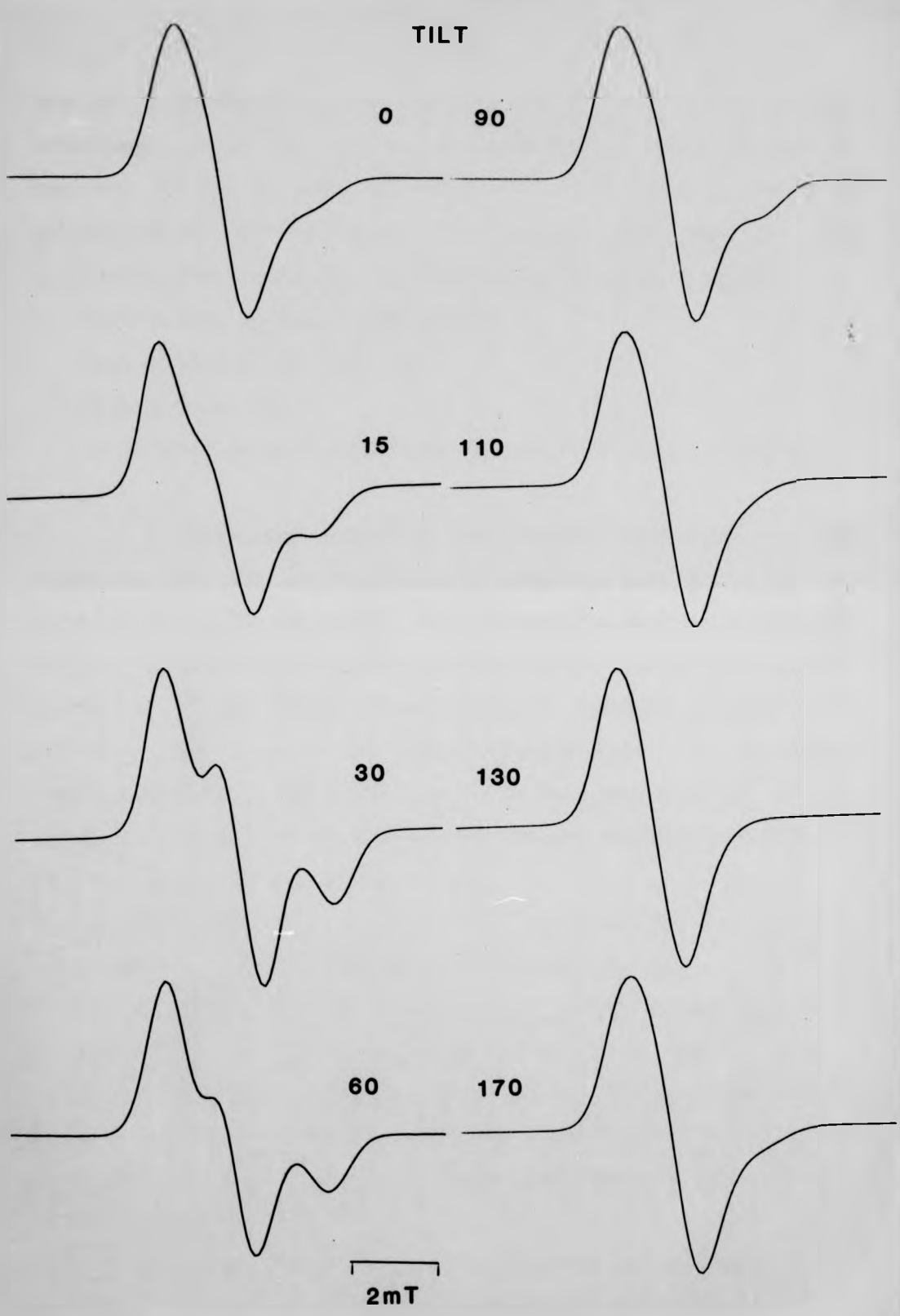


Fig. 5.14b Computer Simulations of the Perpendicular Fibre Spectra for several angles of tilt using a misalignment of 40°.

changes in the simulations. On the other hand an increase in the angle of misalignment to 55° for a tilt of -20° did improve the fit to the parallel spectrum, as may be seen from Fig. 5.15d. The fit to the other orientations of the fibre was not as good, but the simulations are still acceptable. The following set of parameters was therefore obtained.

Angle of tilt, $\theta_2$ = 160 - 180° or 110°

Angle of misalignment = 40 - 55°

Angle of twist: Any.

The principal g- and A-values were the same as in the gel simulation.

A surprising feature of the computer simulations is the suggestion that the free radicals may be orientated with their z-axes at about 110° to the DNA helix axis. This is surprising because, as mentioned earlier, one would expect the triplet splitting observed for the parallel orientation of the fibre to be associated with a parallel arrangement of the $2p\pi$-orbital z-axis and the external magnetic field. The discrepancy between expectation and calculation is no doubt accounted for by the imperfect alignment of DNA in the fibre: for zero misalignment a tilt of 110° does not provide a satisfactory fit.

More significant, perhaps, is the finding that the drug molecules could have a spread of tilt angles in the range 160 - 180°. The free radicals may be orientated at any one of these possible angles of tilt. On the other hand, the existence of a small spread in the angles of tilt cannot be ruled out and may even be more likely. There may also be a fraction of drug molecules tilted at 110° to the helix axis. Unfortunately, these possibilities cannot be distinguished using the ESR results alone.

The X-ray diffraction results showed that at about 92% r h. a reversible conformational transition of the DNA occurred (i.e. the A → B transition). However, this change in conformation had no visible effect on

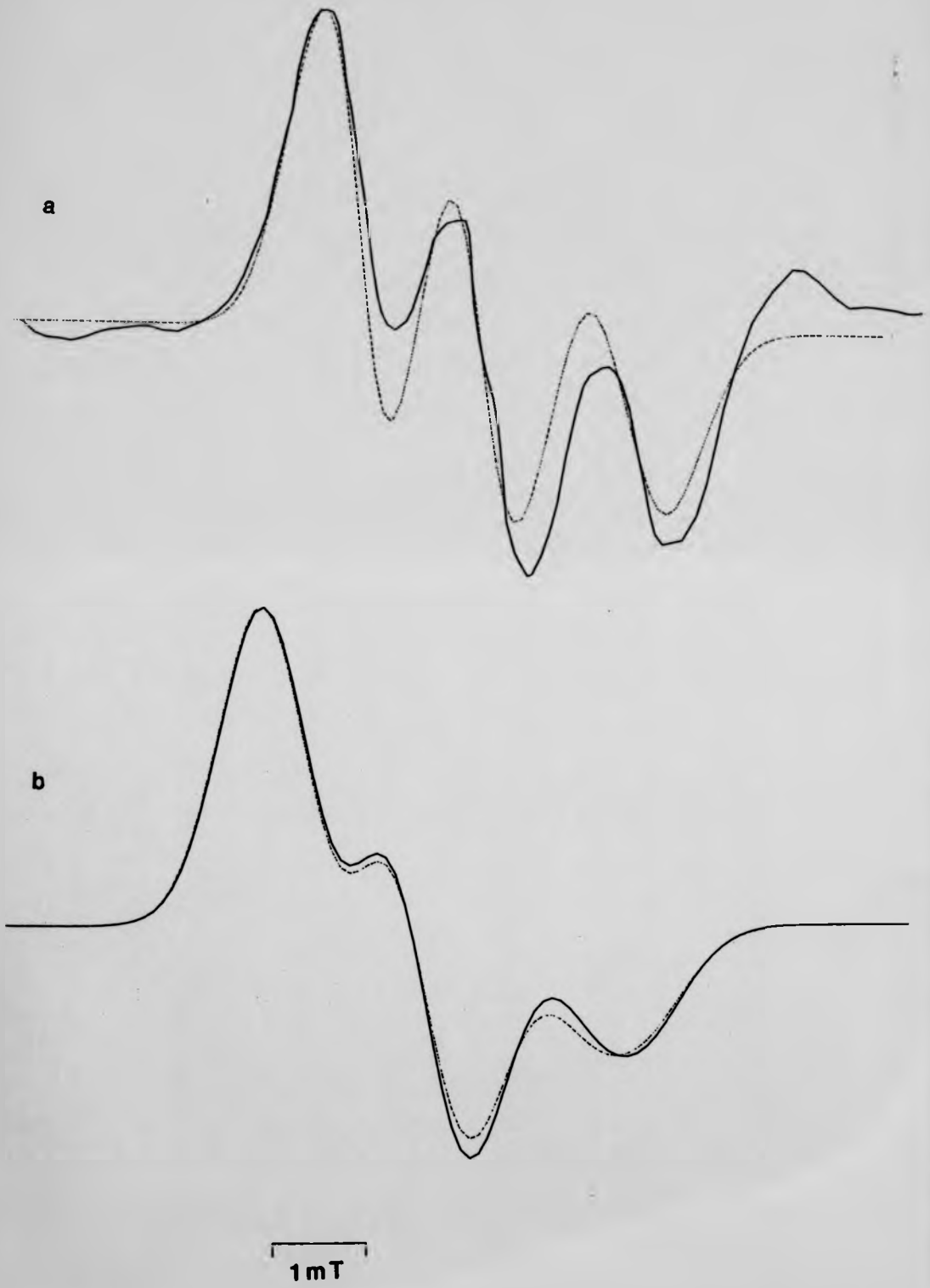


Fig. 5.15(a.b) Computer Simulations of the FPRZ$^{+}$-DNA Fibre Spectra for a misalignment of 40° and a tilt of zero degrees: (a) 0° (b) 45°.

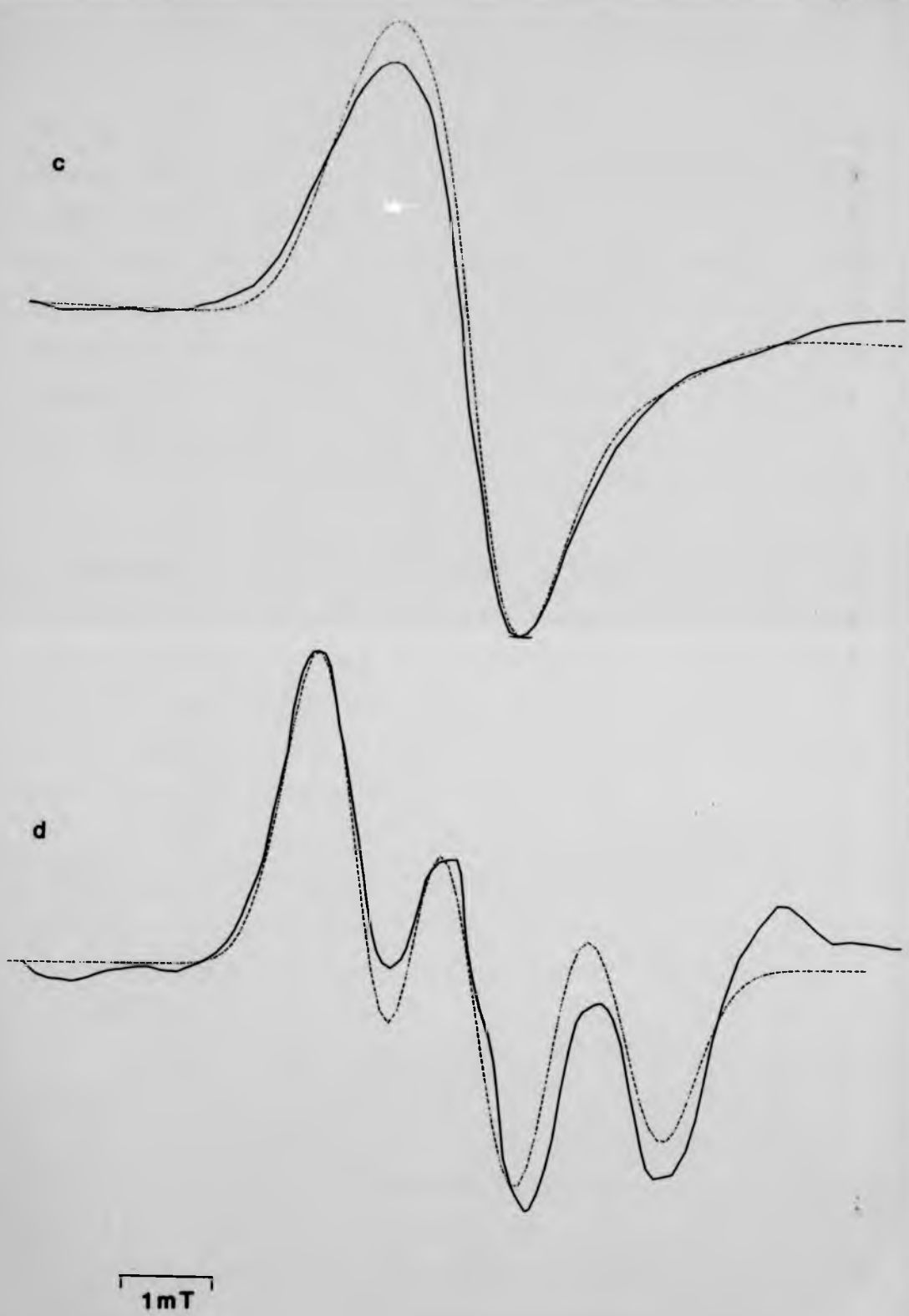


Fig. 5.15(c,d) Computer Simulations of the FPRZ$^{+}$-DNA Fibre Spectra for a misalignment of 40° and a tilt of zero degrees: (c) 90°; and for a misalignment of 55° and a tilt of -20°: (d) 0°.

the ESR spectra. This observation was at first sight puzzling since, judging from the results of the previous chapter, some change in the ESR lineshapes should have been seen. An explanation of the similarity of the A- and B-form spectra is now possible in terms of the results of the above computer simulations. These simulations show that if the helix axis and the $2p\pi$-orbital z-axis are initially parallel, then a transition to a configuration in which these axes are rotated by about 20° may occur without any alteration of the free radical ESR spectrum.

A tilt of zero degrees may indicate that an intercalative mode of binding is present and this is most likely to occur for the high humidity B-conformation. When the relative humidity is lowered and a transition to the A-conformation takes place the drug molecules could be released from their intercalated site and take up any one of a number of external binding sites all of which result in tilt angles to within -20° to the helix axis. It is suggested that such a sequence of events could take place without there being any noticeable effect on the ESR spectra.

However, it is not possible to tell from the ESR data alone whether or not intercalation has taken place: the simulations show that there are simply too many ways in which the binding can occur. On the evidence of the ESR results one could also argue that the drug molecules are externally bound to the DNA.

In order to reveal whether intercalation has occurred, the B-type diffraction patterns were examined and their layer line separations were measured. These measurements gave pitch values no different to those found for normal B-form DNA fibres. This result would normally be taken to mean that intercalation has not taken place. However, as was noted in Chapter 4, the drug concentration in a fibre needs to be reasonably high (about a P/D of 10) before the large scale effects of intercalation become visible in the X-ray patterns. In the present samples, with P/D values of about 60 or more, the drug concentration is probably insufficiently high.

An interesting observation was the fact that the C-conformation was not observed at any humidity for any drug. In experiments involving spin-labelled proflavine it was found that the C-form appeared only at low P/D values. The present result agrees with the findings of Chapter 4 in that, at low drug concentrations, the C-form appears to be prohibited. The possible reasons for this have been noted in the earlier chapter.

**Summary**

It has been shown that the phenothiazine free radicals have a strong affinity for DNA. The binding results in a stabilisation of the free radicals and this is especially true in dry fibres. Except for a few minor differences in the linewidths all the phenothiazine free radical derivatives exhibited the same orientational dependence in their ESR fibre spectra. The results presented here are therefore entirely consistent with the findings of Porumb and Slade (1976), who estimated a tilt angle of 0° for the $CPZ^+$ radical bound to DNA fibres. The results suggest that the interaction between the free radicals and the DNA primarily involves the phenothiazine ring system and that the substituted groups, though important in influencing the cationic charge distribution over the ring, have a negligible effect on the binding process. On the other hand, the substituted groups may play a large part in stabilising the free radicals in the complexes. As noted in Section 5.1, the formation of these complexes could be important in determining the psychotropic activities of the phenothiazines (see Section 5.1).

The ESR results presented above are consistent with the free radicals adopting any one of a number of orientations in the fibres. For this reason no definite answer can be given to the problem of intercalation. Unfortunately, the X-ray diffraction data is also equivocal with regard to intercalation. However, Porumb (1976) measured the dichroic ratios of $CPZ^+$-DNA complexes in fibres and found the results to be

consistent with a perpendicular orientation of the $CPZ^+$ chromophore to the DNA helix axis. This result would rule out the possibility, suggested above, of the drug molecules binding externally to the DNA with a tilt of ~110° to the helix axis. A CPK model also shows this structure to be unlikely, particularly in the A-conformation. If this configuration of the drug-DNA complex is rejected it still leaves the possibility of a spread of drug orientations between 0 and -20° to the DNA helix axis. The results of the previous chapter imply that a large angle of misalignment is associated with a large spread in the orientations of **externally** bound drug molecules. A reasonable fit was found to the fibre spectra in the present case for a misalignment of up to 55°. This result tends to support an external binding mechanism.

In the external binding model it is envisaged that the phenothiazine ring nitrogen interacts electrostatically with the phosphate groups in the backbone. This binding would be further strengthened by an electrostatic interaction between the phosphate oxygens and the protonated groups (e.g. the nitrogen) in the N10 sidechain. This binding is most likely to occur in the major groove. In the B-conformation the sulphur atom in the ring, which is susceptible to oxidation by water, would lie close to the bases which project into the major groove. This close contact would cause water to be excluded from the complex and thus lead to a stabilisation of the free radical. When complexed to A-form DNA the free radical will occupy a deeper and narrower major groove. Water molecules will tend to concentrate along the sugar-phosphate backbone and the sulphur atoms, which project into the inner core of the helix, will be less prone to oxidation. It may be argued, in support of the external binding model, that the non-planarity of the phenothiazines precludes the possibility of their binding by intercalation. However, although a large unwinding angle would probably be required to accommodate the drug, CPK models shows that there is no steric hindrance to intercalation.

Many of the difficulties of interpretation could be avoided if the free radicals were more stable. It would then be possible to carry out a more systematic examination of their interactions with DNA. For example, competition studies with known intercalators were not possible because of the limited lifetime of the radicals. Stable free radicals, however, can easily be used in competition with other drugs. By such studies it should be relatively straightforward to decide unequivocally on the question of intercalation. Attempts were made to bring about a more stable phenothiazine free radical by attaching a spin label to the ring (see Appendix). These attempts were, unfortunately, unsuccessful. However, a spin-labelled analogue of CPZ has recently been prepared elsewhere (Dikanov et al., 1983). It is not known whether this compound binds to DNA (native CPZ has a negligible affinity for DNA, Waring (1970)).

Appendix: Experiments on Spin-Labelled Thionin

A problem which recurred throughout the previous experiments was that of free radical stability. Unlike the spin-labels used in Chapter 5, the phenothiazine free radicals were quite unstable. This meant that not only was the general handling of the compound made difficult but, in addition, many important experiments were either impossible or very difficult to perform. In an attempt to remedy these problems several spin-labelling experiments were made on the phenothiazine derivative **Thionin.**

Thionin possesses amino substituents at C2 and C8 in the ring and the N10 substituent is hydrogen. Thionin was selected rather than one of the other phenothiazine drugs because (a) it is known to bind to DNA without prior oxidation and (b) the presence of the two amino groups suggested that the molecule could be easily spin-labelled (like proflavine). In practice, however, this last assumption proved to be totally unfounded and all attempts to obtain a spin-labelled analogue of thionin failed. Many hours were spent devising a means of achieving a successful reaction, but to no avail. It is felt, however, that a brief description of the main features of the reactions will be useful.

0.45g of thionin free base was placed in a "soxhlet" thimble and covered with fine sand. The thimble was placed in a reflux tube above a round bottomed flask containing 40cm$^3$ of dry THF into which 0.4g of spin-label acid chloride (2,2,5,5-tetramethylpyrrolline-1-oxyl 3-Carboxylic acid) was dissolved. 1g of Mg filings was added and anhydrous reflux followed for two hours. The mechanism behind the reaction is as follows.

The THF boils off and is condensed into the thimble. After a short while the free base dissolves in the THF and is carried into the rb-flask. The amino groups are expected to react with the acid chloride, forming an amide bond with the release of HCl. The HCl is then "picked up" by the Mg filings. However, analysis of the reaction product after two

hours showed that the thionin free base had been converted to thionin-HCl. The probable reason for this unexpected reaction lies with the strong bascicity of the free base. Other experiments were attempted with pyridine as solvent but to no avail. Finally, some success was achieved using a mixture of $30cm^3$ of dry pyridine and $3cm^3$ of N-methylpiperidine, which is $10^6$ times as basic as thionin free base. During the reaction solid precipitates appeared. These were foud to be reasonably soluble in MeOH. TLC analysis exhibited several spots, one of which (a green component under short wave UV) contained spin-label. The green component was found to have a high affinity for DNA. After isolation and purification using column chromatography this component was analysed by mass spectrometry (by Dr. Griffiths, Dept. Chemistry). It was found to have a mass only half that expected for spin-labelled thionin. Apparently, this was a spin-labelled fragment of the thionin molecule. (Interestingly, a fibre prepared using the green compound exhibited only a single exchange narrowed line at all orientations).

Several other experiments were carried out but the result was always the same: either thionin-HCl or a fragment of the heterocyclic ring. It became clear that the project required a considerable knowledge of phenothiazine chemistry and an investment in time which was beyond the limits of this thesis.

# CHAPTER 6

## Spin-Labelled ϕW-14 DNA

### 6.1 Introduction

A virus may be considered to be a fraction of cellular genetic material which, although capable of surviving outside the cell, depends entirely on the cell for its own replication. Viruses can infect animal, plant or bacterial cells and are classified accordingly. Viruses which infect bacteria are known as bacteriophages and ϕW-14 is the name given to the virus which has as host the bacterium Psudonomas Acidovorans (Kropinski and Warren, 1970).

In ϕW-14 DNA, as in many other phage DNAs, one of the four commonly occurring bases is replaced by a modified base. Kropinski et al., (1973) showed, by chemical analysis, that approximately one-half of the normal thymine bases in ϕW-14 are replaced by modified thymine bases in which the C5 methyl groups are exchanged for putrescinyl groups (Fig. 6.1).

The presence of a modified base can alter the physical and chemical properties of the DNA and this may have important biological consequences. For example, the G-C content of ϕW-14 is estimated to be ~51% and, on this basis, the expected values for melting temperature (in 0.15M NaCl) and bouyant density (in neutral CsCl) are 90.1°C and 1.716gcm$^{-1}$ respectively (Warren, 1980). The measured values are 99.3°C and 1.666gcm$^{-1}$. The 9°C increase in melting temperature is believed to arise from the partial neutralisation of the negative phosphate groups by the positively charged amino groups in the putrescine sidechain. This reduces the electrostatic repulsion between the phosphate groups and stabilises the double helix. The decreased bouyant density in CsCl is thought to be due to the direct effect on the density of the methylene groups in the sidechain and to the exclusion of $Cs^+$ ions by the positive amino groups

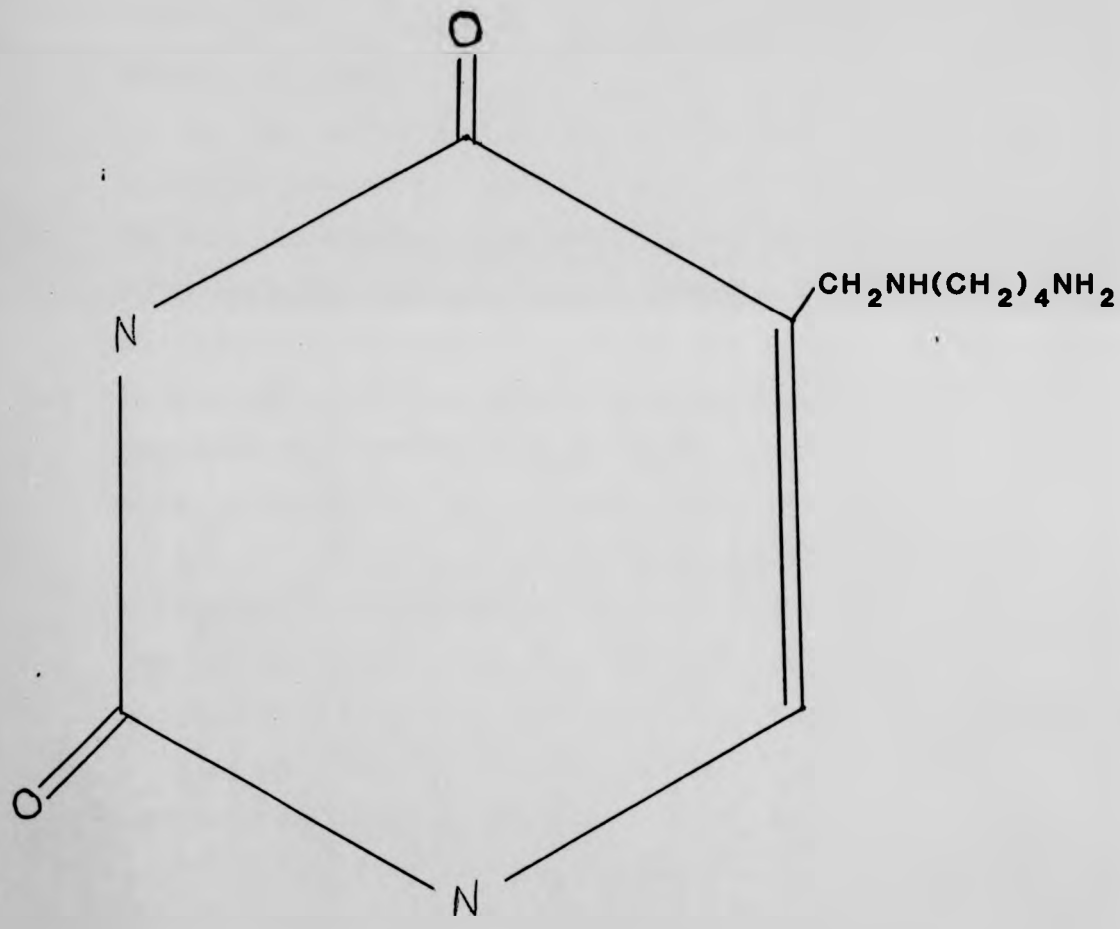


Fig. 6.1 α-Putrescinylthymine

(Warren, 1980).

α-putrescinylthymine is synthesised at the polynucleotide level (Maltman et al., 1981) and the modified bases may not be randomly sequenced since the combination purine-PutThy-purine is twice as frequent as the sequence purine-Thymine-purine (Warren, 1981). The biological significance of the putrescine sidechain is not yet known but it has been shown to be responsible for the high packing density of the DNA in the phage head (Scraba et al., 1983).

The conformation of the putrescine group and its importance in influencing the conformational transitions of ϕW-14 DNA are of considerable interest. Goodwin (1977) reported that ϕW-14 DNA in fibres remained in the A-form up to 98% r. h. whereas normal DNA made a transition to the B-form at 92% r. h. Mahendrasingham (1983) has recently confirmed these observations. A molecular model of ϕW-14 DNA showed that, in the A-form, the amino group on the putrescine sidechain was able to form a hydrogen bond with a phosphate group of the opposite polynucleotide strand. The presence of such a bond would be likely to strengthen the A-form structure in that region of the DNA and thereby result in an increased resistance to conformational change. A similar stabilisation of the double helix would be expected to occur in the case of an electrostatic interaction between the positive amino groups and the phosphate oxygens. Goodwin (1977) calculated the molecular transforms of several models of the A-form and compared the results with the experimentally observed intensity differences between ϕW-14 and normal (Calf Thymus) DNA diffraction patterns. Although the hydrogen-bonding model was consistent with the observed intensity changes, the fit was not altogether satisfactory. Greenall (1982) later re-examined Goodwin's work and claimed that his data was consistent with a normal A-form structure, thus leaving the problem of the putrescine conformation unresolved.

Recently, the circular dichroism of ϕW-14 DNA and its acetylated

derivative have been examined (Warren, private communication). It was found that the rotational strength of the band above 260nm was enhanced for native ϕW-14 DNA compared with that for the acetylated derivative. This was explained by supposing that the conformation of ϕW-14 DNA in solution is modified in the region of an ion-pair interaction between the positively charged primary amines and the phosphate backbone.

In this chapter the conformational properties of the putrescine group and its effects on the conformational transitions of ϕW-14 DNA are examined using ESR spectroscopy. The method consists of attaching a spin-label to the primary amino group on the putrescine sidechain and then observing the ESR spectra obtained from orientated ϕW-14 fibres. If the putrescine group forms hydrogen bonds to the nearest phosphate in the opposite chain then some orientational dependence of the ESR spectra should be observed. On the other hand, if no hydrogen bonding takes place the spin-labelled putrescine groups will be free to adopt any orientation in the DNA. These points will be examined in detail in the next section.

The greatest problem encountered at the outset of the project was how to achieve the spin-labelling at the required position. Site-specific spin-labelling of DNA polymers is difficult to bring about (e.g. see the reviews by Bobst (1979) and Kamzalova and Pos tnikova (1980)). However, after many false starts ϕW-14 DNA was successfully spin-labelled at the required position. The credit for this work goes entirely to Prof. Warren and his colleagues at the Biochemical and Chemical Laboratories at the University of British Columbia.

An important aspect of the present work compared with the earlier studies (apart from being a more direct approach to the problem) is that the importance of $Na^+$ ion concentration on the conformational transitions of DNA is now better understood (Chapter 1). The A → B and A → C transitions in fibres depends not only upon the level of humidity but also on the concentration and type of salt present. By keeping the salt

concentration in ϕW-14 fibres low the orientation of the putrescine group in all three conformations can be examined.

6.2 A- and B-form ϕW-14 DNA

The thymine putrescine groups are exposed in the major groove of the double helix in B-form (and C-form) DNA but lie in the large inner core of the major groove in the A-conformation. The fully extended length of the putrescine group, from the C5 carbon to the amino nitrogen, is calculated to be 6.28A using standard bond angles and bond lengths (Goodwin, 1977). For hydrogen bonding to occur the amino groups are required to lie at about 2.9A from the acceptor atom (in this case a phosphate oxygen). Therefore, the maximum possible distance in which hydrogen bonding can occur is 10.2A.

Since the nearest phosphate oxygen on the chain opposite the major groove in B-form DNA is 11.8A from the C5 carbon atom on the pyrimidine ring (Arnott and Hukins, 1972), the possibility of hydrogen bonding across the major groove in B-form DNA is ruled out.

However, there is a possibility of the putrescine group forming a hydrogen bond (or an ionic bond) with the phosphate groups attached to either the 3' or 5' position of the putrescine nucleoside. This conformation is neither sterically nor energetically favourable in a normal B-form helix since the putrescine chain is no longer fully extended. However, certain small modifications to the B-form may resolve this difficulty (Warren, private communication). Goodwin (1977) examined several other models of hydrogen bonding in B-form DNA including the possibility of inter-molecular hydrogen bonding to an adjacent DNA duplex. These possibilities were rejected because stereochemically satisfactory models could not be built.

Although the groove size in C-form DNA is smaller than in the B-form, the formation of putrescine-phosphate hydrogen bonds across the

major groove can also be ruled out for this conformation. The formation of a hydrogen bond (or ionic bond) to a phosphate group attached to the same chain is not likely in C-form DNA due to the even greater constriction required of the putrescine sidechain in this conformation.

In the A-conformation, however, the separation between the thymine C5 carbon atom and the nearest phosphate oxygen is smaller than for the B-form. The formation of a hydrogen bond between the putrescinyl nitrogen and the nearest phosphate oxygen is therefore quite feasible. The sidechain is restricted both in orientation and in mobility in this structure. By contrast, the extended putrescine group is quite unconstrained in B-form DNA.

## 6.3 Spin-Labelling Experiments

Spin-labelled ϕW-14 DNA was prepared by Prof. Warren at the University of British Columbia, Canada. The samples were received several days later and used immediately. The following method is due to Prof. Warren (private communication).

### (a) Spin-Labelled ϕW-14

A 12cm$^3$ solution of 0.5mg/cm$^3$ of ϕW-14 DNA was prepared in 0.1M TEA (pH = 9.5). 25mg of2,2,5,5-tetramethylpyrroline-1-oxyl-3 Carboxylic acid N-hydroxysuccinimide was dissolved in 6cm$^3$ of acetronitrile. This solution was added slowly to the DNA solution and the mixture was stirred at room temperature (this was done in a fume cupboard since acetronitrile is a class A1 poison). The reaction is shown in Fig. 6.2.

After 5 hours the mixture showed a single, clear phase, with a pH of 8.5. The pH of the solution was adjusted to 5.0 in order to stop the reaction. This was accomplished by the addition of a small volume of 2N HCl. Care was taken not to precipitate the

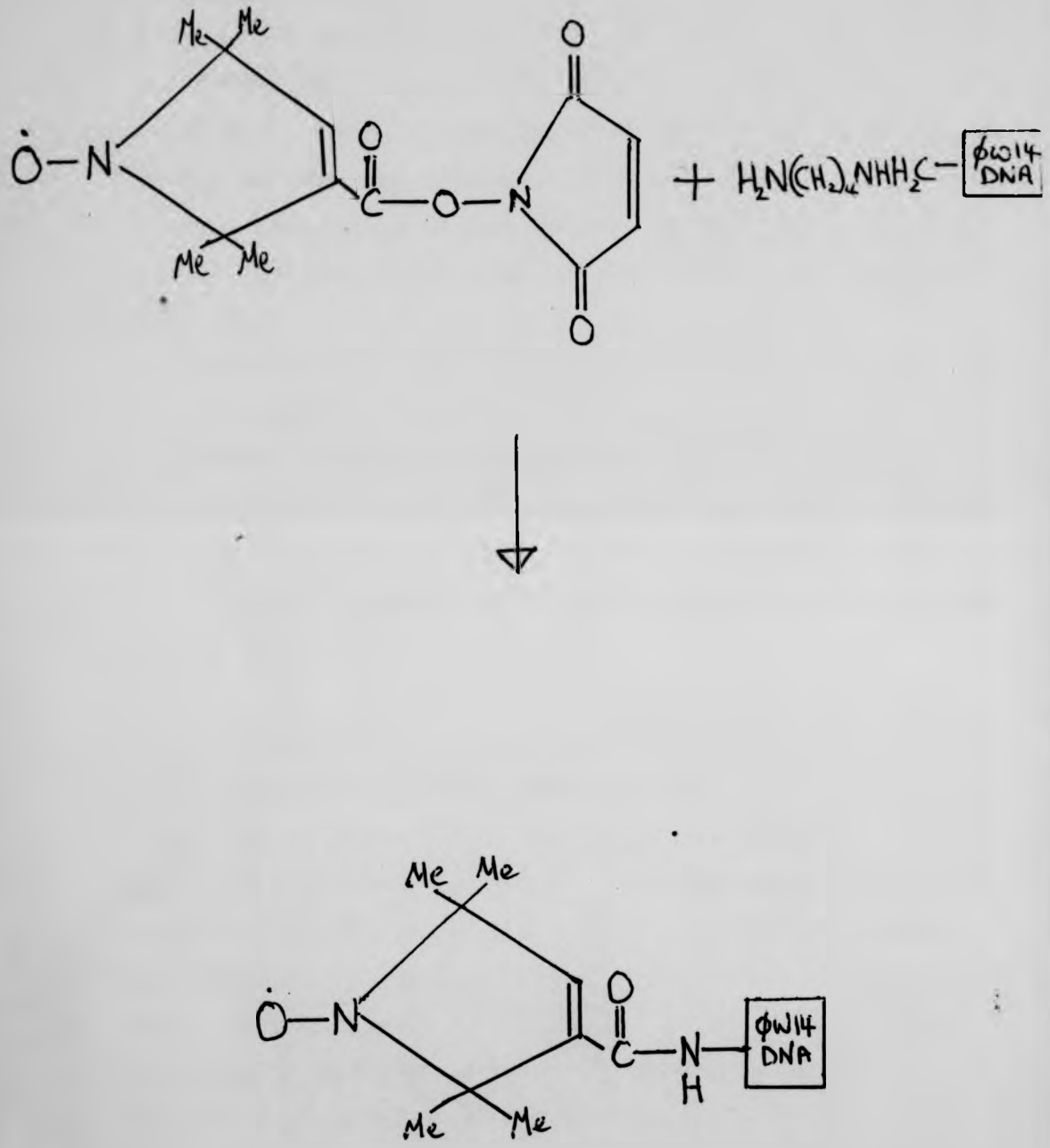


Fig. 6.2 Schematic representation of spin-labelling of φW-14 DNA.

DNA, which was easily done at this pH. The solution was then made up to 0.1M NaCl by the addition of $2cm^3$ of 1M NaCl. The mixture was swirled gently and the DNA was precipitated with 2 volumes of cold propanol. After stirring for a few minutes the liquid was poured off and the precipitated DNA was washed briefly with de-ionised water and then re-suspended in $10cm^3$ of 10mM NaCl and stirred at room temperature, then in the cold room, until it had redissolved.

(b)**Purification**

Excess (unbound) spin-label was removed as follows. When the DNA had redissolved it was again precipitated by the addition of 2 volumes of cold propanol. The DNA was collected on a glass rod and washed in 15mM NaCl for 30 minutes. The DNA was then collected and washed twice more. Finally, the DNA was redissolved in $10cm^3$ of 15mM NaCl. Any remaining spin-label was assumed to be bound to the DNA.

Several samples prepared by Prof. Warren were found, on their arrival to be either denatured or unlabelled. Denaturation of the DNA was no doubt due to the unavoidable variations in the temperature of the samples during their passage from Canada. Unlabelled samples were probably the result of a failure of the original spin-labelling experiment. Prof. Warren reports (private communication) that different DNA preparations often behaved differently even under the same conditions. Nevertheless, a good spin-labelled sample was received and most of the results presented in this chapter were obtained using this sample.

## 6.4 ESR Experiments

6.4.1 Solution Studies

6.4.1 (a) Method

ESR solution spectra were recorded from the original ϕW-14 sample after dilution with de-ionised water. The DNA concentration in this solution was $1.8 \times 10^{-4}$M. Assuming that all the putrescene groups are labelled this corresponds to a spin-label concentration of approximately $4 \times 10^{-5}$M.

6.4.1 (b) Results

The 9.5-GHz spectrum was recorded at room temperature and is shown in Fig. 6.3. The spectrum consists of three motionally narrowed lines centred on g = 2.0052 and separated by 1.6mT. The spin-label correlation time was estimated at 0.03nsec (see Chapter 2 for method).

6.4.1 (c) Discussion

The depth of both the major and minor grooves in B-form DNA in fibres is 8.5Å (Arnott, 1981). The putrescine group spans a distance of 6.28Å from the C5 carbon to the amino nitrogen (see above) and the nitroxide moiety extends some 3Å further into the major groove. If the major groove is ~8.5Å in depth then the N-O bond will jut out of the major groove to beyond the sugar-phosphate backbone. A CPK space-filling model of this structure shows that the extended putrescine group is free to perform rapid tumbling motions within a cone of large semi-angle whilst simultaneously twisting rapidly about its long axis. On this model a motionally narrowed ESR spectrum is to be expected.

On the other hand, if the nitroxide moiety were to remain within the major groove then, as the work of Bobst et al. (1984) has shown, its mobility would be hindered and a broadened spectrum would be observed.

The present work therefore provides additional evidence for the proposed groove depth of B-form DNA in solution.

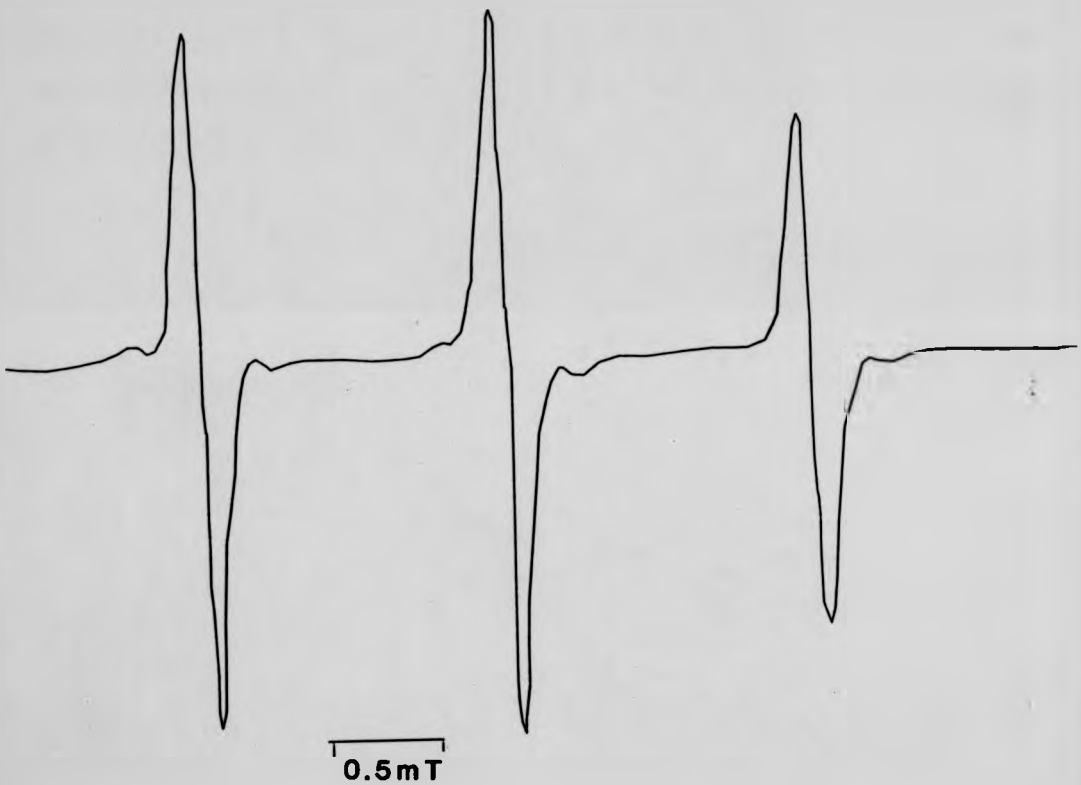


Fig. 6.3 The 9.5-GHz ESR spectrum of spin-labelled ϕW-14 DNA in aqueous solution.

The results of this section do not undermine the claims of Warren and coworkers (see above) that in B-form DNA the putrescine group is at least partially immobilised by an electrostatic interaction with the phosphate backbone. Unfortunately at normal pH levels the spin-label used in these experiments removes the positive charge from the primary amines. Several attempts have so far been made to synthesise a spin-labelled ϕW-14 derivative in which the primary amines retain their positive charge. The most promising method appears to lie in the use of the so called "Spin Imidate" nitroxide which is shown below:

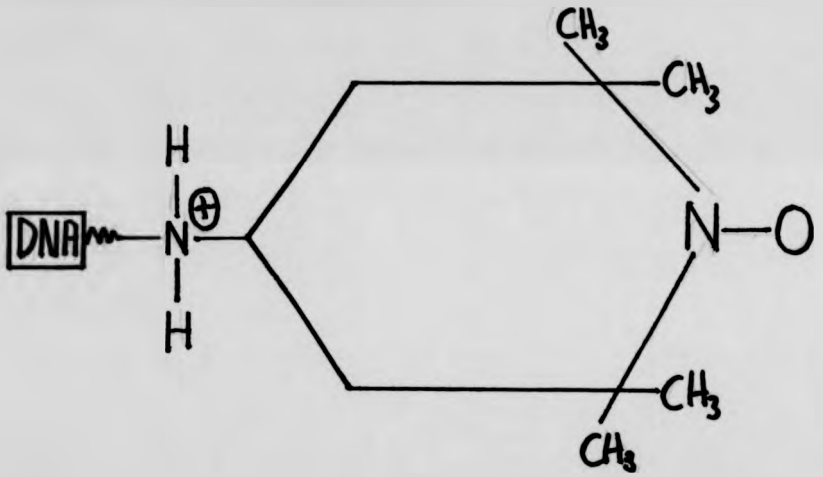


To date only a small fraction of putrescines have reacted with this spin-label.

## 6.4.2 Experimental Fibre Studies

### 6.4.2 (a) Method

Fibres were prepared in the usual way (Chapter 3). The salt concentration of the original ϕW-14 solution was 15mM NaCl but, in order to increase the liklihood of obtaining all three DNA conformations with the same fibre, fibres were also prepared at about 1mM NaCl. In practice it happened that both 1mM and 15mM NaCl fibres gave C-forms. The salt concentration was reduced as follows.

The gel collected after centrifugation of the ϕW-14 in a 3 x 3cm$^3$ rotor was redissolved in 3cm$^3$ of de-ionised water and then re-centrifuged. This procedure was repeated once more and after the final centrifuge run the resulting gel was used to make the fibres. The salt concentration in the gel could have been reduced by diluting the original sample prior to centrifugation. The method actually used was preferred, however, because a reasonably large DNA concentration was maintained throughout (at low salt concentrations and low DNA concentrations precipitation can be difficult). Both X- and Q-band ESR spectra were recorded and except for the following alterations the usual spectrometer settings were used.

The X-band microwave power was varied between 10mW and 50mW and the PSD was set at 100μV sensitivity. This was ten times smaller than in the previous experiments and reflects the high proportion of labelled groups present in these samples. The Q-band experiments were performed at 25mW microwave power.

All experiments were carried out at room temperature and 9.5-GHz ESR spectra were recorded at several relative humidities between 33% and 98%. Because of the physical constraints imposed by the size of the Q-band cavity and by the method of humidification, Q-band spectra were only taken at room humidity (i.e. from 55 to 65% r. h.)

A sufficiently large ESR signal intensity was obtained at all humidities using only a single fibre of dimensions ~250μm diameter and 2mm in length. Gel spectra were recorded from a sample containing roughly the same amount of DNA.

As in the previous experiments several fibres were made from the same gel, one of which was used to obtain X-ray diffraction data at different humidities.

### 6.4.2 (c) Results

The fibre (either 1mM or 15mM NaCl) was initially humidified at

The gel collected after centrifugation of the ϕW-14 in a 3 x 3cm$^3$ rotor was redissolved in 3cm$^3$ of de-ionised water and then re-centrifuged. This procedure was repeated once more and after the final centrifuge run the resulting gel was used to make the fibres. The salt concentration in the gel could have been reduced by diluting the original sample prior to centrifugation. The method actually used was preferred, however, because a reasonably large DNA concentration was maintained throughout (at low salt concentrations and low DNA concentrations precipitation can be difficult). Both X- and Q-band ESR spectra were recorded and except for the following alterations the usual spectrometer settings were used.

The X-band microwave power was varied between 10mW and 50mW and the PSD was set at 100μV sensitivity. This was ten times smaller than in the previous experiments and reflects the high proportion of labelled groups present in these samples. The Q-band experiments were performed at 25mW microwave power.

All experiments were carried out at room temperature and 9.5-GHz ESR spectra were recorded at several relative humidities between 33% and 98%. Because of the physical constraints imposed by the size of the Q-band cavity and by the method of humidification, Q-band spectra were only taken at room humidity (i.e. from 55 to 65% r. h.)

A sufficiently large ESR signal intensity was obtained at all humidities using only a single fibre of dimensions ~250μm diameter and 2mm in length. Gel spectra were recorded from a sample containing roughly the same amount of DNA.

As in the previous experiments several fibres were made from the same gel, one of which was used to obtain X-ray diffraction data at different humidities.

6.4.2 (c) Results

The fibre (either 1mM or 15mM NaCl) was initially humidified at

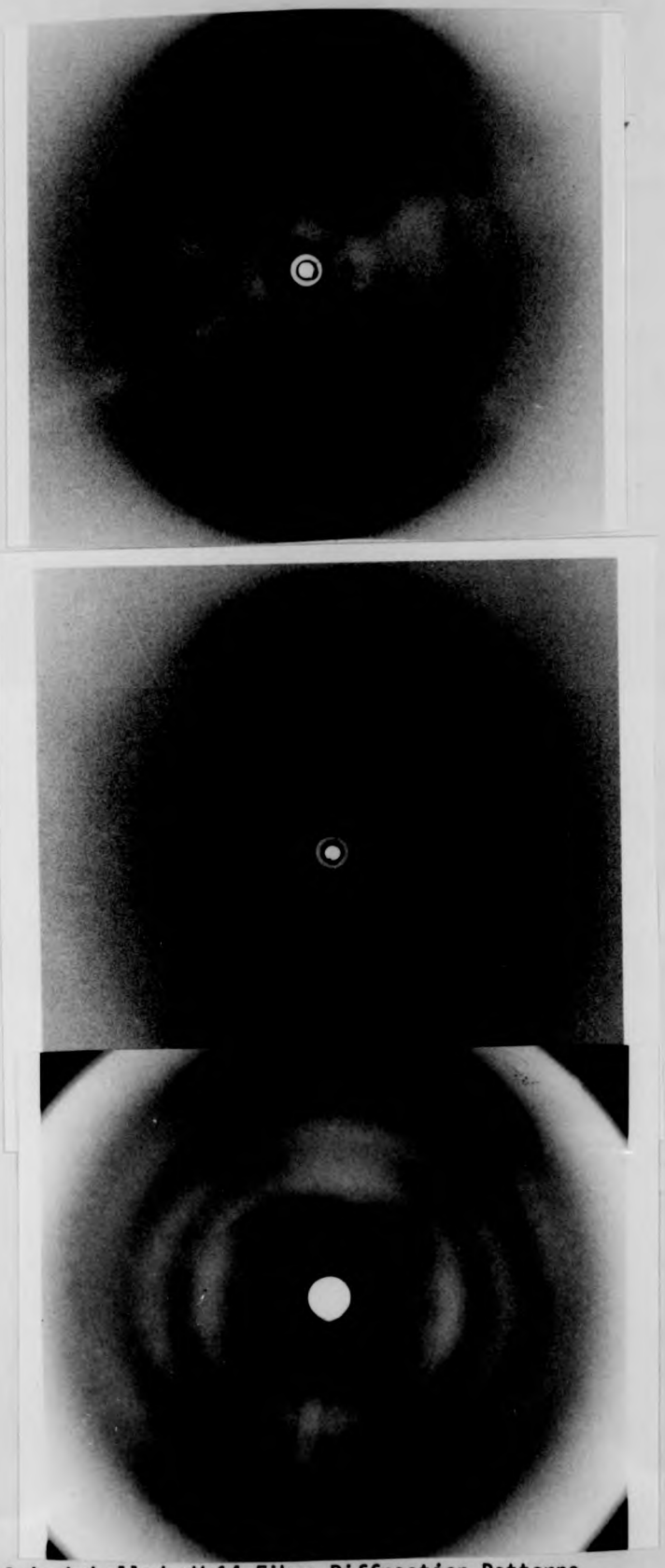

Fig. 6.4 Spin Labelled ϕW-14 Fibre Diffraction Patterns recorded at (a) 33% (b) 66% (c) 98% relative humidities.

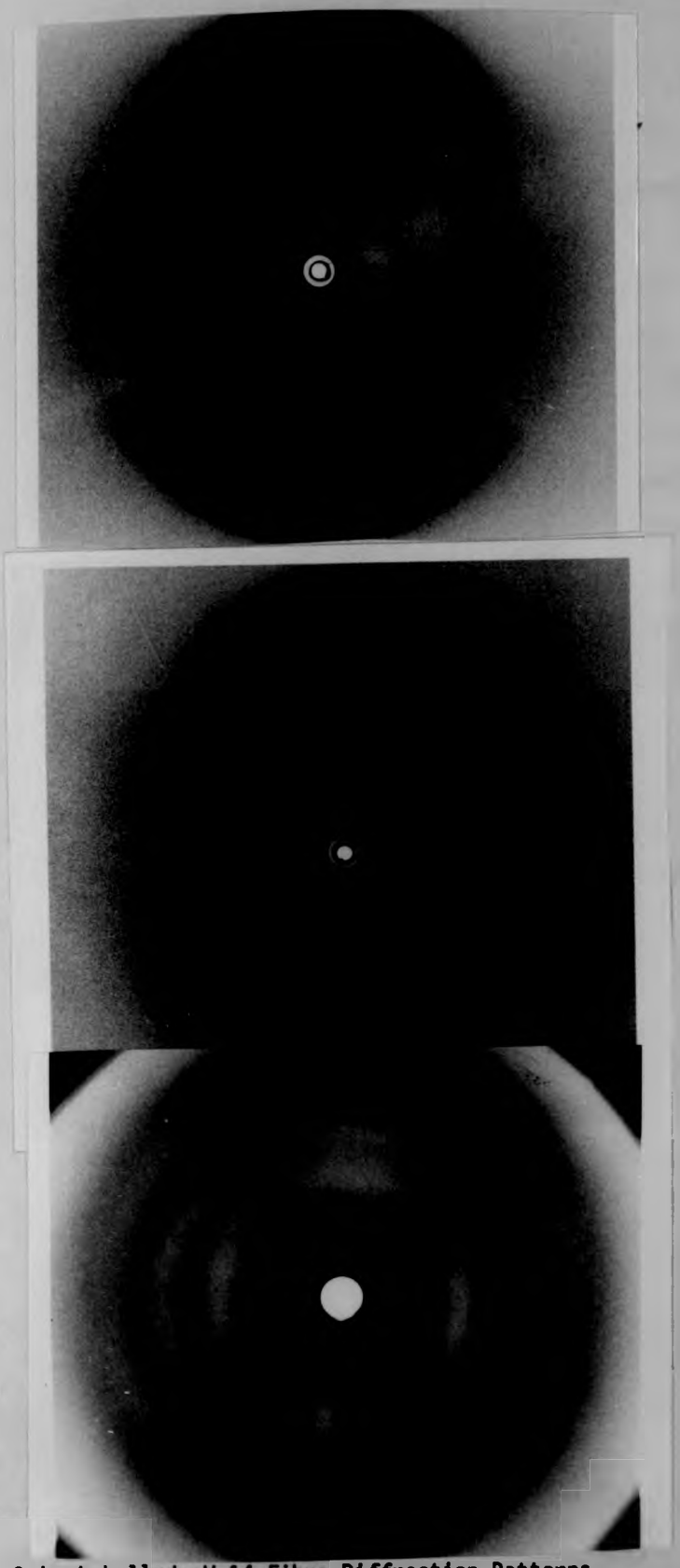

Fig. 6.4 Spin Labelled ϕW-14 Fibre Diffraction Patterns recorded at (a) 33% (b) 66% (c) 98% relative humidities.

33% r h. and its ESR spectrum was recorded periodically over an interval of a few hours until it became clear that equilibrium had been reached. At the same time X-ray diffraction patterns recorded at 33 and 44% r h. showed the DNA to be in the C-conformation. The diffraction pattern obtained at 33% r h. is shown in Fig. 6.4a and the associated ESR spectra for three orientations of the 1mM NaCl fibre are given in Figs. 6.5(a-c). The C-form gel spectrum is shown in Fig. 6.5d. Using the previous notation (see Chapter 4) the maximum hyperfine splittings for these spectra are $\Delta A_{\parallel}^{C} = \Delta A_{\perp}^{C} = 3.62mT$, $\Delta A_{45}{}^{C} = 3.52mT$ and $\Delta A_{g}^{C} = 3.62mT$. The gel and fibre spectra obtained from the samples prepared at 15mM NaCl gave identical lineshapes to the spectra in Figs. 6.5(a-d) but their hyperfine splittings were larger and equal to $\Delta A_{w}^{C} = \Delta A_{\perp}^{C} = 3.98mT$, $\Delta A_{45}{}^{C} = 3.87mT$ and $\Delta A_{g}^{C} = 3.98mT$ respectively.

Between 57 and 92% relative humidities A-form diffraction patterns were obtained (Fig. 6.4b). The ESR spectrum recorded at 75% r h. is shown in Fig. 6.6a. The A-form gel spectrum is identical to the fibre spectrum and is not shown.

At 98% r h. the fibres gave B-form diffraction patterns (Fig. 6.4c). The gel and fibre ESR spectra (Fig. 6.6c) are identical in almost all respects to those previously obtained for the C-conformation and the maximum hyperfine splittings are again larger for the high-salt fibre.

The transitions between the three conformations were reversed when the relative humidity was reduced.

The Q-band spectra (Fig. 6.6b) were identical at all orientations.

### 6.4.2 (d) Discussion

The X-ray diffraction results show that, as for normal ϕW-14 DNA and other natural DNAs, spin-labelled ϕW-14 DNA is able to adopt all of the three usual conformations. Transitions between these conformations were in

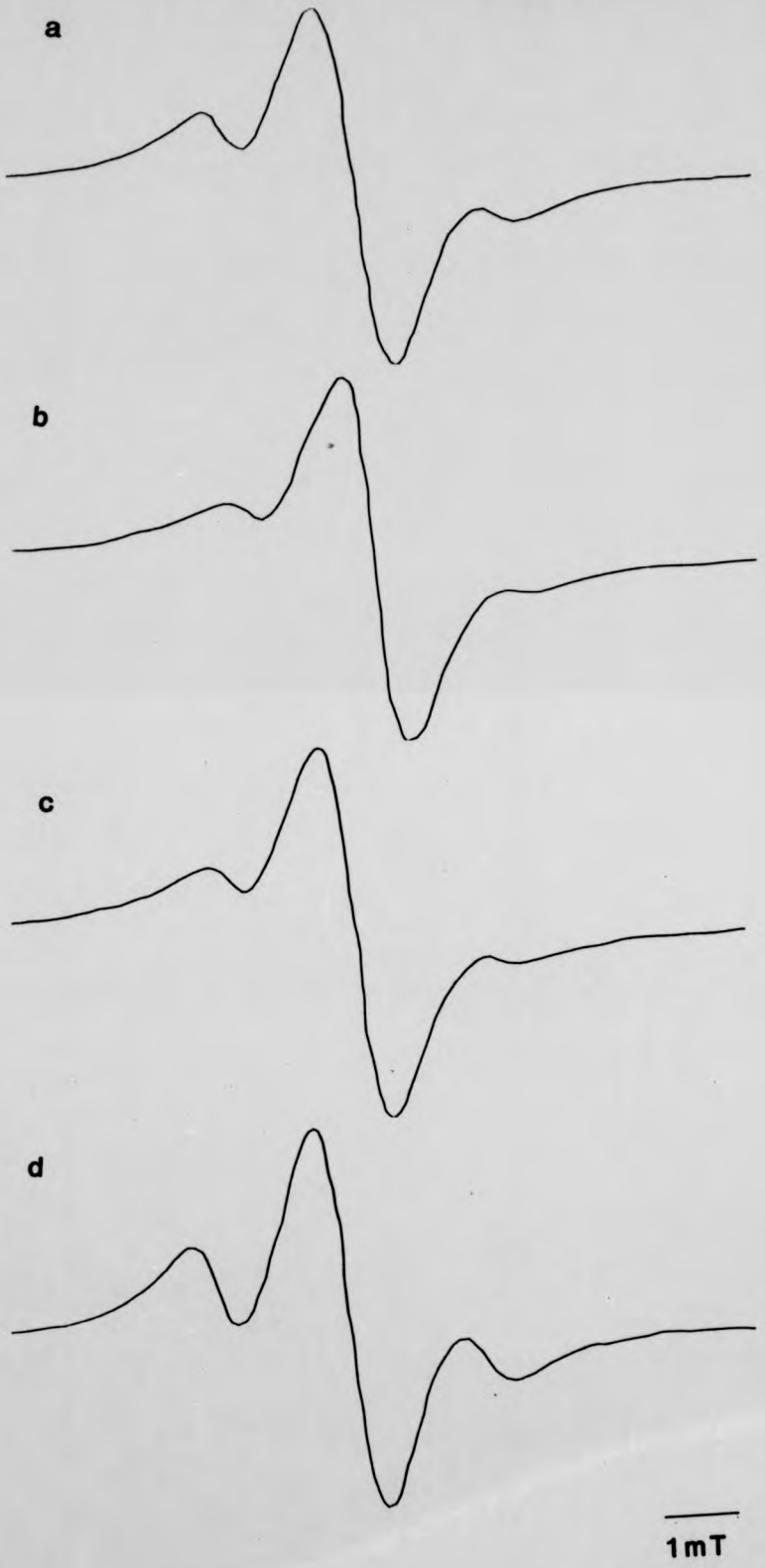


Fig. 6.5 (a-d) The Gel and Fibre ESR spectra corresponding to C-form ϕW-14 DNA: (a) 0° (b) 45° (c) 90° (d) gel.

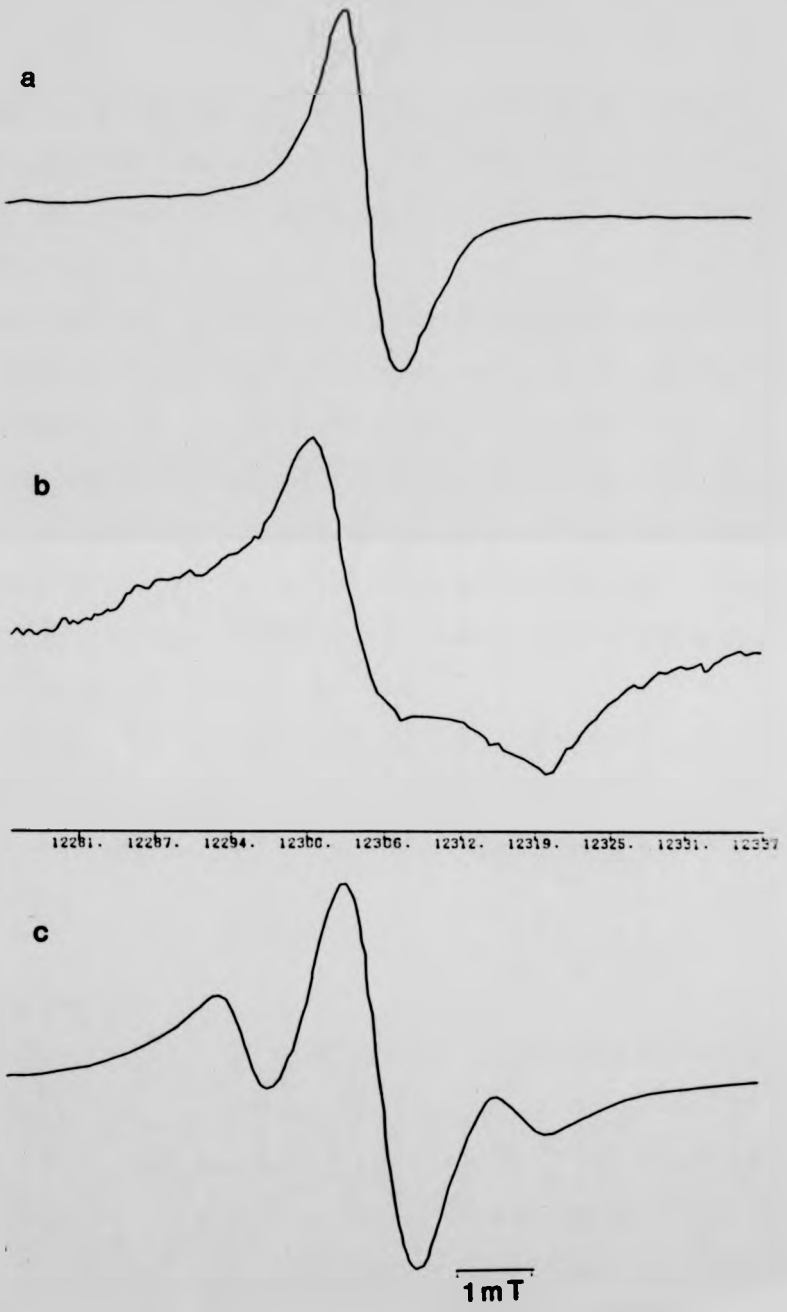


Fig. 6.6 (a) The 9.5-GHz Fibre spectrum corresponding to A-form ϕW-14 DNA.
(b) The 35-GHz Fibre spectrum corresponding to A-form ϕW-14 DNA.
(c) The Fibre spectrum recorded at 98% r h. (B-form ϕW-14 DNA)

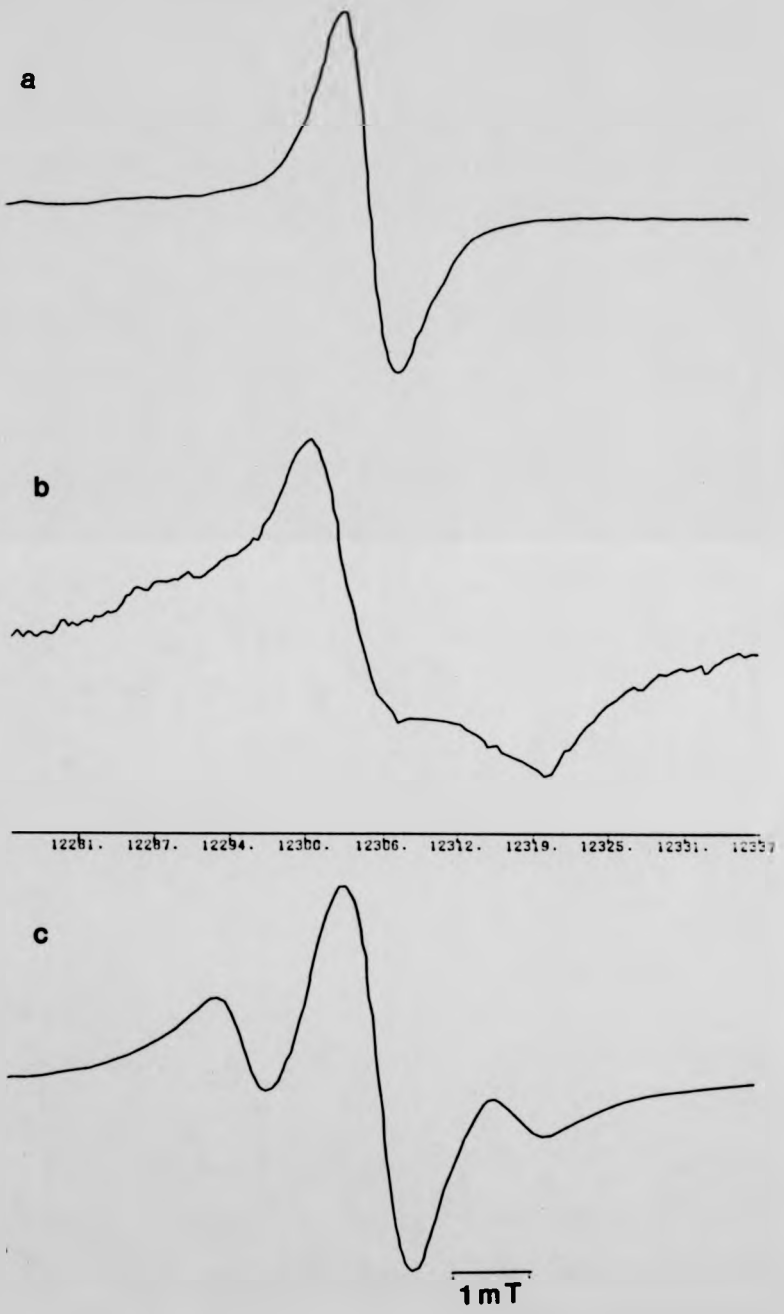


Fig. 6.6 (a) The 9.5-GHz Fibre spectrum corresponding to A-form ϕW-14 DNA.
(b) The 35-GHz Fibre spectrum corresponding to A-form ϕW-14 DNA.
(c) The Fibre spectrum recorded at 98% r h. (B-form ϕW-14 DNA).

practice more difficult to induce in the low-salt fibre. Evidence for this comes from both the X-ray and ESR experiments where prolonged exposure of the fibre at high and low humidities was required before the A → B or A → C transitions occurred. This effect is not thought to be due to the presence of the modified bases but is probably caused by a non-uniform distribution of excess salt in the fibre. The following observation supports this claim.

The 1mM NaCl fibre was allowed to stand for several days at 98% r h. and after this time it was humidified at 33, 66 and 98% relative humidities respectively. The transitions C → A → B were then found to occur as for normal DNA fibres. It is possible that after prolonged exposure at high humidity the salt distribution in the fibre became more uniform. This would allow for a more effective distribution of water into the central parts of the fibre and ensure a more rapid response of the DNA to changes of humidity.

At higher salt concentrations there are more centres of hydration present and the distribution of salt ions is then not so important. Transitions are therefore easier to bring about as was the case for the 15mM NaCl fibre.

**B- and C-form Spectra**

In discussing the ESR results it might be remembered that the nitroxide moiety used in these experiments was also used to spin-label proflavine. It is reasonable to assume, therefore, that the principal g- and A-values previously assigned to this nitroxide are also applicable in the present work (although judging by the ESR solution spectrum the g-values will be slightly modified). If this is the case then a maximum hyperfine splitting of ~7.0mT would be expected for a completely immobilised spin-label. The B- and C-form splittings (Figs. 6.5(a-d) and Figs. 6.6c) are little more than half this value, indicating that some

residual spin-label motion is present.

The equality of the hyperfine splittings of the 1mM (or 15mM) NaCl fibre spectra at both high and low relative humidities suggests that the mobility of the spin-labelled putrescine group is determined primarily by the DNA conformation. The linewidths and lineshapes of the fibre spectra are comparable at both humidities and much broader than those for spin-labelled ϕW-14 DNA in solution. If the lineshape changes and broadening observed in going from solution to the fibre state at 98% r h. are caused largely by the decreased level of hydration in the fibre, then a considerable difference should also be apparent between the ESR fibre spectra recorded at extreme humidities. However, as can be seen from Figs. 6.5(a-d) and Fig. 6.6c only minor lineshape changes are visible between the B- and C-form spectra. One may conclude from this observation that the amount of water in present in the fibres has only a limited affect on the overall characteristics of the ESR spectra.

However, the hyperfine splittings at both high and low humidities are 0.26mT larger for the high-salt fibre than the 1mM NaCl fibre. This effect may be attributable to a change in the polarity of the environment of the spin-label (see Chapter 2). Since at 33% (or 98%) relative humidity the two fibre will be equally hydrated, an increase in polarity can only arise if there is a tendency for water to accumulate within the locality of the spin-label (i.e. in the major groove). This tendency must be related to the concentration and distribution of $Na^+$ ions in the fibre.

The $Na^+$ ion distribution and its relationship to water structure in DNA in fibres is not known, although it is becoming increasingly clear from single-crystal studies that both of these factors are extremely important with regard to DNA conformation and stability (Drew and Dickerson, 1981; Lee et al., 1984; Conner et al., 1982). If the main features of these single crystal studies are extended to the fibre case then the following picture emerges.

Both theoretical calculation (mentioned by Lee et al., 1984) and experimental evidence (Drew and Dickerson, 1981; Conner et al., 1982) suggest that the $Na^+$ ions do not merely neutralise the phosphate groups but instead form a regular zig-zag lattice which minimises $Na^+$ - $Na^+$ ion repulsions. These repulsions are further minimised by the strong attractive forces which exist between the $Na^+$ ions and the lone-pair groups of the water molecules. The water - $Na^+$ ion interactions result in the formation of long chain-like structures which extend from the phosphate backbone into the major and minor grooves (see also the discussion in Chapter 4). The extent and stability of these $Na^+$ - water - $Na^+$ chains would seem to depend (amongst other factors) upon both the amount of water present and on the $Na^+$ ion concentration, e.g. too few water or $Na^+$ ions will result in only small chains or none at all.

Given that these chains do exist in DNA in fibres then one might expect their formation to be more extensive in the 15mM NaCl fibre than in the low salt fibre. That is, in the 15mM NaCl fibre the $Na^+$ - water - $Na^+$ chains will extend further into the major groove, thus increasing the polarity of this region of the DNA relative to that present in the 1mM NaCl fibre. This increase in polarity is then responsible for the larger hyperfine splittings observed for the high-salt fibre.

**A-Form Spectra**

The A-form ESR spectra (Figs. 6.6(a-b)) clearly indicate the presence of exchange phenomena. Viz, the nuclear hyperfine structure has virtually collapsed and only a single line is visible at all orientations. Actually, a closer examination of the spectra reveals the existence of small humps in the wings of the central line. These features are typical of intermediate to fast exchange interactions (see Chapter 2). From the point of view of the original project (i.e. the determination of the conformation of the putrescine in A-form DNA) the existence of these

exchange interactions is rather unfortunate. However, although no orientational information is available it is in any case unlikely that the putrescine groups could form hydrogen bonds in the prescribed manner and at the same time participate in strong exchange phenomena. This will become clear in the following discussion.

The bases in A-form DNA are displaced by nearly 5A from the helix axis (see Chapter 1), forming a large hollow inner core in which the putrescine chains are probably fully extended. Being fully extended they may form hydrogen bonds with the phosphate oxygens. On the other hand, the putrescine groups may merely project into the inner core and remain mobile (although greatly restricted compared with the B- and C-form structures).

The possibility of hydrogen-bonding is not eliminated by the presence of the nitroxide moiety since the remaining secondary amine is available. A CPK space filling model shows that there is no steric hindrance to the formation of hydrogen bonds involving the secondary amines. However, the removal of the positive charge from the (primary) amino-nitrogen will reduce the attraction between the putrescine and the phosphate backbone. The formation of a hydrogen bond will therefore no longer be favourable. (Note: as mentioned above work is in progress to develop a spin-labelled putrescine which retains the positive primary amino). Nevertheless, some interesting information is available from the present study. In order to understand the circumstances under which the observed exchange effects occur and in particular why these effects are prominent in the A-form but not the B- or C-forms, a consideration of the three DNA conformations is necessary.

In the following discussion it is assumed that the base pair sequence in $\phi$W-14 DNA is random and that the probability of a given base being $\alpha$-putrescinylthymine is 0.125. The average separation between the nearest modified thymines is then 4 base pairs.

In B-form DNA there are 10 base pairs per turn of the helix so that the twist angle per base pair is 36° and the rise per residue (i.e. base pair) is 3.4Å (see Table 1.1, Chapter 1). This means that two modified thymine bases belonging to the **same** polynucleotide strand are separated by 13.6Å and rotated by 144° to each other. The nearest modified thymines belonging to **opposite** polynucleotide strands will also be separated by 13.6Å but the angle of rotation is now 324° (or -36°).

In C-form DNA there are 9.33 base pairs per turn of the helix and the twist per base pair is therefore larger and equal to 38.6°. The nearest modified thymines are therefore rotated by 156.4° if on the same polynucleotide strand or by 336.4° (-23.6°) if on opposite polynucleotide strands. The rise per residue is 3.3Å so that the nearest neighbour separation is 13.2Å.

In both the B- and C-conformations exchange interactions between neighbouring putrescine groups belonging to the same polynucleotide strand are prohibited by the steric hindrance which results from their large angular separation. For two modified bases attached to opposite strands the angle of rotation is large enough to allow for some interaction between the spin-labels. However, the putrescine sidechains are able to rotate and wobble over a large angle about their mean positions in the major groove, so a close approach of two spin labels will be infrequent. On this model, therefore, only weak exchange interactions would be expected and a broadening of the three ESR lines should be observed. As can be seen from Figs. 6.5(a-d) and Figs. 6.6c the B- and C-form linewidths are indeed broadened. Motional modulation effects, as described in Chapter 2, are also likely to contribute to the observed linewidths, particularly at the high- and low-field regions of the spectra.

In A-form DNA the twist per residue is 32.7° and the rise per residue is only 2.6Å. Therefore the separation between the nearest modified thymines is 10.4Å and the angle of rotation between them is 130.8°

(if both bases are on the same polynucleotide strand) or 310.8° (-49.2°) (if the bases are on opposite strands). Whereas in the B- and C-conformations the putrescine groups are "outside" the double helix, in the A-conformation they occupy the hollow interior of the structure. This means that (a) the angle of wobble of the putrescine sidechains is smaller than that allowed in the B- and C-conformations and (b) the putrescine groups attached to either the same or opposite polynucleotide strands are in a more favourable configuration for close contact. Since two spin-labelled putrescines together span a distance of some 20A very close contact is possible and exchange interactions between adjacent spin-labels will be strong. This conclusion may also be drawn from a model in which the base-pair sequence is not random. In this case neighbouring modified bases will on average be closer together and exchange interactions will be even more favourable.

If hydrogen-bonding occurs between the secondary amines and the phosphate oxygens then the average separation between adjacent spin-labelled putrescines will be of the order of 10A. Exchange processess may still occur over this distance but the spin-labels will now be more or less fixed in orientation. Spin-spin dipolar interactions will therefore become more important. In this case a broadening of the ESR spectra should be observed and the nuclear hyperfine structure should be visible. The presence of exchange effects suggests, therefore, that the putrescine groups are not bound to the sugar-phosphate backbone.

The Q-band spectra were obtained at a level of humidity at which the fibres gave A-type diffraction patterns. The broadness of these spectra compared with the 9.5-GHz A-form spectra is principally due to the increased spectral resolution obtainable at the higher microwave frequency. In particular, the g-value anisotropy which is hidden at 9.5-GHz is resolved at 35-GHz. This anisotropy is directly responsible for the width

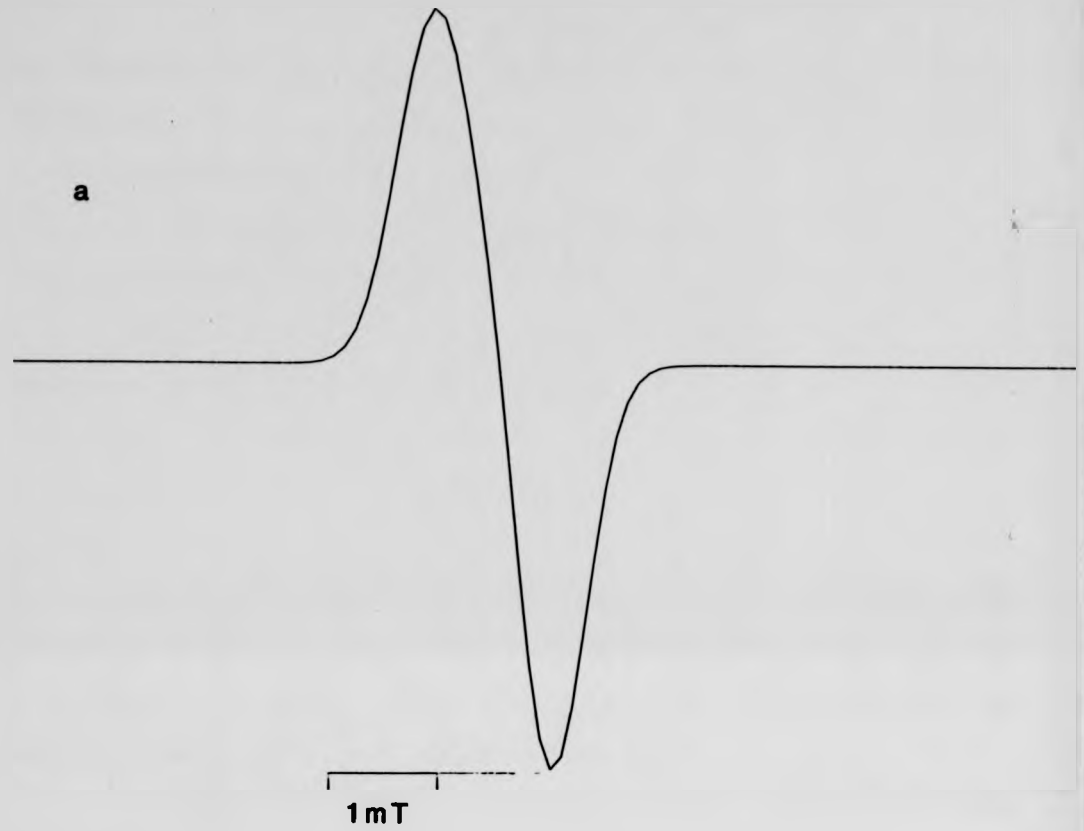


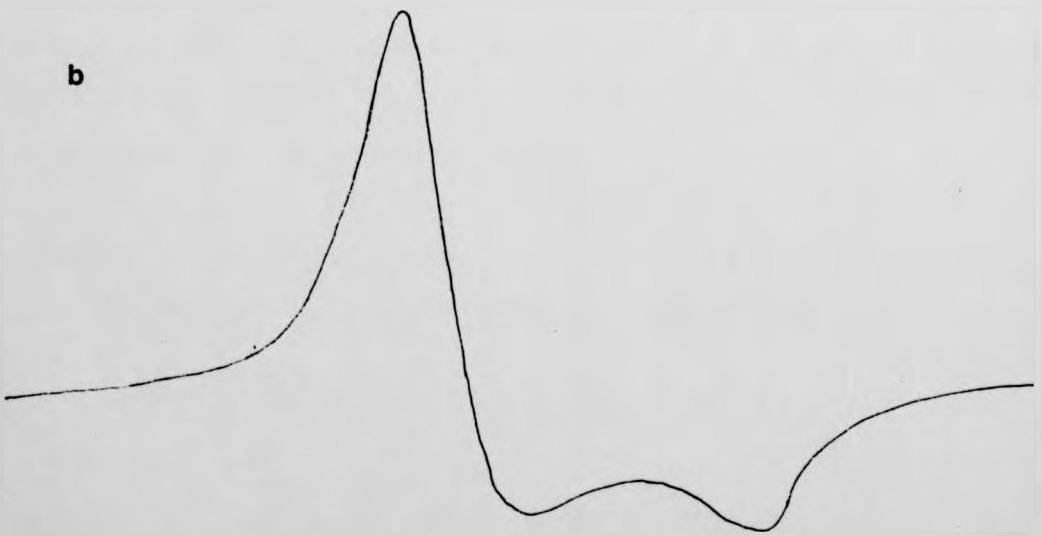


Fig. 6.7 (a) 9.5-GHz Fibre simulation of the A-form spectrum given that the hyperfine term is zero and $\delta = 90°$.
(b) The Q-band simulation demonstrating the line broadening due to the g-value anisotropy.

and shape of the Q-band spectrum of Fig. 6.6b. This is easily seen as follows.

Assume for the moment that

(1) There is no nuclear hyperfine structure,

(2) There is no spin-spin dipolar coupling,

and (3) There are no exchange interactions present,

then the spin-Hamiltonian for this system is

$$h\nu = \beta \mathbf{S}.\mathbf{g}.\mathbf{B}$$

A computer simulated spectrum based upon this Hamiltonian with $g_{xx} = g_{yy} = 2.0065$, $g_{zz} = 2.0027$ and $\nu = 34.5$-GHz is shown in Fig. 6.7b for a Lorentzian lineshape. These g-values were chosen because they give an isotropic g-value equal to the experimental value.

By comparing Fig. 6.6b with Fig. 6.7b it can clearly be seen that, although only g-value anisotropy has been considered, the simulated spectrum has the correct overall shape and width. The 9.5-GHz simulation for this Hamiltonian is shown in Fig. 6.7a and it compares well with the experimental A-form spectrum (Fig. 6.6a).

In practice, assumptions (1) and (2) are likely to hold under conditions in which the electrostatic exchange coupling is strong (contrary to assumption (3)). The **true** Hamiltonian for strong exchange is therefore:

$$h\nu = \beta \mathbf{S}.\mathbf{g}.\mathbf{B} + J\mathbf{S}_1.\mathbf{S}_2$$

where J is the **exchange integral.** The line positions and intensities are therefore dependent upon the exchange term as well as the Zeeman term. Nevertheless, enough has been said here to demonstrate that the X- and Q-band spectra can be interpreted in terms of exchange processes.

**Summary**

The initial objectives of this chapter - a determination of the configuration of the putresine sidechain in ϕW-14 DNA - were not reached, principally because of the difficulties of obtaining a suitably spin-labelled DNA derivative. However, the results do shed some interesting sidelights on the extent of the modification of the thymine bases in the DNA and on the geometry and mobility of the putrescine sidechain in the three DNA conformations. Further work, some of which is in progress, will include (a) using a ϕW-14 derivative with fewer modified groups, to reduce spin-spin interactions, (b) as mentioned above, a spin-label will be prepared which is designed to retain the positive charge of the primary amines and (c) radio-labelled putrescines will be us ed in conjunction with the ESR experiments to monitor the extent of the spin-labelling.

# CHAPTER 7

## CONCLUSIONS AND SUGGESTIONS FOR FURTHER WORK

In this chapter the main results of this thesis and their significance are discussed. Suggestions are also made concerning future ESR studies of drug binding to DNA and its related systems. In general the present work shows that ESR can be successfully applied to study the interactions of drugs with DNA in both fibres and solutions.

### 7.1 Work on spin-labelled proflavine

The interaction between spin-labelled proflavine and DNA was found to result in the formation of a specific geometrical relationship between the drug chromophores and the double helix, implying that the interaction occurs at particular sites in the DNA molecule. It was shown that this interaction depended upon the conformational state of the DNA. Analysis of the drug-binding was possible in terms of simple models in which only one species of bound drug was assumed to be present. Computer simulation showed that external binding was the primary mode of interaction with A- and C-form DNA. The B-form ESR spectra were simulated using a model in which a rapid rotation of the intercalated drug about the helix axis was assumed. Intercalation in B-form DNA was confirmed by X-ray diffraction.

Transitions between the A-, B- and C-forms were not observed for a single fibre: at high P/D values no C-form was seen but a A → B transition was allowed. At lower P/D values the C → B transition occurred but no A-form was present. A possible explanation of this observation was given in Chapter 4.

There was some indication from the fibre studies of a base pair specificity in the binding process, and solution work showed that the

binding affinity of spin-labelled proflavine was some 100 times smaller than that of the native drug.

### 7.1.1 Suggestions for further work

Further ESR studies of drug-DNA interactions should be extended to include many other important drugs or small molecules. The primary aims of any future work seem to lie in the following areas.

(a) Following on from the methods used here, the base pair specificity of the spin-labelled drugs can be examined more thoroughly, both in the liquid and solid (i.e. fibre) states. Solution studies could be carried out using the method outlined below.

Firstly, the spin-labelled drug is bound to the DNA in a solution of known salt content. A solution of drug having a known specificity for AT bases is then added and the resulting change in the ESR spectrum is monitored. By estimating the amount of free to bound spin-labelled drug a Scatchard plot can be produced from which the binding characteristics of the spin-labelled drug may be determined. This experiment could be carried out with native competitor as well as with foriegn species of drug.

To test the feasibility of such a study a brief and qualitative experiment was performed to show that native proflavine easily displaces its spin-labelled analogue. On the other hand, thionin had no effect on the ESR spectrum of bound spinlabelled proflavine. Interestingly, as judged by the colour changes produced, thionin did bind when added to the DNA-spin-labelled proflavine complex. This result suggests that thionin either binds preferably to sites not occupied by proflavine, or that it is forced into these sites by the presence of the bound proflavine. A quantitative study could resolve this problem.

(b) Under aqueous conditions DNA adopts the B-conformation. However, it is believed that the addition of appropriate amounts of alcohol at low salt ( < 1mM) can induce a transition to the A-form (Ivanov et al., 1974). It will be interesting to examine these conformational changes in the presence of (initially) intercalated drug molecules. ESR should be an appropriate technique to use, preferably in combination with circular dichroism studies. The latter technique will provide the same service that X-ray diffraction did for the present work, namely confirming the nature of the conformational changeswhich take place.

(c) The work on DNA-drug binding in fibres can be extended in many ways. Known intercalators similar to proflavine could be spin-labelled and their interactions with DNA in fibres could be examined by the methods used in this thesis. Once the ESR spectra from these "model" systems have been characterised, the results could be used to interpret ESR data obtained from other DNA-drug complexes.

In the fibre context, an attempt could be made to study the binding of drugs to left-handed forms of the synthetic polynucleotide Polyd(GC).Polyd(GC). The possibility of examining left-right handed transitions then arises. It is particularly useful to do this work in conjunction with the X-ray diffraction group at Keele University, which is at present embarked upon a systematic study of the structures of many new synthetic polynucleotides.

(d) The absence of the A-form at high drug concentratiions (and the absence of the C-form at low drug concentrations) is intriguing. The reasons for this effect should be thoroughly investigated by a more systematic method than that employed in this work.

## 7.2 Phenothiazine Derivative-DNA complexes

Solution ESR studies of the oxidised forms of several phenothiazine derivative drugs showed that the unpaired electron spin was largely localised on the ring nitrogen. When bound to DNA fibres a three line hyperfine splitting characteristic of the nitrogen nuclear interaction was observed for a parallel arrangement of fibre and field; in the perpendicular orientation only one line was recorded. These spectra were analysed according to the fibre model (Chapter 4) and it was shown that the drug chromophores were orientated either parallel or at ~160° to the helix axis. No changes in the ESR spectra were observed with relative humidity, but X-ray diffraction studies showed that an A → B transition occurred at ~92% relative humidity. The constancy of the ESR spectra has been explained by supposing that the drug alters its orientation from parallel to the helix to ~160° to the helix as the conformational transition takes place. This could correspond to intercalation and external binding respectively. All the derivatives examined produced identical ESR results, regardless of the substituted groups present.

### 7.2.1 Suggestions for further work

It is clearly desirable to eliminate the ambiguities of the results of the fibre studies and to determine with greater certainty whether intercalation is a possible mode of binding for the phenothiazines. This task may perhaps best be accomplished by preparing a series of spin-labelled analogues of the phenothiazines. The advantages to be had by using spin-labelled compounds have been demonstrated by some of the work in this thesis. With regard to the phenothiazines the major problem encountered was their instability. This difficulty would be eliminated if spin-labelled derivatives are used. Furthermore, the ease with which P/D values can be estimated and controlled will be vastly improved; solution studies will become feasible and the number of fibres required for

orientation studies will be reduced (thus reducing uncertainties in interpretation).

Problems may, however, be encountered in this proposal and some of the more obvious ones should be mentioned.

Firstly, it is not clear that a neutral spin-labelled phenothiazine drug will bind to DNA. The initial interaction between the oxidised derivatives and DNA probably involves an electrostatic attraction between the negative phosphates and the positive drug. This interaction is inhibited at normal pH (Chapter 5). It will therefore be wise to examine the binding of several of the native drugs before embarking on any spin-labelling experiments. If the native drugs do prove to be useless in this respect then other tricyclic "bent" molecules could be looked at. A second problem is the spin-labelling itself. As was seen in the present work a considerable expenditure of time and effort is required in order to search for appropriate materials and methods. However, a spin-labelled derivative of chlorpromazine has recently been synthesised (Dikanov et al., 1983). Work is now in progress in the Physics department to apply the published method to other phenothiazine derivatives.

## 7.3 ϕW-14 DNA

The project involving ϕW-14 DNA was most interesting and it is unfortunate that a sufficient amount of spin-labelled material was not available to enable a full set of experiments to be completed. Some suggestions for the future have already been mentioned in Chapter 6 and, if a suitable spin-label (e.g. "Spin-Imidate") can be found, ESR should prove to be an ideal method for examining the structural properties of the putrescine sidechain.

## REFERENCES


Abragam A., **Principles of Nuclear Magnetism**, Oxford Science Pub. (1961)

Aggarwal A., Islam A., Kuroda R., Neidle S., Biopolymers **23**(6) 1025 (1984)

Anderson P. W., Phys. Rev., **114**, 1002 (1959).

Arnott S., Chandrasekharan R., Birdsall D. L., Leslie A. G. W. Ratcliff R. L., Nature, **283**, 943 (1980)

Arnott S., Hukins D. W. L., Biochim. Biophys. Res. Comm., **47**, 1504 (1972)

Atherton N. M., **Electron Spin Resonance**, Ellis Horwood (1973)

Ayscough P. B., **Electron Spin Resonance in Chemistry**, Methuen (1967)

Berliner L. J. (ed), **Spin-Labelling: Theory and Practice** Academic Press N. Y., Volume 1 (1976), Volume 2 (1979)

Bernier J. L., Henichart J. P., Catteau J. P., J. Biochem., **199**, 479 (1981b)

Bernier, J. L., Henichart, J. P., Catteau, J. P., Anal. Biochem., **117**, 12 (1980).

Blake, A., Peacocke, A. R., Biopolymers **6**, 1225 (1968).

Bloch F., Phys. Rev., **70**, 460 (1946)

Bobst A. M., Kao S. C., Toppin R. C., Ireland J. C., Thomas I. E. J. Mol. Biol., **151**, 835 (1981)

Bobst A. M., in **Spin-Labelling II: Theory and Practice** Berliner L. J. (ed), Academic Press, N. Y. (1979).

Bobst A., Hakam A., Langemenier P., Kouda S. Arch. Biochem. Biophys., **194**(1), 171 (1979)

Bodea C., Silberg I., Adv. Hetero. Chem. **9**, 320 (1968)

Borg D. C., Cotzias C., Proc. Nat. Acad. Sci., **48**, 617 (1962)

Borg D. C., Fed. Proc., **20**(10), 104 (1961)

Bradley, D. F. and Wolf, M. K., Proc. Nat. Acad. Sci., **45**, 944 (1959).

Calendi E., Merco D., Reggian A., Scarpinto B., Valentini T. Biochim. Biophys. Acta., **103**, 25 (1965)

Carrington A., McLachan A. D., **Introduction to Magnetic Resonance** Science Paperbacks, J. Wiley α Sons (1967)

Chan D., Piette L. H., Biochem., **21**(12), 3028 (1982)

Chapman I., Leysko W., Gwozdzinski K., Koter M., Grelinska E., Bartoz G., Radiat. Res., **96**(3), 518 (1983)

Clarke D., Gilbert B., Hanson P., Kirk C., J. C. S. Perkin II, 1103 (1978)

Conner B. N., Takano T., Takana S., Itakura K., Dickerson R. E.
Nature, **295**, 294 (1982)

Cooper P. J., Hamilton L. D., J. Mol. Biol., **16**, 562 (1966)

Crick F. C. H., Barnett L., Brenner S., Watts-Tobin R. J.,
Nature, **192**, 1227 (1961).

Davidson J. N., (ed) **The Biochemistry of Nucleic Acids**
Science Paperbacks, 8$^{tn}$ Edition (1976)

Davis D. R., Baldwin R. L., J. Mol. Biol., **6**, 251 (1963)

Denny W. A., Cain B. F., J. Med. Chem., **21**, 430 (1978)

Dougherty, M., Ph.D Thesis, Keele University (1979).

Drew H. R., Dickerson R. E., J. Mol. Biol., **173**, 63 (1984)

Drew H., Dickerson R. E., J. Mol. Biol., **151**, 1981

Fenner H., Arch. Pharm., **303**, 919 (1970)

Fenner H., in **The Phenothiazines and Structurally Related Drugs**
Forrest I.S., Carr C. T., Usdin E. (eds), 5, Raven Press NY, (1974)

Forrest I. S., Forrest F. M., Berger M.
Biochim. Biophys. Acta, **29**, 441 (1958)

Forrest I. S., in **The Phenothiazines and Structurally Related Drugs**
Forrest I. S., Carr C. T., Usdin E. (eds), 341, Raven Press NY, (1974)

Fraenkel K., J. Phys. Chem., **71**, 139 (1967)

Franklin R. H., Gosling R. G., Acta. Cryst., **6**, 678 (1953)

Freed J. H., Fraenkel K., J. Chem. Phys., **39**, 326 (1963).

Fuller W., Wilkins M. H. F., Wilson H. R., Hamilton L. D.
J. Mol. Biol., **12**, 60 (1965)

Fuller, W. and Waring, M. J., Ber. Bunsenges. Physik Chem., **68**, 805 (1964).

Gersch, N. F. and Jordan, D. O., J. Mol.Biol., **13**, 138 (1965).

Goodwin, D. C., Ph.D Thesis, Keele University (1977).

Greenall R. J., PhD Thesis, University of Keele (1982)

Greenall R. J., Pigram W. J., Fuller W., Nature, **282**, 880 (1979)

Gregori S., Olast M., Bertinchamps A., Radiat. Res., **89**(2), 238 (1982)

Griffith O. H., Cornell D. V., McConnell H. M., J. Chem Phys., **43**, 2909
(1965)

Griffith O. H., McConnell H. M., Proc. Nat. Acad. Sci., **55** (1966)

Hamilton L. D., Fuller W., Reich E., Nature, **198**, 538 (1963)

Hanson P., Isham W., Lewis R., Stockburn W., J. C. S. Perkin II, 1492 (1981)

Hanson P., Norman R., J. C. S. Perkin II, 264 (1973)

Harris J. P., Phillipson O. T., Walkins G. A., Whelpton R. Psychopharm., **79**(1), 49 (1983)

Herman D., Fazerkeley G., Biopolymers **23**(3), 945 (1984)

Hollister L. E., Rational Drug Ther., **16**(8), 1 (1982)

Hong S. J., Piette L. H., Cancer Res., **30**, 1159 (1976)

Hong S. J., Piette L. N., Arch. Biochem. Biophys., **185**(2), 307 (1978)

Hudson A., Luckhurst G. R., Chem. Rev., **69**, 191 (1968)

Hurley I., Osei-Gyimah P., Archer S., Scholes C. P., Lerman L. S. Biochemistry, **21**, 4999 (1982)

Ivanov I., Raikova E., Raikova Z., Yaneova I., Kaffalieva D., Int. J. Biochem., **15**(3), 433 (1983)

Ivanov V. I., Minchenkova L. E., Minyat E. E., Frank-Kamenetskii M. P., Schoylinka A. K., J. Mol. Biol., **87**, 817 (1974)

Jost P. C., Griffith O. H., in **Spin-Labelling I: Theory and Practice** Berliner L. J., (ed), Academic Press, N. Y. (1976)

Kamzalova S. G., Postnikova G. B., Quart. Rev. Biophys., **14**, 244 (1981)

Kauffman J. J., Kerman E., in **The Phenothiazines and Structurally Related Drugs**, Forrest I.S., Carr C. T., Usdin E. (eds), 55, Raven Press NY, (1974)

King H. D., Wilson W. D., Gabbay E. J., Biochem., **21**, 4982 (1982)

Kirkpatrick M. W., Klysik J., Singleton C. K., Zaling D. A. Jovin J. M., Hanau L. H., Eleger B. F., Wells R. D. J. Biol. Chem., **259**, 7268 (1984)

Kolpak F. J., Crawford J., Van Boom J. H., van der Marel G., Rich A. Nature **282**, 680 (1979)

Kropinski A. M. B., Warren R. A. J., J. Gen. Virol., **6**, 85 (1970)

Kropinski A., Bose R. J., Warren R. A. J., Biochem., **12**, 151 (1973)

Krugh T. R., Reinhardt C. G., J. Mol. Biol., **97**, 133 (1975)

Langercrantz C., Acta. Chem. Scand., **15**, 1545 (1961)

Langridge R., Marvin D. A., Seeds N. E., Wilson H. R. J. Mol. Biol., **2**, 19 (1960)

Lawrence J. J., Bernier L., Ouvrier-Buffet J. L., Piette L. H.
Euro. J. Biochem., **107**, 263 (1980)

Le Pecq J. B., Paoletti C., J. Mol. Biol., **27**, 87 (1967)

Lee N. K., Gao Y., Prokhofsky E. W., Biopolymers **23**(2), 257 (1984)

Lerman L. S., Proc. Nat. Acad. Sci., **49**, 94 (1963)

Lerman, L. S., J. Mol. Biol., **3**, 18 (1961).

Libertini L. J., Burke C. A., Jost P. C., Griffith O. H.,
J. Magn. Res., **15**, 460 (1974)

Libertini L. J., Griffith O. H., J. Chem. Phys., **53**, 1359 (1970)

Libertini L. J., Waggoner A.S., Jost P.C., Griffith O. H.,
PNAS **64**, 13 (1969)

Low L. C., Drew H. R., Waring M., Nucl. Acid Res., **12**(12), 4865 (1984).

Luzzatti, V., Mason, F., Lerman, L. S., J. Mol. Biol., **3**, 634 (1961).

Mahendrasignham A., PhD Thesis, University of Keele (1983)

Mahendrasignham A., Pigram W. J., Fuller W., Brahms J., Vergne J.
J. Mol. Biol., **168**, 879 (1983a)

Mahendrasingham A., Rhodes N. J., Goodwin D. C., Nave C., Pigram W. J.
Fuller W., Brahms J., Vergne J., Nature, **301**, 535 (1983b)

Malmstrom M. C., Corder A. W., J. Hetero. Chem., **9**, 323 (1972)

Malreau T., Pullman B., Theoret. Chim. Acta, **2**, 293 (1964)

Maltman K. L., Neuhard J., Warren R. A. J., Biochem., **20**, 3586 (1981)

Marsau P., Acta. Crystall., **B27**, 42 (1971)

Marvin D. A., Spencer M., Wilkins M. H. F., Hamilton L. D.
J. Mol. Biol., **3**, 574 (1961)

Massie H. R., Zimm B. H., PNAS **54**, 1641 (1965)

McConnell H. M., McFarland B. G., Quart. Rev. Biophys., **3**, 91 (1970)

McConnell H., Robertson R. E., J. Phys. Chem., **61**,1018 (1958)

McDowell J. J. H., in **The Phenothiazines and Structurally Related Drugs**
Forrest I. S., Carr C. T., Usdin E. (eds), 33, Raven Press NY, (1974)

Meeham T., Gauper H., Becker T. F., J. Biol. Chem., **257**, 10479 (1982)

Meselson M., Stahl F. W., Proc. Nat. Acad. Sci., **66**, 671 (1958)

Muller W., Crothers D. M., Euro. J. Biochem., **54**, 267 (1975)

Muller W., Crothers D. M., J. Mol. Biol., **35**, 251 (1968)

Muller W., Crothers D. M., Waring M. J., Euro. J. Biochem., **39**, 223 (1973)

Nelson H. P., DeVoe H., Biopolymers **23**(3), 879 (1984)

Neville, D. M. and Davies, D. R., J. Mol. Biol., **17**, 57 (1966).

Newlin D., Millar K. J., Bioploymers **23**(1), 139 (1984)

Noji S., Ser. A: Phys. Chem., **44**(1), 119 (1980)

Nonhebel D. C., Tedder J., Walton J., **Radicals**, CUP (1979)

Nordio P. L. in **Spin-Labelling I: Theory and Practice**
Berliner L. J. (ed), Chapter 2, Academic Press, N. Y. (1976)

Onishi S., McConnell H., J. Amer. Chem. Soc., **87**, 2293 (1965)

Ozinkas A., Deranesau P., Keller S., Bobst A.,
Nucl. Acid Res., **9**(20), 5483 (1981)

Pake G. E., Estle T. E., **The Physical Principles of Paramagnetic Resonance**, W. A. Benjamin, Mass. (1973)

Pan E., Bobst A., Bioploymers, **13**, 1079 (1974)

Pan E., Bobst A., Biopolymers, **12**, 367 (1973)

Peacocke A. R., Skerrett J. N. A., Trans. Farad. Soc., **52**, 261 (1956)

Peacocke, A. R., **The Acridines**, Acheson (ed) (1970).

Petrov A. I., Sukharokov B., Biofizika, **28**(5), 736 (1983)

Piette L. H., Biochim. Biophys. Acta., **88**, 120 (1964)

Piette L. H., Forrest I. S., Biochim. Biophys. Acta., **57**, 419 (1962)

Poole C. P., "**Electron Spin Resonance: A comprehensive Experimental Treatise**", 2nd Edition, John Wiley and Sons (1983).

Porumb H., PhD Thesis, Keele University (1976)

Porumb T., PhD Thesis, University of Keele (1976)

Porumb T., Slade E. F., Euro. J. Biochem., **65**, 21 (1976)

Raikova E., Ivanov I., Kaffalieva D., Demirov G., Raikov Z.
Int. J. Biochem., **14**(1), 41 (1982)

Raikova E., Kaffalieva D., Ivanov I., Zakhariev S., Golorinskii E.,
Biochem. Pharmacol., **32**(4), 587 (1983)

Rhodes N. J., Mahendrasingham A., Pigram W. J., Fuller W., Brahms J.
Vergne J., Warren R. A. J., Nature, **296**, 267 (1982)

Robinson B. H., Forgacs G., Dalton L. R., Frisch H. L.,
J. Chem. Phys., **73**(9), 4688 (1980)

Robinson B. H., Lerman L. S., Bethe A. H., Frisch H. L., Dalton L. R.,
Auer C., J. Mol. Biol., **139**, 13 (1980).

Rodley G. A., Scobie R. S., Bates P. H. T., Lewitt R., M.
Proc. Nat. Acad. Sci., **73**, 2959 (1979)

Roland F., Int. Res. Comm. Syst., **9**(4), 365, 1981

Rozantsev **Free Nitroxide Radicals**, Plenum Press, N. Y. (1970).

Ruperez F. L., Conesca J. C., Soria J., J. C. S. Perkin II, 1157 (1982)

Scatchard, G., Ann. N. Y. Acad. Sci., **51**, 660 (1949).

Scraba D. G., Bradley R. D., Leynitz-Wills M., Warren R. A. J.
J. Virol., **124**, 152 (1983)

Segal E., Giraultt J. P., Muzard G., Chottard G., Chottard J. C.,
Le Pecq J. P., Biopolymers, (23)**9**, 1623 (1984).

Shakkad Z., Rabinovich D., Kennard O., Cruse W. B. T., Salisbury A.
Viswamitra M. A., J. Mol. Biol., **166**, 183 (1983)

Shafer R. H., Brown S. C., Debarre A., Wade D.,
Nucl. Acid Res., **12**(11), 4679 (1984).

Shearman L. W., Forgette M. M., Loeb L. A., J. Biol. Chem., **258**, 4485
(1983)

Shine H., Mach E. E., J. Org. Chem., **30**, 2130 (1965)

Sinha B. K., Cox M. G., Chignall C. F., Csysk R. L.
J. Med. Chem., **21**(9), 1051 (1979)

Sinha B. K., Csysk R. L., Millar D. B., Chignall C. F.
J. Med. Chem., **19**, 994 (1976)

Sinha B. K., Csysk R.L., Chem.-Biol. Int., **34**(3), 367 (1981a)

Sinha B. K., Lewis G. S., Biochem. Pharmacol., **30**(18), 2626 (1981b)

Sinha, B. K., Chignall, C. F., Wee, V. T.,
Nucleic Acid Res., **6**(11), 3703 (1979)

Slichter C. P., **Principles of Magnetic Resonance**, Springer-Verlag (1980)

Sobell, H. M. and Jain, S. C., J. Mol. Biol., **83**, 487 (1972).

Sobell, H. M., **Nucleic Acid Geometry and Dynamics**, Sarma, R. (ed) (1980).

Stone T. J., Buckman T., Nordio P. L., McConnell H. M.,
Proc. Nat. Acad. Sci., **54**, 1010 (1965)

Sullivan P. D., Bolton J. R., J. Magn. Res., **1**, 356 (1969)

Sweatt J. D., Palmer G. C., Jackson T. G., Mannion A. A.
Arch. Int. Pharm. Ther., **257**(2), 188 (1982)

Thiery C. C., Meunier J., Leternier F., J. Chim. Phys., **66**, 234 (1968)

Topol M. D., Biochem., **23**(1), 237 (1984)

Tozer T. N., Tuck L. D., J. Pharm. Sci., **54**, 1169 (1965)

Van Vleck J. H., Phys. Rev., **74**, 1168 (1948)

Van, S. P., Birrell, G. B., Griffith, O. H., J. Magn. Res., **15**, 444 (1974).

Wakelin, L. P. G. and Waring, M. J., J. Mol. Biol., **144**, 183 (1980).

Wang A. H., Quigley G., Kolpak F. J., Crawford J. L., van Boom J. H.,
Marel G., Rich A., Nature, **282**, 680 (1979)

Waring M. J., J. Mol. Biol., **54**, 247 (1970)

Warren R. A. J., Ann. Rev. Microbiol., **34**, 137 (1980)

Warren R. A. J., Current Microbiol., **6**, 85 (1981)

Watson J. D., Crick T. H. C., Nature **171**, 737 (1953)

Wilkins M. H. F., Stokes A. R., Wilson H. R., Nature **171**, 738 (1953)

Wilson W. D., Keel R. A., Jones R. C., Masher C. W.
Nucl. Acid Res., **10**, 4093 (1982)

Yamaoka K., Noji S., Chemm. Lett., 449 (1977)

Yamaoka,K. and Sumihare,N., Chem. Lett., 1351 (1976).

Yielding L., Yielding K., Donaghue E., Bioploymers **23**(1), 83 (1984)

Zdhanov R., Paritikova V., Rozantsev E., Synthesis, **4**, 267 (1979)

Sweatt J. D., Palmer G. C., Jackson T. G., Mannion A. A.
Arch. Int. Pharm. Ther., **257**(2), 188 (1982)

Thiery C. C., Meunier J., Leternier F., J. Chim. Phys., **66**, 234 (1968)

Topol M. D., Biochem., **23**(1), 237 (1984)

Tozer T. N., Tuck L. D., J. Pharm. Sci., **54**, 1169 (1965)

Van Vleck J. H., Phys. Rev., **74**, 1168 (1948)

Van, S. P., Birrell, G. B., Griffith, O. H., J. Magn. Res., **15**, 444 (1974).

Wakelin, L. P. G. and Waring, M. J., J. Mol. Biol., **144**, 183 (1980).

Wang A. H., Quigley G., Kolpak F. J., Crawford J. L., van Boom J. H.,
Marel G., Rich A., Nature, **282**, 680 (1979)

Waring M. J., J. Mol. Biol., **54**, 247 (1970)

Warren R. A. J., Ann. Rev. Microbiol., **34**, 137 (1980)

Warren R. A. J., Current Microbiol., **6**, 85 (1981)

Watson J. D., Crick T. H. C., Nature **171**, 737 (1953)

Wilkins M. H. F., Stokes A. R., Wilson H. R., Nature **171**, 738 (1953)

Wilson W. D., Keel R. A., Jones R. C., Masher C. W.
Nucl. Acid Res., **10**, 4093 (1982)

Yamaoka K., Noji S., Chemm. Lett., 449 (1977)

Yamaoka,K. and Sumihare,N., Chem. Lett., 1351 (1976).

Yielding L., Yielding K., Donaghue E., Bioploymers **23**(1), 83 (1984)

Zdhanov R., Paritikova V., Rozantsev E., Synthesis, **4**, 267 (1979)